Molecular regulation of neuroblast migration in the postnatal brain

Gajendra, Sangeetha

Awarding institution:
King's College London

Molecular regulation of neuroblast migration in the postnatal brain

A thesis for the degree of Doctor of Philosophy

Sangeetha Gajendra

Wolfson Centre for Age-Related Diseases

King's College London

Abstract

The subventricular zone (SVZ) is one of the main neurogenic niches in the postnatal brain. Neural precursors derived from SVZ stem cells migrate in chains to the olfactory bulb (OB) via the rostral migratory stream (RMS) through channels (glial tubes) formed by the processes of astrocytes. Importantly, these precursors have the capacity to migrate away from their native route to areas of pathological damage in the adult brain. Therefore, studying the migratory properties of these cells is essential, not only to understand basic aspects of adult neurogenesis, but also to exploit the potential of adult neural stem cells in neuroregenerative strategies. Whilst considerable progress has been made in the field of SVZ neural precursor migration, the exact molecular mechanisms regulating this process remain to be fully elucidated.

The endocannabinoid system is known to play an important role in the regulation of neural stem cell proliferation. Here, we show that CB signalling also regulates the migration of SVZ-derived neural precursors. In addition, stimulation of G-protein coupled cannabinoid receptors, CB1 and CB2, leads to significant activation of RalA, a Ras-like GTPase involved in the control of neuronal morphology and polarity. siRNA-mediated knockdown of RalA or the expression of dominant negative RalA abolished cannabinoid-induced stimulation of migration. Time-lapse imaging revealed that depletion of RalA strongly impaired nucleokinesis: a crucial step for efficient migration. Analysis of RalA function *in vivo*, using wild type and mutant constructs electroporated into the SVZ, showed that the loss of RalA function results in both altered morphology and direction of migration. Finally, selective deletion of RalA in RMS neuroblasts *in vivo* further confirms that RalA is required for correct polarised morphology of migrating neuroblasts in the RMS.

In summary, RalA is activated by CB agonists, and is required for CB-promoted migration of RMS neuroblasts. Furthermore, RalA expression is necessary for polarised morphology and efficient migration of RMS neuroblasts both *in vitro* and *in vivo*.

Acknowledgements

I would like to take this opportunity to thank my supervisor Dr Giovanna Lalli for her support, advice, and encouragement throughout the four years of my PhD. I am extremely grateful for the time and effort she has taken to train me in the lab, and for passing on her passion and enthusiasm for Science. I would also like to express my deepest gratitude to my second supervisor Professor Patrick Doherty, who gave me the BBSRC studentship that has funded this PhD. I am especially thankful for his invaluable advice, which has helped to guide this project.

I would also like to thank all the staff at the Wolfson, namely Brenda Williams, John Chesson and Ralph Wilson. You have all gone out of your way to help me on more than one occasion, for which I am extremely grateful. Also, a special thanks to Carl Hobbs for the endless supply of antibodies, and for his help and contribution to this thesis.

I would also like to express my gratitude to my husband Myuran. It was his encouragement that led me to undertake this PhD, and it has been his endless support that has made this journey that much easier. Thank you.

Finally, I would like to express my sincerest thanks to Martina Sonego and Katarzyna Falenta from the Lalli Lab; Fiona Howell, Melina Reisenberg, Madeleine Oudin, Praveen Singh, Zhou Ya, Rachel Lane and Dr Gareth Williams from the Doherty Lab; and all my colleagues on the 3rd floor. I have enjoyed the laughs, the banter, and the great food and wine that seem to be a part of life at the Wolfson. You have all made my PhD a memorable experience and I will miss you all.

Contents

List of Figures

Chapter 1: Introduction

Chapter 2: Materials and methods

Chapter 3: Endocannabinoids regulate RMS neuroblast migration

Chapter 4: RalA is required for CB-promoted migration of RMS neuroblasts

Chapter 6: Potential effectors and activators of RalA

Chapter 7: General discussion

Abbreviations

2/3D	2/3-dimensional
2-AG	2-arachidonoylglycerol
a.a	Amino acid
Ang1	Angiopoietin1
AEP	Anterior entopeduncular area
aPKC	Atypical protein kinase C
BDNF	Brain derived neurotrophic factor
BL	Basal Lamina
BMP	Bone Morphogenetic Protein
BrdU	Bromodeoxy-Uridine
CA	Constitutively active
Ca^{2+}	Calcium
CAM	Cell adhesion molecule
cAMP	Cyclic adenosine monophosphate
CB	Cannabinoid
CB1	Cannabinoid receptor 1
CB2	Cannabinoid receptor 2
CDK5	Cyclin-Dependent Kinase 5
cDNA	Complementary deoxyribonucleic acid
CFP	Cyan fluorescent protein
CNS	Central nervous system
CP	Choroid plexus
Cre	Cyclic Recombinase
CSF	Cerebrospinal Fluid
DAG	Diacylglycerol
DAG-L	Diacylglycerol lipase
DCX	Doublecortin
DG	Dentate Gyrus
Dlx2	Distal-Less Homeobox 2
DMEM	Dulbecco's modified eagle medium

DNA	Deoxyribonucleic Acid
DN	Dominant negative
DSE	Depolarization-induced suppression of excitation
DSI	Depolarization-induced suppression of inhibition
E	Embryonic day
EV	Empty vector
eCB	Endocannabinoid
ECL	Enhanced chemiluminescence
ECM	Extracellular Matrix
EGF	Epidermal growth factor
EGFP	Enhanced green fluorescent protein
EGFr	Epidermal growth factor receptor
EPL	External plexiform layer
FAAH	Fatty acid amide hydrolase
FAK	Focal adhesion kinase
FC	Fast cycling
FCS	Foetal calf serum
FGF	Fibroblast growth factor
FRET	Fluorescence resonance energy transfer
GABA	γ-Aminobutyric acid
GAP	GTPase-activating protein
GC	Granule cell
GCL	Granule cell layer
GDNF	Glial cell line derived neurotrophic factor
GEF	Guanine nucleotide exchange factor
GFAP	Glial fibrilliary astrocyte protein
GFP	Green fluorescent protein
GL	Granular layer
GPCR	G-Protein Coupled Receptor
GPR55	G-protein coupled receptor 55
GSK3β	Glycogen Synthase Kinase3β
HGF	Hepatocyte growth factor

IGF	Insulin growth factor
INM	Inter-kinetic nuclear migration
IRES	Internal ribosome entry site
LGE	Lateral Ganglionic Eminence
MAG-L	Monoacylglycerol lipase
MAPK	Mitogen-Activated Protein Kinase
MC	Mitral cell
MGE	Medial Ganglionic Eminence
mGluR	Metabotropic glutamate receptor
MI	Migratory Index (Total displacement/Total distance)
ML	Molecular Layer
MLC	Myosin light chain
MMPs	Matrix metalloproteinases
MRI	Magnetic Resonance Imaging
mRNA	Messenger RNA
NAPE	N-arachidonoylphosphatidylethanolamine
NAT	N-Acyltransferase
NCAM	Neural cell adhesion molecule
NMDA	N-methyl-D-aspartate
nIPC	neural intermediate progenitor cell
NRK	Normal Rat Kidney cells
NS cell	Neural stem cell
OB	Olfactory bulb
OD	Optical density
OE	Olfactory Epithelia
OPCs	Olfactory precursor cells
OSN	Olfactory Sensory Neuron
P	Postnatal day
PAK	p21-activated kinase
PAR	Partitioning defective
PBS	Phosphate buffered saline
PCR	Polymerase Chain Reaction

PET	Positron emission tomography
PGC	Periglomerular cell
PI	Phosphatidylinositol
PIP2	Phosphatidylinositol 4,5-bisphosphate
PI3K	Phosphatidylinositide-3 kinase
PKA	Protein kinase A
PKC	Protein kinase C
PLC	Phospholipase C
PLD	Phospholipase D
PNS	Peripheral Nervous System
PSA	Polysialic Acid
PSA-NCAM	Polysialylated neural cell adhesion molecule
Ral	Ras-like GTPase
RalBP1	Ral binding protein 1
Ral-GDS	Ral guanine nucleotide dissociation stimulator
RG	Radial glia
RMS	Rostral migratory stream
RNA	Ribonucleic Acid
RRP	Readily releasable pool
SDF-1	Stromal-derived factor
SGZ	Subgranular zone
shRNA	Small hairpin ribonucleic acid
siRNA	Short interfering ribonucleic acid
SVZ	Subventricular zone
TBS	Tris-Buffer Saline
TGFα	Transforming growth factor α
TH	Tyrosine hydroxylase
ΔTHC	Δ-tetrahydrocannabinol
VEGF	Vascular endothelial growth factor
VEGFR	Vascular endothelial growth factor receptor
WT	Wild type
YFP	Yellow fluorescent protein

Chapter 1: Introduction

1.1 Adult neurogenesis

1.1.1 Adult neurogenesis: A brief history

The absence of mitosis in neurones of higher vertebrate adults, coupled with the complexity and specificity of neural networks, had created the long held belief that the adult human central nervous system (CNS) is an immutable structure (Gage 2002). As a result, the concept of neurogenesis had been viewed as a process largely restricted to embryonic, foetal, and early postnatal development. However, ground breaking work during the last few decades has questioned this dogmatic view and replaced it with one in which ongoing cell replacement occurs in specific regions of the CNS (Ortega-Perez et al. 2007).

In 1962, Joseph Altman of the Massachusetts Institute of technology published his findings that incorporation of [^{3}H]-thymidine (a marker of cell proliferation) could be detected in hippocampal neurones of young adult rats. He went on further to suggest that these labelled neurones are likely to have been generated by undifferentiated precursors, and that the absence of "mitotic figures" in neurones may not be sufficient to rule out neurogenesis entirely (Altman 1962). Over a decade later, Michael Kaplan also documented the presence of adult neurogenesis in the hippocampus and olfactory bulb, this time proving the neuronal nature of the labelled cells using electron microscopy. Unlike Altman, Kaplan suggested the existence of dividing neurones (Kaplan and Hinds 1977). His work was therefore received by the scientific community with considerable scepticism, since the notion of mature neurones undergoing mitosis did not seem feasible (Kempermann 2006). Despite continued reports of adult neurogenesis in rodents, cats, and songbirds throughout the 60's, 70's and 80's (Altman 1962; Altman 1963; Altman and Das 1965; Altman 1969; Kaplan and Hinds 1977; Goldman and Nottebohm 1983; Alvarez-Buylla and Nottebohm 1988), little progress was made in establishing this radical concept as also applying to primates and humans (Rakic 1985). The pivotal point in the history of adult neurogenesis came about during the 1990s, an era

coined “the decade of the brain”, when newborn neurones were identified in the dentate gyrus of cancer patients (Eriksson et al. 1998). Coupled with isolation and characterisation of adult NS cells (Reynolds and Weiss 1992; Gage et al. 1995), the concept of ongoing neurogenesis in the mammalian brain was finally acknowledged and accepted as scientific fact.

1.1.2 Neurogenic regions of the adult CNS: Subventricular zone and Hippocampus

The subventricular zone (SVZ) of the lateral ventricles and the subgranular zone (SGZ) of the dentate gyrus (DG) of the hippocampus are now recognised as the two neurogenic regions of the adult CNS. Of the two compartments, the SVZ is by far the most mitotically active (Abrous et al. 2005) and houses four different types of cells: SVZ astrocytes (type B cells), transient amplifying progenitors (type C cells), migrating neuroblasts (type A cells), and multi-ciliated ependymal cells (type E cells) (Figure 1.1). The SVZ astrocyte, currently believed to be the resident stem cell of this neurogenic region, slowly divides to give rise to transient amplifying progenitors. These daughter cells undergo rapid proliferation to generate neuroblasts, which leave the SVZ and migrate tangentially to the olfactory bulb (OB) via the rostral migratory stream (RMS). Employing a unique mode of migration, SVZ-derived neuroblasts migrate collectively in chains through a channel (glial tube) formed by astrocytes (Figure 1). Upon reaching the OB, neuroblasts leave the glial tube and migrate radially to their eventual destination, where they differentiate into granule and periglomerular interneurones, and integrate into the existing neural circuitry (Doetsch et al. 1997). Each of the different SVZ cells types can be distinguished by their distinctive morphology, behaviour, location, and expression of markers. For example, type B cells express astrocytic marker glial fibrilliary acidic protein (GFAP) (Bignami and Dahl 1974), neural precursor marker vimentin (Cochard and Paulin 1984; Alvarez-Buylla et al. 1987; Sancho-Tello et al. 1995), have a stellate morphology, and divide asymmetrically (Doetsch et al. 1997). Migratory neuroblasts on the other hand can be identified by their expression of PSA-NCAM, a cell adhesion molecule commonly expressed in regions of neuronal plasticity (Rousselot et al. 1995); neuron specific β tubulin (β lll tubulin), a marker of immature neurones (Easter et al. 1993); doublecortin (DCX), a microtubule

associated protein expressed by migrating neurones during embryonic and postnatal development (Gleeson et al. 1999; Yang et al. 2004; Koizumi et al. 2006; Ocbina et al. 2006); and Dlx2, a transcription factor known to be involved in the development of GABAergic neurones (Porteus et al. 1994; Doetsch et al. 2002; Panganiban and Rubenstein 2002). Neuroblasts typically have an elongated cell body with either a single leading process or bipolar morphology, and can undergo limited cell division (Doetsch et al. 1997). Transient amplifying progenitors express Dlx2 (Doetsch et al. 2002), as well as pro-neural transcription factor Mash1 (Casarosa et al. 1999; Horton et al. 1999; Parras et al. 2004). They are the most proliferative cells of the SVZ, dividing symmetrically at a rate 10 times greater than that of type B cells, and are found in clusters scattered along the tangential network of neuroblasts in the SVZ, but are absent in the RMS (Doetsch et al. 1997).

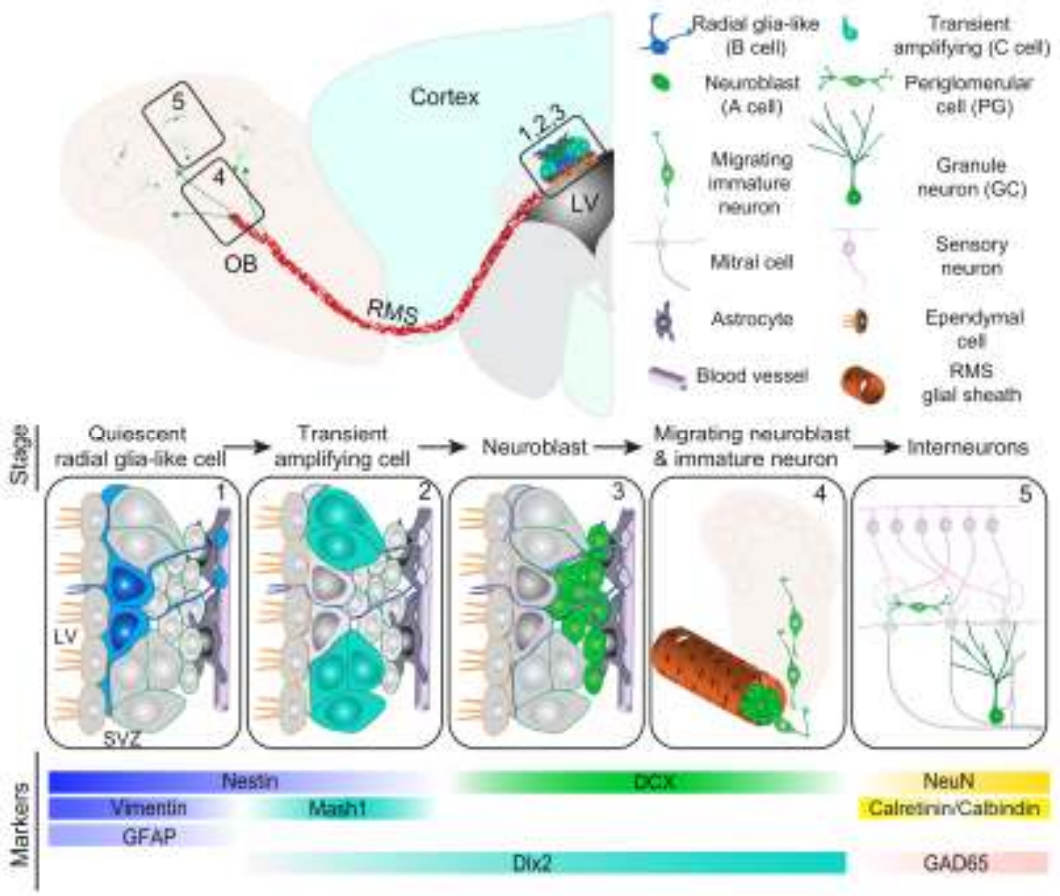

Figure 1.1: Neurogenesis in the adult SVZ. A schematic diagram of a sagittal cross section of a rodent brain showing the migratory path undertaken by neuroblasts from the SVZ to the OB (top left), the cell types found in the SVZ/RMS/OB (top right), different stages in SVZ neurogenesis (middle), and markers expressed by different neuronal lineages (bottom). Adapted from Ming and Song (2011).

The second neurogenic region of the adult brain, the subgranular zone (SGZ), is located at the border between the granule cell layer (GCL) and hilus of the dentate gyrus of the hippocampus (Abrous et al. 2005) (Figure 1.2). In the SGZ a specialised astrocyte, which extends a radial process through the GCL and contacts the molecular layer (ML), has been identified as the stem cell of this region. These radial astrocytes (type B cells) give rise to rapidly dividing transient amplifying progenitors (type D cells), which in turn generate neuroblasts (Seri et al. 2001; Seri et al. 2004). Unlike SVZ-derived neuroblasts, those originating in the SGZ do not undergo extensive tangential migration. Instead, neuroblasts of the SGZ move radially into the adjacent GCL as they differentiate and mature into mostly glutamatergic dentate granule cells. These newly formed neurones extend dendrites into the ML and axons into the CA3 region of the hippocampus, forming synaptic connections with resident cells (Ehninger and Kempermann 2008).

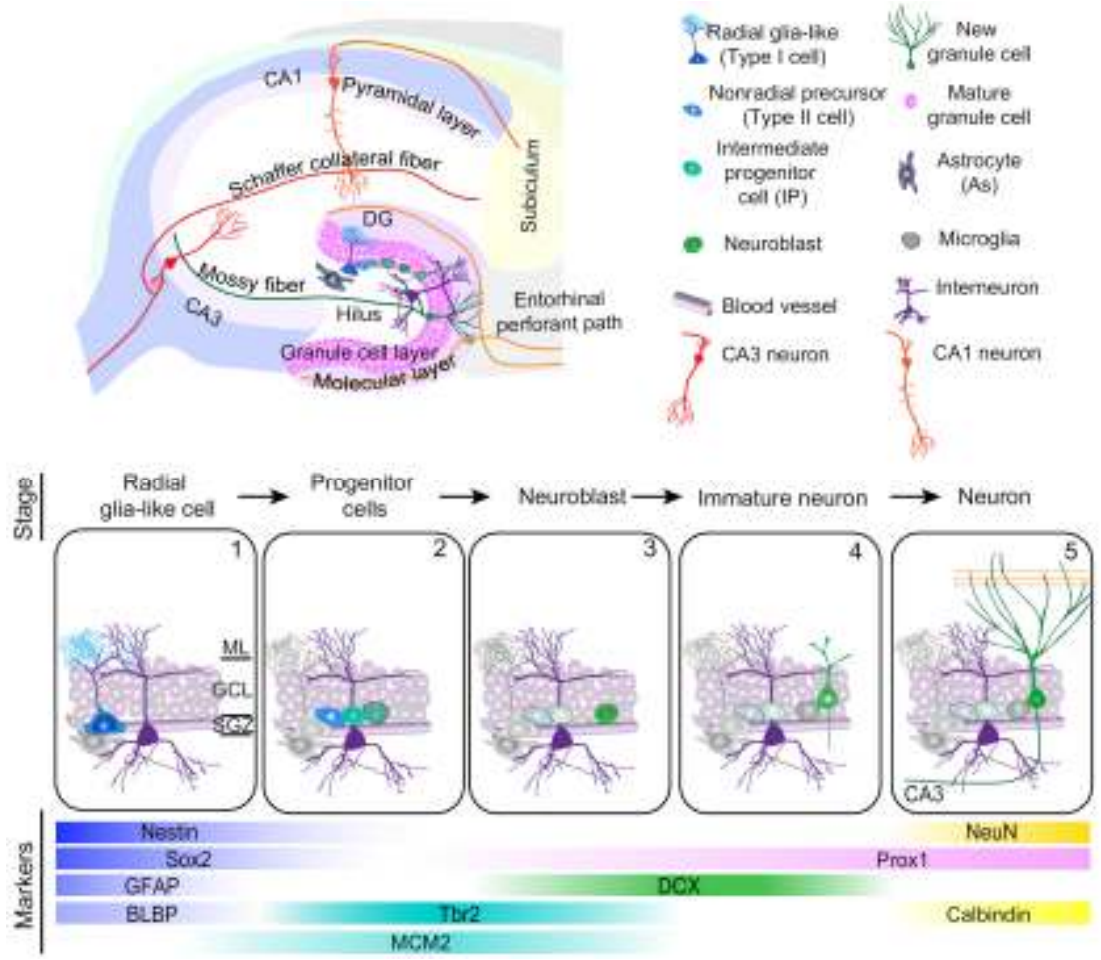

Figure 1.2: Neurogenesis in the adult hippocampus. A sagittal cross section of the rodent hippocampus showing the neurogenic niche in the dentate gyrus (top left), the different cells types in this region (top right), stages of neurogenesis in the DG (middle), and markers expressed by different cell types (bottom). Adapted from Ming and Song (2011).

1.1.3 SVZ neurogenesis

The identity of the adult SVZ neural stem cell

Adult NS cells, like their embryonic counterpart, are multipotent cells capable of giving rise to all three constituents of the CNS: neurones, astrocytes and oligodendrocytes. Unlike the NS cells of the developing brain, which undergo rapid cell division to give rise to the entire nervous system, it appears that those residing in the adult CNS are relatively quiescent. Progenitor cells, the offspring of NS cells, although more proliferative than their predecessors, are more limited in terms of their capacity for self-renewal and differentiation (Doetsch et al. 1997). One of the greatest challenges in the field of NS cell research, has been uncovering the nature of the adult NS cell. The lack of specific markers has been a significant drawback which has hindered progress in this area of research, and led to much debate over the identity of these cells.

Based on the known dormant nature and multipotency of adult NS cells, transient amplifying progenitors and proliferating neuroblasts were ruled out early on as potential candidates. This left the SVZ astrocyte and ependymal cell as the main contenders for this role. Initially, ependymal cells were suggested as the source of newly generated neurones in the SVZ (Johansson et al. 1999). This assumption was based on incorporation of BrdU by cells in the ependymal layer, and *in vitro* studies demonstrating self-renewal and multipotency of isolated ependymal cells. However, not long after the publication of these results, contradictory evidence questioning the proliferative ability of ependymal cells came to light. Doetsch et al. (1999) demonstrated that the NS cell of this region is in fact a specialised astrocyte. Here, the authors show using electron microscopy, that BrdU-incorporating cells in the SVZ are in fact astrocytes and not ependymal cells. Proliferating astrocytes were found to reside close to the ventricular wall, and easily mistaken for being in the ependymal layer when viewed by light microscopy alone. Compelling evidence, which include selective ablation and fate mapping studies performed in transgenic mice (Imura et al. 2003; Morshead et al. 2003; Garcia et al. 2004), now point to GFAP expressing SVZ astrocytes as the main source of neurones in the adult OB.

On the origin of adult NS cells

In the developing mammalian brain, NS cells correspond to neuroepithelium-derived radial glia (RG) found in the ventricular zone (VZ). During the neurogenic phase of development, RG proliferate asymmetrically to self-renew and generate a lineage-restricted neural intermediate progenitor cell (nIPC) or differentiated neuron (Kriegstein and Alvarez-Buylla 2009). The embryonic SVZ is now also acknowledged as a major site of neurogenesis (Noctor et al. 2004). Here, RG-derived nIPCs proliferate symmetrically to either expand the progenitor population or generate neurones. This raises the important question, as to whether NS cells residing in the adult SVZ (B cells) are direct descendents of ventricular zone RG, or nIPCs of the embryonic SVZ.

Early studies of mammalian CNS development had indicated that the VZ is lost following birth, with RG differentiating into astrocytes or ependymal cells that line the ventricle (Schmechel and Rakic 1979; Voigt 1989). Thus, nIPCs of the embryonic SVZ were thought to be a likely source of adult NS cells. However, recent data in which the cytoarchitecture of the SVZ was examined in detail, revealed that a subtype of B cell (B1) resides immediately beneath ependymal cells and makes direct contact with the ventricles through an apical process (Mirzadeh et al. 2008). Also, in some instances, rather than extending an apical process, part of the B1 cell body itself was found squeezed between ependymal cells, making direct contact with the ventricle. Interestingly, the presence of these B1 apical processes causes a conformational change in the surrounding ependymal cells, resulting in a formation resembling a pinwheel, with the B1 process at its centre. Ventricle contacting B1 cells were found only in neurogenic regions and were found to divide asymmetrically. The authors also describe for the first time, a basal process arising from B1 cells which wrap around chains of neuroblasts, continue for several hundred μm along the chains, and eventually terminate on blood vessels. These observations draw remarkable similarities to RG which also possess a short ventricle contacting apical process, a long basal process extending to the pial surface, and specialised endfeet terminating on blood vessels (Takahashi et al. 1990; Mission et al. 1991). Thus, it appears that the adult NS cell provides a

supportive structure for neuroblast migration in a similar manner to which RG provide a migratory scaffold for newborn neurones in development. In stark contrast, nIPC of the embryonic SVZ are multipolar cells that have no contact with the ventricle, divide symmetrically, and have no role as a migratory scaffold (Haubensak et al. 2004). Furthermore, during proliferation, B1 cells display evidence of interkinetic nuclear migration (INM) (Tramontin et al. 2003), a characteristic feature of RG cells in which the nucleus travels back and forth in response to cell cycle progression (Kosodo 2012). In light of these data, the concept that the ventricular zone ceases to exist in the adult may need to be revised. Instead, there is an accumulation of evidence pointing to the existence of a modified ventricular zone containing RG-derived adult NS cells.

The neurogenic niche

Although stem cells have been shown to exist throughout the CNS, only those that reside in the SVZ and SGZ appear to be involved in neurogenesis in the adult (Gould 2007). Interestingly, transplantation of SGZ astrocytes induces neurogenesis in conventionally non-neurogenic regions of the CNS, as well as from differentiated neurones in culture (Alexanian and Kurpad 2005; Jiao and Chen 2008). Moreover, SGZ precursors transplanted into the RMS differentiate into tyrosine hydroxylase-positive interneurones in the OB (Suhonen et al. 1996). Thus it appears that neurogenic regions of the CNS house a specialised niche that not only permits stem cell proliferation, but also instructs resident and transplanted precursors to take on a specific neuronal fate (Gage 2000).

One of the unique features of the neurogenic niche is the extensive interaction between different populations of resident cells (Doetsch et al. 1997) (Figure 1.3). Astrocytes in particular, which contain multiple processes that make contact with all neighbouring cells, and are extensively coupled via gap junctions, are well adapted to receive and translate signals from cells in the germinal region. The processes of astrocytes have also been known to occasionally extend between ependymal cells, and make direct contact with the lateral ventricles, thereby allowing the capture of factors secreted by the choroid plexus (Doetsch et al. 1999;

Doetsch 2003; Mirzadeh et al. 2008). In addition, astrocytes isolated from the neurogenic regions are able to promote proliferation of neural precursors as well as direct their differentiation into a neural fate. This property is absent from astrocytes of non-neurogenic sites, and therefore appears to be essential for the creation of the neurogenic niche (Lim and Alvarez-Buylla 1999; Song et al. 2002). The ependymal cells also promote lineage restriction to a neural fate by secreting noggin, an antagonist of gliogenesis inducing molecule bone morphogenetic protein (BMP) (Lim et al. 2000).

Another notable feature of the SVZ and SGZ is the close physical association between endothelial cells and neural precursors. Mature endothelial cells secrete mitogens and survival factors that influence the survival and differentiation of both groups of precursors (Leventhal et al. 1999; Palmer et al. 2000; Yang et al. 2011). This suggests that neurogenesis and angiogenesis may be co-regulated to some extent. In support of this hypothesis, disruption of the neuro-angiogenic relationship by radiation, results in the cessation of neurogenesis and the differentiation of remaining precursors into a glial fate. The fact that irradiated neural precursors form neurones, when grown in culture, suggests that the absence of neurogenesis arises from the disruption of the microvasculature, and is not due to alterations in the properties of the stem cells (Monje et al. 2002).

An additional feature of the SVZ is the presence of a specialised basal lamina (mats of extracellular matrix) which extends from the blood vessels, makes contact with all cell types in the region, and terminates in bulbs near the ependymal cell layer (Mercier et al. 2002). In peripheral organs such as the liver, bone marrow, and mammary glands, the basal lamina is an essential component of the microenvironment that is required for cell proliferation, migration, and differentiation (Kruegel and Miosge 2010). Similarly, in the SVZ the basal lamina forms an integral part of the extracellular matrix (ECM) and is believed to anchor cells as well as sequester factors - such as laminins, tenascin-C, collagen-1, heparan sulphate proteoglycans, and chondroitin sulphate proteoglycans - that regulate the migration and proliferation of neural precursors (Gates et al. 1995; Jankovski and

Sotelo 1996; Jacques et al. 1998; Kerever et al. 2007; Mercier and Arikawa-Hirasawa 2012). Recent studies have shown that SVZ NS cells upregulate their expression of laminin receptor α6β1 integrin when they are stimulated to become mitotically active (Kazanis et al. 2010). Thus, interaction with the ECM appears to be a crucial event in the regulation of SVZ neurogenesis.

The neurogenic zones of the CNS are structurally unique. The resident cells and the peculiar architecture of these regions results in the creation of a specialised niche that is permissive of neurogenesis. Thus, measures undertaken to comprehend the role of this complex environment, will heighten our understanding of the factors that are essential for neurogenesis, and assist in developing effective transplantation techniques.

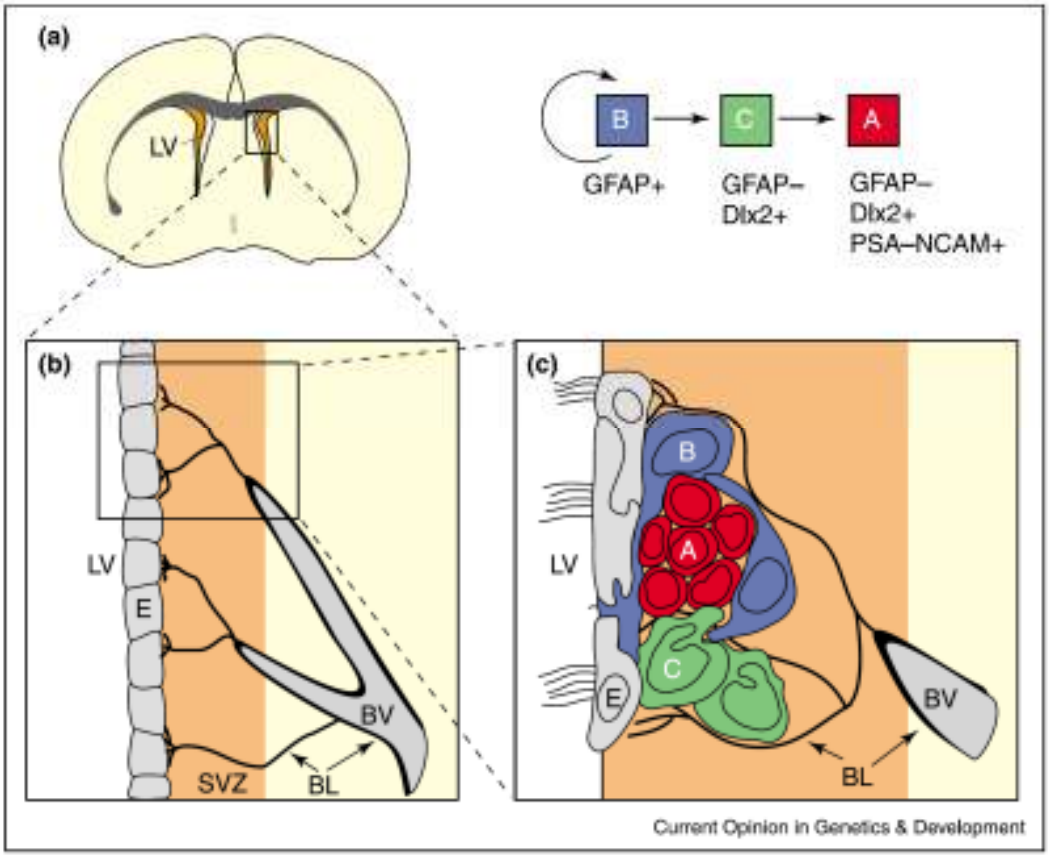

Figure 1.3: The neurogenic niche of the adult SVZ. A diagram showing the organisation of the ependymal cells (E), astrocytes (B), neural progenitors (C) and migrating neuroblasts (A) in relation to the lateral ventricles (LV), blood vessels (BV), and basal lamina (BL) in the SVZ. Taken from Doetsch (2003).

1.1.4 The structure and cell types of the OB

A single odorant receptor, from a family of over 1000 subtypes, is expressed by each olfactory sensory neurone (OSN) in the nasal epithelium (Buck and Axel 1991). Groups of OSNs expressing the same receptor converge onto one glomerulus, which contains the axonal terminals of mitral cells and tufted cells that project to the olfactory cortex (Shepherd 1972) (Figure 1.4). Neuronal activity in the OB is tightly regulated by two populations of inhibitory interneurones - periglomerular cells (PGC) and granule cells (GC) - that are replenished throughout adulthood (Lledo et al. 2008). Two morphologically distinct subtypes of GCs (deep and superficial) make dendrodendritic synapses with projection neurones in the external plexiform layer (EPL). Deep GCs project into the deep lamina of the EPL synapsing with mitral cells, whereas superficial GCs project into the superficial lamina of the EPL and contact tufted cells (Orona et al. 1983). PGCs on the other hand are found within the glomerular layer and can synapse with cells within a single glomerulus or from different glomeruli. They can be classified into three subtypes based on their expression of tyrosine hydroxylase (TH), calbindin, or calretinin (Parrish-Aungst et al. 2007). The majority of newly generated neurones in the adult OB are GABAergic granule cells, with a small percentage (1-25%) differentiating into either GABAergic or dopaminergic periglomerular cells (Luskin 1998; Petreanu and Alvarez-Buylla 2002). Interneuron identity in the OB is regulated both temporally and spatially. For example, TH+ and calbindin+ PGC production is greatest during embryogenesis and declines postnatally, whilst calretinin+ GC and PGC generation increases (Batista-Brito et al. 2008). Also, dorsal regions of the adult SVZ have been shown to give rise to primarily superficial GC and TH+ PGC, whereas ventral regions generate mostly deep GC and Calbindin+ PGC (Young et al. 2007). The majority of calretinin+ neurones are generated from an embryonic cortex-derived region of the adult SVZ (Young et al. 2007). Interestingly, SVZ precursors from specific regions continue to generate the same subtypes of interneurones when cultured *in vitro* or grafted heterotopically (Merkle et al. 2007). Thus, the production of specific interneurones by adult NS cells is an intrinsic property determined by the region of origin in the SVZ, and is independent of environmental influences.

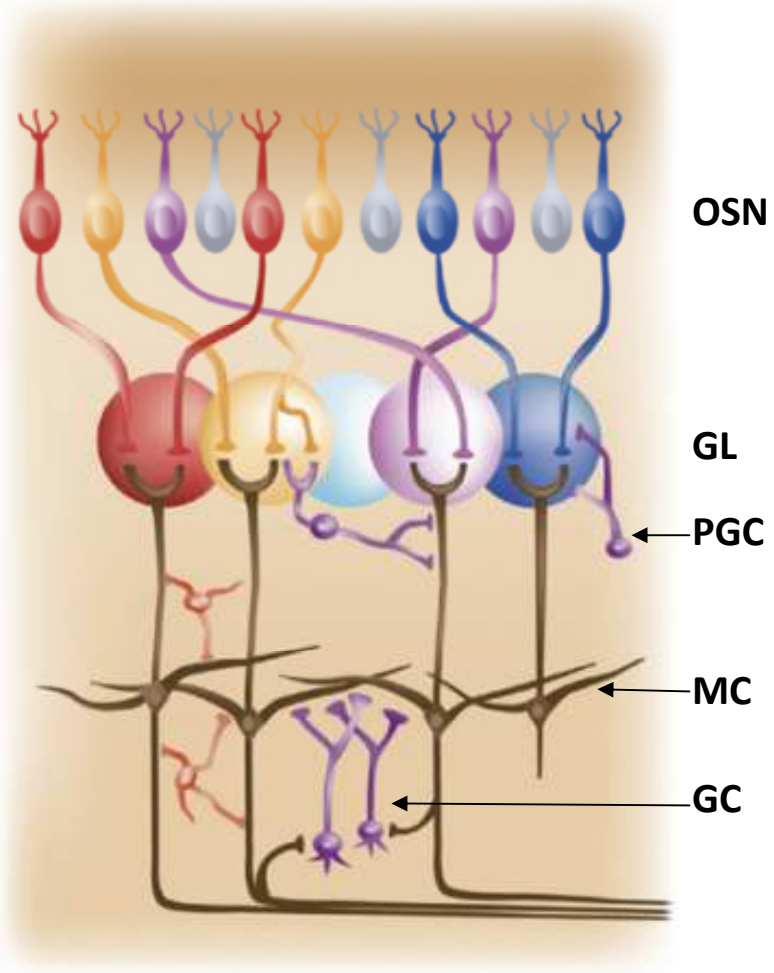

Figure 1.4: Structure of the olfactory bulb neural circuit. Olfactory sensory neurones (OSN) in the olfactory epithelium that express a particular odorant receptor project onto one or more glomeruli (GL). The two types of SVZ derived interneurones, periglomerular cells (PGC) and granule cells (GC), are shown in purple. PGC synapse with cells within a glomerulus or between glomeruli whilst GC form dendrodentritic synapses with Mitral cells (MC) that project to the olfactory cortex. Adapted from Lledo et al. (2008)

1.1.5 The function of adult SVZ neurogenesis

Adult neurogenesis in the SVZ produces a surplus of neurones destined for the OB. Following arrival and maturation in the OB, almost 50% of newborn neurones are eliminated from the bulbar circuit within 45 days from birth, in an activity dependent manner (Petreanu and Alvarez-Buylla 2002). Even fewer cells (10%) survive within a year (Winner et al. 2002). The exact role of this continual replacement of interneurones and refinement of its circuits on OB function is still not fully understood. Currently, an overwhelming number of publications investigating the function of adult neurogenesis and reporting numerous olfactory deficits, often contradictory to one another, has led to much confusion over the real function of newborn olfactory neurones in adulthood. Changes in response to predator odours and olfaction dependent sexual behaviour (Sakamoto et al. 2011); diminished fear responses to conditioned odours (Valley et al. 2009); reduced short-term olfactory memory only (Breton-Provencher et al. 2009; Sultan et al. 2010); reduced long-term olfactory memory only (Lazarini et al. 2009); and increased survival of newborn neurones in odour rich environments (Rochefort et al. 2002) are amongst the list of attributes currently ascribed to adult neurogenesis. More recently, a study in which selective activation of adult born interneurones was paired with an odour discrimination task, revealed that high frequency activation of adult born interneurones facilitates learning and improves memory (Alonso et al. 2012). Here, the authors used injection of a lentiviral vector encoding channel rhodopsin-YFP (yellow fluorescent protein) under the control of the synapsin 1 promoter and a miniature LED implanted over the dorsal bulb to specifically label and activate adult born interneurones. Interestingly, activation of early postnatal born interneurones had no effect on learning of difficult tasks, implying that adult born OB neurones have a specific role in fine tuning recognition of odours (Alonso et al. 2012). Similarly, another group showed increased survival of newborn inhibitory neurones following learning of odour discrimination tasks, with learning being delayed if neurogenesis was inhibited before or after the training period (Moreno et al. 2009).

Differences in the techniques used to inhibit neurogenesis, variations in the behavioural tests used to assess olfactory behaviour, as well as the specific behaviour being examined may account for the different conclusions drawn from these studies. In addition, it is worthy to note that most of these studies look at global activation or elimination of a heterogenous population of olfactory neurones. Whether each subtype of newborn neurone contributes to a distinctive olfactory function is yet to be examined, and may shed some light on this issue.

1.1.6 Evidence of SVZ neurogenesis in the human brain

Despite numerous reports of ongoing neurogenesis in the mammalian and non-human primate brains (Altman and Das 1965; Altman 1969; Morest 1970; Kaplan and Hinds 1977; Goldman and Nottebohm 1983; Alvarez-Buylla and Nottebohm 1988; Eriksson et al. 1998; Pencea et al. 2001; Sawamoto et al. 2011), the existence of active neurogenic regions in the adult human brain remains a topic of controversy. In 1998 Eriksson et al. (1998), described for the first time, the existence of neurogenesis in the hippocampus of adult human brains. In this study, post-mortem analysis of cancer patients, who had received BrdU as part of their therapy, showed incorporation of BrdU by neurones in the hippocampus. Before long, similar reports of neurogenesis in the SVZ, and anatomical descriptions of the human RMS were also published (Curtis et al. 2007). Here, the authors demonstrated the presence of dividing neural progenitors in the SVZ, and described the existence of an RMS organised around a ventricular extension, which takes a ventro-caudal route before joining the olfactory tract. However, a recent study examining neurogenesis in human brains, from ages 1 week to 84 years, shows a steep decline in neurogenic potential with age (Sanai et al. 2011). The infant SVZ (up to 6 months) was found to contain chains of migrating neuroblasts that converge to form a prominent RMS extending to the olfactory peduncle. Similar to rodents, neuroblast chains were encased by glial tubes and were closely associated with blood vessels. However, between the ages of 6 - 18 months, a steady decline in neurogenesis results in the loss of migratory neuroblasts and the formation of a hypocellular gap in the region once occupied by the SVZ. Importantly, no evidence of chain migration was observed in the SVZ or RMS of adults or children over 2

years, though single or pairs of migratory neuroblasts were found occasionally. This limited neurogenic capacity of the adult human brain was also demonstrated in another study using post-mortem human tissue and a novel technique measuring ^{14}C levels in DNA to assess the age of OB neurones (Spalding et al. 2005; Bhardwaj et al. 2006). This study suggests that all OB neurones may be produced at around the time of birth. However, the authors also emphasise the limitations of their method, which may not be sensitive enough to detect potential low levels of neurogenesis in adulthood. In addition, data from rodent studies suggests that unlike OB neurones born during development, those born in adulthood do not survive long-term, but are continually replaced (Winner et al. 2002). Coupled with the information that neurogenesis also declines with age (Sanai et al. 2011), it is not altogether surprising that only neurones formed at birth could be detected in this study.

Though neurogenesis has been shown to be extremely restricted in the adult human brain, the existence of even limited neurogenesis itself is a monumental leap from the once held belief that "the nerve paths are something fixed, ended and immutable"(May 1991). Moreover, evidence of proliferation and recruitment of neural progenitors in humans following CNS injury, raises the possibility of activating a typically dormant system to aid neuronal repair (Arvidsson et al. 2002; Jin et al. 2006; Martino and Pluchino 2006; Sohur et al. 2006; Ekonomou et al. 2011; Ekonomou et al. 2012). Though we are far from achieving this somewhat ambitious task, detailed research of the individual stages of neurogenesis - proliferation, migration, and differentiation – is essential for progress in this field.

1.2 Neuronal migration

1.2.1 Neuronal migration in the developing CNS

The migration of cells in response to extracellular cues is a highly regulated process that is fundamental to the evolution, development, and maintenance of multi-cellular organisms (Wedlich 2005). This complex interplay between cells and their environment is nowhere more apparent than in the central nervous system (CNS). During mammalian brain development, neural precursors migrate from their point of origin to their eventual residence via one of two distinct forms of migration: radial (in a direction perpendicular to the surface of the brain) and tangential (in a direction parallel to the surface of the brain) (Park et al. 2002). Both forms of migration are particularly evident during corticogenesis. In the early stages of cortical development, when the cerebral wall is relatively thin, neurones that give rise to the plexiform layer or preplate, undergo a form of radial migration known as nuclear translocation. In this mode of migration, terminally differentiated neurones that initially contact both the ventricular and pial surfaces lose contact with the ventricle and translocate their soma towards the pial surfaces. (Nadarajah et al. 2001; Nadarajah et al. 2003). The subsequent group of migrating neuroblasts also use nuclear translocation to invade the plexiform layer, splitting it into the subplate and marginal zone, and giving rise to the first layer of glutamatergic projection neurones (pyramidal neurones) in the cortical plate (Gupta et al. 2002). As the size of the cerebral wall increases, neuroblasts are no longer able to translocate across the rapidly expanding width of the neocortex (Nadarajah et al. 2003). Thus, an alternative form of radial migration, known as locomotion, is adopted by precursors in the latter stages of corticogenesis. Neurones that migrate by locomotion crawl along a glial scaffold formed by the processes of radial glia which extend from the ventricular zone to the pial membrane. Each wave of migrating neurones, travel past the existing layers, thus generating the six layers of the neocortex in an inside-out manner (Figure 1.5) (Hatten 1999; Nadarajah et al. 2001; Kanatani et al. 2005).

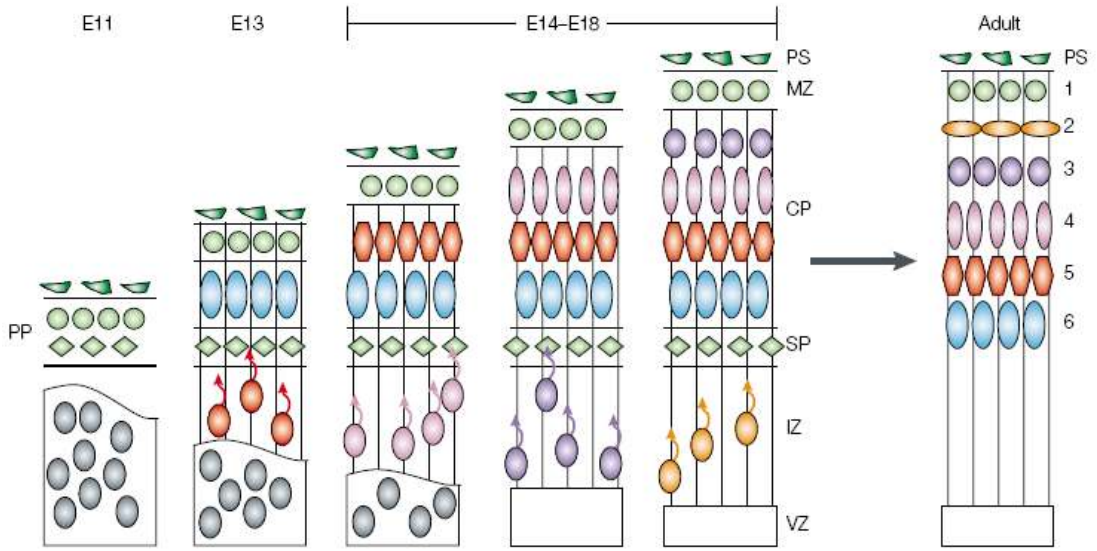

Figure 1.5: Formation of the six layers of the neocortex by radially migrating cells. A schematic diagram showing the formation of the six layers of the neocortex during mammalian brain development. By embryonic day 11 (E11), the first wave of neuroblasts have migrated from the ventricular zone (VZ) to the pial surface (PS) forming the preplate (PP). At E13, the PP has been split into the marginal zone (MZ) and subplate (SP) by a second wave of migrating neuroblasts. During E14 to E18, the remaining layers of the cortical plate are generated in an inside-out manner by neuroblasts migrating along the processes of glia (vertical lines). In the adult, the SP degenerates to leave behind a six layered neocortex. Adapted from Gupta et al. (2002).

Although the majority of neurones in the developing cortex undergo radial migration, a small pool of tangentially migrating neurones have also been described in corticogenesis (Austin and Cepko 1990; Walsh and Cepko 1992; Reid et al. 1995). It is now believed that nearly all GABAergic interneurones of the cortex are derived from tangentially migrating neurones born from precursors in the subpallial telencephalon (Anderson et al. 1997; Stuhmer et al. 2002). Several proliferative zones in this region, which include the lateral ganglionic eminence (LGE), medial ganglionic eminence (MGE) and anterior entopeduncular area (AEP), all give rise to populations of neurones with distinct migratory routes that are spatially and temporally regulated (Marin and Rubenstein 2001) (Figure 1.6). Unlike radially migrating neurones of the cortical plate, tangentially migrating interneurones move independently of a glial scaffold (O'Rourke et al. 1995). Exactly how these cells are guided via multiple tangential pathways to distinct CNS regions is still unclear, though there is some evidence to suggest that axons of other neurones may act as a physical guide (Metin et al. 2000).

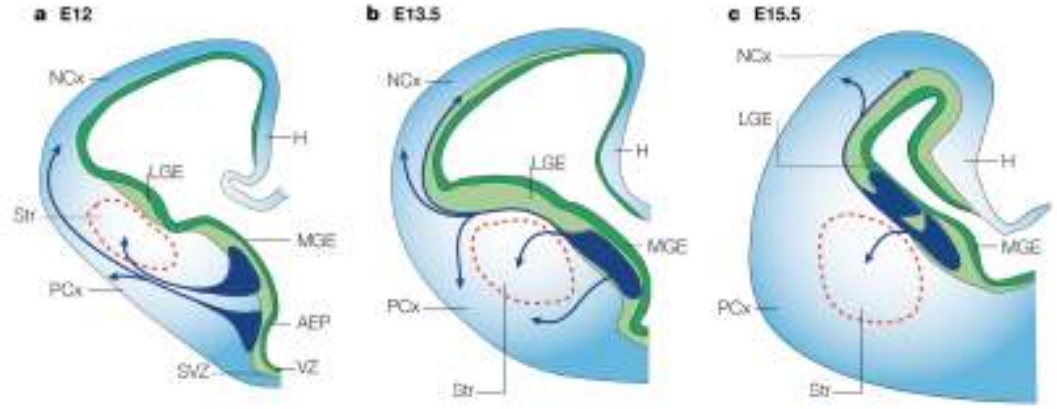

Figure 1.6: Tangential migration by precursors of the subcortical telencephalon during corticogenesis. A schematic diagram of transverse sections of an embryonic telencephalon showing the routes of tangential migration undertaken by neurones of the subcortical telencephalon at embryonic day 12 (a), 13.5 (b) and 15.5 (c). AEP, anterior entopeduncular area; H, hippocampus; LGE, lateral ganglionic eminence; MGE, medial ganglionic eminence; NCx, neocortex; PCx, piriform cortex; Str, striatum; SVZ, subventricular zone; VZ, ventricular zone. Adapted from Marin and Rubenstein (2001).

1.2.2 Neuronal migration in the adult CNS

Long-distance tangential migration of neural precursors in the adult brain is restricted to the subventricular zone of the lateral ventricles, one of two sites known to accommodate ongoing neurogenesis (Luskin 1993; Lois and Alvarez-Buylla 1994). Within the SVZ, running parallel to the walls of the lateral ventricles exist a network of interconnected tangential chains composed of migratory neuroblasts encased by a tube formed by the processes of SVZ astrocytes. These migratory chains of cells can vary in their thickness from just a single line of neuroblasts to thick bundles formed of 10 or more cells (Doetsch and Alvarez-Buylla 1996; Doetsch et al. 1997). As they approach the anterior horn, the majority of chains converge to form the rostral migratory stream (RMS), a highly restricted path running from the SVZ to the olfactory bulb (OB) (Doetsch and Alvarez-Buylla 1996). Migratory neuroblasts are mostly unipolar, having a characteristic elongated cell body and a single leading process tipped with a dynamic lamellipodium. Occasionally they may also have a trailing process or display bipolar morphology (Nam et al. 2007). Neuroblasts move towards the bulb using a unique form of collective migration, whereby the cells in a chain slide over one another (Lois et al. 1996). Despite the presence of a glial tube extending from the SVZ to the entrance of the OB, current evidence suggests that this structure is not required to guide neuroblasts along the stream (Wichterle et al. 1997; Law et al. 1999). Hence neuroblasts of the adult brain are capable of migrating between 4-8 mm through the complex environment of the adult CNS independently of a glial scaffold. It is most likely that a multitude of factors acting at different points along the RMS are required to guide neuroblast along this highly restricted path. Over the last decade a considerable effort has been made to uncover these mechanisms and a picture of how neuroblasts are regulated along the stream is slowly beginning to emerge (discussed in depth in Section 1.3).

Similar to the developing brain, radial migration of neurones also persist in the adult. Upon reaching the OB, neuroblasts exit the glial tube, detach from the RMS chain, and migrate radially as single cells into the layers of the bulb (Alvarez-Buylla 1997; Luskin 1998; Carleton et al. 2003). Although much of the research on

neuroblast migration in the adult CNS has focused primarily on tangential migration in the stream, there is an increasing amount of work investigating the transition from tangential to radial migration and the cues that direct neurones to their final position in the layers of the bulb. Hack et al. (2002) recently showed that reelin, a secreted extracellular matrix protein, acts as a detachment signal. Reelin was found to be expressed in an increasing gradient from the granule cell to the mitral cell layer and was absent in the RMS. Most notably, addition of reelin to explants cultures induced neuroblasts to migrate as single cells rather than in chains, whilst an accumulation of precursors was observed in the entrance to the OB in the *reeler* mouse (transgenic mouse line deficient of reelin). Similarly tenascin-R, another ECM protein, is also exclusively expressed in the granule and plexiform layers of the OB and induced detachment of neuroblasts from chains *in vitro* (Saghatelyan et al. 2004). In addition to promoting single cell migration, tenascin-R was also found to behave as a chemoattractant, since ectopic expression of the protein re-routed neuroblasts away from the RMS and towards these sites. Furthermore, the expression of tenascin-R was found to be activity-dependent since odour deprivation caused a significant reduction in expression of the protein and a subsequent reduction in BrdU labelled neuroblasts being recruited to the bulb (Saghatelyan et al. 2004). Thus, in addition to promoting detachment and providing directional guidance, activity-dependent regulation of tenascin-R expression may be a mechanism of regulating neuroblast recruitment to the OB. More recently, prokineticin 2, a diffusible secreted protein that acts via G-protein coupled receptors, has also been proposed as both a detachment signal and chemoattractant in the OB (Ng et al. 2005).

1.2.3 Pathological influences on neuronal migration in the adult SVZ

A remarkable feature of SVZ neuroblasts is that they can be recruited away from their native migratory path to sites of injury or degeneration in the CNS. For example, in the R6/2 mouse and quinolinic acid lesion rat models of Huntington's disease, which is characterised by neurodegeneration of GABAergic medium spiny neurones in the striatum, proliferation of NS cells in the SVZ is increased. Moreover, in these models, SVZ NS cell-derived neuroblasts migrate into the striatum and

differentiate into neurones (Tattersfield et al. 2004; Batista et al. 2006). Similarly in the 6-hydroxydopamine lesion induced model of Parkinson's disease, neuroblasts were recruited into the adjacent striatum (Winner et al. 2008). Multiple observations of compensatory neurogenesis and long-distance migration of SVZ neuroblasts to areas of focal ischaemia have also been documented in rodent models of stroke (Nakatomi et al. 2002; Zhang et al. 2004; Ohab et al. 2006; Massouh and Saghatelyan 2010). Studies investigating the specific mediators that divert neural precursors to sites of pathological insult showed that brain derived neurotrophic factor (BDNF), caused progenitor cell expansion as well as recruitment of new neurones into the neostriatum when infused into the CNS or expressed after adenoviral transfection (Benraiss et al. 2001). In addition, there is now a body of evidence to suggest that chemotactic factors, such as stromal-derived factor (SDF-1), and angiopoietin 1 (Ang1) secreted by newly formed un-perfused branches of the vascular endothelium in the peri-infarct region, may recruit neuroblasts through activation of CXCR4 and Tie2 receptors respectively (Ohab et al. 2006; Robin et al. 2006; Thored et al. 2006). Interestingly, SDF-1 is also an important chemoattractant for migrating neurones in the developing brain (Stumm et al. 2003; Stumm and Hollt 2007), and thus implies that adult neural precursors have the potential to respond to guidance cues traditionally associated with development. Also, close examination of peri-infarct areas in models of stroke has revealed that newborn neuroblasts (BrdU/DCX^{+}) specifically associate with areas of active vascular re-modelling in this region (Ohab et al. 2006). Furthermore, inhibiting angiogenesis with endostatin caused a drastic reduction in stroke-induced recruitment of neuroblasts (Ohab et al. 2006). Hence, an association between neural and endothelial precursors appears to regulate NS cell proliferation in both the neurogenic niches of the SVZ and SGZ (Leventhal et al. 1999; Palmer et al. 2000; Doetsch 2003), as well as at sites of CNS injury, thus highlighting the importance of the relationship between angiogenesis and neurogenesis**.**

Whether SVZ NS cell proliferation and migration in response to CNS injury also occurs in humans, or is a unique feature of rodent brains has been an extensively discussed topic. Evidence from post-mortem analysis of human brains following

stroke has revealed both an increase in SVZ NS cell proliferation, as well as migration of SVZ neuroblasts to the infarct area, with some cells displaying markers of differentiated neurones (Jin et al. 2006; Ekonomou et al. 2011; Ekonomou et al. 2012). Thus, the adult human CNS is permissive to NS cell recruitment and neuronal replacement following injury, and contains an existing pool of NS cells which may be exploited in neuroregenerative strategies.

1.3 What's guiding neuroblast migration in the RMS?

The RMS is not an easy path to follow: it is a tortuous route that dips and curves steeply before reaching the OB. Yet neuroblasts along the stream adhere tightly to its constraints, never venturing beyond its boundaries. Given the restrictive nature of the RMS, it is highly unlikely that this form of long-distance migration is reliant on a single factor. Instead, research carried out during the last two decades, suggests the existence of multiple chemorepulsive, chemoattractive, motogenic, and physical guidance cues acting at different points along the stream to co-ordinate the migration of neuroblasts to their eventual destination in the bulb (Cayre et al. 2009; Leong and Turnley 2011). Here we review a comprehensive but not exhaustive list of the proposed guidance molecules recognised for their contribution to postnatal neuroblast migration. A detailed list of factors involved in RMS neuroblast migration can be found in Table 1.1 below.

1.3.1 Architectural guides

The flow of cerebrospinal fluid

The flow of cerebrospinal fluid (CSF) is now recognised as an important factor directing neuroblast migration in the SVZ (Sawamoto et al. 2006). Fluoroscopic imaging reveals that the orientation of ependymal cilia beating correlates with CSF flow, which runs rostrally along the dorsal section of the lateral ventricle before turning ventrally in the anterior SVZ (Sawamoto et al. 2006). The concentration of the chemorepellent Slit, which is secreted by the choroid plexus (CP) and septum and is known to repel SVZ neuroblasts (Wu et al. 1999; Nguyen-Ba-Charvet et al. 2004), was also found to be dictated by CSF flow, with the gradient becoming weaker rostrally. Interestingly, the orientation of neuroblasts was found to be determined specifically by the flow of CSF and not the relative position of the RMS or OB. For example, in the anterior SVZ neuroblasts are oriented ventrally, away from the RMS, but in line with CSF flow. Furthermore, disruption of cilia beating resulted in loss of the Slit concentration gradient, gross disorientation of neuroblasts in the SVZ, and significantly fewer neuroblasts entering the RMS (Sawamoto et al. 2006). However, once neuroblasts entered the stream, they

remained strictly oriented towards the bulb and migrated normally despite the loss of the chemorepulsive gradient, which suggests the existence of different guidance cues present in the SVZ and RMS. Thus, directed migration at the beginning of the stream is highly reliant on CP- and septum-derived chemorepulsive gradients created by the beating of ependymal cilia.

Astrocytes

Chains of migrating neuroblasts in the SVZ and RMS of the adult brain are encased within a glial tube formed by the processes of astrocytes (Lois et al. 1996). To date, the exact role of these astrocytes, as far as neuroblast migration is concerned, is still unclear. At first glance, it may appear as if the astrocytic tube may be responsible for the chain-like structure of migrating neuroblasts. However, the glial tube itself does not form until after P7 in mice, yet chain migration of neuroblasts is evident in the SVZ and RMS well before this period (Law et al. 1999; Peretto et al. 2005). In addition neuroblasts are able to migrate as chains *in vitro* in the absence of any glial scaffold (Wichterle et al. 1997; Ward and Rao 2005). Another possibility is that the vasculature may act as a physical barrier to contain migrating neuroblasts or concentrate signalling molecules. However, microscopic analysis shows that the ensheathing astrocytes do not form a continuous barrier, and the density of astrocytic processes is in fact greater within the RMS than around it, as would not be expected of a physical barrier (Whitman et al. 2009). Interestingly, the average speed of migrating neuroblast is greater in the glial tube containing adult RMS (31 μm/hour) than in the RMS of P5 mice (24 μm/hour) (Bovetti et al. 2007). One suggestion for this observed difference in migratory speed is that, in the absence of the astrocytic tunnel neuroblasts have to migrate through the extracellular matrix to reach the OB (Bovetti et al. 2007). Instead, formation of the astrocytic tube creates a path of low resistance, which may facilitate neuroblast migration and account for the perceived increase in speed. This theory is supported by the fact that inhibitors of matrix metalloproteinases (MMP), proteolytic enzymes that re-model the extracellular matrix (ECM), perturb neuroblast migration in the early postnatal brain, but not in the adult brain (Bovetti et al. 2007). This observation raises the question as to why neuroblasts need to increase their

migration speed at all if they are perfectly capable of migrating to the OB in the absence of a glial tube. One possibility is that, as the brain develops, the distance between the SVZ and OB becomes ever-greater. Thus faster migration speeds may be required to maintain the population of newborn neurones arriving at the bulb each day. Thus, greater speeds necessary for long distance migration in the adult brain may be achieved via the creation of a path of low resistance by astrocytes.

Vasculature

The vasculature within the RMS is highly organised. Unlike the rest of the CNS where blood vessels appear to be randomly arranged, in the RMS they run parallel to the direction of the stream and are considerably denser here than in the surrounding areas (Snapyan et al. 2009; Whitman et al. 2009). This organisation is unique to the adult RMS as it is absent in the embryonic brain, and only starts to emerge during the late stages of development (Nie et al. 2010). In the adult brain, neuroblasts form a close association with the vasculature, with the majority being less than 3 μm distance from a neighbouring blood vessel (Snapyan et al. 2009). Similarly, the processes of astrocytes are also closely associated, often forming a barrier between neuroblasts and endothelial cells (Whitman et al. 2009). The close association of migrating neuroblasts with the vasculature suggests several possibilities. One is that being in close proximity to blood vessels facilitates the supply of diffusible guidance signals, as well as oxygen and nutrients to support the high metabolic demand of migrating cells, or the vasculature itself acts as a physical guide to migrating neuroblasts. Time lapse imaging has revealed that neuroblasts do in fact use the vasculature as a scaffold, and can be seen migrating along blood vessels throughout the RMS. In addition, Snapyan et al. (2009) also demonstrated that endothelial cells in the RMS release BDNF, which enhances migration by activation of p75NTR on neuroblasts. Contrary to these findings, Nie et al. (2010) published data showing that proliferating cells in the RMS are juxtaposed to blood vessels, and proliferation not migration is reliant on the vasculature. However, it is important to note that whilst studies demonstrating migration of neuroblasts along blood vessels in the RMS were performed in adult brains (> 2months old), those performed by Nie et al. (2010) were done on P4 mice based on observations that

organisation of blood vessels in the RMS is complete by this stage. However, new evidence now suggests that the architecture of the vasculature in the RMS is re-modelled following the emergence of the glial tube, which does not take place until after P7 (Bozoyan et al. 2012). Secretion of vascular endothelial growth factor (VEGF) by glial tube astrocytes has now been shown to be important for the formation of the parallel arrangement of blood vessels characteristic of the adult RMS (Bozoyan et al. 2012). In addition, several studies have demonstrated that different modes of migration are utilised by neuroblasts before and after formation of the glial tube (Bovetti et al. 2007; Bozoyan et al. 2012), and that feedback mechanisms involving neuroblasts, astrocytes and endothelial cells may be important for this difference (Snapyan et al. 2009). Hence, failure to see vasculature guided migration of neuroblasts in P4 mice may be due to the difference in the glial-blood vessel architecture of the stream at this point in development, and does not rule out the vasculature as a migratory scaffold for neuroblasts in the adult brain.

1.3.2 Adhesion molecules

PSA-NCAM

Neural cell adhesion molecule (NCAM) is a homophilic receptor involved in cell-cell interactions and has been implicated in several developmental functions including axon guidance and neural crest cell migration (Doherty et al. 1990; Doherty et al. 1990; Bronner-Fraser et al. 1992). Post-translational modification of this molecule by the addition of polysialic acid (PSA) reduces its adhesiveness and is necessary for NCAM's role in regulating morphogenesis and cell migration in the developing CNS (Rutishauser et al. 1985). In the adult brain, the SVZ/RMS is one of few regions where PSA-NCAM expression persists. Here, it is exclusively expressed by migrating neuroblasts (Seki and Arai 1993). Interestingly, the RMS in NCAM-deficient mice still forms a continuous stream, and although less pronounced, migrating chains of neuroblasts can still be observed (Chazal et al. 2000). Thus, chain formation itself does not appear to be reliant on the expression of PSA-NCAM. However, the OB in these mice is notably smaller despite no obvious defect in proliferation in the SVZ. Also, fewer BrdU-labelled neuroblasts reach the OB in mutant mice, hence

suggesting the existence of a migration defect (Tomasiewicz et al. 1993; Cremer et al. 1994). Similarly, enzymatic removal of PSA *in vivo* with Endo N also resulted in fewer BrdU positive cells reaching the OB, thus phenocopying the migratory defect seen with NCAM deficient mice, and implying that the glycosylation of NCAM is essential for its function in the RMS (Ono et al. 1994). Surprisingly, NCAM deficient neuroblasts migrate normally when transplanted into a WT postnatal SVZ, whilst WT neuroblasts struggle to migrate in an NCAM deficient or PSA deficient SVZ environment (Hu et al. 1996). Given that neuroblasts migrate by sliding over each other, glycosylation of NCAM and a consequent reduction in adhesiveness may be a requirement for this process to occur. So, it appears that although PSA-NCAM is not a necessity for the formation of neuroblast chains and does not regulate intrinsic motility, the reduced adhesiveness of NCAM following addition of PSA may allow neuroblasts to use each other as a substrate for migration.

Integrins

Integrins are heterophilic binding receptors consisting of an α and β chain. They are involved in cell-cell and cell-ECM interactions and play an important role in transducing information about the ECM to the cell (Hynes 2002). There is now an increasing amount of evidence to suggest that the integrin family of cell adhesion molecules play a vital role in neuroblast migration in the SVZ. Belvindrah et al. (2007) showed that β1 integrins are expressed by neuroblasts throughout the RMS. Interestingly, the authors also found that the expression of α1, α6, and α7 subunits, which dimerise with β1 subunits to form laminin receptors, was increased in the RMS in comparison to the SVZ. Furthermore, laminin was found to be concentrated around the surface of neuroblasts. Analysis of Itgb1-CNSKo mice - where β1 deficiency is restricted to nestin expressing cells – revealed an RMS in which cells failed to assemble in chains. A similar defect was also seen in laminin α2 and α4 deficient mice where the chains of neuroblasts were less compact (Belvindrah et al. 2007). Moreover, *in vitro* migration assays also showed that neuroblasts from Itgb1-CNSKo mice migrate as single cells without any change to the distance migrated (Belvindrah et al. 2007). The concept that the interaction between integrins and laminin is required for the formation of chains is further supported by observations

that neuroblast migration in a collagen matrix can be switched from single cell to chain migration by the introduction of laminin (Belvindrah et al. 2007), whilst neutralising antibodies to α6β1 integrin reduces the cohesive nature of neuroblasts (Emsley and Hagg 2003). More recently, a role for β8 integrin has also been suggested based on a loss of migrating chains in β8-/- and nestin-Cre β8 flox/flox mutants. In these mice, neuroblasts fail to form chains and are found as rosette-shaped aggregates throughout the RMS (Mobley et al. 2009). Though there seems to be a general consensus that integrins are involved in neuroblast migration, there is still considerable dispute as to which integrins are the key players in this system. For example, Murase and Horwitz (2002) showed using immunohistochemistry that the expression of different integrin subunits by neuroblasts changed throughout development. This study found that β1 and β8 were only expressed in the early postnatal period (up to P10), whilst β6 and β10 persisted into adulthood. They also showed that function blocking antibodies to the individual integrin subunits perturbed neuroblast migration in slice cultures, but only if used at the time of expression. Contrary to these findings, Belvindrah et al. (2007) detected β1 and β5 subunits in FACS sorted neuroblasts from the adult RMS. Another group has also reported the expression of β1, β5, and β8 subunits in neuroblasts from P14 mice (Mobley and McCarty 2011). Taken together, most studies implicate β1 and β8 integrins as the main forms responsible for neuroblast migration in the adult brain.

PSA-NCAM and integrins are emerging as important regulators of RMS neuroblast migration, each with distinctive roles in this process. Whilst integrins seem to be responsible for the formation of chains, PSA-NCAM appears to create an environment that is permissive to migration.

1.3.3 Guidance molecules

Slit proteins

The discovery that cultures of the septum and CP repel SVZ neuroblasts *in vitro* led to the identification of the Slit proteins as one of the major regulators of neuroblast migration in the SVZ (Hu and Rutishauser 1996; Hu 1999; Wu et al. 1999). In the developing brain, the repulsive activity of Slit proteins plays a vital role in axon

guidance (Brose et al. 1999; Kidd et al. 1999; Nguyen Ba-Charvet et al. 1999; Nguyen-Ba-Charvet et al. 2002). In a similar way, a gradient of Slit created by the beating of cilia in the lateral ventricles is believed to propel neuroblasts from the SVZ into the RMS (Sawamoto et al. 2006). A role for Slit proteins as a chemorepellent in the SVZ is further supported by evidence that migrating neuroblasts re-orient their leading process in the opposite direction when presented with a source of Slit (Ward et al. 2003), whilst cultures of septum and choroid plexus derived from Slit1 and Slit2 deficient mice fail to show chemorepulsive activity towards neuroblasts *in vitro* (Nguyen-Ba-Charvet et al. 2004). Moreover, neuroblasts migrate outside their putative route and invade the corpus callosum in Slit1$^{-/-}$ mice, thus confirming the role of Slits as a chemorepulsive cue for SVZ neuroblasts (Nguyen-Ba-Charvet et al. 2004).

Growth factors

Several growth factors are now recognised as important chemoattractants and/or motogens regulating neuroblast migration in the RMS. Both glial derived neurotrophic factor (GDNF) and hepatocyte growth factor (HGF) have been proposed as chemoattractants directing neuroblasts to the OB (Paratcha et al. 2006; Garzotto et al. 2008). Indeed, neuroblasts express receptors for GDNF and HGF (GFRα1 and Met respectively), and the expression of both factors follows a rostro-caudal gradient, with the highest expression being in the bulb. *In vitro* chemotaxis assays also confirmed the roles of GDNF and HGF as chemoattractants to neuroblasts (Paratcha et al. 2006; Garzotto et al. 2008).

Another study showed that vascular endothelial growth factor (VEGF) acts as both a chemoattractant and motogen for RMS neuroblasts. Here the authors show that VEGF acts specifically through VEGFR2, and that expression of this receptor was reliant on the presence of FGF-2 (Zhang et al. 2003). FGF-2 itself did not have a chemotactic or motogenic effect in this study, which contradicts reports by Garcia-Gonzalez et al. (2010) who report that FGF-2 was a motogen for neuroblasts. Insulin like growth factor (IGF) is another molecule whose function in regulating neuroblast migration is also unclear. Whilst exogenous addition of IGF significantly enhanced

neuroblast migration from explants cultures, $IGF^{-/-}$ explants show no disruption of migration (Hurtado-Chong et al. 2009).

Brain derived neurotrophic factor (BDNF), which is known for directing long-distance migration of tangentially migrating cortical interneurones in development (Polleux et al. 2002), has also been recognised as a regulator of neuroblast migration in the RMS. BDNF has been shown to behave as a motogen when presented in a uniform concentration (Chiaramello et al. 2007), and as a chemoattractant to neuroblasts when presented in a gradient (Chiaramello et al. 2007; Snapyan et al. 2009). While some studies report a higher expression of BDNF and its receptor in the OB in comparison to the RMS, and suggest that the primary function of this growth factor is as a chemoattractant (Chiaramello et al. 2007), others have shown a uniform expression of BDNF along the stream (Petridis and El Maarouf 2011). This is consistent with reports that blood vessels are the main source of BDNF in the RMS and would therefore lead to the creation of a uniform concentration of BDNF along the length of the RMS (Snapyan et al. 2009). In theory BDNF could act as both chemoattractant and motogen in this situation. For example, BDNF secreted by blood vessels may help to draw neuroblasts towards the vasculature, an association that has been shown to be important for neuroblast migration (Snapyan et al. 2009); while the motogenic activity of BDNF may help to enhance migration of cells towards the bulb. There is currently some dispute as to which receptors are responsible for mediating the effects of BDNF. Snapyan et al. (2009) suggest that neuroblasts predominantly express p75NTR. They also report that GABA released by neuroblasts activates $GABA_A$ receptors on astrocytes, which in turn express the high affinity Trk receptor that leads to sequestering of BDNF in the RMS. This mechanism has been suggested as a means by which neuroblasts negatively regulate their own migration. In contrast to these findings, others have shown that neuroblasts mostly express Trk receptors and that activation of this receptor and subsequent stimulation of the PI3K and MAPK pathways is responsible for the migratory effects of BDNF (Chiaramello et al. 2007; Bagley and Belluscio 2010). Hence, despite the general agreement that BDNF has a vital role in the

regulation of RMS neuroblast migration, the specifics as to how this is achieved is yet to be established.

In contrast to most growth factors, epidermal growth factor receptor (EGFr) activation has been suggested as a negative regulator of neuroblast migration (Kim et al. 2009). Previous reports show that EGFr is predominantly expressed by C cells in the SVZ and is not expressed by neuroblasts. Recently Kim et al. (2009) showed that a subpopulation of cells in the RMS display low expression of EGFr ($EGFr^{low}$) negatively correlating with the expression of neuroblast markers (PSA-NCAM, DCX, and βIII tubulin), possibly indicative of the transition stage from C cell to neuroblast. $EGFr^{low}$ neuroblasts display a slower less directed migration compared to EGFr negative neuroblasts. Exogenous addition of the EGFr ligand TGF-α to brain slice cultures caused a drastic reduction in the number of motile cells and a small increase in proliferative cells in the RMS, though the authors did not investigate exactly which cells in the RMS were proliferating (Kim et al. 2009). The role of EGFr in migration is complicated by the fact that activation of this receptor can change committed neural progenitors into a more premature state (Doetsch et al. 2002; Gonzalez-Perez et al. 2009). Thus, it is not clear whether the observed reduction in motile cells is caused by a change in the identity of $EGFr^{low}$ neuroblasts into a progenitor type phenotype or whether it directly affects motility without cell fate.

Neurotransmitters

Migrating neuroblasts in the RMS express both glutamate and GABA receptors in a mosaic fashion. Whilst nearly all neuroblasts express the ionotropic $GABA_A$ receptor, a small population of these cells express either GLU_{k5} or mGluR or both (Platel et al. 2008). Exogenous application of GABA significantly reduces the migration speed of neuroblasts (Bolteus and Bordey 2004). Interestingly, neuroblasts themselves are the source of GABA in the stream, and regulate their own migration via GABA-mediated activation of $GABA_A$ receptors and subsequent inhibition of Ca^{2+} release from IP_3 sensitive intracellular stores. Astrocytes within the RMS express the high affinity GABA transporter GAT4, and thereby influence neuroblast migration indirectly by managing the availability of GABA (Bolteus and

Bordey 2004). The lack of a glial tube in the OB, and hence the loss of GABA transporters may expose neuroblasts to higher concentrations of GABA in the bulb, which may be a mechanism by which differentiating neurones eventually stop migrating. Surprisingly, exogenous administration of glutamate, which increases intracellular Ca^{2+}, also inhibited neuroblast migration when applied exogenously to slice cultures. This effect is specifically mediated by GLU_{k5} receptors and is independent of mGluR activation (Platel et al. 2008).

Olfactory bulb derived chemoattractants

It seems only natural that long-distance migration, such as that seen in the adult RMS, should require a chemoattractant at the final destination. Hence, there was much surprise upon the discovery that neuroblasts continue to migrate along the entire length of the RMS even after surgical removal of the OB (Kirschenbaum et al. 1999). Given that the RMS is a meandering path approximately 5 mm in length (Lois et al. 1996), it is highly unlikely that neuroblast migration is regulated by a single OB derived attractant. Instead it is most probable that gradients of several factors at different parts of the stream direct neuroblasts towards the bulb (Cayre et al. 2009; Leong and Turnley 2011). Hence, a chemoattractant secreted by the OB may only be involved in regulating the final leg of this journey. In support of this concept, Liu and Rao (2003) have published data showing the existence of an OB derived chemoattractant. This factor seems to arise from the glomerular and mitral cell layers of the OB and its properties do not fit with any of the known chemoattractants. The authors also show that although the OB is not an absolute necessity for neuroblasts from the SVZ to migrate along the stream, loss of the OB increases the number of cells migrating in the opposite direction. Thus, an OB-derived chemoattractant may be involved in guiding neuroblasts in the final stage of their migration.

Table 1.1: Regulators of RMS neuroblast migration

Regulators of RMS neuroblast migration	Reference
CSF flow	(Sawamoto et al. 2006)
Matrix metalloproteinases	(Bovetti et al. 2007)
Vasculature	(Snapyan et al. 2009; Whitman et al. 2009; Bozoyan et al. 2012)
DCX	(Koizumi et al. 2006; Ocbina et al. 2006)
Drebrin	(Song et al. 2008)
PSA-NCAM	(Tomasiewicz et al. 1993; Cremer et al. 1994; Ono et al. 1994; Hu et al. 1996; Chazal et al. 2000)
Integrins	(Emsley and Hagg 2003; Belvindrah et al. 2007; Mobley et al. 2009; Mobley and McCarty 2011)
ADAM2	(Murase et al. 2008)
Galectin-3	(Comte et al. 2011)
Connexins	(Marins et al. 2009)
Slit	(Hu and Rutishauser 1996; Hu 1999; Wu et al. 1999; Nguyen-Ba-Charvet et al. 2002; Ward et al. 2003; Nguyen-Ba-Charvet et al. 2004)
Ephrins	(Conover et al. 2000)
Neuroregulins	(Anton et al. 2004)
Netrin1	(Murase and Horwitz 2002; Hakanen et al. 2011)
Ganglioside 9-O-acetyl GD3	(Miyakoshi et al. 2012)
ApoER2/VLDL receptor	(Andrade et al. 2007)
GDNF	(Paratcha et al. 2006)
HGF	(Garzotto et al. 2008)
BDNF	(Chiaramello et al. 2007)
VEGF	(Zhang et al. 2003; Wittko et al. 2009)
FGF-2	(Garcia-Gonzalez et al. 2010)
IGF	(Hurtado-Chong et al. 2009)

EGF	(Kim et al. 2009)
GABA	(Bolteus and Bordey 2004)
Glutamate	(Platel et al. 2008; Platel et al. 2008)
MIA	(Mason et al. 2001)
Tenascin-R	(Saghatelyan et al. 2004)
Reelin	(Hack et al. 2002)
Prokineticin-2	(Ng et al. 2005)

1.4 The role of endocannabinoids in the CNS

Cannabis Sativa has been used throughout history for both medicinal and recreational purposes (Aggarwal et al. 2009). We now know that Δ-tetrahydrocannabinol, the main bioactive compound in cannabis (Mechoulam and Gaoni 1965), exerts its many biological effects through the activation of cannabinoid (CB) receptors (Matsuda et al. 1990; Munro et al. 1993), and that endogenous cannabinoids or endocannabinoids (eCBs) play vital roles in both the developing and adult CNS (Harkany et al. 2007; Mechoulam and Parker 2012). In recent years, the eCB system has also been implicated in the regulation of adult neurogenesis (Oudin et al. 2011). The expression of a functional eCB system in adult SVZ neural precursors (Aguado et al. 2006; Palazuelos et al. 2006; Goncalves et al. 2008; Gao et al. 2010), coupled with the ability of eCBs to regulate the migration of both cortical interneurones during development and immune cells (Berghuis et al. 2005; Miller and Stella 2008), suggests a possibility for this system to be involved in RMS neuroblast migration. Here we provide a brief overview of the eCB system and outline some of its recognised functions in the CNS.

1.4.1 Synthesis and degradation

Endocannabinoids (eCB), 2-arachidonyl-glycerol (2-AG) and anandamide, are lipid mediators synthesised on-demand from membrane phospholipids (Figure 1.7). Anandamide synthesis is a multi-step process involving conversion of phosphatidylethanolamine (PE) into N-arachidonyl-PE (NAPE) by the enzyme N-acetyl-transferase, and subsequent hydrolysis by phospholipase D (PLD) (Di Marzo et al. 1994; Cadas et al. 1997). 2-AG, the most abundant eCB in the brain, is generated from hydrolysis of 1,2-diacylglycerol (DAG) by the enzyme DAG-lipase (DAG-L) (Farooqui et al. 1989; Bisogno et al. 2003). The precursor DAG is synthesised by the actions of PLC on PIP_2 to generate DAG and IP_3, both of which are secondary messengers. Whist IP_3 induces release of Ca^{2+} from intracellular stores; DAG activates protein kinase C (PKC). Thus, DAG is both the end-product of one pathway, and the precursor of another (Piomelli 2003). The secondary messenger activity of DAG is regulated by the enzyme DAG-kinase, which converts

the precursor into phosphatidic acid, thus terminating its biological activity (Kanoh et al. 2002). The synthesis of both anandamide and 2-AG are Ca^{2+} dependent processes and can be initiated artificially in cultured neurones by increasing intracellular Ca^{2+} using Ca^{2+} ionophore ionomycin (Cadas et al. 1996). eCB synthesis has also been linked to activation of G protein coupled receptors (GPCRs) such as muscarinic acetylcholine and metabotropic glutamate receptors (Varma et al. 2001; Kim et al. 2002). Interestingly, high frequency stimulation in hippocampal cultures increases 2-AG levels but not anandamide, whereas dopamine receptor 2 activation in the striatum specifically increases anandamide production without affecting 2-AG (Stella et al. 1997; Stella and Piomelli 2001). Thus the production of each eCB can be regulated independently in neurones. Unlike Δ-tetrahydrocannabinol, the main bioactive component of cannabis, the eCBs are rapidly degraded following synthesis (Giuffrida et al. 2001). Whist anandamide is hydrolysed by fatty acid amide hydrolase (FAAH) to arachidonic acid and ethanolamine (Cravatt et al. 1996), 2-AG is degraded by both FAAH and monoacylglycerol lipase (MAG-L) into fatty acid and glycerol (Dinh et al. 2002).

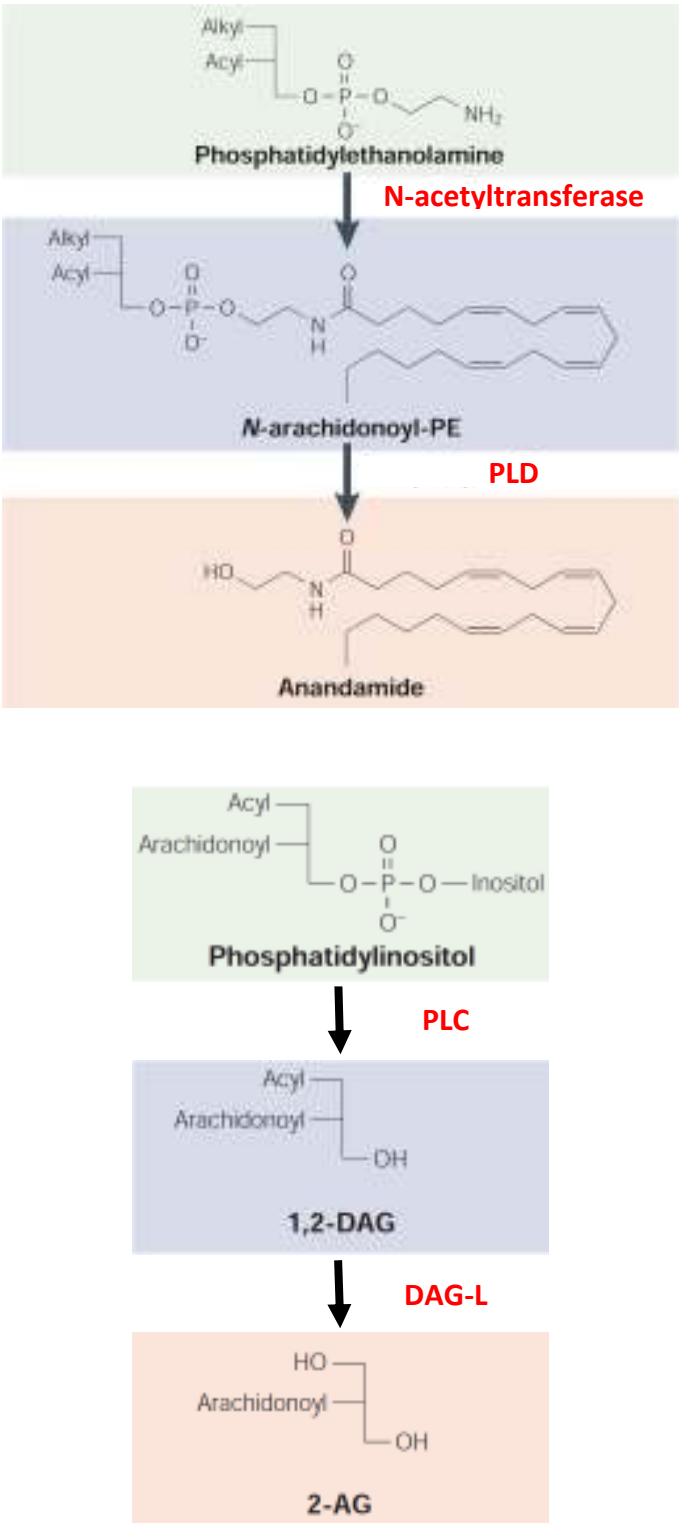

Figure 1.7: The synthetic pathways of endocannabinoids. A diagram showing the main synthetic pathways for anandamide and 2-AG from membrane phospholipids. Adapted from Piomelli (2003). Abbreviations: Diacylglycerol lipase (DAG-L), phospholipase C (PLC), phospholipase D (PLD).

1.4.2 CB receptors

The many diverse functions of the eCBs are mediated through the activation of G-protein coupled receptors CB1 and CB2, both of which couple to the $G_{i/o}$ family of monomeric G proteins. The CB1 receptor, the most abundant GPCR in the brain, is expressed as early as E11 in the neural tube, and in the adult is found throughout the central and peripheral nervous systems (Buckley et al. 1998). The CB2 receptor on the other hand is absent in the developing nervous system and is most abundantly expressed in the liver during embryogenesis (Buckley et al. 1998). In the adult, CB2 receptors are predominantly expressed by cells of the immune system, and have been shown to modulate migration of these cells (Cabral et al. 2008; Miller and Stella 2008). However, the discovery that select groups of neurones in the brainstem and cerebellum, as wells as neural progenitors in the subventricular zone (SVZ) express the CB2 receptor, has instigated newfound interest into its role in the brain (Palazuelos et al. 2006; Goncalves et al. 2008). CB receptors can be activated by local production of eCBs. Due to the hydrophobic nature of 2-AG and anandamide, they have a tendency to remain within the lipid membrane following synthesis. This unusual property allows them to activate CB receptors within the same cell by a process of lateral membrane diffusion (Song and Bonner 1996; Xie et al. 1996). At the same time, eCBs have also been shown to activate CB receptors on the terminals of adjacent axons (Kreitzer and Regehr 2001; Wilson and Nicoll 2001). Exactly how they are transported through the aqueous environment is still unknown, though there is some speculation that lipid binding proteins may be involved in facilitating this process (Piomelli 2003).

1.4.3 CB receptor signalling

Activation of either CB1 or CB2 receptor results in classical signalling associated with the $G_{i/o}$ family of G proteins. In neurones, CB1 receptor activation leads to inhibition of N and P/Q type voltage gated Ca^{2+} channels and opening of K^+ channels. The effect on Ca^{2+} channels is believed to occur through direct interaction of the $\beta\gamma$ subunit of the G protein with the channel, whilst the effect on K^+ channels result from attenuation of PKA activity following inhibition of adenyl cyclase and subsequent reduction in intracellular cAMP. This is the main mechanism by which

CB receptors inhibit neurotransmitter release in the adult CNS (Pertwee 2006). Another feature of CB receptor signalling, is the activation of several kinases including focal adhesion kinase (FAK), extracellular signal related kinase (ERK), PI3K, and the MAPK pathway (Derkinderen et al. 1996; Adams and Sweatt 2002; Derkinderen et al. 2003). Interestingly, in the absence of $G_{i/o}$ proteins, CB receptors can couple to G_s proteins, thus resulting in an increase in cAMP and activation of PKA (Glass and Felder 1997).

1.4.4 Functions of the eCB system in the CNS

eCB function in the adult CNS

In the adult brain, the main function of the CB1 receptor is inhibition of neurotransmitter release via retrograde signalling (Pertwee 2006; Uchigashima et al. 2007) (Figure 1.8). Here, 2-AG produced post-synaptically, acts on pre-synaptic CB1 receptors to inhibit neurotransmitter release via its actions on Ca^{2+} and K^+ ion channels. The majority of CB1 receptors are located on cholecystokinin-8 (CCK-8) positive GABA interneurones (Tsou et al. 1998). In the hippocampus, depolarisation of pyramidal neurones leads to postsynaptic synthesis of eCBs, activation of presynaptic CB1 receptor on GABAergic interneurones, and inhibition of neurotransmitter release that ultimately increases the excitability of the target cell (Wilson and Nicoll 2001). This process, termed depolarisation-induced suppression of inhibition (DSI), is thought to be a mechanism by which synaptic plasticity and long term potentiation is achieved in the hippocampus (Alger 2002). In contrast, activation of CB1 receptors on glutamatergic presynaptic terminals has the opposite effect and is known as depolarisation induced suppression of excitation (DSE) (Alger 2002). Much of the characteristics effects of cannabis (altered perception, euphoria, hallucination, enhanced appetite, reduced spontaneous motor activity, immobility, analgesia and impairment of short-term memory) can be attributed to regulation of neurotransmitter release by CB1 receptors in discrete regions of the CNS (Piomelli 2003).

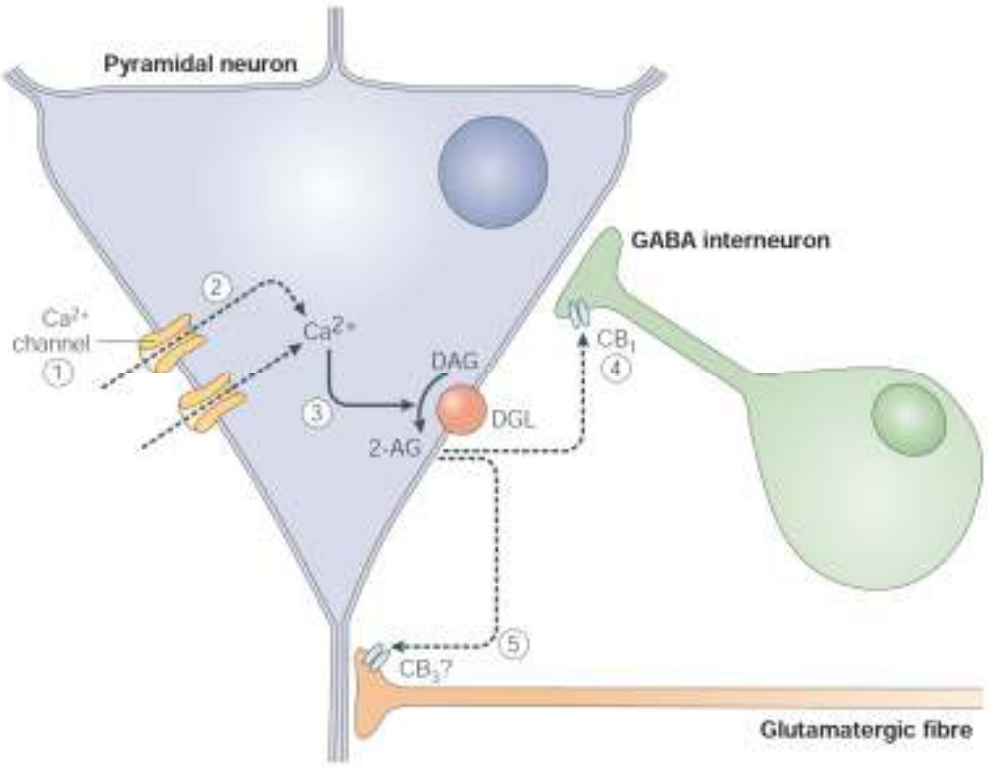

Figure 1.8: Retrograde signalling by endocannabinoids. Membrane depolarisation in pyramidal neurones in the hippocampus leads to activation of DAG-L and synthesis of 2-AG. Activation of CB receptors on adjacent GABAergic and glutamatergic neurones leads to suppression of neurotransmitter release via retrograde signalling. Adapted from Piomelli (2003).

eCB function in the developing brain

During development, the eCB system actively participates in axon growth and guidance through its actions on the CB1 receptor (Williams et al. 2003). In fact, the appearance of CB1 receptor expression throughout the developing brain coincides with differentiation of cells into a neuronal fate (Begbie et al. 2004). Thus it appears that CB1 receptor expression may be required by cells taking on a neuronal phenotype in order to guide their growing axons to the correct target. The function of the CB1 receptor in axonal guidance occurs downstream of signalling through cell adhesion molecules (Williams et al. 1994; Williams et al. 2003). Specifically, information regarding the extracellular environment is transduced via activation of the FGF receptor by FGF or adhesion molecules NCAM, N-Cadherin and L1 (Williams et al. 2001; Sanchez-Heras et al. 2006). Classical signalling associated with this receptor tyrosine kinase ultimately leads to the activation of PLC and production of the precursor DAG. An unknown mechanism couples FGF receptor signalling to the activation of DAG-L, which results in the production of the eCB 2-AG (Williams et al. 2003). In contrast to the adult nervous system, the eCB synthetic enzyme and CB1 receptor are both expressed within the growing axon terminal, which allows locally produced lipid mediators to activate receptors within the same membrane, and thus creates a local signalling circuit. Interestingly, activation of the CB1 receptor during development leads to opening of voltage gated Ca^{2+} channels which may arise from the ability of CB receptors to couple to different signalling molecules under certain conditions (Glass and Felder 1997). The following increase in intracellular Ca^{2+} has been shown to be a pivotal step in steering axonal growth (Doherty et al. 1991; Williams et al. 1994).

eCB function in adult neurogenesis

The eCB system is now recognised as having an important role in the regulation of adult neurogenesis. An underlying eCB tone in the SVZ regulates the proliferation of NS cells through the activation of CB1 and CB2 receptors on dividing cells (Jin et al. 2004; Aguado et al. 2006; Palazuelos et al. 2006; Goncalves et al. 2008). Furthermore, DAG-Lα knockout animals have severely reduced neurogenesis, suggesting that 2-AG is the main eCB contributing to this process (Gao et al. 2010).

Interestingly, in young animals, where neurogenesis is maximal, administration of a CB2 agonist did not increase NS cell proliferation any further (Goncalves et al. 2008). However, in older animals, where proliferation of NS cells has declined, administration of a CB2 agonist was able to restore neurogenesis to levels similar to those seen in young animals (Goncalves et al. 2008). Much of the scepticism surrounding the therapeutic potential of adult neural stem cells, has arisen from the limited neurogenesis present in the adult human brain (Sanai et al. 2011). Thus, these findings raise the exciting possibility that neurogenesis may possibly be re-activated in the adult brain through stimulation of the eCB system.

1.5 Molecular regulation of neuronal migration

Like all migratory cells, neuroblasts undergo a series of cytoskeletal re-arrangements to mediate motion. The initiating step, polarisation of the cell and extension of a leading process, occurs in response to the integration of extracellular signals, resulting in a polarised distribution of intracellular signalling molecules and preferential polymerisation of actin on one side of the cell (Lambert de Rouvroit and Goffinet 2001). This is followed by forward movement of the soma and its organelles, a process termed somal translocation or nucleokinesis, and results in net movement of the cell (Lambert de Rouvroit and Goffinet 2001). Uncovering the signalling cascade regulating neuronal migration has been complicated by the existence of diverse morphologies and modes of migration adopted by different populations of migrating neural precursors. For example, SVZ neuroblasts have a short compact single leading process, precerebellar neurones in the pons have long leading processes extending for several hundred μm, whilst cortical interneurones have branched leading processes (Marin et al. 2006). Thus, it was largely believed that a unique migratory mechanism was responsible for each form of migration. However, recent evidence showing that the same neurones can switch between radial and tangential migration (Lois and Alvarez-Buylla 1994; Nadarajah et al. 2002; Nadarajah and Parnavelas 2002), as well as alter their morphology at different stages of migration (Kriegstein and Noctor 2004; Noctor et al. 2004; Marin et al. 2006), suggests the existence of a common underlying mechanism that is modulated to achieve the diverse modes and morphologies observed by migrating neural precursors. Thus, although very little is known about the molecular regulation of SVZ neuroblast migration, our current understanding of neuronal migration in other contexts may assist in elucidating the key players controlling migration in the adult CNS.

1.5.1 Leading process extension

The leading process in SVZ migratory neuroblasts is tipped with a dynamic lamellipodial structure that resembles growth cones in axons (Nam et al. 2007). Finger-like filopodial protrusions, found at the edges of lamellipodia, constantly

probe the extracellular environment for guidance cues. Both lamellipodia and filopodia are based on an underlying actin framework, and are required for translating differences in extracellular chemical gradients into polarisation of signalling molecules within the cell (Luo 2000; Lambert de Rouvroit and Goffinet 2001; Marin et al. 2006). Ultimately, polymerisation of actin monomers, a process regulated by numerous actin binding proteins, generates the protrusive force required for leading process extension (Ridley et al. 2003), whilst microtubule assembly helps to stabilise and establish the leading process (Schliwa et al. 1999; Gopal et al. 2010). In addition, adherence to the extracellular matrix via formation of adhesion complexes is also required to generate force for migration to occur (Ridley et al. 2003). We now know from studies in neuronal and non-neuronal cells that selective activation of PI3K at the leading front following G-protein coupled receptor or tyrosine kinase receptor activation is a crucial event in directed migration (Funamoto et al. 2002; Weiner 2002). For example, the motogenic effects of BDNF and HGF in cortical interneurones, as well as the chemotactic effect of reelin on radially migrating projection neurones, are both dependent on localised activation of PI3K (Beffert et al. 2002; Polleux et al. 2002; Segarra et al. 2006). Both Rac1 and Cdc42, members of the Rho family of GTPases responsible for the formation of lamellipodia and filopodia (respectively) in other cell types, act downstream of PI3K in migrating neurones (Konno et al. 2005). In non-neuronal cells, both Rac1 and Cdc42 are found at the leading front, where Cdc42 is believed to orient the MTOC ahead of the nucleus and Rac1 is involved in formation of protrusions (Ridley et al. 2003; Marin et al. 2006). Inhibition of Rac1 or Cdc42 activity in radially migrating cortical neurones perturbs migration (Konno et al. 2005). In migrating cortical neurones Rac1 is distributed along the plasma membrane, and expression of mutant Rac1 leads to the loss of the leading process. Instead, Cdc42 is concentrated in the perinuclear region and may be involved in regulating orientation of the microtubule organising centre (MTOC) (Konno et al. 2005). In line with these observations, the chemorepellent activity of Slit proteins on SVZ neuroblasts was shown to occur through local suppression of Cdc42 following activation of Rho GAPs (GTPase activating proteins) (Wong et al. 2001).

Thus, Rac1 and Cdc42 may be involved in leading process formation and centrosome positioning in RMS neuroblasts, respectively.

1.5.2 Nucleokinesis

Nucleokinesis is regarded as a two-step process. The first step is characterised by the occurrence of a cytoplasmic swelling directly in from of the nucleus. This results from transmission of force generated in the leading process to the centrosome, which moved forward to form a dilatation that contains the Golgi apparatus, mitochondria, and rough endoplasmic reticulum. A microtubule cage that surrounds the nucleus keeps it constantly attached to the centrosome. In the second step, pulling forces generated by the dynein motor complex, as well as acto-myosin contraction and loss of cell-substrate adhesion at the rear of the cell propel the nucleus forward and completes the migration cycle (Tsai and Gleeson 2005) (Figure 1.9).

PAR complex

There are now several lines of evidence to suggest that the PAR3-PAR6-aPKC complex, which is known for its role in establishing cell polarity (Etienne-Manneville and Hall 2003; Henrique and Schweisguth 2003; Goldstein and Macara 2007), is involved in localisation of the centrosome during neuronal migration. Studies investigating glial-guided migration of cerebellar granule cells have highlighted that mPar6α and PKCζ are required for correct positioning of the centrosome (Solecki et al. 2004). In SVZ neuroblasts, Slit mediated repulsion is associated with formation of a new leading process in the opposite direction, and re-orientation of the centrosome towards the new leading process. Furthermore, pharmacological inhibition of PKCζ or its target glycogen synthase kinase 3 β (GSK3β), specifically results in the loss of centrosome re-orientation (Higginbotham et al. 2006).

Dynein motor complex

The forward movement of the nucleus in the final step of nucleokinesis is achieved by the dynein motor complex, a minus-end directed microtubule motor that is fundamental for the regulation of nuclear movement in fungi and animals (Morris

2003). Mutations in genes coding for dynein-interacting proteins in humans, such as Lis1 and doublecortin (DCX), are responsible for the condition Lissencephaly, which is characterised by abnormal neuronal migration. DCX is expressed by migrating neurones during development, as well as RMS neuroblasts, and is thought to regulate neuronal migration via its ability organise and stabilise microtubules (Gleeson et al. 1999). Investigations in migrating cerebellar granule cells revealed that Lis1 was localised to the MTOC, whilst DCX was localised along the microtubule cage enveloping the nucleus (Tanaka et al. 2004). This study also showed that inhibition of dynein or deletion of Lis1 resulted in centrosome-nuclear uncoupling, as evidenced by an increase in the distance between the centrosome and nucleus. Interestingly, overexpression of DCX was able to rescue this migratory defect. In RMS neuroblasts, loss of DCX also resulted in a migratory defect associated with centrosome-nuclear uncoupling. In addition, neuroblasts also displayed a shortening of the leading process and an increase in secondary branching (Koizumi et al. 2006). Hence, DCX may participate in two aspects of neuroblast migration by regulating centrosome-nuclear coupling through an interaction with the dynein motor complex, and maintaining the morphology of RMS neuroblasts through its ability to stabilise microtubules (Tanaka et al. 2004; Koizumi et al. 2006).

Cyclin-dependent kinase 5

Cyclin dependent kinase 5 (CDK5) is a serine/threonine kinase that regulates the activity of a diverse range of proteins, and is therefore able to participate in numerous cell functions which include regulation of the actin cytoskeleton, microtubule stability, axon guidance, membrane transport, synaptic function, dopamine signalling and drug addiction (Dhavan and Tsai 2001). However, it is most well known for its regulation of the CNS cytoarchitecture as evidenced by the gross morphological abnormalities seen in CDK5 knockout mice (Ohshima et al. 1996; Chae et al. 1997). One of the most striking phenotypes in these mice is the inverted layering of the cortex, which is believed to arise from failure of neuronal migration during development (Ohshima et al. 1996; Chae et al. 1997). More recently, a role for CDK5 in tangentially migrating cortical neurones (Rakic et al. 2009) as well as SVZ neuroblast has also been demonstrated (Hirota et al. 2007). Also, the pro-

migratory effect of GDNF on RMS neuroblasts appears to be reliant on the activity of CDK5 (Paratcha et al. 2006).

The exact mechanism by which CDK5 regulates neuroblast migration is yet to be determined. Since CDK5 can regulate a vast number of proteins involved in actin and microtubule dynamics, there are several potential target proteins that may be downstream of CDK5 in neuroblast migration. One such example is p27kip1. The phosphorylation of this protein by CDK5 has been suggested as a mechanism by which CDK5 regulates F-actin dynamic in the leading processes of migrating cortical neurones (Kawauchi et al. 2006). CDK5 also induces hyperphosphorylation and subsequent inhibition of p21-activated kinase 1 (Pak1), a Rac effector involved in the control of neuronal morphology through the regulation of actin and microtubule dynamics (Rashid et al. 2001; Jacobs et al. 2007; Nikolic 2008). Furthermore, cortical neuron migration is now recognised as being dependent on the activity of Pak1 (Causeret et al. 2009). CDK5 also phosphorylates focal adhesion kinase (FAK), a regulator of cell adhesion in migrating non-neuronal cells (Hanks et al. 1992; Schaller et al. 1992). Importantly, FAK has been shown to regulate glia-dependent cortical neuron migration by promoting neuron-radial glia interaction through regulation of Connexin-26-containing gap junctions (Valiente et al. 2011). In cultured neurones, FAK was found localised to the microtubule fork that contacts the nucleus. Moreover phosphorylation of FAK by CDK5 was found to be crucial for efficient nucleokinesis as well as the specific localisation of FAK to the microtubule fork (Xie et al. 2003). In addition, CDK5 can phosphorylate proteins associated with the dynein motor complex such as the Lis1 interacting protein Nudel (Niethammer et al. 2000), whilst phosphorylation of DCX has been shown to regulate its localisation to the perinuclear microtubule cage of migrating neurones (Tanaka et al. 2004). Thus, CDK5 may single headedly orchestrate several stages of the migratory cycle by activating or inactivating target proteins that regulate different aspects of neuronal migration.

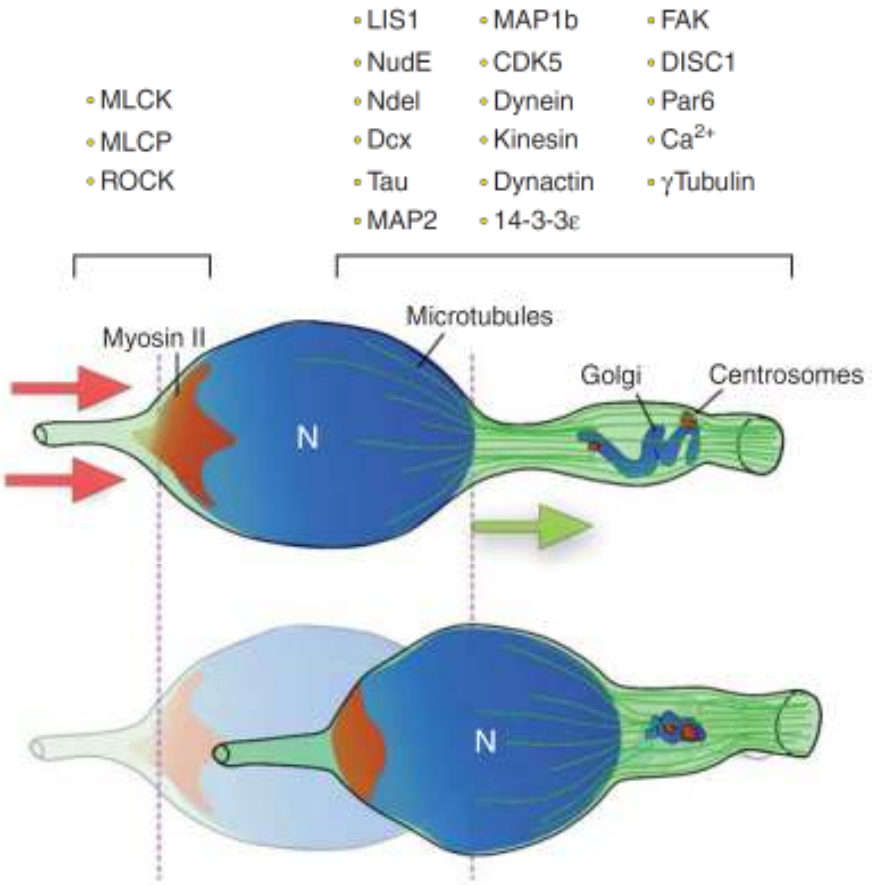

Figure 1.9: Nucleokinesis in neuronal migration. In the first stage of nucleokinesis, the centrosome and Golgi move into a cytoplasmic swelling directly in front of the nucleus (top). In the second part, actomyosin contraction at the rear of the cell and pulling forces generated by the dynein motor complex propels the nucleus forward towards the leading process (bottom). The molecules believed to regulate each of these stages are shown above. The green arrow indicates the direction of motion. N = nucleus. Adapted from Marin et al. (2010)

1.6 Ral GTPases

1.6.1 Ral GTPase: History, structure and function

Small GTPases are monomeric G proteins that play a pivotal role in the regulation of signal transduction, and modulate a diverse range of cell biological functions. Over 100 identified G proteins have been categorised into 5 main families based on their structural similarity: Ras, Rho, Gα, Arf and Rab. Members of the Ras family are generally known to regulate gene expression, cell proliferation, and adhesion (Takai et al. 2001). The Rho family members are most well known for their regulation of the actin cytoskeleton, with formation of stress fibres, lamellipodia, and filopodia being associated with the activities of RhoA, Rac1 and Cdc42, respectively (Ridley et al. 2003; Jaffe and Hall 2005). Rab and Arf family members are involved in the management of vesicle trafficking, whilst Ran family members, which constitute a branch of the Rab family, co-ordinate nucleocytoplasmic transport during mitosis (Takai et al. 2001). All GTPases cycle between a GDP bound inactive and GTP bound active form (Figure 1.10). The exchange of GDP for GTP initiates binding and modulation of the biological activity of an effector molecule, which is responsible for mediating the unique cellular functions of each G protein. Association with the effector in turn activates the catalytic domain, resulting in hydrolysis of GTP, and return of the small GTPase into its inactive state. This cycling process is under tight spatial and temporal regulation by a specific set of guanine nucleotide exchange factors (GEFs) that promote the exchange of GDP for GTP, and GTPase activating proteins (GAPs) that stimulate the hydrolysis of GTP (Feig 2003; Bos et al. 2007). Thus, GTPase activity can be locally "turned on and off" by GEFs and GAPs respectively, and are often referred to as molecular switches for this reason.

Ras-like GTPase A (RalA) is a monomeric G-protein belonging to the Ras family. It shares almost 85% identity with its closely related family member RalB, and only differs in the C-terminal region, the site of post-translational modification that is believed to be responsible for the localisation of RalA mainly on the plasma membrane and RalB mostly on endomembranes (Shipitsin and Feig 2004; Fenwick et al. 2009). A large portion of the Ral protein comprises the catalytic GTPase

domain, which contains 4 GTP binding motifs and an effector-binding region (switch l and switch ll). Whilst the N-terminus contains a PLC/PLD binding domain that acts independently of GTP loading, the C-terminus contains a Ca^{2+} dependent calmodulin binding site, and a RalA specific phosphorylation site for Aurora kinase A (van Dam and Robinson 2006) (Figure 1.10). Though much of the early work on Ral GTPases did not distinguish between the two isoforms, RalA and RalB are now recognised for having both distinct and overlapping functions (Oxford et al. 2005; Martin and Der 2012). So far several Ral-GEFs such as Ral-GDP dissociation stimulator (Ral-GDS), Rgl1, Rgl2/Rlf, Rgl3, Rgr, and RalGPS1-2 have been identified (Feig et al. 1996; Quilliam et al. 2002). Although the nature of the GAPs that regulate Ral activity is less well known, recent studies have identified large heteromeric complexes resembling the tuberous sclerosis tumor suppressor complex as potential GAPs for Ral GTPases (Shirakawa et al. 2009).

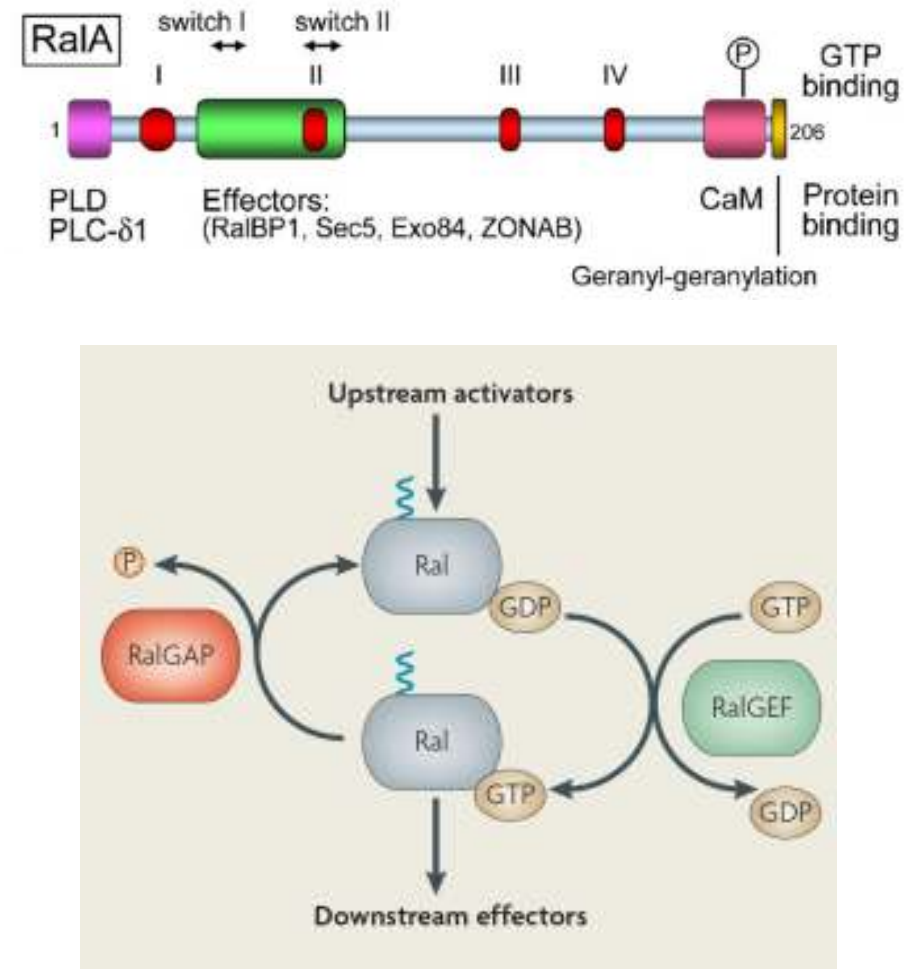

Figure 1.10: Structure and activation cycle of RalA. (Top) A schematic representation of the different domains of RalA showing PLD1 and PLC δ1 binding domains at the N-terminal region, four GTP binding motifs (I-lV), effector binding regions (switch l and switch ll), calmodulin binding site, post translational lipid modification site at the C terminus, and an Aurora kinase A phosphorylation site at Ser194 which is unique to RalA. Adapted from van Dam and Robinson (2006). (Bottom) Schematic representation of the Ral activation/inactivation cycle. Adapted from Bodemann and White (2008)

1.6.2 Regulation of Ral GTPase activation

Ras GTPases are now recognised as important activators of RalA and RalB. This unexpected discovery was made following identification of Ral-GDS as one of the main effectors for active Ras. Since Ras proteins can be activated by a range of extracellular signals such as growth factors and GPCR agonists, as well as second messengers which include DAG and Ca^{2+}, Ras proteins are aptly placed to couple Ral activation to several signalling pathways (Feig et al. 1996). Besides delivering Ral-GDS to Ral proteins in the plasma membrane, Ras regulation of PI3K is also believed to be a simultaneous mechanism of enhancing Ral activation. Here, PI3K promotes the association of PDK1 with the N-terminus of Ral-GDS. Formation of this complex relieves autoinhibition of the catalytic domain of Ral-GDS by its N-terminal domain, and thus enhance intrinsic GEF activity in a manner that is independent of the kinase activity of PDK1 (Tian et al. 2002). Rap proteins, another member of the Ras GTPase family, have also been suggested as regulators of Ral activity. In *Drosophila* Rap GTPases have a higher affinity for Ral-GEFs than Ras, and are the main upstream regulators of Ral proteins in this system (Mirey et al. 2003). Although the reverse appears to be true in mammalian cells, recent evidence suggests that at least in some contexts, such as neurite outgrowth, Rap GTPases may be responsible for the activation of Ral (He et al. 2005).

Ral GTPases can also be stimulated by mechanisms that are independent of Ras (Figure 1.11). For example, growth factor-induced activation of PLC and subsequent increase in intracellular Ca^{2+} has also been shown to be responsible for initiation of Ral activity under certain conditions (Hofer et al. 1998). Exactly how an increase in Ca^{2+} is translated to Ral activation is not entirely clear, though there is some thought that this effect may be mediated by an unknown Ca^{2+} sensitive GEF (Wolthuis et al. 1998). In addition, Ral GTPases also have a calmodulin binding site at the C-terminus, suggesting a possible mechanism for coupling changes in intracellular Ca^{2+} concentrations to Ral activity. Although the interaction of calmodulin with RalA and RalB has been shown to be Ca^{2+} dependent, whether this interaction is directly involved in activating the GTPases has not yet been demonstrated (Clough et al. 2002). Signalling via certain GPCRs can also lead to Ral

activation in a Ras-independent manner. β-arrestins, which are responsible for agonist-mediated desensitisation of GPCRs, can exist in the cytosol as a complex with Ral-GDS. Activation of GPCRs that lead to recruitment of β arrestins, results in translocation of the complex to the plasma membrane and dissociation of Ral-GDS, which is then able to bind and activate RalA (Bhattacharya et al. 2002). In addition, Ral function can be negatively regulated by phosphorylation of the N-terminal domain of Ral-GDS by PKC. This in turn prevents removal of the inhibitory N-terminal domain from the catalytic region of the GEF and hence prevents Ral activation (Rusanescu et al. 2001).

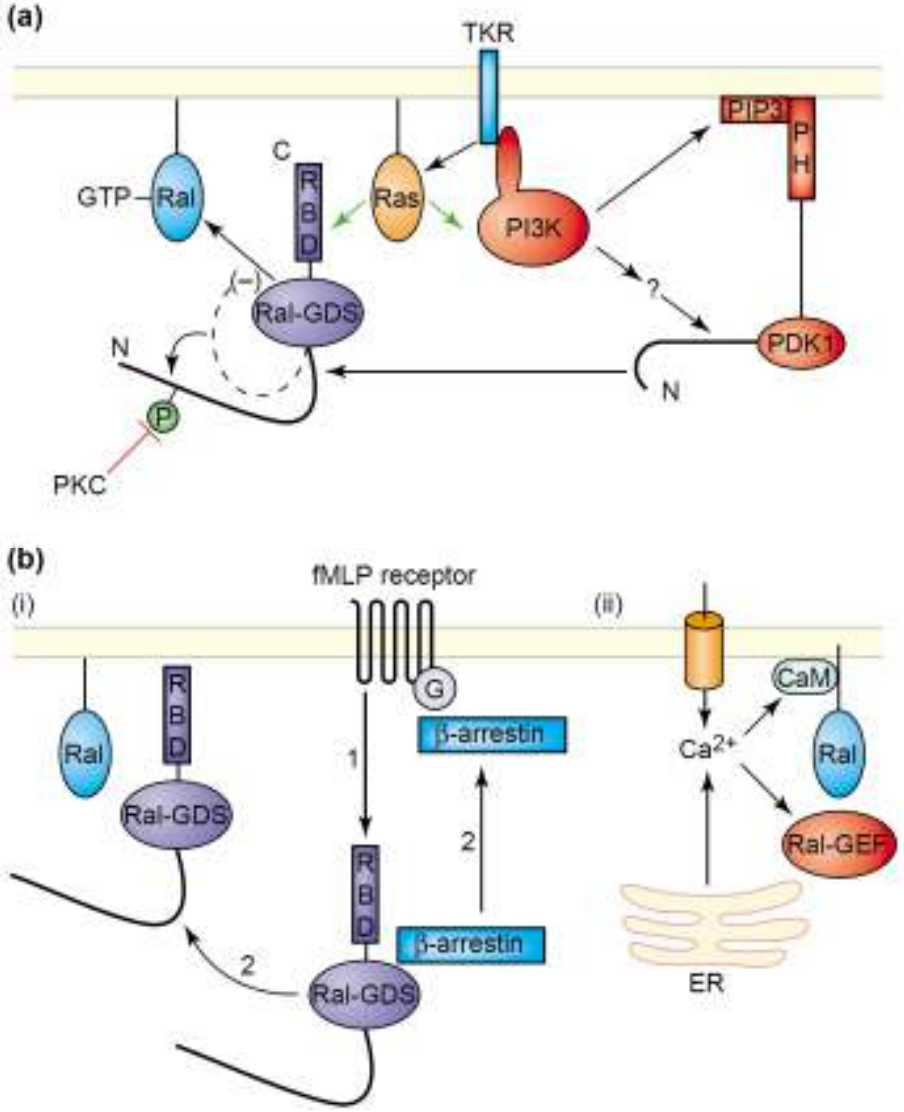

Figure 1.11: Regulation of Ral GTPases activation. (a) Ras dependent mechanisms of Ral GTPase activation. Active Ras binds Ral-GDS and delivers it to Ral in the plasma membrane. Simultaneous activation of PI3K promotes the association of PDK1 and Ral-GDS, resulting in enhancement of GEF activity. **(b)** Ras independent mechanisms of Ral activation. Ral-GDS and β arrestin form an inactive complex in the cytosol. Signalling via GPCR leads to recruitment of the complex to the plasma membrane followed by dissociation, thus releasing Ral-GDS **(i)**. A rise in intracellular Ca^{2+} activates Ral, either through a Ca^{2+} sensitive GEF or Calmodulin **(ii)**. Adapted from (Feig 2003).

1.6.3 Effectors of Ral GTPases

Ral binding protein 1 (RalBP1), the first molecule identified as an effector of Ral GTPases, associates with AP2, POB1, and Reps1, which regulate endocytic pathways. Regulation of endocytosis by RalA is now primarily attributed to its association with RalBP1 (Cantor et al. 1995; Jullien-Flores et al. 2000; Han et al. 2009). In addition to its established function in endocytosis, RalBP1 has also been found to negatively regulate Rho GTPases Cdc42 and Rac1 through a GAP domain (Cantor et al. 1995; Park and Weinberg 1995). Although this suggests a possible mechanism of actin cytoskeletal regulation via RalBP1, the consequences of its negative regulation of the Rho GTPases remains unclear.

The exocyst is another major effector of RalA. This protein complex, which is found in regions of the plasma membrane undergoing expansion or secretion is formed of 8 subunits (sec3, sec5, sec6, sec8, sec10, sec15, Exo70 and Exo84), and was originally recognised for its role in the delivery of secretory vesicles to the plasma membrane in the budding yeast *Saccaharomyces cerevisiae*, and Golgi-derived vesicles to the basolateral membrane in polarised epithelial cells (TerBush et al. 1996; Grindstaff et al. 1998). Current evidence suggests that the exocyst is a dynamic complex formed of two subcomplexes: a targeting unit on the plasma membrane (Sec3, Sec5, Sec6, Sec8 and Exo70) and a vesicle-associated unit (Sec10, Sec 15, and Exo84), which directs and tethers secretory vesicles to the plasma membrane (Moskalenko et al. 2003). Two subunits of the complex, Sec5 and Exo84, bind active Ral in a competitive manner (Figure 1.12). The association of Ral with the exocyst subunits appears to be involved in both assembly and stabilisation of the full octameric complex (Moskalenko et al. 2002; Jin et al. 2005). The Ral-exocyst interaction has also been linked to the formation of filopodia in fibroblasts. Interestingly, this function was found to be due to direct regulation of the actin cytoskeleton since dominant negative RalA inhibited filopodia formation induced by Cdc42, whilst blockade of general secretion with brefeldin A did not affect RalA-induced protrusions (Sugihara et al. 2002). Although both RalA and RalB have been implicated in Ral-exocyst mediated processes, RalA has been shown to have a greater affinity for this complex than RalB (Shipitsin and Feig 2004). Ral GTPases

may also regulate actin cytoskeletal dynamics through another effector molecule, the actin binding protein filamin, which has been implicated in the formation of filopodia (Ohta et al. 1999). Recently the transcription factor ZONAB, which regulates cell proliferation, was identified as a novel effector of Ral GTPases (Frankel et al. 2005). Association of active RalA with ZONAB was found to relieve its transcriptional repression. This mechanism has been proposed as a method by which the oncogenic effects of the Ras proteins may be translated via RalA.

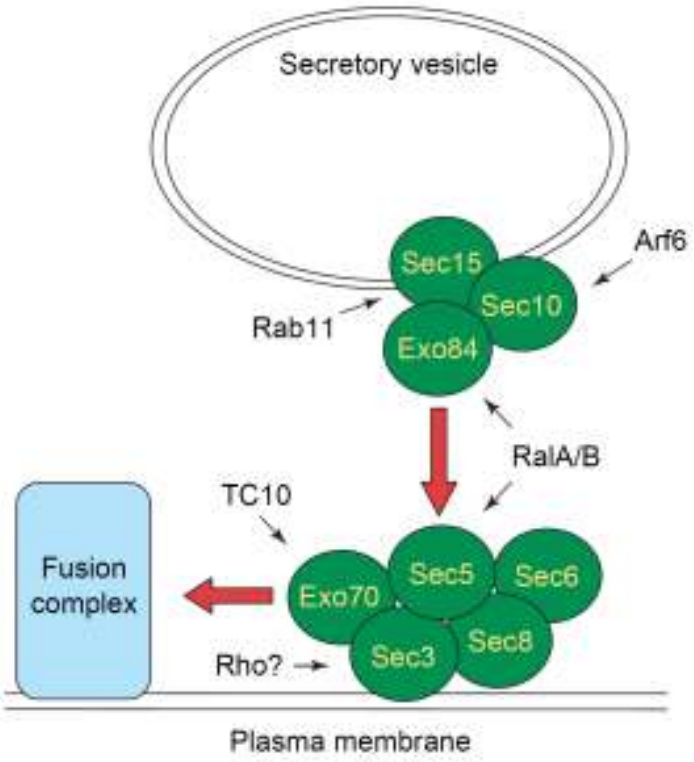

Figure 1.12: Ral-Exocyst interaction. A schematic model of the localisation of the exocyst subunits as predicted by published reports. RalA/B regulates exocyst assembly and function through binding of the Exo84 or Sec5 subunits. Other GTPases may also modulate exocyst activity by binding to specific subunits. Adapted from Camonis and White (2005).

1.6.4 Biological functions of Ral GTPases

Ral GTPases are multifunctional proteins involved in a variety of cellular functions including endocytosis, exocytosis, cell migration, proliferation, and cell polarity (Jullien-Flores et al. 2000; Feig 2003; Wang et al. 2004; Lalli and Hall 2005; van Dam and Robinson 2006; de Gorter et al. 2008; Lalli 2009; Chen et al. 2011). Recently, an additional role for Ral GTPases has been described in the regulation of mitochondrial fission (Kashatus et al. 2011). Here we examine a few of the known functions of Ral GTPases, particularly focussing on roles in neurones and events related to cell migration.

Cell morphology

Besides influencing cytoskeletal remodelling in non-neuronal cells (Ohta et al. 1999; Sugihara et al. 2002), Ral GTPases have also been shown to regulate neuronal cell morphology. For example, neurite branching in cortical and sympathetic neurones has been shown to be reliant on the effects of both RalA and RalB (Lalli and Hall 2005). Here, active RalA or RalB enhanced the formation of neurite branches, which were enriched in actin filaments. Ral activation also correlated with PKC-mediated phosphorylation of growth-associated protein GAP-43, which regulates branching and axonal regeneration. Interestingly, RalA appeared to preferentially act through the exocyst complex to induce neurite branching possibly downstream of integrin signalling, whilst RalB promoted neurite branching mainly through its association with PLD (Lalli and Hall 2005). Thus, although both Ral isoforms appear to contribute to modelling of the actin cytoskeleton, the end result appears to be achieved via different effector molecules

Cell polarity

Several studies have highlighted an important role for the Ral-exocyst interaction in cell polarity (Moskalenko et al. 2002; Shipitsin and Feig 2004; Lalli 2009). In polarised epithelial cells, inhibiting Ral function or its interaction with the Sec5 subunit of the exocyst, results in mislocalisation of basolateral membrane proteins to the apical surface. This suggests that the Ral-exocyst interaction does not influence fusion of vesicles itself, but specifically directs them to the appropriate

location (Moskalenko et al. 2002). Detailed investigation has revealed that RalA is the isoform that associates with Sec5 to regulate vectorial delivery. This preferential association with RalA over RalB was found to be due to a greater affinity of RalA for the exocyst as well as differences in the localisation of the two proteins. Whilst both RalA and RalB were enriched at the plasma membrane, only RalA was enriched at recycling endosomes (Shipitsin and Feig 2004).

Regulation of the exocyst by Ral has also been implicated in initial axon specification in neurons. Depletion of RalA, but not RalB, in developing cortical neurones inhibited axon establishment, and resulted in unpolarised cells capable of extending only minor neurites. Interestingly, RalA was found at the tips of growing axons where it co-localised with exocyst complex subunits as well as the component of the polarity complex PAR-3. Perturbing the function of either RalA or the exocyst inhibited localisation of PAR-3 to the tips of growing neurites, thus impairing neuronal polarisation. Importantly, biochemical studied revealed an interaction between the exocyst and PAR-3, which was reliant on the activity of RalA. These results imply that RalA may influence neuronal polarity by controlling the localisation of the PAR (polarity) complex via an interaction with the exocyst to initiate axon growth (Lalli 2009).

Cell migration

Directed cell migration requires dynamic changes to the cell cytoskeleton as well as alterations to the cell membrane, key events that can be regulated by Ral GTPases. However, the specific isoform responsible for modulating migration as well as the effector that the Ral proteins associate with appear to differ depending on the system being examined. For example, chemotaxis of myoblasts in response to FGF-2, HGF or IGF-1 is mediated via Ras activation of Ral. In particular, the motogenic effect on myoblasts and activation of Ral by IGF-1 was also reliant on a rise in intracellular Ca^{2+}. Mutant Ral proteins unable to bind RalBP1 or PLD abolished chemotaxis of myoblasts in response to growth factors, thus pointing to RalBP1 and PLD as the main Ral effectors involved myoblast migration (Suzuki et al. 2000). In contrast, Rosse et al. (2006) found that a RalB-exocyst interaction was required for

directed migration of Normal Rat Kidney (NRK) cells in a scratch-wound migration assay. Here the authors report a need for RalB to bring about exocyst assembly and localisation to the leading edge, and therefore suggest that the delivery of secretory vesicles to the plasma membrane via RalB is a mechanism of bringing about the necessary morphological changes to promote cell migration (Rosse et al. 2006).

Migration of B cells and multiple myeloma cells in response to stromal cell-derived factor-1 (SDF-1) is also linked with activation of RalB. However, in this system induction of RalB activity was independent of both Ras and PI3K signalling (de Gorter et al. 2008). A similar observation was made in invasive human prostate and bladder cancer cell lines, in which depletion of RalB but not RalA inhibited motility (Oxford et al. 2005). Unexpectedly, depleting cells of both RalA and RalB did not affect migration, a phenomenon also observed in migrating NRK cells by an independent group (Rosse et al. 2006). These findings propose a possible antagonistic relationship between RalA and RalB in certain forms of migration.

One of the key steps that underlie metastasis is the loss of adhesiveness. In a prostate cancer cell line, loss of E-Cadherin resulted in re-location of the exocyst complex from Cadherin based adherens junctions found at the lateral membranes between adjacent cells, to the leading edge of migrating cells. In this situation, an interaction between RalA or RalB with the Sec5 subunit was found to be necessary for delivery of Golgi-derived vesicles containing α5 integrin to the leading edge. This study proposes a novel mechanism for Ral GTPases in migration, where the invasive phenotype of metastatic cells is achieved via Ral-mediated formation of new cell-substratum adhesions at the advancing edge (Spiczka and Yeaman 2008).

Secretion

The identification of the exocyst as an effector for Ral GTPases as well as the enrichment of Ral proteins on secretory vesicles soon instigated a flood of research investigating the potential role of Ral proteins in secretion. To date, a diverse range of cell types and extracellular signals have been associated with Ral-mediated secretion. These include exocytosis of secretory granules in response to membrane

depolarisation in PC12 cells (Moskalenko et al. 2002), thrombin induced release of Weibel-palade bodies containing von Willebrand factor by endothelial cells (Rondaij et al. 2004), and secretion of dense granules by platelets (Kawato et al. 2008). In all systems, an interaction between Ral and the Sec5 exocyst subunit was necessary to mediate this role of Ral GTPases. The regulation of secretion appears to be a role that is predominantly associated with RalA rather than RalB. Indeed, only RalA is specifically expressed by pancreatic β cells, and membrane depolarisation which leads to insulin secretion, activates RalA in a Ral-GDS dependent manner. Depletion of RalA inhibited insulin secretion in response to both depolarisation and glucose, and closer examination revealed fewer insulin containing vesicles docked at the plasma membrane (Lopez et al. 2008; Ljubicic et al. 2009).

RalA has also been implicated in the regulation of neurosecretion. The pre-synaptic terminal is abundant in secretory vesicles, yet only those docked at the plasma membrane, known as the readily releasable pool (RRP), are involved in secretion. It is currently believed that the size of this pool is regulated by both PKC and Ca^{2+}. Whilst activation of PKC via metabotropic glutamate receptors is thought to increase the size of the RRP, Ca^{2+} entry following depolarisation is thought to enhance refilling of the pool. In transgenic mice expressing DN RalA, glutamate release following membrane depolarisation was unaffected. However, PKC mediated enhancement of glutamate release, a mechanism thought to be involved in regulating synaptic plasticity, was markedly reduced. Similar to the findings in pancreatic β cells, there was a marked reduction in the number of glutamate vesicles docked at the plasma membrane in cells lacking RalA. In this manner, RalA may participate in regulating synaptic plasticity mediated by PKC by orchestrating the docking of glutamate vesicles to the pre-synaptic membrane (Polzin et al. 2002).

1.7 Aim: Investigate the molecular mechanisms that regulate RMS neuroblast migration in the postnatal brain

The vast majority of research examining neuroblast migration in the postnatal/adult brain has focussed on determining the extracellular signals present in the SVZ and RMS. We were particularly interested in how these diverse signals are interpreted and co-ordinated by migrating neuroblasts in this region. Since the eCB system is involved in the control of adult neurogenesis (Aguado et al. 2006; Palazuelos et al. 2006; Goncalves et al. 2008; Gao et al. 2010) and is instrumental in translating extracellular signals to direct axonal growth (Williams et al. 2003), we questioned whether it could also regulate RMS neuroblast migration. During our studies we also investigated signalling downstream of the CB receptors by examining a functional role for Ral GTPases in neuroblast migration, since these proteins can co-ordinate a number of biological processes including neuronal polarisation and migration (Lalli and Hall 2005; Lalli 2009; Jossin and Cooper 2011).

Thus, our primary aim was to investigate whether eCB-signalling and Ral GTPases regulate the migration of RMS neuroblasts in the postnatal brain. To achieve our goal we aimed to establish a range of *in vitro* and *in vivo* migration assays, which could be used to screen and validate regulators of neuroblast migration.

Chapter 2: Materials and Methods

2.1 Materials

2.1.1 Animals

P2-P3 mouse pups were bred from CD1 mice obtained from Charles River. P5-P7 Sprague Dawley Rat pups were obtained from Harlan. $RalA^{lox/lox}$, $RalA^{lox/lox}/RalB^{-/-}$, and wild type mice were a kind gift from Chris Marshall and Pascal Peschard (Institute of Cancer Research, London). Details regarding the generation of the transgenic mice can be found in Peschard et al, 2012, Current Biology, *in press*. All procedures were performed in accordance with U.K. Home Office regulations (Animals Scientific Procedures Act, 1986).

2.1.2 General solutions

Phosphate Buffered Saline (PBS)

One PBS tablet (Oxoid) dissolved in a 100 ml of water and autoclaved: KCl (0.20 g/l), KH2PO4 (0.2 g/l), NaCl (8 g/l) and Na2HPO4 (1.15 g/l).

Tris-buffered saline (10x)

0.5 M Tris-HCl pH 8, 1.5 M NaCl

TBS-T

1X TBS containing 0.1% Tween20

2.1.3 Cell culture

Cor-1 cell line

The Cor-1 cell line was kindly provided by the laboratory of Austin Smith (University of Cambridge, UK). Details regarding the derivation of this cell line can be found in Conti et al. (2005).

NS cell media

NS-A medium (Euroclone) supplemented with EGF (10 ng/ml; Peprotech), FGF-2 (10 ng/ml; Peprotech), 2 mM L-glutamine (Invitrogen), and N2 supplement (Invitrogen).

Dissection media

Hank's Buffered Salt Solution (HBSS; Invitrogen) containing 5 mM HEPES (Sigma), 100 units/ml penicillin G and 100 µg/ml streptomycin (Invitrogen).

Dissociation media

HBSS containing 0.25% trypsin (Gibco) and 40 µl of DNAse l (1 mg/ml; Worthington).

Neurobasal complete media

Neurobasal medium (Gibco) containing B27 supplement, 2 mM L-glutamine (Invitrogen), and 0.6% glucose (Sigma).

3D migration gel

BD Matrigel™ (Basement Membrane Matrix, Growth Factor Reduced (GFR), Phenol Red-free; BD Bioscience) and Neurobasal complete media mixed in a 3:1 ratio respectively.

Brain slice collection media

Gey's Balanced Salt Solution (Invitrogen) supplemented with 0.45% glucose (Invitrogen)

Brain slice imaging media

Phenol red-free Dulbecco's Modified Eagle Medium (DMEM) supplemented with 0.5% glucose, B27 supplement, 4 mM L-glutamine, 10 mM HEPES (pH 7.4), 100 units/ml penicillin G and 100 µg/ml streptomycin (Invitrogen) and 5% foetal calf serum (FCS).

2.1.4 Western Blotting

General lysis buffer

50 mM Tris-HCl (pH 8), 150 mM NaCl, 10 mM $MgCl_2$, 1% Triton-X, 5% glycerol, and 2 mM $CaCl_2$ supplemented with 10 mM NaF, 1 mM Na_3VO_4, 1 mM PMSF, and complete protease inhibitors (Roche) prior to use.

4x Laemmli (Loading sample buffer)

100 mM Tris pH 6.8, 30% glycerol, 4% SDS, 0.2% bromophenol blue, 0.1 M DTT

SDS polyacrylamide gel

% Separating Gel	**7%**	**8%**	**10%**	**12%**
1.5 M Tris pH 8.8	5 ml	5 ml	5 ml	5 ml
Water	10.03 ml	9.37 ml	8.03 ml	6.7 ml
Acrylamide 30%	4.67 ml	5.33 ml	6.67 ml	8 ml
SDS 10%	200 µl	200 µl	200 µl	200 µl
APS 10%	75 µl	75 µ	75 µ	75 µ
TEMED	20 µl	20 µl	20 µl	20 µl

Stacking Gel	**4%**
0.5 M Tris pH 6.8	1.25 ml
Water	3 ml
Acrylamide 30%	0.70 ml
SDS 10%	20 µl
APS 10%	37.5 µl
TEMED	10 µl

Running buffer (10x)

0.25 M Tris, 1.92 M Glycine, 1% SDS (Flowgen Bioscience)

Transfer buffer

25 mM Tris, 0.19 M glycine, 20% methanol, and 0.01% SDS.

Blocking/Primary antibody/Secondary antibody solution

TBS-T containing 5% semi-skimmed milk.

Antibody stripping solution

Re-blot plus strong (Millipore)

Antibodies used for Western blot analysis

Antibody	Source	Species/Conjugate	Dilution
Actin	Cell signalling	Rabbit	1:4000
RalA	BD Bioscience	Mouse	1:4000 - 1:5000
RalB	R&D systems	Rat	1:500
Rap1 A/B	Cell signalling	Rabbit	1:1000
Rap1B	Sigma	Rabbit	1:1000
PAK1	Cell signalling	Rabbit	1:4000
PAK2	Cell Signalling	Rabbit	1:1000
PAK3	Cell signalling	Rabbit	1:1000
PAK4	Cell signalling	Rabbit	1:1000
PAK1 (αPak C-19)	Santa Cruz	Rabbit	1:500
Total Pak (Pak 1,2,3)	Santa Cruz	Rabbit	1:1000
P27kip1	Santa Cruz	Rabbit (SC-528)	1:100 – 1:500
p-P27kip1	Abcam	Rabbit (S10)	1:2000
MLC2	Cell Signalling	Rabbit	1:1000
P-MLC2 (ser19)	Cell Signalling	Mouse	1:1000
DAG-Lα	Gift from Dr. Masahiko Watanabe	Goat	1:3000
DAG-Lβ	(Bisogno *et al.*, 2003)	Rabbit	1:5000
FAAH	Abcam	Mouse	1:1000
MAG-L	Abcam	Rabbit	1:100
Goat-Anti Mouse	Thermo Scientific	HRP	1:5000
Goat-Anti Rabbit	Thermo Scientific	HRP	1:5000
Goat- Anti Rat	Thermo scientific	HRP	1:5000

2.1.5 Pull down assay reagents

RalA pull down lysis buffer

50 mM Tris-HCl pH 7.5, 10 mM $MgCl_2$, 200 mM NaCl, 2% NP-40, 10% glycerol, supplemented with 1 mM PMSF, 10 µg/ml aprotinin, 10 µg/ml leupeptin, 1 mM Na_3VO_4 and 1 mM DTT prior to use.

RalA pull down wash buffer

25 mM Tris-HCl pH 7.5, 30 mM $MgCl_2$, 40 mM NaCl, 1% NP-40, supplemented with 1 mM PMSF, 10 µg/ml aprotinin, 10 µg/ml leupeptin, and 1 mM DTT prior to use.

Rap1 pull down lysis/wash buffer

50 mM Tris-HCl pH 7.4, 2.5 mM $MgCl_2$, 500 mM NaCl, 1% NP-40, 10% glycerol supplemented with 10 µg/ml aprotinin and 10 µg/ml leupeptin prior to use.

GTPase activation assay

Ral assay reagent (300 µg of RalBP1 in 600 µl of agarose slurry; Millipore). Rap1 assay reagent (650 µg of Ral GDS-RBD in 1 ml glutathione-agarose slurry; Millipore).

2.1.6 Molecular Biology

Small interfering RNA

RalA siRNA: AGACTACGCTGCAATTAGA (Dharmacon) (Lalli and Hall 2005)

Small hairpin RNA (shRNA) plasmid vectors

The following shRNA sequence duplexes (designed on the Ambion website) were cloned in-between the ApaI and EcorV sites of the pCA-b-EGFPm5 silencer 3 expression vector (Bron et al. 2004), a kind gift from Matthieu Vermeren. The control was based on a published sequence (Kawauchi et al. 2006). The Ral shRNA sequences were chosen in order to target RalA in different regions. Ral (3) was designed to target the same region as the RalA siRNA.

Control: CGCGCATAAGATTAGGGAATTCAAGAGATTCCCTAATCTTATGCGCGTATTTTTT
CCGGGCGCGTATTCTAATCCCTTAAGTTCTCTAAGGGATTAGAATACGCGCATAAAAAA

Target sequence: TACGCGCATAAGATTAGGGAA

RalA (1): GTGCAGATCGACATCTTAGTTCAAGAGACTAAGATGTCGATCTGCACTTTTTT
CCGGCACGTCTAGCTGTAGAATCAAGTTCTCTGATTCTACAGCTAGACGTGAAAAAA
Target sequence: AAGTGCAGATCGACATCTTAG

RalA (2): CAAGAGAATCAGAGAAAGATTCAAGAGATCTTTCTCTGATTCTCTTGGCTTTTTT
CCGGGTTCTCTTAGTCTCTTTCTAAGTTCTCTAGAAAGAGACTAAGAGAACCGAAAAAA
Target sequence: GCCAAGAGAATCAGAGAAAGA

RalA (3): ACTATGCTGCAATTAGAGATTCAAGAGATCTCTAATTGCAGCATAGTCCTTTTTT
CCGGTGATACGACGTTAATCTCTAAGTTCTCTAGAGATTAACGTCGTATCAGGAAAAAA
Target sequence: GGACTATGCTGCAATTAGAGA

RalA (4): GGCAGGTTTCTGTAGAAGATTCAAGAGATCTTCTACAGAAACCTGCCTTTTTT
CCGGCCGTCCAAAGACATCTTCTAAGTTCTCTAGAAGATGTCTTTGGACGGAAAAAA
Target sequence: AAGGCAGGTTTCTGTAGAAGA

pCAG vectors

pCX-EGFP was a kind gift from Dr Masaru Okabe (Osaka University, Japan).

Human WT RalA, constitutively active RalA (RalA72L), fast cycling RalA (RalA39L), and dominant negative RalA (RalA28N) sequences were obtained by PCR from a pRK5-myc construct (Lalli and Hall 2005; Lalli 2009) using the following primers:
5'GAATTGGCTAGCATGGAGCAGAAGCTGATCTCCGAGGAGG3'
5'TCTGCAGATCGATTTATAAAATGCAGCATCTTTCTCTG3'
PCR products were inserted into a pCAG-IRES-EGFP plasmid vector (Jacobs et al. 2007; Causeret et al. 2009), a kind gift from Dr Meggie Nikolic (Imperial College School of Medicine, London, UK).

pCAG-Cre-IRES2-EGFP (plasmid 26646; Addgene) (Woodhead et al. 2006).

RalA FRET sensor

Raichu-RalA was kindly provided by M. Matsuda (Takaya et al. 2004; Yoshizaki et al. 2006)

2.1.7 Drugs and factors

List of drugs used

Drug	Description	Concentration Range	Source
ACEA	CB1 receptor agonist	0.5 µM-1 µM	Tocris Bioscience
AM-251	CB1 receptor antagonist	0.5 µM-1 µM	Tocris Bioscience
LY-320135	CB1 receptor antagonist	0.5 µM	Tocris Bioscience
JWH-133	CB2 receptor agonist	0.5 µM-1 µM	Tocris Bioscience
JWH-056	CB2 receptor agonist	1 µM	Tocris Bioscience
JTE-907	CB2 receptor antagonist	0.5 µM-1 µM	Tocris Bioscience
AM-630	CB2 receptor antagonist	0.5 µM	Tocris Bioscience
HGF	Growth factor	50 ng/ml	Peprotech
GDNF	Growth factor	100 ng/ml	Peprotech
Roscovitine	CDK5 antagonist	1 µM	Sigma
Mitomycin C	Applichem	50-100 ng/ml	Applichem

Pharmacology of eCB drugs

Agonist/ Antagonist	Drug	Ki value (nM) at CB1	Ki value (nM) at CB2	Selectivity	Reference
CB1 agonist	ACEA	1.4	>2000	1400 fold selectivity over CB2	(Hillard et al. 1999)
CB1 antagonist	AM-251	7.49	2290	300 fold selectivity over CB2	(Gatley et al. 1996; Gatley et al. 1997)
CB1 antagonist	LY-320135	141	14900	100 fold selectivity over CB2	(Felder et al. 1998)
CB2 agonist	JWH-056	10000	32	312 fold selectivity over CB1	(Molina-Holgado et al. 2007)
CB2 agonist	JWH-133	677	3.14	200 fold selectivity over CB1	(Huffman et al. 1999)
CB2 antagonist	JTE-907	1050	0.38	2760 fold selectivity over CB1	(Iwamura et al. 2001)
CB2 antagonist	AM-630	5152	31.2	165 fold selectivity over CB1	(Ross et al. 1999)

2.1.8 Immunocytochemistry

Fixative

4% paraformaldehyde (PFA) in PBS, pH 7.4

Blocking/Permeabilising solution

2% bovine serum albumin (BSA), 0.25% porcine skin gelatin type A (Sigma), 0.2% glycine, 15% FCS, 0.1% Triton-X.

Primary/Secondary antibody solution

1% BSA, 0.25% porcine skin gelatin type A (Sigma)

Blocking/Permeabilising/primary/secondary antibody solution for explants in Matrigel

15% goat serum, 0.3% Triton-X, 0.1% BSA in PBS

Mounting media

Fluorescent mounting media (Dako)

Antibodies for immunocytochemistry and other fluorescent reagents

Antibody/Dye	Source	Species/Conjugate	Dilution
PSA-NCAM	Sigma	Mouse monoclonal	1:100
DCX	Abcam	Rabbit polyclonal	1:100
βIII Tubulin	Sigma	Mouse monoclonal	1:100
GFAP	Dako	Rabbit polyclonal	1:200
RalA	BD Bioscience	Mouse monoclonal	1:250
GFP	Invitrogen	Rabbit polyclonal	1:4000
N-Cadherin (cytoplasmic)	BD Bioscience	Mouse monoclonal	1:200
N-Cadherin (external)	Sigma	Mouse monoclonal	1:100
Pak1 (αPak c-19)	Santa Cruz	Rabbit polyclonal	1:100
γ tubulin	Sigma	Mouse monoclonal	1:400
DAG-Lα	Abcam	Goat	1:100
CB1 receptor	Gift from Dr. Maurice Elphick	Rabbit	1:100
CB1 receptor	Gift from Dr. Ken Mackie	Rabbit	1:100
CB2 receptor	Cayman	Rabbit	1:300
Cleaved caspase 3	Cell signaling	Rabbit	1:1600
cMyc	Abcam	Mouse	1:1000
Phalloidin A488	Invitrogen	N/A	1:400
Phalloidin Texas Red	Invitrogen	N/A	1:400
Hoechst	Sigma (B-2883)	N/A	1:10000
Goat Anti-Mouse	Invitrogen	Alexa 488	1:200
Goat Anti-Mouse	Invitrogen	Texas Red	1:200
Goat Anti-Rabbit	Invitrogen	Alexa 488	1:200
Goat Anti-Rabbit	Invitrogen	Texas red	1:200

2.1.9 Immunohistochemistry

Fixative for gelatine embedding

4% PFA in PBS

Block/Permeabilising/Primary antibody/Secondary antibody solution for PFA fixed gelatine embedded slices

1% BSA, 0.1% Triton-X, 0.1% sodium azide in PBS

Mounting media for gelatine embedded slices

Fluorescent mounting media (Dako)

Blocking buffer/Primary/Secondary antibody solution

1% BSA in 50 mM TBS pH7.6 and 0.1 % sodium azide

Dewaxing/Dehydrating

Xyelene and industrial methylated spirits (IMS) were used.

Antigen Retrieval Solutions

Stock solution: 20 g citric acid dissolved in 500ml of water. For working solutions of citric acid, stock solutions were diluted 1:100 and adjusted to pH6 using 5 M sodium hydroxide.

StreptABComplex/HRP

Equal parts of streptavidin and biotinylated HRP were mixed.

DAB Stock Solution (10%)

5 g of Diaminobenzidine tetrahydrochloride (Sigma D5637) were gradually dissolved in a fume hood in 50 ml of water heated to 45^0C. For a working solution 10% DAB stock was mixed with 200 µl hydrogen peroxide and 0.1 M Tris buffer (pH 7.6).

Antibodies for immunohistochemistry

Antibody/Dye	Source	Species/Conjugate	Dilution
Anti-GFP	Invitrogen	Rabbit polyclonal	1:1000
Hoechst	Sigma (B-2883)	N/A	1:5000
N-Catherin cytoplasmic	ECM Biosciences	Mouse monoclonal	1:1000
N-Catherin a.a 811-824	ECM Biosciences	Rabbit polyclonal	1:1000
Goat anti-rabbit	Invitrogen	Alexa488	1:1000
Goat anti-rabbit	Dako	biotinylated HRP	1:200
Goat anti-mouse	Dako	biotinylated HRP	1:200

2.2 Methods

2.2.1 Cell culture

Cor-1 Cell line

Cor-1 cells were cultured in 0.1% gelatine-coated T75 flasks (Nunc), and maintained at 37^0C and 8% CO_2 (standard conditions), in NS cell media. To passage confluent flasks, cells were trypsinised and collected in NS-A medium. The cell suspension was centrifuged at 13,000 rpm for 3 minutes, and the resulting pellet was re-suspended in 500 µl of NS cell media. Cells were plated out at a density of approximately $2x10^6$ cells per flask, and passaged every 2-3 days or upon reaching 80% confluency. For immunofluorescence, cells were plated onto 0.1% gelatin-coated glass coverslips at a density of 30,000-40,000 cells per well.

Primary RMS neuroblasts/explants

CD1 mice/Sprague Dawley rat pups, postnatal day 5-7 (P5-P7), were sacrificed by cervical dislocation and then decapitated. Brains were collected in dissection medium. The most caudal third of the brain was removed and discarded. The remaining section of the brain was cut into 1.4 mm coronal slices using a McIlwain Tissue Chopper. Slices were separated and the RMS was isolated from the tissue with the aid of a dissecting microscope. RMS explants were cut into fragments approximately 200-300 µm in diameter (Ward and Rao 2005).

Dissociated RMS neuroblasts

To obtain dissociated neuroblasts, RMS fragments were triturated with 2 ml of HBSS containing 0.25% trypsin (Gibco) and 40 µl of DNAse I (1 mg/ml; Worthington), and left at 37^0C for 2 minutes. The trypsin was inactivated with 5 ml of DMEM (Gibco) containing 10% FCS and the solution was centrifuged at 1,500 rpm for 5 minutes. After another two washes with DMEM + 10% FCS to remove any traces of trypsin, the pellet was re-suspended in pre-equilibrated (37^0C/5% CO_2) Neurobasal complete medium (Gibco) containing B27 supplement, 2mM L-glutamine (Invitrogen), and 0.6% glucose (Sigma). Cells were plated onto 6 well plates (1,000,000 cells/well) or glass coverslips (30,000-50,000 cells/coverslip) coated with polyornithine (0.5 mg/ml; Sigma) and laminin (10 µg/ml; Sigma). Cells were maintained in Neurobasal complete medium at 37^0C/5% CO_2 for 48-72 hours.

2.2.2 Nucleofection and electroporation

Nucleofection of RMS neuroblasts

Dissociated neuroblasts were obtained as previously described. Cells were pelleted and re-suspended in rat neuron nucleofection solution (Lonza) at a final concentration of approximately $3.5x10^6$ cells/100 µl for each nucleofection. Each sample was mixed with 3-9 µg of a DNA/shRNA vector or siRNA oligonucleotides, and transfected using program G-013 on the Nucleofector™ 2 device (Lonza). Each nucleofected sample was transferred to a Falcon tube containing DMEM + 10% FCS and centrifuged at 1,500 rpm for 5 minutes. For Western blot analysis, the resulting pellet was re-suspended in Neurobasal complete medium and cells were plated onto polyornithine (0.5 mg/ml; Sigma) and laminin (10 µg/ml; Sigma) coated 6 wells plates at a density of 1,000,000 cells/well. To create aggregates for 3D migration assays, the pellet was re-suspended in 30 µl of DMEM + 10% FCS, pipetted as a drop onto the inside of a p35 dish lid, and inverted over a dish containing 2 ml of Neurobasal complete medium. Hanging drops were transferred from the lid into the dish 5 hours later and cultured in suspension for 24-48 hours before embedding in Matrigel.

Electroporation of mouse pups

Postnatal day 2 (P2) mouse pups were anaesthetised with isofluorane (0.6 L/min). DNA vectors (approximately 3 µg) were injected into right ventricle using a pulled glass capillary (diameter 1.5mm; Clark) and electroporated using the following settings: 5 pulses 99.9 V, pulse on 50 ms, and pulse off 850 ms. Pups were returned to the mother and sacrificed 3-14 days later by cervical dislocation.

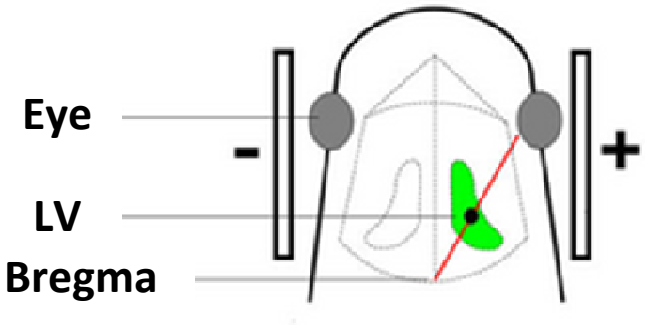

Figure 2.1: Electroporation. A schematic diagram showing the point of injection into the lateral ventricle. An imaginary line (red line) running from the bregma to the right eye was used as a positional marker. The injection site was determined as the point which is 1/3 of this distance from the bregma. Lateral ventricle (LV). Adapted from Boutin et al. (2008).

2.2.3 Western Blotting

Cells cultured in 6-well plates were placed on ice, washed with ice cold PBS three times, and lysed in 50-100 µl of the following lysis buffer: 50 mM Tris pH 8.0, 150 mM NaCl, 10 mM $MgCl_2$, 1 mM $CaCl_2$, 1% Triton-X-100, 5% glycerol, 10 mM NaF, 1 mM Na_3VO_4, 1 mM PMSF, and complete protease inhibitors (Roche). A higher concentration of NaF (15 mM) was used for analysis of phosphorylated proteins. For Cor-1 cell lysates, samples were rotated for 30 minutes at 4^0C, and then centrifuged at 12,000 rpm for 10 minutes at 4^0C. Protein concentration of the supernatant was determined using a BCA protein assay kit (Thermo Fisher Scientific). For primary RMS neuroblast cultures whole cell lysates were used. Samples were run on 7-12% SDS-polyacrylamide gel for 2 hours at 100 V, transferred onto PVDF membranes (Millipore) for 1 hour at 100 V, and blocked with 5% milk in TBS-T for 1 hour. All primary antibodies were diluted in 5% milk in TBS-T

and incubated overnight at 4^0C. Horseradish peroxidase (HRP)-conjugated secondary antibodies were also diluted in 5% milk in TBS-T and incubated for 1 hour at room temperature. Protein bands were visualised with Amersham Enhanced Chemiluminescence Western Blotting reagent (GE Healthcare) and Amersham hyperfilm (GE Healthcare).

2.2.4 RalA/Rap1 pulldown assay

RMS neuroblasts plated onto polyornithine and coated 6 well plates were lysed in 100 µl of RalA pull down lysis buffer or Rap1 pull down lysis/wash buffer. Lysates were collected and centrifuged at 14,000 rpm at 4^0C for 2 minutes. For each sample, 5 µl of the supernatant (input) was transferred to a clean tube, boiled with loading sample buffer at 100^0C for 5 minutes, and stored at -20^0C until required. The remaining supernatant was incubated with either 15 µl of Ral assay reagent or 40 µl of Rap1 assay reagent. A further 600 µl of lysis buffer was added to each sample before being subjected to gentle agitation on a rotator for 1 hour at 4^0C. The samples were then centrifuged for 5 seconds at 14,000 rpm to pellet the beads. The supernatant was discarded and the beads were washed with 900 µl of RalA pull down wash buffer or Rap1 pull down lysis/wash buffer. The beads were pelleted and washed 3 times before being boiled with loading sample buffer at 100^0C for 5 mins and stored at -20^0C until ready to be run on an SDS-PAGE gel.

2.2.5 Fluorescence resonance energy transfer (FRET)

FRET analysis was performed on fixed neuroblasts embedded in Matrigel expressing the Raichu-RalA construct. The acceptor photobleaching method (Kenworthy 2001) was used to evaluate FRET efficiency. The CFP and YFP fluorophores were excited with 458 nm and 514 nm lasers respectively. Bleaching of the acceptor fluorophore was achieved using the 514 nm laser set to 100% and 30 iterations. Pre- and post-bleaching images were captured on the LSM 710 Zeiss confocal microscope, and at least 15 or more cells were analysed per condition for each independent experiment. FRET efficiency was calculated using the AccPbFRET plugin in Image J software.

The following formula was used to calculate FRET efficiency:

$$\mathbf{FRET}_{\text{Efficiency}} = \frac{(\mathbf{Donor}_{\text{Post}} - \mathbf{BkGrd}_{\text{Post}}) - (\mathbf{Donor}_{\text{Pre}} - \mathbf{BkGrd}_{\text{Pre}})}{(\mathbf{Donor}_{\text{Post}} - \mathbf{BkGrd}_{\text{Post}})} \times 100$$

Donor$_{Post}$ = Donor emission after photobleach

BkGrd$_{Post}$ = Background emission after photobleach

Donor$_{Pre}$ = Donor emission prior to photobleach

BkGrd$_{Pre}$ = Background emission prior to photobleach

2.2.6 Migration assays

Scratch wound assay

Cor-1 cells were plated onto 0.1% gelatin-coated 24 well image-lock plates (Essen Instruments) containing 1 ml of growth medium, at a density of 800,000 cells/well. Cells were allowed to attach at room temperature for 30 minutes prior to incubation at 37^0C/8% CO_2 to reduce clumping. Once cells had become fully confluent (typically after 24 hours), a single uniform scratch (~800 µm in width) was made along the centre of each well using a scratch wound device (Essen Instruments). The medium was removed and the wells were washed twice with PBS to remove cell debris. NS cell medium containing drugs or vehicle was added to the wells immediately before filming. Three pre-determined points along each scratch were imaged using the Incucyte automated imaging platform (Essen Instruments) every 2 hours for 24 hours. The area of the wound infiltrated by migrating cells at 12 hours was calculated from the data generated by the Essen Incucyte software.

Explant migration assay/ Aggregate migration assay

RMS explants/aggregates were embedded in growth factor-reduced phenol red-free Matrigel (BD) on sterile glass coverslips and allowed to migrate for 24 hours in Neurobasal complete medium at 37^0C/5% CO_2. Drugs were added to the Matrigel solution as well as the culture media and were present throughout the incubation period. Images of fixed and immunostained explants/aggregates were captured on

the Zeiss Apotome at 5X, 10X and 20X objectives. For quantification of distance migrated, the distance from the edge of the explant/aggregate to the furthest migrated neuroblast perpendicular to the edge, was measured at 6 points around the periphery of the explant/aggregate using ImageJ software. Approximately 10 to 20 explants/aggregates were measured for each independent experiment. Explants/aggregates in direct contact with other explants/aggregates were excluded from the analysis. Explants/aggregates of varying sizes were used in the analysis, since we did not find a correlation between explant/aggregate size and distance migrated (verbal communication from Madeleine Oudin).

For live imaging of explant migration, RMS explants were embedded in Matrigel in a 4 chamber 35mm Hi-Q4 culture dish (Nikon). Images were captured on the Nikon Biostation (an automatic multipoint time-lapse imaging system with controlled environment maintained at 37^0C/5% CO_2) with a 20X and 40X objectives every 3 minutes for 24 hours. Frames were played at a frequency of 10 frames per second. Tracking analysis was performed using Volocity software (Perkin Elmer), and limited to the first 9 hours of filming. Since neuroblasts from within the explant emerged at different times during the filming period, cells were tracked for the first 4 hours of migration upon exiting the explant core. At least 40 cells were tracked for each condition in each experiment.

Migration in living brain slices

Mouse pups were sacrificed by cervical dislocation followed by decapitation 3-7 days post-electroporation. Brains were hemisected, and the right hemisphere (electroporated side) was mounted (midline face down) onto the Vibratome platform (Leica) using Roti Coll. Brains were cut into 300 µm-thick sagittal sections, and slices containing the olfactory bulb were examined under a microscope for GFP positivity along the RMS. Slices with a GFP signal were cultured on a Milli cell insert (30 mm Organotypic PTFE 0.4µm; Millipore) submerged in brain slice imaging media in a p35 dish for 1 hour. Milli cell inserts were then transferred to a p35 glass bottom dish (MatTek), containing the same media, for imaging. Z-stack (every 2-4 µm) images of GFP positive cells in the RMS were taken every 3 minutes for 3 hours

at 20X magnification on a Perkin Elmer UltraView VoX spinning disk system equipped with an inverted Nikon Ti-E microscope using a Nikon CFI Super Plan Fluor ELWD 20X/0.45 objective and a Hamamatsu Orca R2 camera. Movies were acquired and analysed using the Perkin Elmer Volocity software. For tracking analysis only cells that were present within the imaging area for the entire duration of the movie were analysed. Between 15 to 30 cells were tracked for each experiment.

2.2.7 Immunocytochemistry

Immunocytochemistry on cells in 2D

Coverslips were washed with PBS three times and fixed with 4% PFA for 20 minutes at room temperature. Cells were quenched with 50 mM ammonium chloride for 20 minutes, then permeabilised and blocked at room temperature for 15 minutes with PBS containing 0.1% Triton-X-100, 1% BSA, 0.1% Sodium Azide, 0.025% gelatin, and 10% FCS. Primary antibodies were diluted in PBS containing 1% BSA and 0.025% gelatin, and incubated overnight at 4^0C. Coverslips were then rinsed with PBS and incubated with Alexa Fluor 488 or Texas red-conjugated secondary antibody and Hoechst for 25 minutes. Coverslips were mounted using a commercial mounting solution (Dako).

Immunocytochemistry on Matrigel-embedded explants (3D)

Coverslips were fixed in 4% PFA at room temperature for 40 minutes, washed three times with PBS, and blocked and permeabilised with 15% goat serum, 0.3% Triton-X, 0.1% BSA in PBS for 1 hour at room temperature. Primary antibodies were diluted in the same solution and incubated overnight at 4^0C. Coverslips were washed three times with PBS and incubated with secondary antibodies and Hoechst (1:10,000; Sigma) - diluted in the same solution - for 2 hours at room temperature. Coverslips were washed with PBS and mounted using a fluorescent mounting medium (Dako). For the detection of external N-Cadherin, Triton-X-free block/antibody solution was used.

2.2.8 Immunohistochemistry

Gelatin-embedded sections

Electroporated brains were hemisected, fixed in 4% PFA overnight at 4^0C, and then embedded in 4% gelatine, which was left to set overnight at 4^0C. Gelatin-embedded brains were fixed in 4% PFA overnight at 4^0C to harden the gelatin, and then cut on a Vibratome into 75 µm-thick sagittal sections. Slices were blocked and permeabilised for 1 hour at room temperature in 1% BSA, 0.1% Triton-X, 0.1% sodium azide in PBS, and incubated with primary antibody overnight at 4^0C in the same solution. Secondary antibodies were also diluted in the same solution and incubated for 2 hours at room temperature. Slices were washed in PBS, mounted onto glass slides using Dako mounting media, and covered with a 22x50 mm coverslip. Z-stack (every 0.5 – 1.5 µm) images of the stream were captured on a Zeiss LSM 710 confocal microscope using a 40X objective.

For the purpose of quantification, the RMS was classified into four anatomically distinct regions (Region A: injection site; Region B: descending arm of the RMS; Region C: "elbow" preceding the RMS just before the OB; Region D: within the OB) as previously described (Belvindrah et al. 2011). Process length was measured as the distance from the base of the cell body to the tip of the leading process using ImageJ software. Measurements were taken from all cells in each image. To determine orientation, all cells with their leading process outside a 180^0 angle relative to the position of the OB were considered to be misoriented.

Paraffin-embedded section

Formalin-fixed P8 mouse brains were embedded in paraffin and cut into 6 µm-thick sagittal sections. Slices were deparaffinised and rehydrated prior to heat-induced antigen retrieval using a sodium citrate buffer. Slices were then blocked and incubated with the primary antibody overnight at 4^0C. Biotinylated secondary antibodies were incubated at room temperature and detected with StreptABComplex/HRP, and subsequently developed in DAB solution and counter stained with haematoxylin. Sections were dehydrated in 100% IMS, cleared in Xyelene and mounted in DPX plastic.

2.2.9 Statistical analysis

Student's 2-sided T-test was used for all statistical analysis where variance was equal, or a Mann Whitney U test was used if equal variance was not present. Where shown, * $P < 0.05$, ** $P < 0.01$, *** $P < 0.001$. For all graphs, the error bars represent the standard error of the mean (SEM). We have used the SEM in order to describe the confidence in the estimated value of the mean, rather than the use of the standard deviation (SD) to describe the variability within the data set (Altman and Bland 2005).

Chapter 3: Endocannabinoids regulate RMS neuroblast migration

3.1 Introduction

The eCB system has been previously implicated as a regulator of cell migration (Song and Zhong 2000; Berghuis et al. 2005; Miller and Stella 2008). Whilst CB2 receptor activation in immune cells has been associated with both enhancement and inhibition of migration depending on the specific cell type (Miller and Stella 2008), activation of the CB1 receptor appears to be necessary for chemotaxis of GABAergic cortical interneurones (Berghuis et al. 2005). During CNS development, signalling via the CB1 receptor is a crucial event in the guidance of axons to their target regions (Williams et al. 1994; Williams et al. 2003). Both axon guidance and neural precursor migration are closely related processes, and rely on cytoskeletal changes in response to extracellular cues (Lambert de Rouvroit and Goffinet 2001). Moreover, molecules traditionally associated with axon guidance, such as Slits and netrin-1, have also been shown to regulate the migration of adult neural precursors (Hu 1999; Wu et al. 1999; Murase and Horwitz 2002; Ward et al. 2003; Hakanen et al. 2011). The evidence of a functional eCB tone regulating neurogenesis in the adult SVZ (Jin et al. 2004; Aguado et al. 2006; Palazuelos et al. 2006; Goncalves et al. 2008; Gao et al. 2010), and the expression of both CB1 and CB2 receptors on adult neural precursors (Jiang et al. 2005; Palazuelos et al. 2006; Molina-Holgado et al. 2007), raises the question as to whether CB signalling also regulates the migration of neural precursors in the adult brain. Thus, based on the ability of the eCB system to participate in cell migration and axon guidance, and the existence of a functional eCB system in the SVZ, we set up a series of *in vitro* and *in vivo* migration assays to explore whether the eCB system may also regulate RMS neuroblast migration.

3.2 Results

3.2.1 Activation of CB receptors increases the motility of Cor-1 cells

In the first stage of this project, we used the Cor-1 NS cell line as a model system to assess the ability of CB receptor agonists to regulate neural precursor migration. Even though the range of transcription factors present in these cells may be influenced by the *in vitro* environment, and may not reflect the true neural progenitor state, this cell line represent a valuable model system for initial studies that can be further validated in primary neural progenitors. The Cor-1 cell line is a NS cell line derived from the cortex of E16.5 mouse embryos, and can be continuously expanded in the presence of epidermal growth factor (EGF) and fibroblast growth factor-2 (FGF-2). Cor-1 cells express markers that are characteristic of neurogenic radial glia (nestin, RC2, vimentin, 3CB2, SSEA1/Lex1, Pax6, and prominin), are comparable to NS cells derived from ES cells and the adult SVZ, and can be differentiated into both neurones and astrocytes (Conti et al. 2005; Pollard et al. 2006). In addition, they display an elongated bipolar morphology and migratory ability with inter-kinetic nuclear movement similar to neuroepithelial and radial glia cells *in vivo* (Conti et al. 2005). Interestingly, Cor-1 cells express neuroblast markers (DCX, βIII tubulin, and PSA-NCAM) (Doetsch et al. 1997; Koizumi et al. 2006; Ocbina et al. 2006) (Figure 3.1A), as well as components of the eCB system including DAG-Lα/β, MAG-L, FAAH (Figure 3.1B), and CB1/CB2 receptors (Dr Phillip Sutterlein et al, Molecular and Cellular Neuroscience, *in press*). Hence, this cell line lends itself as a useful model for screening potential regulators of neural progenitor migration and can be used to evaluate the role of CB signalling in this process.

To test the hypothesis that the CB system regulates neuronal migration, we examined the effect of CB2 receptor activation on random cell motility using time-lapse imaging of Cor-1 cells treated with the CB2 agonist JWH-056 (1 μM) (Arevalo-Martin et al. 2007; Molina-Holgado et al. 2007). Our initial assessment was focused on the CB2 receptor due to the fact that activation of this CB receptor alone enhanced neurogenesis in the aged SVZ (Goncalves et al. 2008).

A

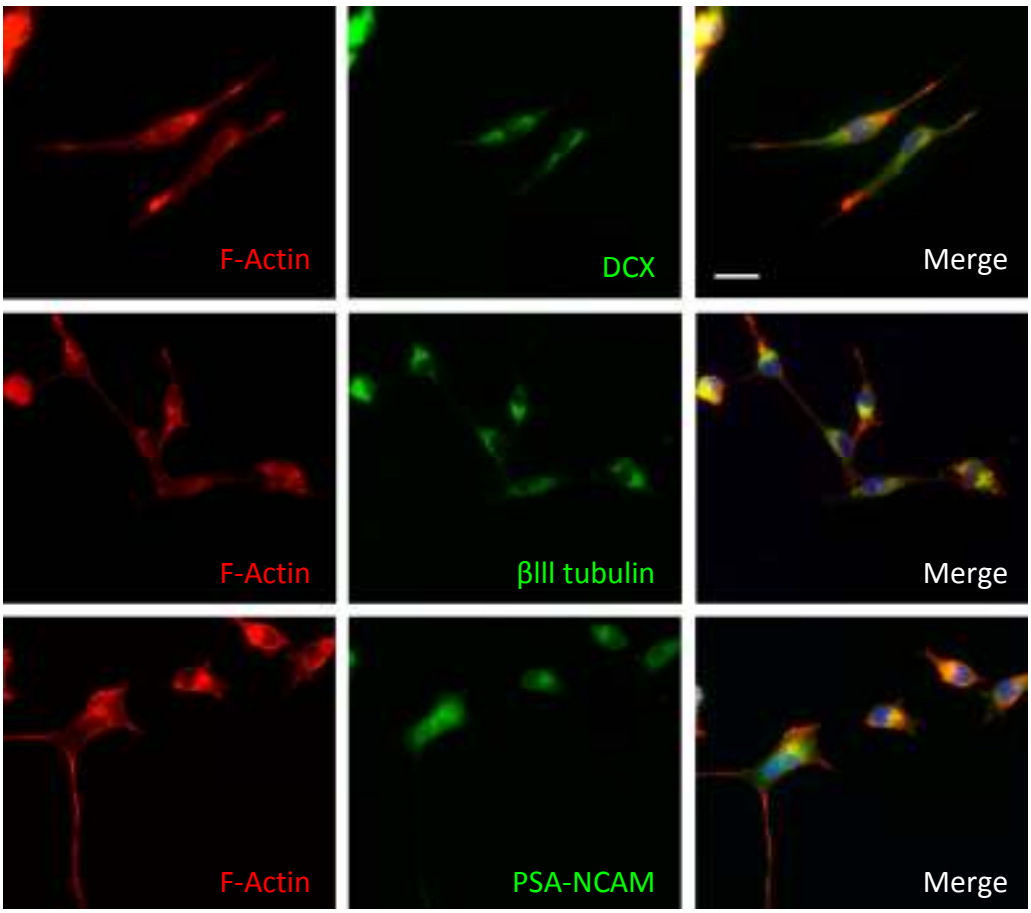
F-Actin
DCX
Merge
F-Actin
βIII tubulin
Merge
F-Actin
PSA-NCAM
Merge

B

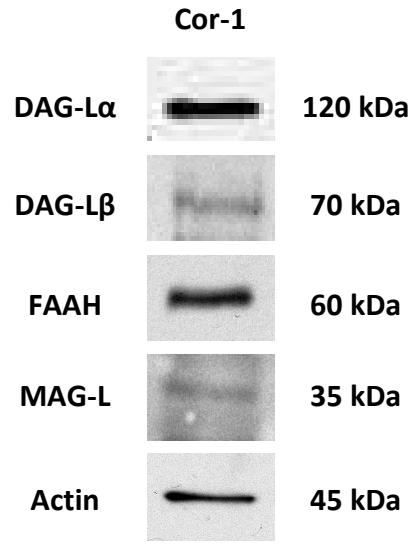
Cor-1
DAG-Lα
120 kDa
DAG-Lβ
70 kDa
FAAH
60 kDa
MAG-L
35 kDa
Actin
45 kDa

Figure 3.1: Cor-1 cells express markers of neural precursors and eCB synthesising/metabolising enzymes. (A) Cor-1 cells show positive staining for markers of neural precursors (DCX, βIII-Tubulin, and PSA-NCAM). Bar = 20 µm. **(B)** Western blot analysis of Cor-1 cell lysates shows expression of eCB synthesising enzymes (DAG-Lα and DAG-Lβ) and metabolising enzymes (MAG-L and FAAH) (PhD thesis of Madeleine Oudin).

Since cells from different flasks showed variation in basal motility (general observation), each treatment group was compared against control cells derived from the same flask. The experiment was repeated on two separate occasions (Test 1 and Test 2). As previously described by the creators of the cell line, Cor-1 cells display a bipolar morphology and show evidence of inter-kinetic nuclear movement (Supplementary movie 1). Interestingly, contact-mediated inhibition of locomotion can also be observed in these cells (Supplementary movie 2): a phenomenon first described by Michael Abercrombie (Abercrombie and Heaysman 1953; Abercrombie and Heaysman 1954) and now attributed to adhesion molecules and signaling via Rho GTPases (Huttenlocher et al. 1998; Grosheva et al. 2001). The trajectories of all cells tracked from Test 1 are shown in Figure 3.2A. Though at first glance the trajectories of JWH-056 treated Cor-1 cells appear longer than those of the control, it was not possible to compare the lengths of trajectories between groups since tracking was terminated if the cells underwent division or collided with one another, and was only resumed once the cells were moving freely. This resulted in the software program registering more than one trajectory for the same cell. Hence, in reality, the trajectories are actually longer than those shown. The mean velocity of JWH-056 treated Cor-1 cells in Test 1 (1.33 μm/min ± 0.06), was significantly greater (71%) than that of its control (0.78 μm/min ± 0.07) (Figure 3.2B). Similarly, the mean velocity of Cor-1 cells treated with JWH-056 in Test 2 (1.58 μm/min ± 0.03) was also significantly greater (22%) than its corresponding control (1.29 μm/min ± 0.04) (Figure 3.2B). Despite considerable variability in basal motility in the two tests, on both occasions the CB2 agonist significantly enhanced Cor-1 cell migration.

3.2.2 Stimulation of CB receptors promotes migration of Cor-1 cells in the scratch wound assay

The scratch wound assay is a simple, effective, and well-established method for studying the migration of cells *in vitro* (Liang et al. 2007). In this assay, a scratch is made in a confluent monolayer of cells, and the rate of wound closure is used as a measure of migration. One of the advantages of using this assay, is that it is a reconstruction of *in vivo* migration of cells in response to a wound, and is also

A

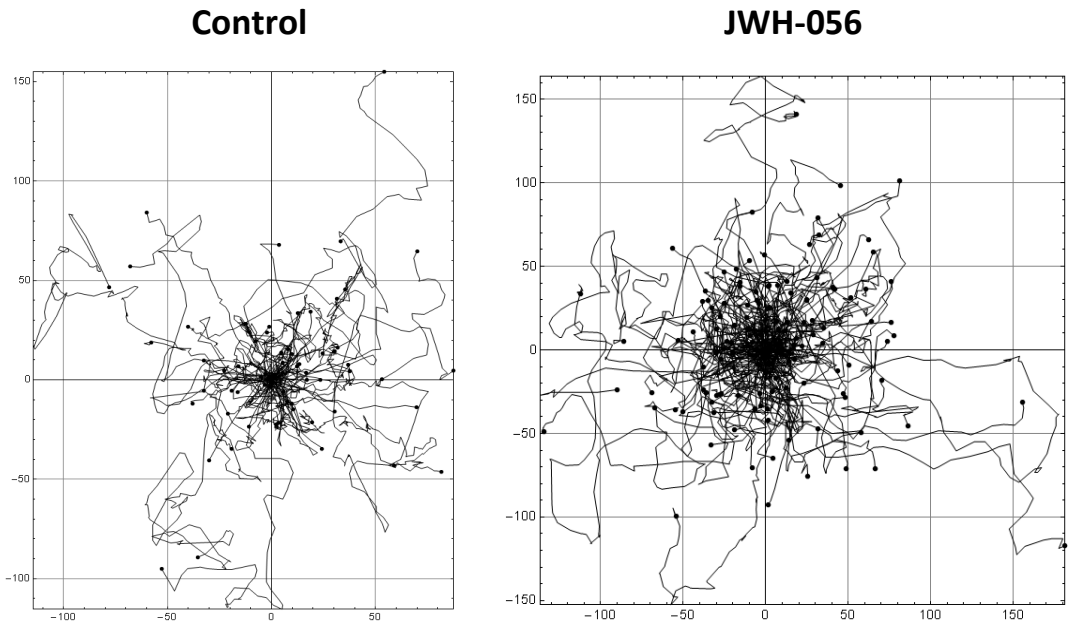
Control
JWH-056
150
100
50
0
−50
−100
−150
−100
−50
0
50
100
150

B

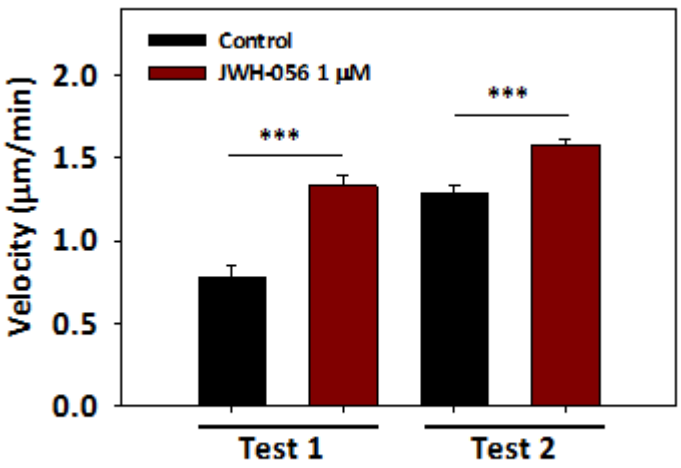
Control
JWH-056 1 µM
Velocity (µm/min)
2.0
1.5
1.0
0.5
0.0
***
***
Test 1
Test 2

Figure 3.2: A CB2 agonist increases random migration of Cor-1 cells. Cor-1 cells plated onto P35 dishes at a density of 70,000 cells per dish, were imaged every 3 minutes using time-lapse microscopy ± CB2 agonist JWH-056 (1 μM). The experiment was repeated on 2 separate occasions (Test 1 and Test 2). The trajectory of every cell imaged during the first 6 hours was tracked manually using the Andor tracking software and analysed with the Mathematica software. Tracking was terminated if the cells stopped to divide or if they were in direct contact with another cell. Tracking was resumed once the cell was freely moving. **(A)** Trajectories of control and JWH-056 treated cells from a single experiment (Test 1) with the origin set at 0 are shown as vector plots with the x and y axis scaled in μm. **(B)** Mean velocity of tracked cells from Test 1 and Test 2. Cor-1 cells treated with JWH-056 have a greater average velocity in comparison to the control in both Test 1 and 2. Each bar represents the mean ± SEM; ***$P < 0.001$; $331 \geq n \geq 63$, where n is the number of cells.

useful for investigating cell-cell interactions as well as the interaction of cells with the extracellular matrix (Liang et al. 2007). We used the Essen Instruments scratch wound device to achieve uniform scratches in all wells of a 24 well Essen image-lock plate (Figure 3.3, please refer to Methods page 97), and used the automated Incucyte imaging platform (Essesn Instruments) to acquire images of the wounds every 2 hours. In order to verify that the closure of the wound is a result of cell migration and not proliferation, we investigated the effects of the anti-proliferative agent Mitomycin C (Tomasz and Palom 1997) on the scratch wound test using Cor-1 cells. When Cor-1 cells are plated at approximately 10% confluence, Mitomycin C (50 ng/ml and 100 ng/ml) is able to inhibit proliferation by 70% (Figure 3.4A-B). Cells appear healthy and show no morphological evidence of toxicity following treatment with 100 ng/ml of Mitomycin C (Figure 3.4B). The same concentrations of the anti-proliferative drug had no effect on the rate of wound closure (Figure 3.4C), thereby proving that in our conditions the scratch wound assay is a measure of migration and not proliferation. It is also worthy to note that the rate of proliferation plateaus when cells approach 100% confluence. Therefore, it is unlikely that proliferation would have an impact in this assay, where the cells are already at maximum confluence.

The scratch wound test was used to examine the role of CB receptors in Cor-1 cell migration. Visual inspection of scratch wounds at 12 hours and 24 hours (Figure 3.5B), reveals that the CB1 agonist ACEA (0.75 µM) (Pertwee 2006) increases the migration of cells into the wound area in comparison to the control. This is particularly evident at 24 hours where the wound is entirely closed in CB1 agonist-treated wells. Quantification of the relative rate of migration (wound area infiltrated by migrating cells) (Figure 3.5A), shows that CB1 (ACEA 0.75 µM) and CB2 (JWH-133 1 µM) (Pertwee 2006) agonists enhance rate of wound closure, and this effect is inhibited by their respective antagonists (AM-251 1 µM and JTE-907 1 µM) (Gatley et al. 1997; Iwamura et al. 2001). Notably, the CB1 antagonist not only inhibited the pro-migratory effect of ACEA, but also inhibited the rate of wound closure to a level significantly lower than that of the control, thus suggesting the existence of an intrinsic eCB tone.

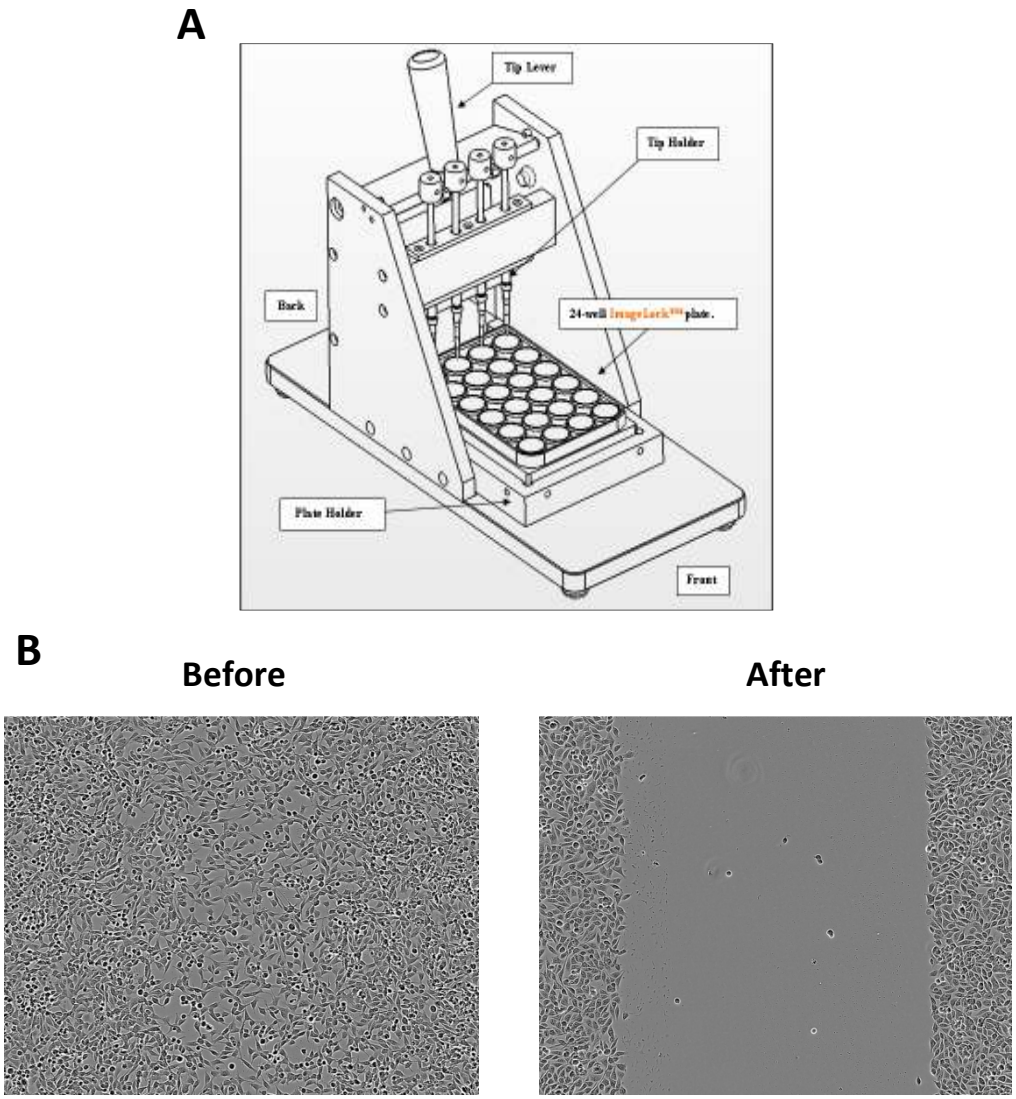

Figure 3.3: Scratch wound assay. (A) Schematic representation of the Essen Instruments scratch wound device. **(B)** Cor-1 cells were plated at a density of 800,000 cells/well in 24 well image-lock plates (Essen Instruments) and incubated for 24 hours. A single uniform scratch (~ 800 µm in width) was made in each well using the Essen Instruments scratch wound device, and the wounds were imaged every 2 hours using the Incucyte automated imaging platform (Essen Instruments). Images show snapshots of a well before (left) and immediately after (right) a scratch.

A

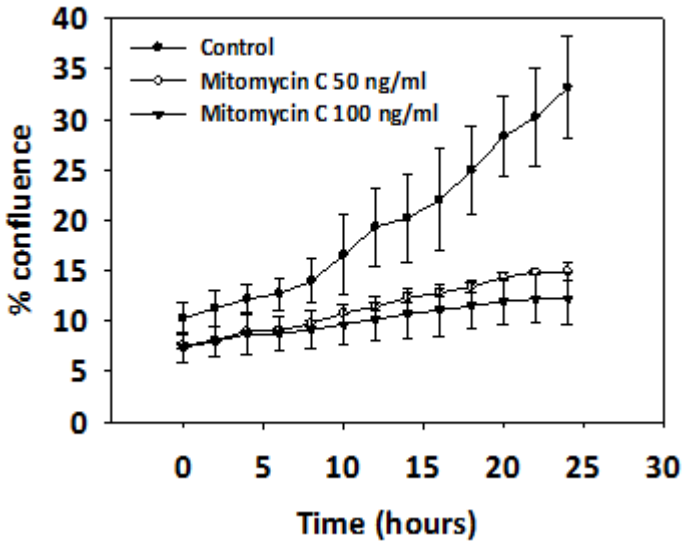
Control
Mitomycin C 50 ng/ml
Mitomycin C 100 ng/ml
% confluence
0
5
10
15
20
25
30
35
40
0
5
10
15
20
25
30
Time (hours)

B

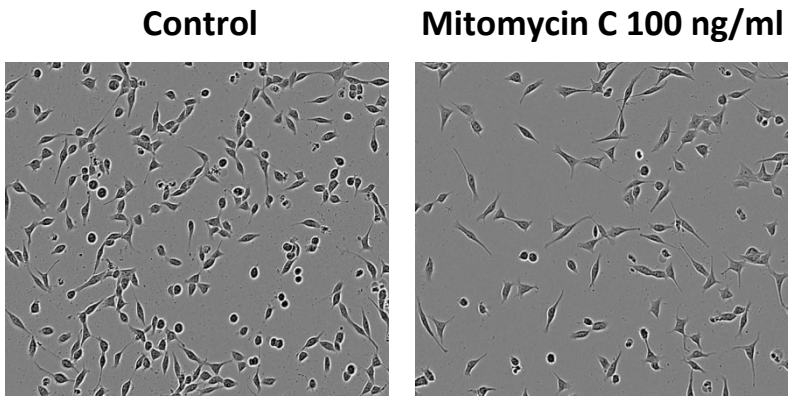
Control
Mitomycin C 100 ng/ml

C

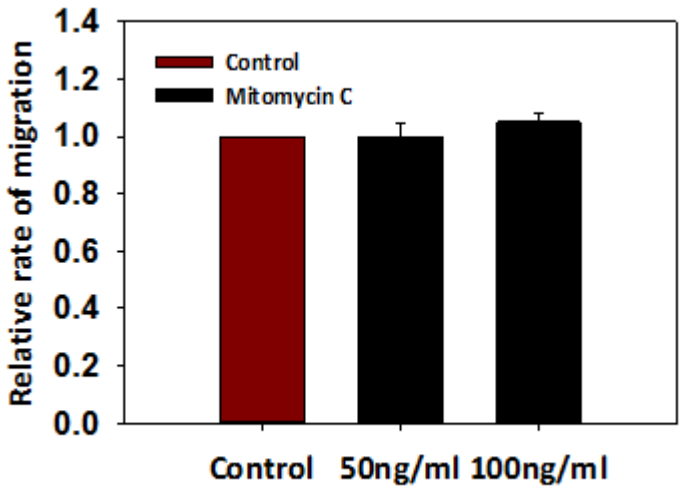
Control
Mitomycin C
Relative rate of migration
0.0
0.2
0.4
0.6
0.8
1.0
1.2
1.4
Control
50ng/ml
100ng/ml

Figure 3.4: Rate of migration is independent of proliferation in the scratch wound assay. (A) Cor-1 cells plated at a density of 100,000 cells/well in 24 well plates were incubated with the anti-proliferative agent Mitomycin C and imaged every 2 hours for 24 hours. Mitomycin C 100 ng/ml inhibits proliferation by approximately 70%. **(B)** Snapshots of control Cor-1 cells and Mitomycin C (100 ng/ml) treated Cor-1 cells taken 24 hours after addition of pharmacological agents. **(C)** Cor-1 cells were plated at a density of 500,000 cells/well in 24 well image-lock plates (Essen Instruments), and cultured overnight to obtain a confluent monolayer. Wells were scratched the following day and incubated with the indicated concentrations of Mitomycin C. Wounds were imaged every 2 hours for 24 hours. The rate of migration, as measured by the rate of wound closure, is unaffected by Mitomycin C. Each bar represents the mean ± SEM; n = 3 independent experiments. (Data from the PhD thesis of Madeleine Oudin).

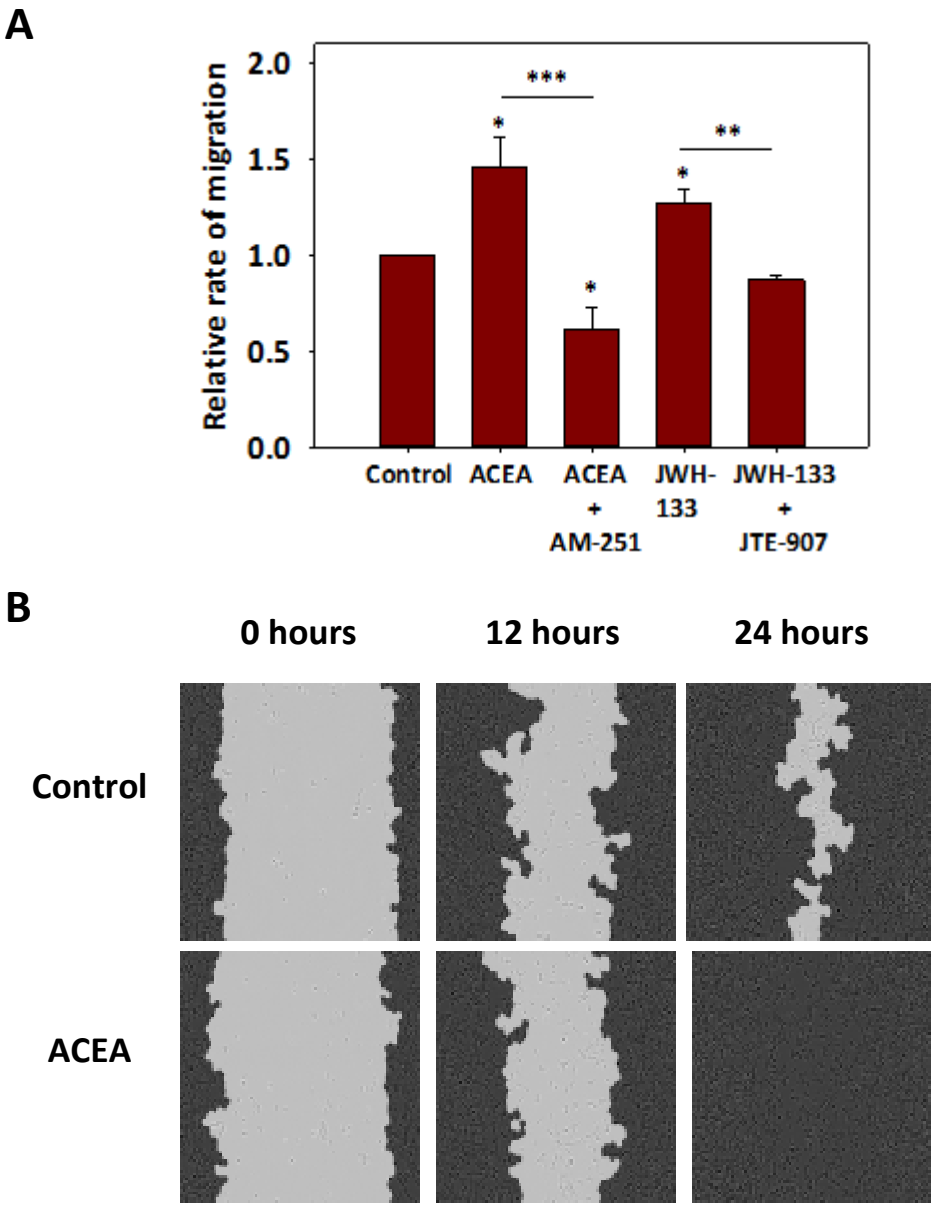

Figure 3.5: CBs regulate Cor-1 cell migration in the scratch wound assay. Cor-1 cells were plated at a density of 800,000 cells/well in image lock plates (Essen Instruments) and incubated overnight under standard condition to achieve a confluent monolayer of cells. The wells were scratched the following day and the wounds were imaged every 2 hours after addition of the indicated pharmacological agents: ACEA 0.75 µM (CB1 agonist), JWH-133 1 µM (CB2 agonist), AM-251 1 µM (CB1 antagonist), and JTE-907 1 µM (CB2 antagonist). **(A)** Quantification of the rate of migration (wound area infiltrated by migrating cells) reveals that CBs significantly increase the rate of migration of Cor-1 cells. This effect is successfully inhibited by their respective antagonists **(B)** Snapshots of control and ACEA treated cells at 0, 12 and 24 hours after the scratch show that ACEA causes faster closure of the wound. Grey regions indicate the area infiltrated by migrating cells. Each bar represents the mean ± SEM; *P < 0.05; **P < 0.01; n = 3 independent experiments.

3.2.3 Establishing an *in vitro* migration assay using primary RMS neuroblast cultures

Having ascertained that CB signalling can regulate the migration of a NS cell line in a 2-dimensional (2D) migration assay, we then decided to establish migration assays using primary cultures of RMS neuroblasts. This would provide a suitable model system to validate the role of CB signaling in RMS neuroblast migration, and also allow us to investigate the signaling cascade regulating migration downstream of the CB receptors.

We followed a published protocol describing a 3-dimensional (3D) neuroblast migration assay which can recapitulate the typical chain migration seen *in vivo* (Ward and Rao 2005). We isolated the RMS of P5-P6 mice (Figure 3.6A), which was cut into explants and embedded in the 3D matrix Matrigel. RMS explants cultures embedded in Matrigel show substantial migration of neuroblasts out of cultures after 24 hours (Figure 3.6B). Time-lapse imaging of these cultures shows that neuroblasts migrate mostly as chains, sliding over one another, and have a highly dynamic single leading process that extends and retracts as it senses the external environment (Supplementary movie 3). Once the leading process becomes established, a swelling forms in front of the nucleus, which then jumps towards the leading process, thereby propelling the cell forward (Schaar and McConnell 2005) (Figure 3.6C and Supplementary movie 3). Neuroblasts also display periods of immobility, during which the leading process extends and retracts, apparently sensing the extracellular environment. They can also change direction rapidly by re-organising the leading process and can migrate back into the explants as well as out (Supplementary movie 3). When cultured in Matrigel, these primary neuroblasts do not show evidence of proliferation (Supplementary movie 3), as confirmed by the virtual absence of immunoreactivity for the proliferation marker Ki67 (Madeleine Oudin, unpublished observations). However, evidence of neuroblast proliferation within the RMS *in vivo* has been described by several groups (Thomas et al. 1996; Doetsch et al. 1997; Nie et al. 2010).

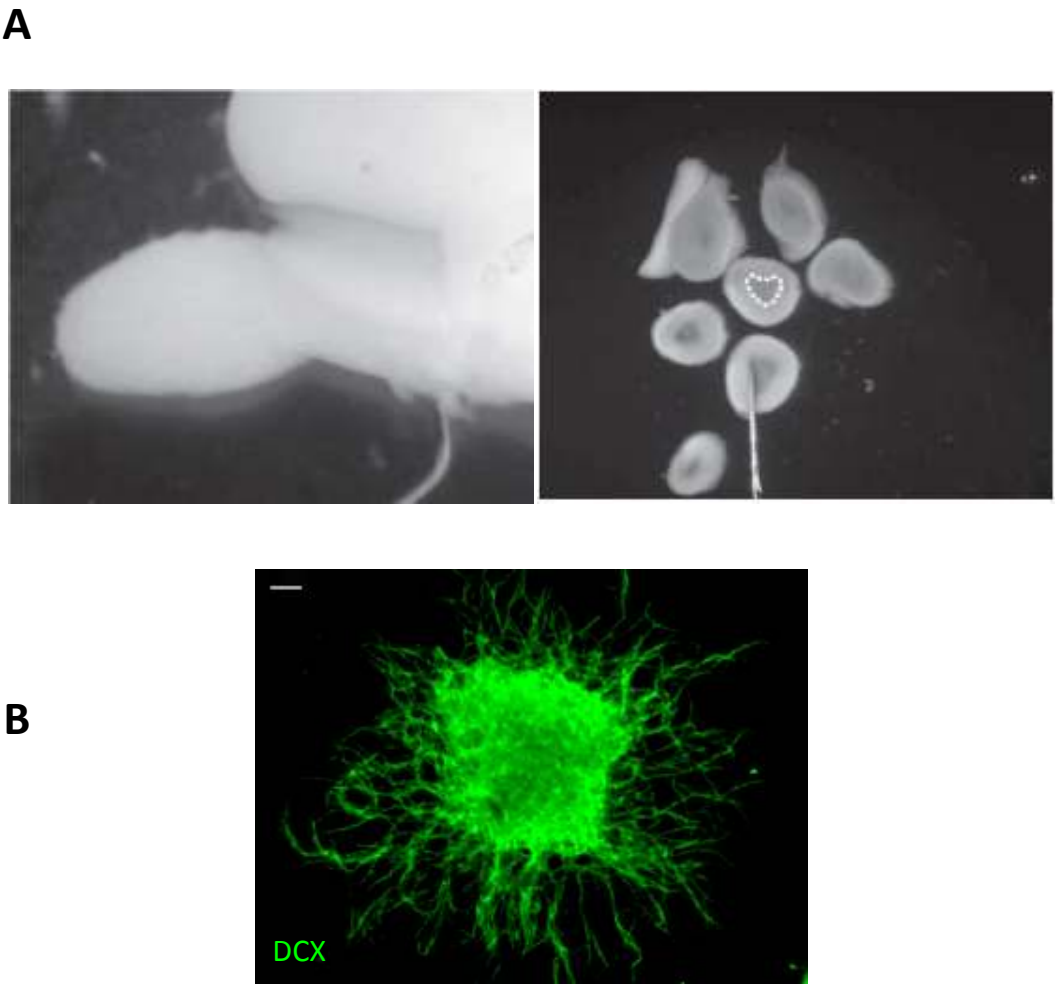

Figure 3.6: Mouse RMS neuroblasts migrate out of explants as chains when embedded in Matrigel. Mouse RMS explants were embedded in Matrigel, and allowed to migrate for 24 hours prior to fixation. **(A)** High magnification view of a mouse olfactory bulb (left) and coronal sections (~1.5mm in diameter) of the olfactory bulb (right). The dotted line outlines the RMS, which can be seen as a triangular, translucent, area in the centre of the section. Adapted from (Ward and Rao 2005) **(B)** Representative image of an RMS explants in Matrigel stained for the migratory neuroblast marker DCX. Neuroblasts migrate out of explants as chains, similar to their migratory behaviour *in vivo*. Bar = 50 µm. **(C)** Phase contrast images from time-lapse movies demonstrating the characteristic movement of a neuroblast migrating in Matrigel: (left) Establishment of a single leading process and swelling in front of the nucleus; (middle) movement of the nucleus towards the leading process (nucleokinesis); (right) extension of a new leading process.

Characterisation of RMS explant cultures by immunostaining for markers of migratory neuroblasts (DCX and PSA-NCAM) reveals that virtually all cells within the cultures are positive for both proteins (Figure 3.7). To assess the purity of the cultures, cells were stained for the neuronal marker βIII tubulin and the astrocytic marker GFAP (Bignami and Dahl 1974; Easter et al. 1993). The vast majority of cells isolated from the RMS express βIII tubulin. Very few cells express GFAP, and the expression of GFAP and βIII tubulin is mutually exclusive. GFAP-positive astrocytes are also morphologically distinct from βIII tubulin positive neuroblasts, having a typical astrocytic stellate morphology (Figure 3.8). RMS neuroblasts also express DAG-L, the enzyme responsible for the synthesis of the main eCB 2-AG, as well as both CB1 and CB2 receptors (Figure 3.9 A-B).

In order to examine the functional role of signaling pathways in neuroblast migration, we decided to establish a 3D migration assay using transfected primary neuroblasts. We initially optimized our experimental conditions by transfecting dissociated RMS neuroblasts with GFP via nucleofection. Cells were then re-aggregated into clusters using the hanging drop procedure (see Methods page 94). These re-aggregated cells successfully migrate out of clusters when embedded in Matrigel (Figure 3.10). Inspection of GFP expression reveals a high level of transfection, with more than 70% of neuroblasts expressing GFP (Figure 3.10). Importantly, nucleofection and expression of GFP does not impair neuroblast migration, as shown by comparison of the distance migrated by transfected and untransfected cells (Refer to chapter 5 Figure 5.14).

In summary, we successfully established a 3D *in vitro* migration assay, which allows us to assess the influence of pharmacological agents on RMS neuroblast migration, as well as perturb signaling cascades using nucleofection and re-aggregation procedures.

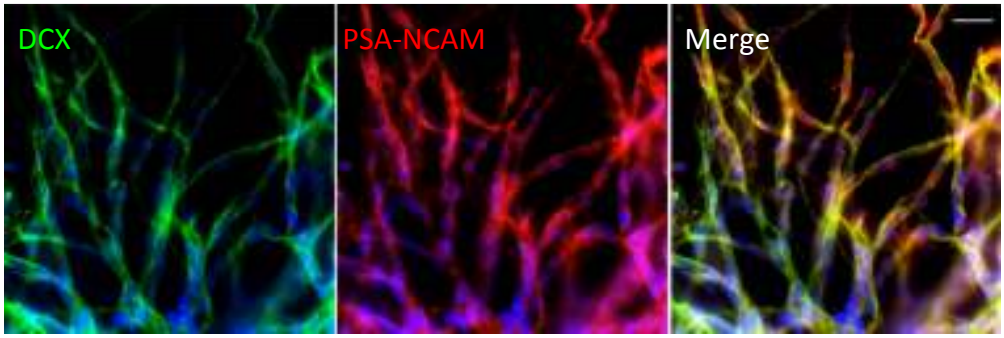

Figure 3.7: Mouse RMS explants cultures express markers of migratory neuroblasts. Mouse RMS explants were embedded in Matrigel, and allowed to migrate for 24 hours prior to fixation. All cells migrating out of RMS explants cultures express markers of migratory neuroblasts (DCX and PSA-NCAM). Bar = 20 µm.

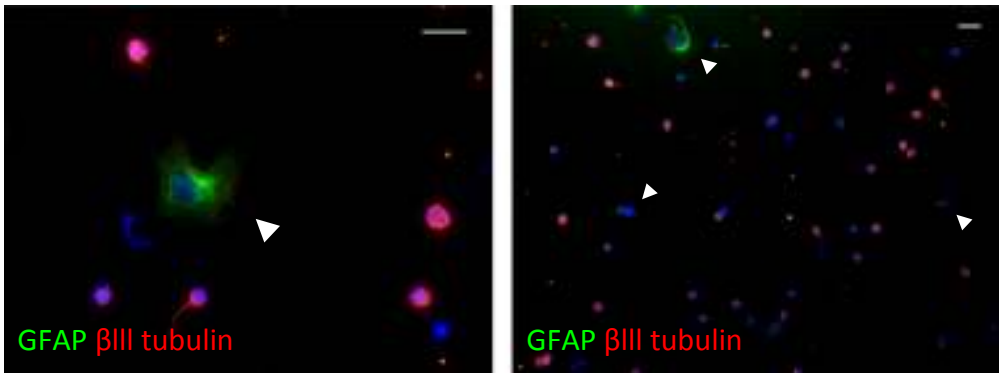

Figure 3.8: Mouse RMS cultures consist mostly of migratory neuroblasts. Dissociated mouse RMS cultures were plated on polyornithine/laminin coated coverslips and stained for markers of SVZ astrocytes (GFAP) and neuroblasts (βIII tubulin) 24 hours after plating. Cell nuclei are visualised by DAPI. GFAP and βIII tubulin expression are mutually exclusive, with the great majority of cells expressing βIII tubulin. White arrowheads point to GFAP positive astocytes. Bar = 20 µm

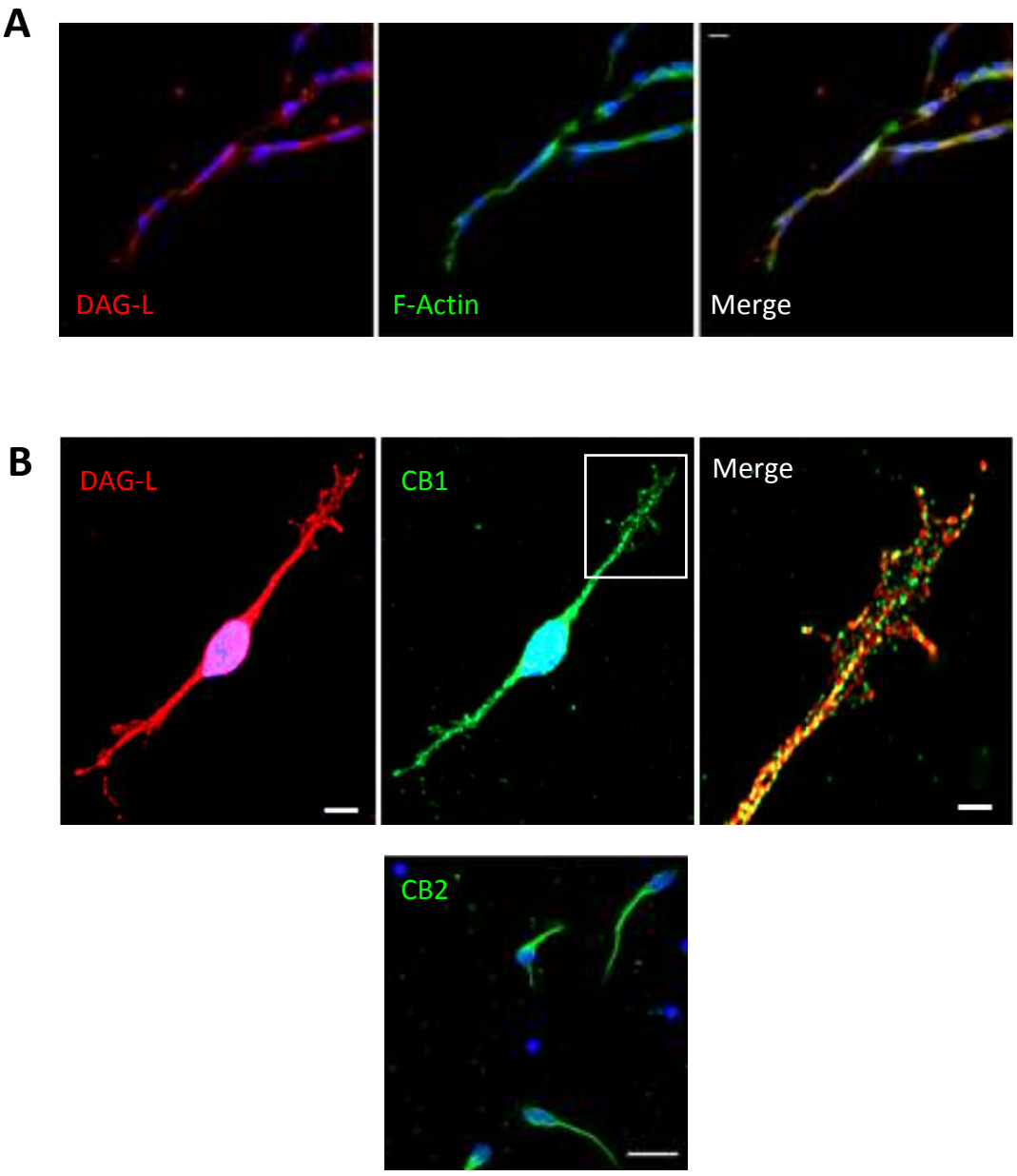

Figure 3.9: Mouse RMS neuroblasts express DAG-L and CB1/CB2 receptors. (A) Mouse RMS explants were embedded in Matrigel and allowed to migrate for 24 hours prior to fixation. Migratory neuroblasts show positive immunostaining for DAG-L (red), the enzyme that synthesises the endocannabinoid 2-AG. Bar = 20 µm. **(B)** Dissociated mouse RMS neuroblasts plated on polyornithine/laminin-coated coverslips were immunostained for DAG-L (red), CB1 receptor (green, top middle panel), and CB2 receptor (green, bottom panel). (Top right panel) High magnification image of the boxed area showing punctuate staining for both DAG-L and CB1 receptor that does not co-localise. Bars = 4 µm (top left and top right panel), 10 µm (bottom panel). Images in **(B)** are adapted from the PhD thesis of Madeleine Oudin.

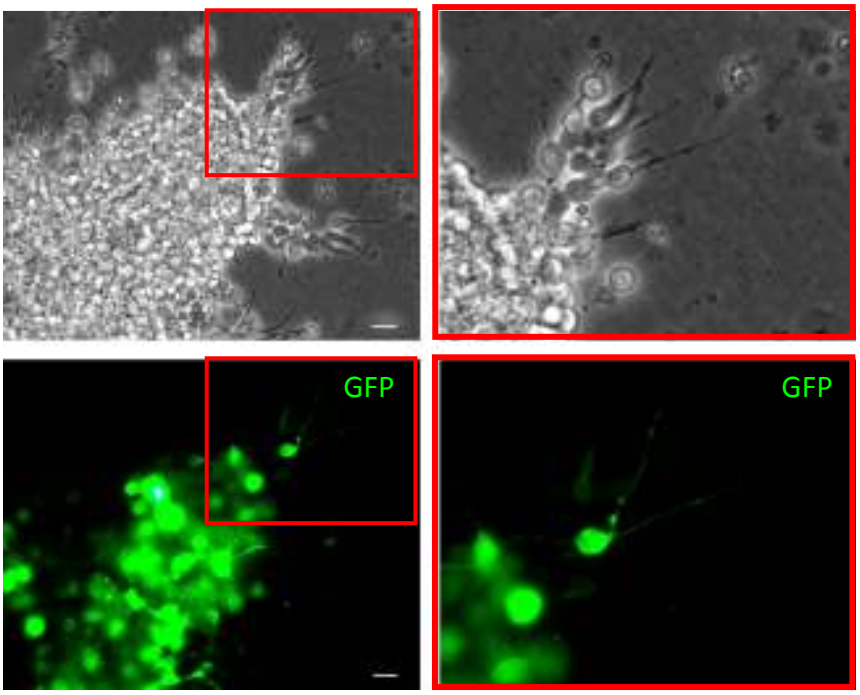

Figure 3.10: Dissociated RMS neuroblasts can be successfully nucleofected and re-aggregated. Mouse RMS explants were dissociated with trypsin and nucleofected with GFP. Neuroblasts were re-aggregated into clusters using the hanging drop procedure. Clusters were embedded in Matrigel and allowed to migrate for 6 hours prior to fixation. Re-aggregated neuroblasts are able to migrate out of embedded clusters (top panel) and show a high efficiency of transfection (bottom panel). Bar = 20 µm.

3.2.4 Activation of CB receptors increases migration of mouse RMS neuroblasts *in vitro*

Having established the necessary tools to study primary neuroblast migration, we tested whether the CB system can regulate this process using specific CB receptor agonists and antagonists. Both CB1 and CB2 agonist (ACEA and JWH-133 respectively) significantly promoted the migration of RMS neuroblasts, and this effect was inhibited by their respective antagonists AM-251 and JTE-907 (Figure 3.11A and Figure 3.11B). Although combined addition of both CB1 and CB2 agonists enhanced migration out of explants, this effect was not greater than either one of the agonists on their own (Figure 3.11B). This could be due to either saturation of a shared pathway or a limit in the migratory capacity of RMS neuroblasts in this *in vitro* system. Analysis of the number of neuroblasts at set distances from the edge of the explant reveals that CB1 activation significantly increases the number of neuroblasts migrating out of the explants at all set distances from the border (Figure 3.11C). Similarly, CB2 activation also caused a significant increase in the number of neuroblasts migrating out of explants (Figure 3.11C). This effect was inhibited by the corresponding CB1 and CB2 antagonists.

More detailed analysis of the CB system in RMS neuroblasts migration revealed that CB1 antagonists, CB2 antagonists, and DAG-L inhibitors, were all capable of inhibiting neuroblast migration *in vitro* (Oudin et al. 2011). On the other hand, a MAG-L inhibitor, which prevents degradation of the endocannabinoid 2-AG, mimicked the effect of the CB agonists and increased migration of neuroblasts out of RMS explants. This increase in migration could not be inhibited by either CB1 or CB2 antagonist on their own, and required either a DAG-L inhibitor or both antagonists to fully counter the effect of the MAG-L inhibitor (Oudin et al. 2011). These results provide further evidence for the existence of an eCB tone in our system, and also suggest that RMS neuroblast migration can be regulated by both CB1 and CB2 receptors, which appear to exhibit a degree of redundancy.

Time-lapse imaging of explant cultures in Matrigel revealed that treatment with CB agonists or MAG-L inhibitor increased the number of saltatory nuclear movements

A

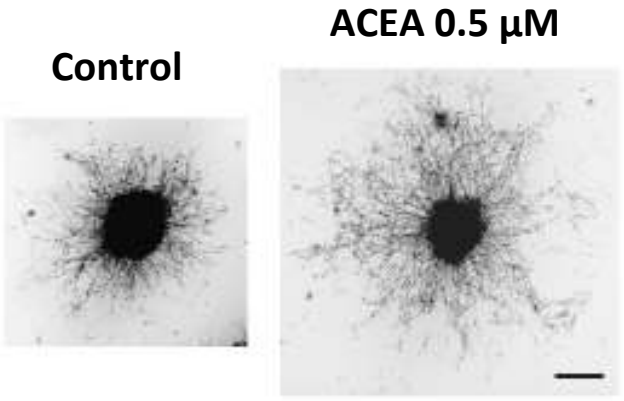
Control
ACEA 0.5 µM

B

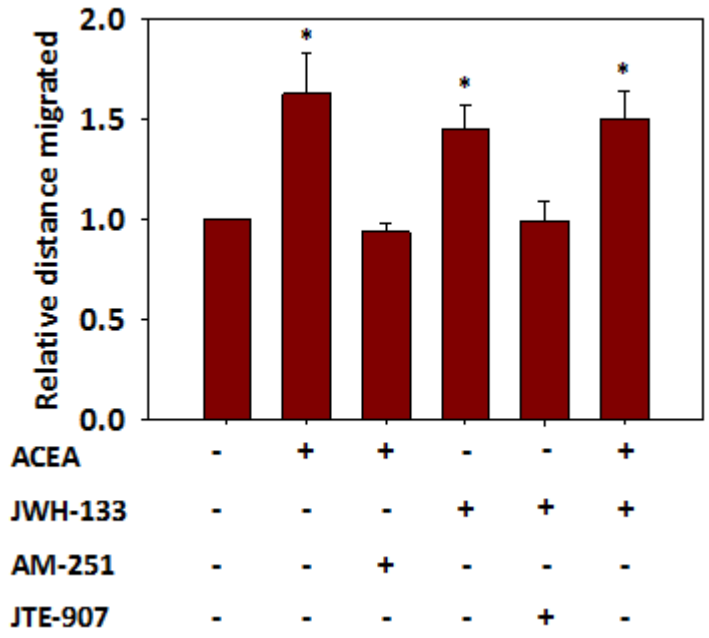
Relative distance migrated
2.0
1.5
1.0
0.5
0.0
ACEA - + + - - +
JWH-133 - - - + + +
AM-251 - - + - - -
JTE-907 - - - - + -

C

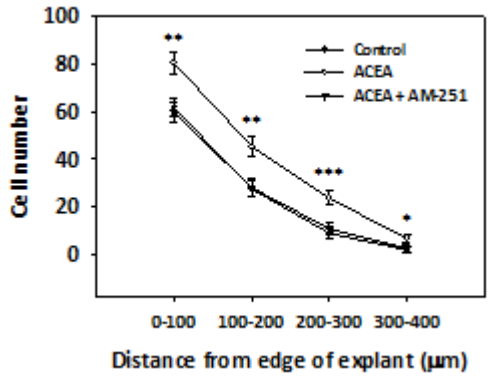
Cell number
Control
ACEA
ACEA + AM-251
0-100
100-200
200-300
300-400
Distance from edge of explant (µm)

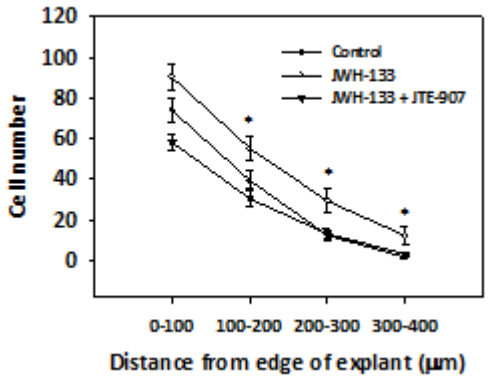
Cell number
Control
JWH-133
JWH-133 + JTE-907
0-100
100-200
200-300
300-400
Distance from edge of explant (µm)

Figure 3.11: CB agonists promote migration of mouse RMS neuroblasts *in vitro*. Mouse RMS explants were embedded in Matrigel, incubated with the indicated drugs, and allowed to migrate for 24 hours prior to fixation. Drugs were left in the medium throughout the duration of the experiment. **(A)** Representative images of explants in Matrigel showing enhanced migration of RMS neuroblasts caused by the CB1 agonist ACEA. Bar = 200 μm. **(B)** Both CB1 agonist (ACEA 0.5 μM) and CB2 agonist (JWH-133 0.5 μM) significantly increase migration of RMS neuroblasts. This effect is blocked by their respective antagonists AM251 (1 μM) and JTE-907 (1 μM). **(C)** Quantification of the number of cells at set distances from the edge of the explant. The CB1 agonist ACEA (0.5 μM) significantly increase the number of cells migrating out of the explant. This effect is blocked by the CB1 antagonist AM251 (1 μM). Each bar represents the mean ± SEM. *P < 0.05; **P < 0.01; ***P < 0.001; n = 4 independent experiments.

(nuclear movement > 5 μm), whilst CB antagonists caused a significant reduction in large nuclear translocations (Oudin et al. 2011). Interestingly, CB antagonists also caused a 3-5 fold increase in the number of secondary branches originating from the leading process; whereas CB agonist or MAG-L treated neuroblasts often extended just a single leading process in a similar fashion to control cells. In contrast to CB antagonists, which caused a significant reduction to average process length, CB agonists notably increased the length of the leading process (Oudin et al. 2011).

Together, this data suggests the presence of an eCB tone in RMS explant cultures, which regulates neuroblast migration and polarised morphology via the CB1 and CB2 receptors.

3.2.5 Activation of CB receptors increases the migration of mouse RMS neuroblasts in situ

Having verified a role for the CB system in primary neuroblast migration *in vitro*, we proceeded to investigate whether this role is conserved *in vivo*. To achieve this, we labelled RMS neuroblasts by electroporating a pCX-EGFP plasmid (a kind gift from Dr. Masaru Okabe, Osaka University, Japan) into the lateral ventricle of P2 mouse pups (Figure 3.12, left). This procedure has been previously validated as an efficient method of labelling SVZ neuroblasts, with transgene expression being robust for at least 15 days post electroporation (Boutin et al. 2008). Several days later (3-7 days), brains were fixed, sectioned, and stained for GFP to visualise neuroblasts migrating in the stream (Figure 3.12, right). For the purpose of quantification, the RMS was classified into four anatomically distinct regions (Region A: injection site; Region B: descending arm of the RMS; Region C: “elbow” preceding the RMS just before the OB; Region D: within the OB) (Figure 3.12, left), as previously described (Belvindrah et al. 2011). We have recently shown that systemic administration of CB antagonists, following GFP-labelling of neuroblasts in the RMS, resulted in a shorter process length and increased secondary branching, as observed in fixed brain slices (Oudin et al. 2011). These results mirror our observations *in vitro*, and provide evidence that eCBs are important for maintaining correct neuroblast morphology

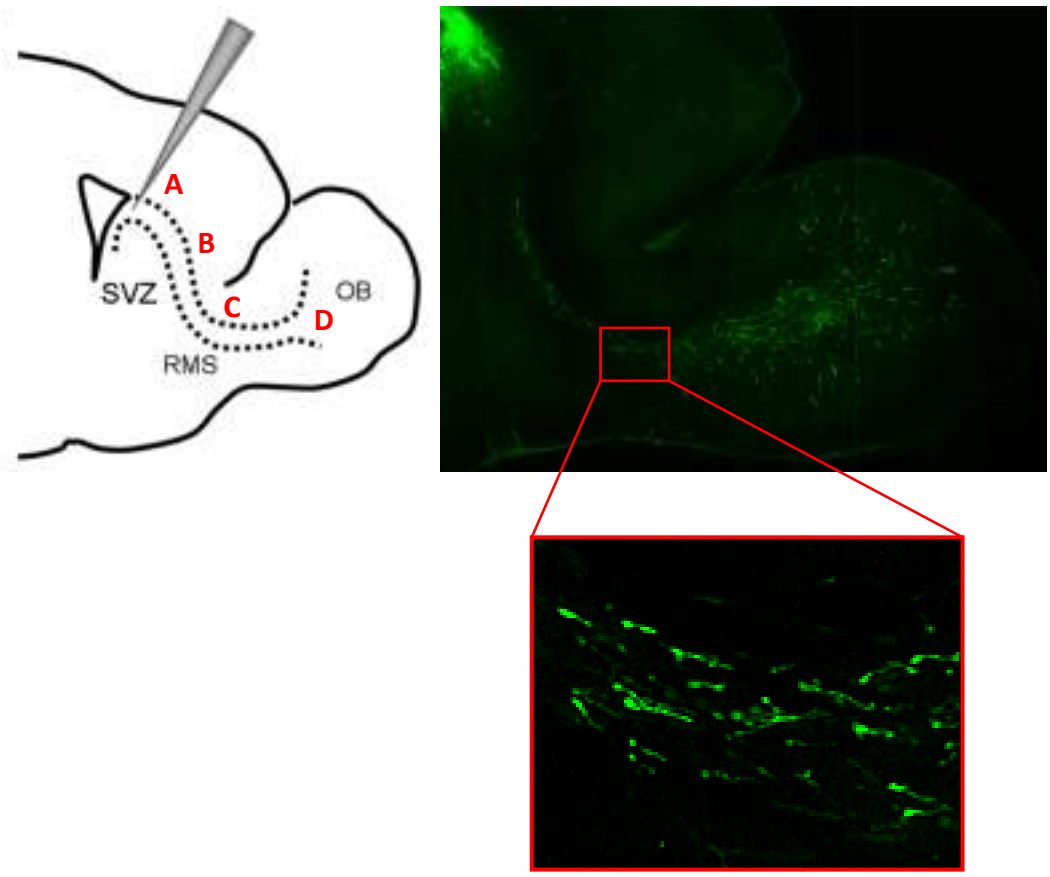

Figure 3.12: Labelling migratory neuroblasts by *in vivo* electroporation. A pCX-EGFP plasmid was electroporated into the right lateral ventricle of P2 mouse pups. (Left) A schematic diagram showing the site of injection in the lateral ventricle. The RMS (dotted lines) was divided into anatomically distinct regions for the purpose of quantification. Region **A** is the injection site, region **B** is the descending arm of the RMS, region **C** is the RMS "elbow" preceding the OB, and region **D** is within the OB. (Right) A fixed brain slice (7 days after electroporation) immunostained for GFP showing labelled neuroblasts migrating from the SVZ along the RMS to the OB. (Bottom enlarged panel) The vast majority of neuroblasts have their leading process directed towards the OB in the direction of migration.

in vivo, and may therefore also be important for proper neuroblast migration.

To validate this hypothesis, we labelled RMS neuroblasts by *in vivo* electroporation of pCX-EGFP, and used time-lapse spinning disk confocal microscopy to monitor their migration in acute brain slice cultures (Figure 3.13). Supplementary movie 4 shows GFP-labelled neuroblasts migrating in region B of the RMS. Neuroblasts move in a similar manner to that observed in the *in vitro* explant migration assay: cells extend a single leading process, followed by swelling of the region in front of the nucleus, and forward propulsion of the nucleus in the direction of migration (Supplementary movie 4). Neuroblasts also showed alternation between periods of rapid migration and immobility, and were able to change direction rapidly by retracting and re-forming their leading process. In contrast to observations made from the Matrigel migration assay, neuroblasts migrating within the brain slice were also able to change direction by drastically curving their leading process in another direction. This may be due to the highly compacted nature of the RMS, where neuroblasts may be forced to curve their processes around adjacent cells. Interestingly, neuroblasts did not move uni-directionally in the stream, often going backwards or in circles and occasionally leaving the stream altogether (Supplementary movie 4). However, this is unlikely to be the case *in vivo* since in fixed brain slices almost all neuroblasts in the RMS are oriented towards the bulb and are tightly contained within the RMS (Figure 3.12). Hence, this effect is likely to be an artefact of either compromising the architecture of the RMS or dilution of the regulatory molecules guiding neuroblast migration *in vivo*. Nevertheless, this assay provides a useful tool to study the effects of pharmacological agents and their downstream targets on the dynamics of neuroblast migration in an environment as close as possible to native RMS.

Figure 3.14 shows the combined effect of CB1 and CB2 agonists (ACEA and JWH-133 1 µM each) on neuroblast migration in the brain slice assay. RMS neuroblasts in slices treated with CB agonists migrated a greater distance (190.8 µm ± 9.6) than control neuroblasts (129.6 µm ± 10.9) and also had a greater average velocity (63.6 µm/hour ± 3.1) than control cells (43.3 µm/hour ± 3.6).

0 hours

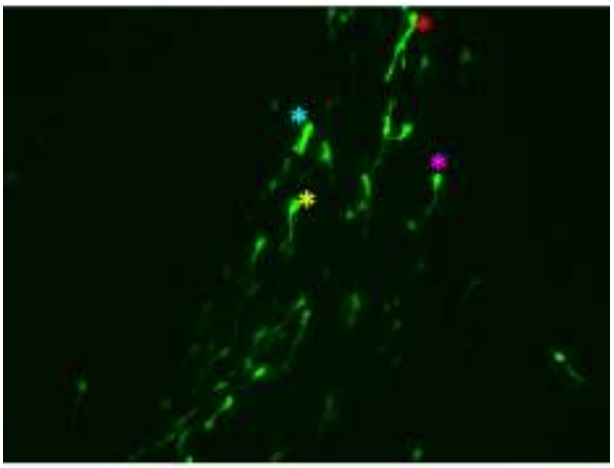

3 hours

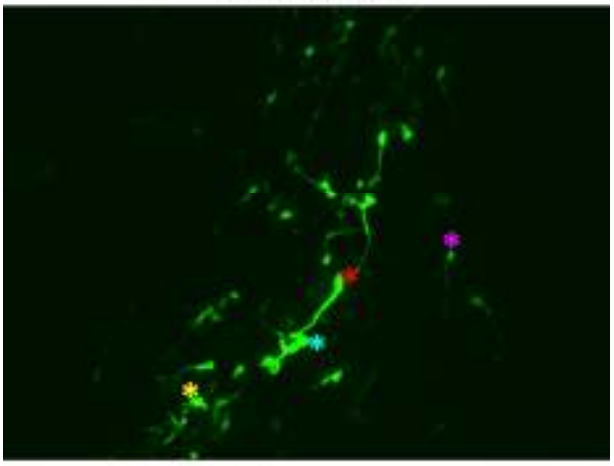

3 hours

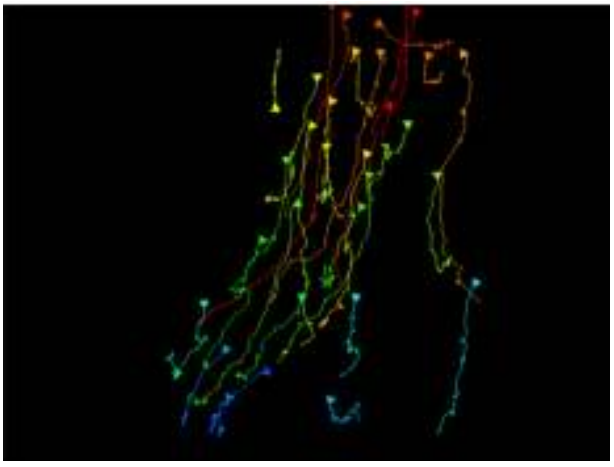

Figure 3.13: Snapshots of pCX-EGFP-expressing neuroblasts migrating in a living brain slice. A pCX-EGFP plasmid was electroporated into the right lateral ventricle of P2 mouse pups. Animals were sacrificed 3 – 7 days later, the right hemispheres were cut into 300 µm thick sagittal sections, and GFP-positive slices were cultured for imaging. Z-stack images (2-4 µm) of RMS neuroblasts in cultured brain slices were acquired every 3 mins for 3 hours using the UltraVIEW VoX System (Perkin Elmer). Migrating cells were tracked and analysed using Volocity software (Perkin Elmer). Panels show snapshots taken at the start (top panel) and end (middle panel) of filming. Coloured asterisks indicate the start and end positions of neuroblasts. Coloured tracks shown in the bottom panel show the trajectory of neuroblasts that were tracked for analysis (Supplementary movie 4).

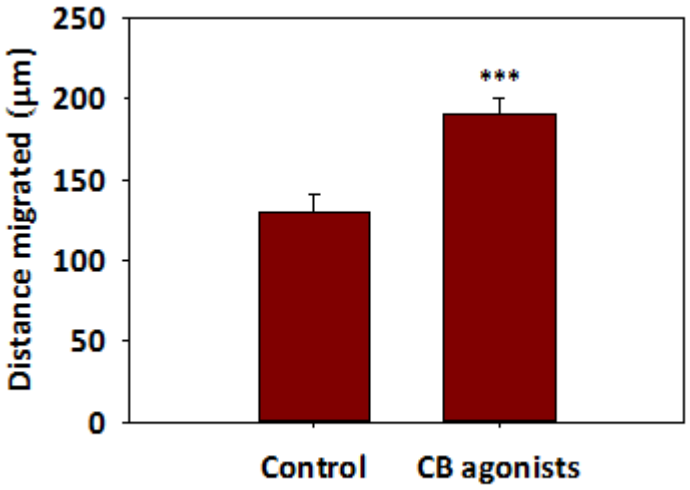
Distance migrated (µm)
250
200
150
100
50
0
***
Control
CB agonists

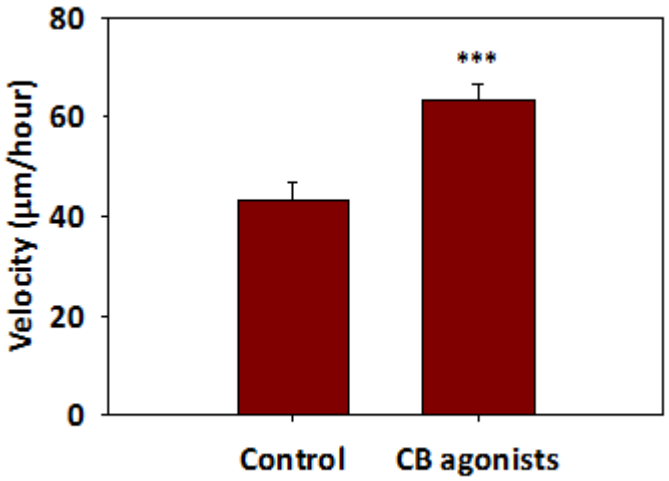
Velocity (µm/hour)
80
60
40
20
0
***
Control
CB agonists

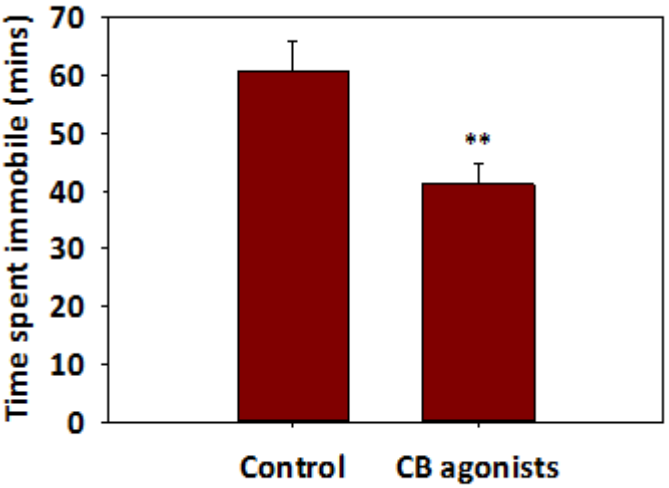
Time spent immobile (mins)
70
60
50
40
30
20
10
0
**
Control
CB agonists

Figure 3.14: Cannabinoids increase migration of neuroblasts in the brain slice assay. Brain slices with GFP-labelled neuroblasts were prepared 3-7 days after *in vivo* electroporation of pCX-EGFP. Slices were incubated with or without cannabinoid agonists (ACEA 1 µM + JWH-133 1 µM) for 1 hour prior to imaging. Slices were imaged at the beginning of the stream (region B) every 3 minutes for 3 hours. Drugs were present throughout the imaging period. CB receptor agonists increase the distance migrated (top) and velocity (middle), and reduce the length of time spent immobile (bottom). Each bar represents the mean ± SEM; **P < 0.01; ***P < 0.001; n = 8 for control; n = 9 for CB agonists, where n = independent experiments. Approximately 15 to 30 cells were tracked for each experiment.

Neuroblasts in CB agonists-treated slices also spent significantly less time immobile (41.2 min ± 3.7) compared to control samples (60.7 min ± 5.2). Comparison of the parameters that describe persistence of directional motility (Figure 3.15) reveals that there was no significant difference between control and CB agonists-treated slices. The total displacement, although slightly greater with CB agonists (94.7 μm ± 6.3) was not statistically different from the control (77.9 μm ± 8.6) (Figure 3.15, top panel). The average meandering index (MI; total displacement/total distance) was also similar between the two groups (control: 0.53 ± 0.026; CB agonists: 0.50 ± 0.021) (Figure 3.15, middle panel). Based on the MI, neuroblasts were also classified as migratory (MI > 0.6), intermediate (MI 0.4 – 0.6) or exploratory (MI < 0.4) using the same parameters defined by published reports describing neuroblast migration in the RMS (Nam et al. 2007). No significant difference was observed in the percentages of cells that were migratory, intermediate, or exploratory between control and CB agonists treated neuroblasts (Figure 3.15, bottom panel). From these results we conclude that CBs have a motogenic effect on RMS neuroblasts *in vivo*. Although we did not observe an effect of CBs on displacement or the MI in the brain slice assay, we cannot say with certainty that CBs have no effect on persistence since there appears to be a loss of directionality even in control cells, probably arising from disruption of the stream architecture and dilution of native migratory signals.

3.2.6 Comparison of rat and mouse RMS cultures

One of the main limitations of using mouse RMS cultures is the relatively low yield of neuroblasts obtained per brain: approximately 500,000 cells per brain of a P5-P7 mouse. Transfection procedures with reasonably high efficiency such as nucleofection, which facilitate the functional study of candidate molecules/signalling pathways in neuroblasts, require at least 3,000,000 cells per nucleofection. Rat RMS cultures on the other hand, can produce more than 1,000,000 neuroblasts per brain of a P5-P7 rat pup. Since the organisation of the rat and mouse SVZ and RMS are remarkably similar (Peretto et al. 2005), we can assume that the two species are interchangeable, at least in this context. For this reason, we examined rat RMS explants as an alternative source of neuroblasts.

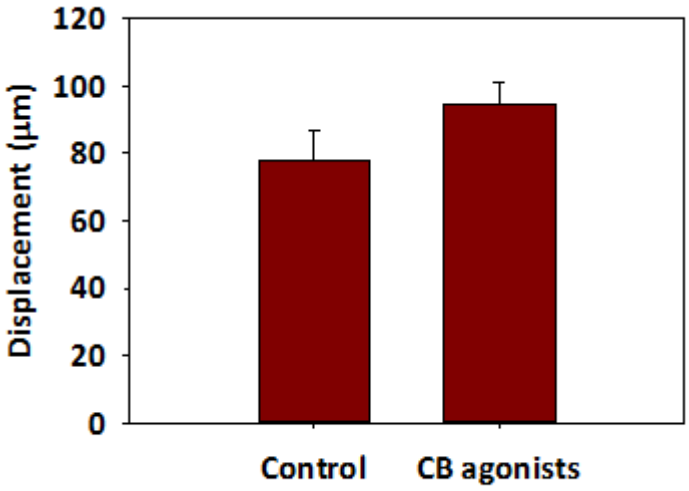
120
100
80
60
40
20
0
Displacement (µm)
Control
CB agonists

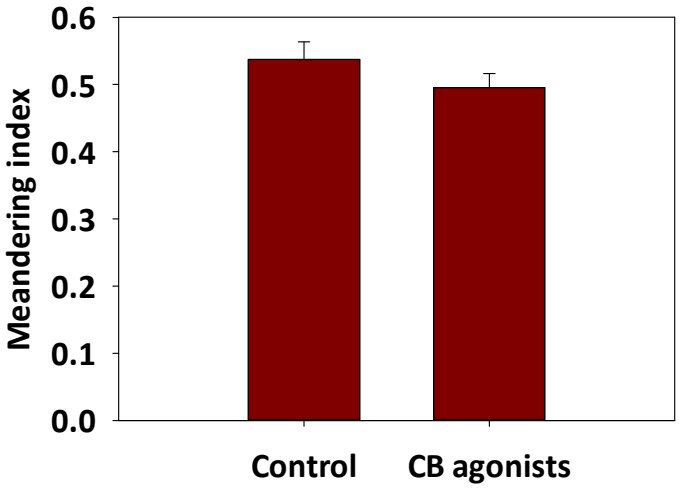
0.6
0.5
0.4
0.3
0.2
0.1
0.0
Meandering index
Control
CB agonists

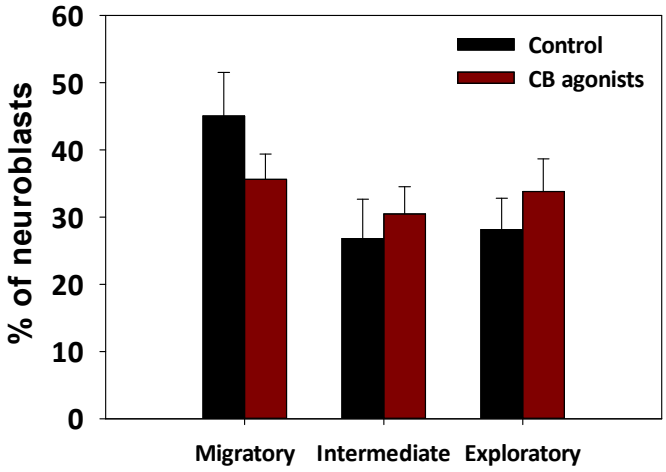
60
50
40
30
20
10
0
% of neuroblasts
Control
CB agonists
Migratory
Intermediate
Exploratory

Figure 3.15: CB agonists do not affect persistence in the brain slice assay. The persistence of neuroblast movement was analysed using the meandering index (MI; total displacement/total distance). The migratory behaviour of neuroblasts was classified as exploratory (MI < 0.4), intermediate (MI 0.4 – 0.6) or migratory (MI > 0.6). Cannabinoid agonists did not significantly affect the displacement (top); average meandering index (middle); or the % of neuroblasts with exploratory, intermediate, or migratory phenotype (bottom). Each bar represents the mean ± SEM; n = 8 for control; n = 9 for CB agonists, where n = independent experiments. Approximately 15 to 30 cells were tracked for each experiment.

Rat RMS neuroblasts migrate out of explants embedded in Matrigel in a similar manner to neuroblasts derived from the mouse RMS (Figure 3.16A). The distance migrated out of explants by rat RMS neuroblasts over a 24 hour period (224.2 μm ± 7.4) is marginally greater, but not significantly different from that observed in mouse explants (204.2 μm ± 10.8) (Figure 3.16B). The vast majority of cells in rat RMS explant cultures are migratory neuroblasts, as confirmed by the expression of neuroblast markers DCX and βIII tubulin (Figure 3.17). As seen in mouse RMS explant cultures, the few astrocytes that are occasionally present, have a distinctive star-like morphology, and do not express the neuronal marker βIII tubulin (Figure 3.18). As a final confirmation that rat RMS cultures can be used for our investigations as an alternative to mouse cultures, we treated rat RMS explants with CB agonists and antagonists to see if we could reproduce the same results seen with the mouse model. Figure 3.19A-B shows that both CB1 (ACEA) and CB2 (JWH-133) agonists were able to significantly increase neuroblast migration, and this effect was inhibited by their corresponding antagonists. Thus, we can conclude that rat RMS neuroblast cultures are similar to those derived from the mouse brain in both their composition and response to CBs, and can therefore be used as an alternative model system.

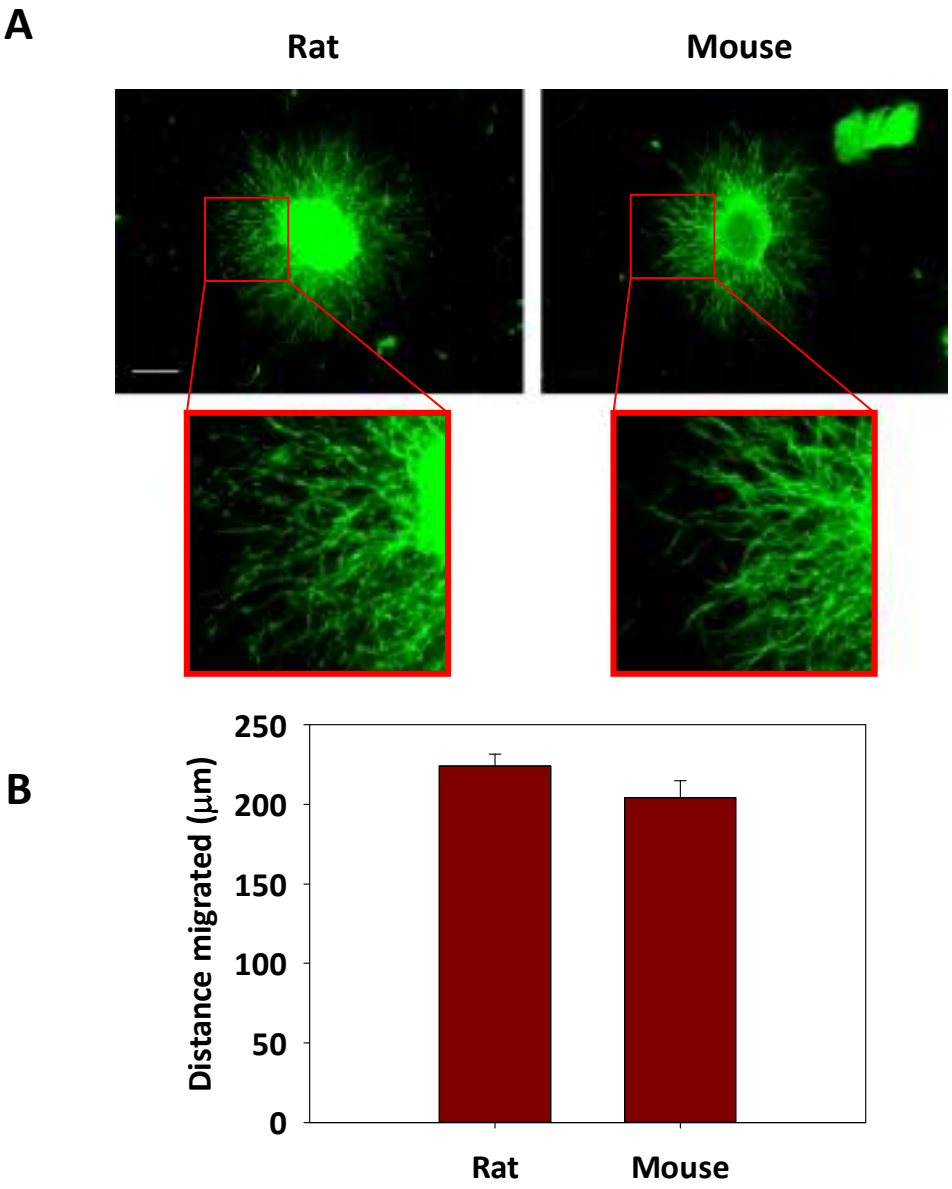

Figure 3.16: Comparison of rat and mouse RMS explants in Matrigel. The RMS was dissected from P5-P7 rat and mouse pups. Explants were embedded in Matrigel, and allowed to migrate for 24 hours prior to fixation. Explants were stained for F-actin to allow comparison of morphology. **(A)** Representative images of rat and mouse explants after 24 hours of migration in Matrigel. Both mouse and rat neuroblasts migrate in a similar manner, although mouse neuroblasts appear to form thicker chains. **(B)** Rat and mouse neuroblasts migrate to a similar extent, as shown by quantitative comparison of their migration distance over a period of 24 hours. Bar = 200 µm. Each bar represents the mean ± SEM; n = 33 and 39 explants for rat and mouse respectively.

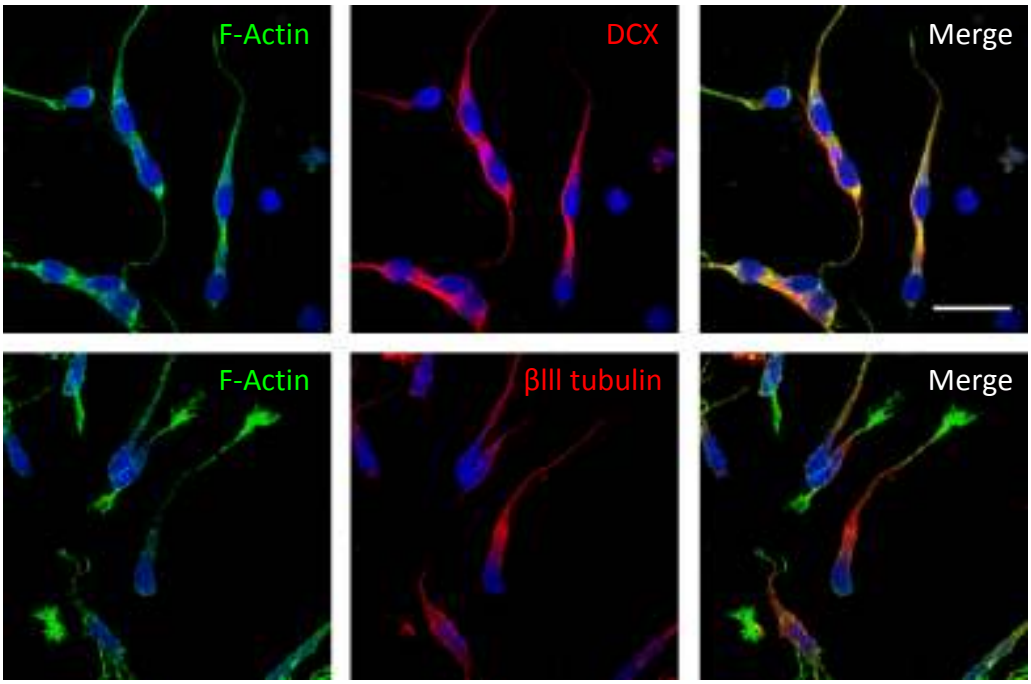

Figure 3.17: Rat RMS cultures express markers of migratory neuroblasts. Rat RMS explants were dissociated and plated onto polyornithine/laminin-coated coverslips. Cells were fixed and stained 48 hours after plating. Like mouse RMS cultures, the vast majority of cells in rat RMS explants cultures express markers of migratory neuroblasts (DCX and βIII tubulin). Bar = 20 µm.

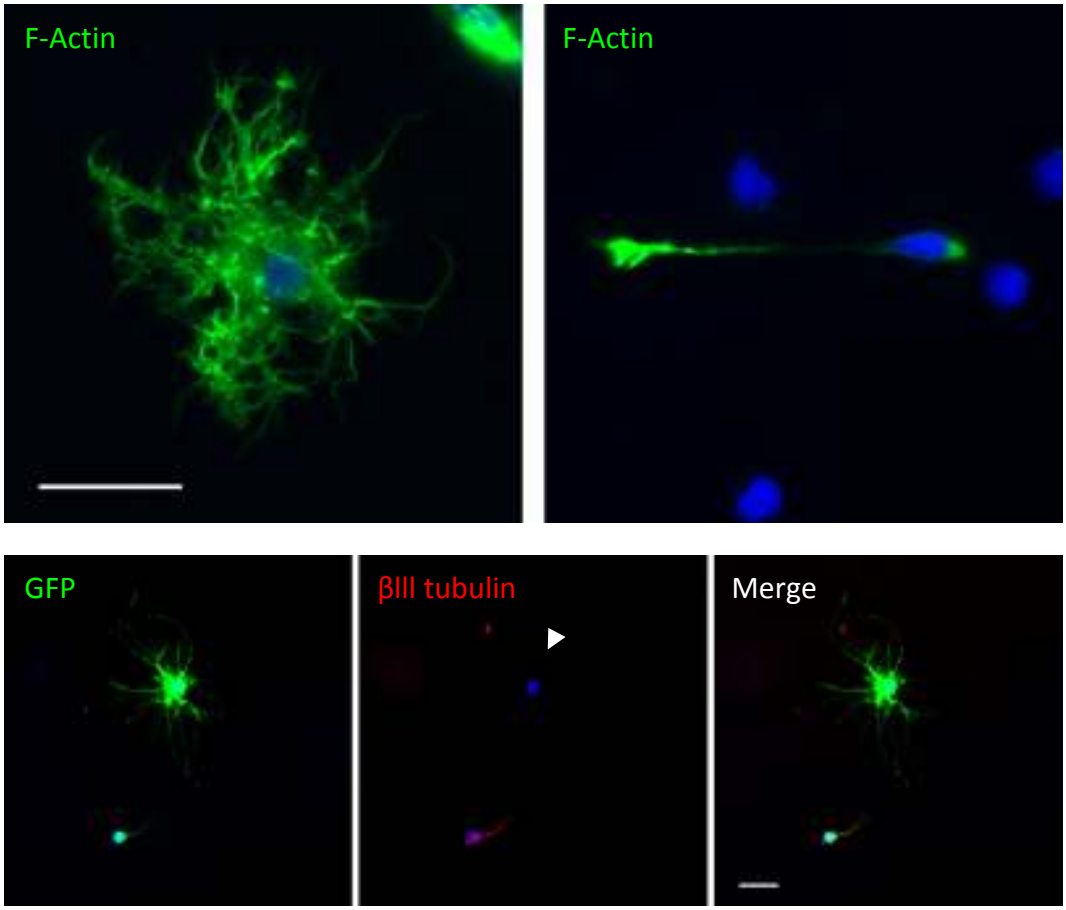

Figure 3.18: Rat RMS astrocytes have distinct morphology and do not express neuronal marker βIII tubulin. (Top panel) Rat RMS explants embedded in Matrigel were stained for F-actin. Astrocytes (left) have a distinctive star-like morphology, whereas neuroblasts (right) have a single leading process. Bar = 20 µm. (Bottom panel) Dissociated rat explants cultures nucleofected with GFP and embedded in Matrigel were stained for GFP and neuronal marker βIII tubulin. Occasional astrocytes that are present in cultures can be recognised by their lack of βIII tubulin expression. White arrowhead points to astrocyte. Bar = 20 µm.

A

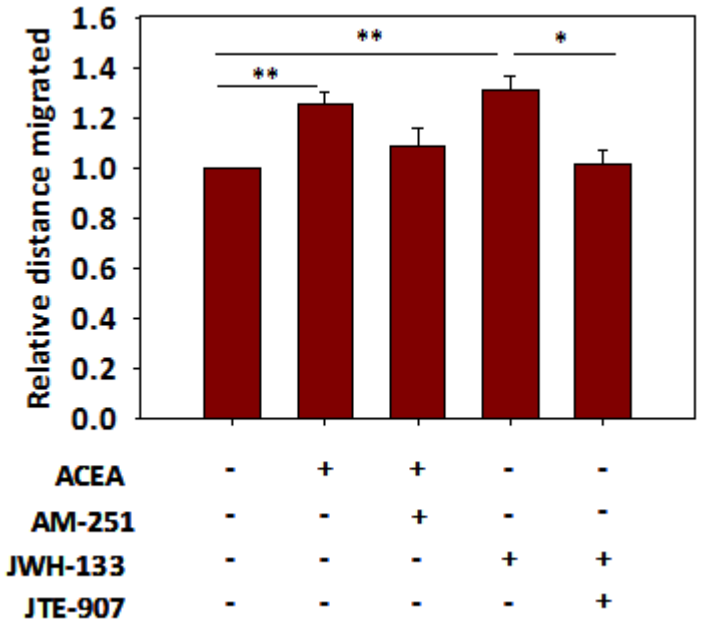
Relative distance migrated
1.6
1.4
1.2
1.0
0.8
0.6
0.4
0.2
0.0
**
**
*
ACEA - + + - -
AM-251 - - + - -
JWH-133 - - - + +
JTE-907 - - - - +

B

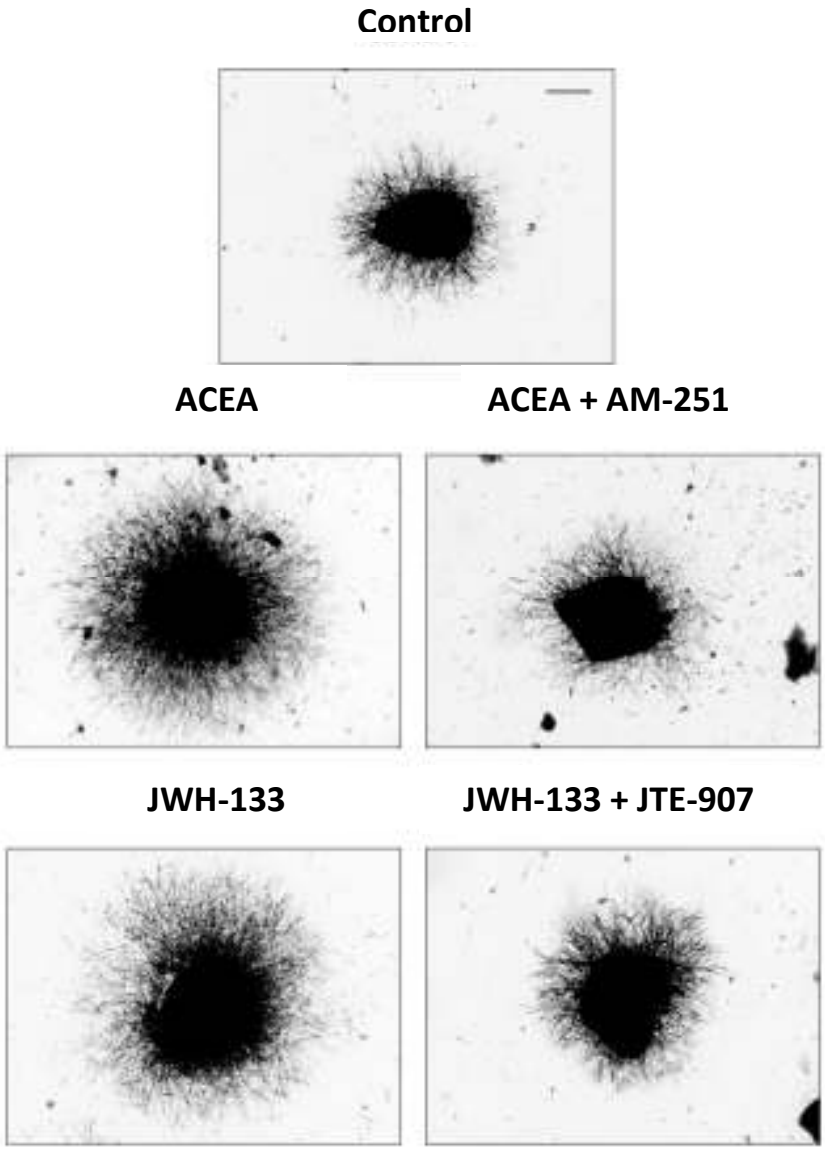
Control
ACEA
ACEA + AM-251
JWH-133
JWH-133 + JTE-907

Figure 3.19: CB agonists promote migration of rat RMS neuroblasts *in vitro*. Rat RMS explants were embedded in Matrigel, incubated with the indicated drugs, and allowed to migrate for 24 hours prior to fixation. **(A)** Both CB1 agonist (ACEA 0.5 μM) and CB2 agonist (JWH-133 0.5 μM) significantly increase migration of RMS neuroblasts, and this effect is blocked by their respective antagonists AM251 (1 μM) and JTE-907 (1 μM). Each bar represents the mean ± SEM. *P < 0.05; **P < 0.01; n = 4 independent experiments. **(B)** Representative images of explants in Matrigel showing enhanced migration of RMS neuroblasts by CB1 agonist ACEA (0.5 μM) and CB2 agonist JWH-133 (0.5 μM), and inhibition of this effect by their respective antagonists AM251 (1 μM) and JTE-907 (1 μM). Bar = 200 μm.

3.3 Discussion

The primary objective for the first part of this study was to determine whether the CB system can regulate the migration of neural precursors in the post-natal brain. In order to investigate this hypothesis, we devised a number of migration assays, using the Cor-1 NS cell line and primary neuroblast cultures.

Our initial observations showed that pharmacological activation of the CB2 receptor significantly enhanced random migration of Cor-1 cells. Similarly, polarised cell migration, as measured by the rate of wound closure in the scratch wound assay, was also significantly increased following activation of the CB1 or CB2 receptor. Although CB receptor agonists have been shown to increase proliferation in these cells (Goncalves et al. 2008), the increased rate of wound closure observed here is unlikely to arise from this effect since the high cell density used in this assay is inhibitory to proliferation (Figure 3.4).

To extrapolate our initial findings in Cor-1 cells to primary neuroblasts, we established a 3D migration assay using RMS explants derived from postnatal mouse brains and embedded in Matrigel (Ward and Rao 2005). Our results show that all constituents of the eCB system are expressed by RMS neuroblasts. Notably, DAG-L appears to be exclusively expressed by neuroblasts in the native RMS, and is absent in GFAP-positive astrocytes (Oudin et al. 2011). This suggests that eCBs may have an autocrine function in this system. Indeed, due to their hydrophobic nature, eCBs are known to remain within the phospholipid bilayer following synthesis and activate CB receptors within the same membrane by means of lateral membrane diffusion (Song and Bonner 1996; Xie et al. 1996; Piomelli 2003). In addition, the close association between neuroblasts, arising from the formation of chains, may facilitate the interaction between 2-AG and CB receptors on neighbouring cells, thereby achieving a paracrine effect. Given the short half life of 2-AG (Giuffrida et al. 2001), it is highly unlikely that a diffusion gradient of this molecule is present in the stream. Instead, eCBs are more likely to be involved in short-range signalling, acting on cells near their site of production (Piomelli 2003).

Treatment of neuroblasts with a CB1 or CB2 agonist significantly increased the distance migrated out of explants. Interestingly, the combined effect of the agonists was not greater than either agonist alone. This could either suggest that the CB1 and CB2 receptors share a common downstream signalling pathway which is already saturated with just one agonist, or that there is a physical limit to the extent to which migration can be enhanced. In addition, both the CB1 and CB2 agonist increased the number of cells migrating out of explants. Thus, CB receptor activation not only enhances the speed of migration, but also appears to have a motogenic effect. This is particularly interesting since these two attributes are not necessarily interconnected. For example, BDNF is able to enhance the number of cells migrating out of explant cultures, but has no effect on the migrated distance (Chiaramello et al. 2007). This implies that CB receptor activation may be involved in two distinct pathways: one that stimulates migration and one that enhances speed.

Next, we sought to confirm the existence of an active endogenous eCB tone in primary neuroblasts using pharmacological tools. We found that inhibiting DAG-L activity significantly reduced neuroblast migration, whilst enhancing eCB tone with an inhibitor of MAG-L, the main enzyme responsible for the hydrolysis of 2-AG in the brain (Blankman et al. 2007), drastically increased neuroblast migration. Importantly, enhancement of migration in response to a MAG-L inhibitor could not be blocked by either a CB1 or CB2 antagonist alone, and required both CB antagonists to fully counter this effect (Oudin et al. 2011). Thus, regulation of neuroblast migration appears to be reliant on both CB1 and CB2 receptors. Moreover, our results also suggest that 2-AG may be the main eCB involved in this process.

We turned to time-lapse imaging of RMS explants in Matrigel to further analyse the effect of CB receptor activation on the dynamics of neuroblast migration. Activation of CB receptors or enhancement of endogenous eCB tone increased the number of large saltatory nuclear movements; whilst CB receptor antagonists significantly reduced the frequency of productive nuclear translocation events. Moreover, CB

receptor antagonists significantly disrupted unipolar neuroblast morphology, causing a 3-5 fold increase in the number of secondary branches formed per hour, as well as a shortening of the leading process (Oudin et al. 2011). Consistent with these observations, a single systemic administration of CB receptor antagonists was able to drastically disrupt the polarised morphology of neuroblasts *in vivo*, causing a shortening of their leading process and substantially increasing secondary branching (Oudin et al. 2011). Taken together, these findings show that an eCB tone is present in the RMS, and is involved in the regulation of neuroblast morphology and migration *in vitro* and *in vivo*. In the context of axonal guidance, information regarding the extracellular environment is relayed to the eCB system, which in turn mediates changes that promote axonal growth (Williams et al. 2003). If a similar mechanism exists in neuroblast migration, antagonising CB receptors would in effect inhibit the responses to extracellular guidance signals, thus leading to a loss of polarised migration. This may explain the phenotype seen here, and suggests the requirement of the eCB system to translate extracellular guidance cues.

Finally, we sought to provide evidence that the regulation of neuroblast migration by eCBs also occurs within the native architecture of the stream, and is not an artefact of explant cultures in Matrigel. To achieve this, we labelled SVZ neuroblasts by electroporation of a GFP-expressing plasmid (Boutin et al. 2008), and administered pharmacological agents targeting the endocannabinoid system, either systemically for analysis of fixed brain slices, or directly to brain slices cultured for time-lapse imaging. Tracking analysis of neuroblasts migrating in the RMS revealed that they move in a similar manner to that observed in the explant migration assay, and to that described by others using the slice culture assay (Nam et al. 2007; Martinez-Molina et al. 2011). Although these studies report that neuroblasts adhere within the constraints of the RMS boundary (Nam et al. 2007; Martinez-Molina et al. 2011), we found that they occasionally migrated out of the stream altogether. One possible explanation for this anomaly could be that whilst we have conducted our studies in early postnatal mouse pups (P5-P9), the mentioned reports have used adult mouse brains. Since the glial tube and associated vasculature only begins to form after P7, the tendency to migrate out of the RMS in

our system may be accounted for by the lack of this physical structure, which has been shown to be an important guide for neuroblast migration (Saghatelyan 2009; Snapyan et al. 2009; Whitman et al. 2009). Thus, in the early postnatal mouse brain, neuroblast migration may be more reliant on diffusible guidance cues, which are lost in the slice culture assay. In line with the observations of others, we also found that neuroblasts did not always move towards the OB, with a significant proportion moving in the opposite direction or in circles (Nam et al. 2007; Martinez-Molina et al. 2011). However, analysis of fixed brain slices show that neuroblasts are strictly oriented towards the OB, with few, if any oriented in the wrong direction. Again, this may be indicative of the loss of guidance factors associated with this assay. Nevertheless, the slice culture assay is a close representation of neuroblast migration in the RMS, and provides a system in which the dynamic behaviour of neuroblasts may be examined in their native environment.

We report that activation of CB receptors significantly increased the average distance travelled by neuroblasts. Whilst control neuroblasts were stationary for almost an hour during a 3 hour filming period, treatment with CB receptor agonists reduced the length of the stationary period by a third. In addition, CB agonists significantly enhanced the speed of migration. These results are consistent with our findings in the explant migration assay, and further confirm that CB agonists enhance the speed of migration as well as having a motogenic effect on RMS neuroblasts. Although the eCB system is known to be involved in cell adhesion molecule-mediated axon guidance (Williams et al. 1994; Saffell et al. 1997; Williams et al. 2003), we did not observe any changes in the persistence of directional motility following activation of the CB receptors. However, in axon guidance, activation of the CB receptors is restricted to specific regions of the growth cone (Bisogno et al. 2003; Harkany et al. 2007; Oudin et al. 2011). Thus, a function for CB signalling in directional guidance of RMS neuroblasts may require activation of the CB receptors to be confined to localised regions, rather than the global activation occurring in the slice assay.

In summary, the CB system is an important regulator of RMS neuroblast migration both *in vitro* and *in vivo*. CB receptor agonists have a motogenic effect on RMS neuroblasts, and also increase the speed of migration. Moreover, the eCB system appears to be essential for correct polarised morphology of migrating neuroblasts.

Chapter 4: RalA is required for CB-promoted migration of RMS neuroblasts

4.1 Introduction

A diverse range of guidance molecules are involved in regulating neuroblast migration in the RMS. Our recent work on the eCB system has now established these lipid mediators as important contributors to this process (Oudin et al. 2011). Whilst considerable progress has been made in identifying the various guidance cues present in the RMS, exactly how these signals are translated to the cell's migratory machinery is still not fully understood. We know from current studies that the chemoattractive effect of BDNF is reliant on activation of both the MAPK and PI3K pathways (Chiaramello et al. 2007), whilst GDNF interaction with NCAM is believed to activate CDK5 (Paratcha et al. 2006), and the effects of HGF is reliant on signalling via MAPK but not PI3K (Garzotto et al. 2008). In order for these diverse extracellular signals to be relayed to the molecular components that mediate cell migration, there may be a common pathway(s) on which different signalling cascades can converge. Here, we propose the small GTPase RalA as an ideal candidate for this role.

Ras-like GTPases (Ral) are members of the Ras family of small G proteins that are known to regulate a number of biological functions, including cell polarity, exocytosis, endocytosis, proliferation and migration (Feig 2003; Lalli and Hall 2005; van Dam and Robinson 2006; Lalli 2009; Chen et al. 2011). The two Ral isoforms, RalA and RalB, share over 85% sequence identity and are known for having both distinct and overlapping biological functions (Takai et al. 2001). Ral activation has been previously linked to polarisation events in neurones (Lalli and Hall 2005; Lalli 2009), as well as migration of cortical neurones during development (Jossin and Cooper 2011). Moreover, activation of Ral GTPases downstream of CB signalling has also been suggested as a potential mechanism regulating neurite outgrowth (He et al. 2005). These observations prompted us to investigate whether Ral activation

occurs downstream of CB signalling in the regulation of RMS neuroblast migration in the postnatal brain.

4.2 Results

4.2.1 RalA is expressed in rat RMS neuroblasts

To date, the expression of RalA and its closely related family member RalB, have not been examined in RMS neuroblasts. Immunostaining reveals that RalA is strongly expressed in rat RMS neuroblasts, and is enriched at sites along the surface of the cell membrane (Figure 4.1). Western blot analysis also confirms the presence of RalA in neuroblast lysates, with a single band being detectable at 25 kDa as expected (Figure 4.2A). In contrast, RalB could not detected in neuroblast lysates, was weakly expressed in SVZ and embryonic rat cortex homogenates, and showed strong expression in Cor-1 cells (Figure 4.2B). The apparently different abundance of RalA and RalB in the SVZ and RMS, suggests the existence of distinct roles for the two Ral isoforms in these brain areas. Moreover, it implicates RalA as the main Ral isoform present in RMS neuroblasts.

4.2.2 CB agonists activate RalA in rat RMS neuroblasts

Next, we sought to investigate whether RalA acts downstream of CB receptors. To verify our hypothesis, we performed a pulldown assay where dissociated rat RMS lysates treated with CB1 or CB2 agonist (ACEA 0.5 µM and JWH-133 0.5 µM respectively, for 5 minutes, 30 minutes and 1 hour) were incubated with agarose beads bound to the RalA effector RalBP1 (Ral-binding protein 1), which only binds the active form of RalA (RalA-GTP) (Goi et al. 1999). Figure 4.3 shows that a basal level of active RalA is present in control conditions; however, CB agonists increase activation of RalA beyond basal levels at all time points, with statistical significance occurring after 30 minutes and 1 hour of incubation with ACEA 0.5 µM. Surprisingly, pre-treatment of neuroblasts with a CB1 antagonist (AM-251 1 µM) or a CB2 antagonist (JTE-907 1 µM) for 1 hour prior to the addition of their respective agonists (ACEA 0.5 µM and JWH-133 0.5 µM for 30 minutes), resulted in an increase in RalA activation that was greater than either agonist alone (Figure 4.4).

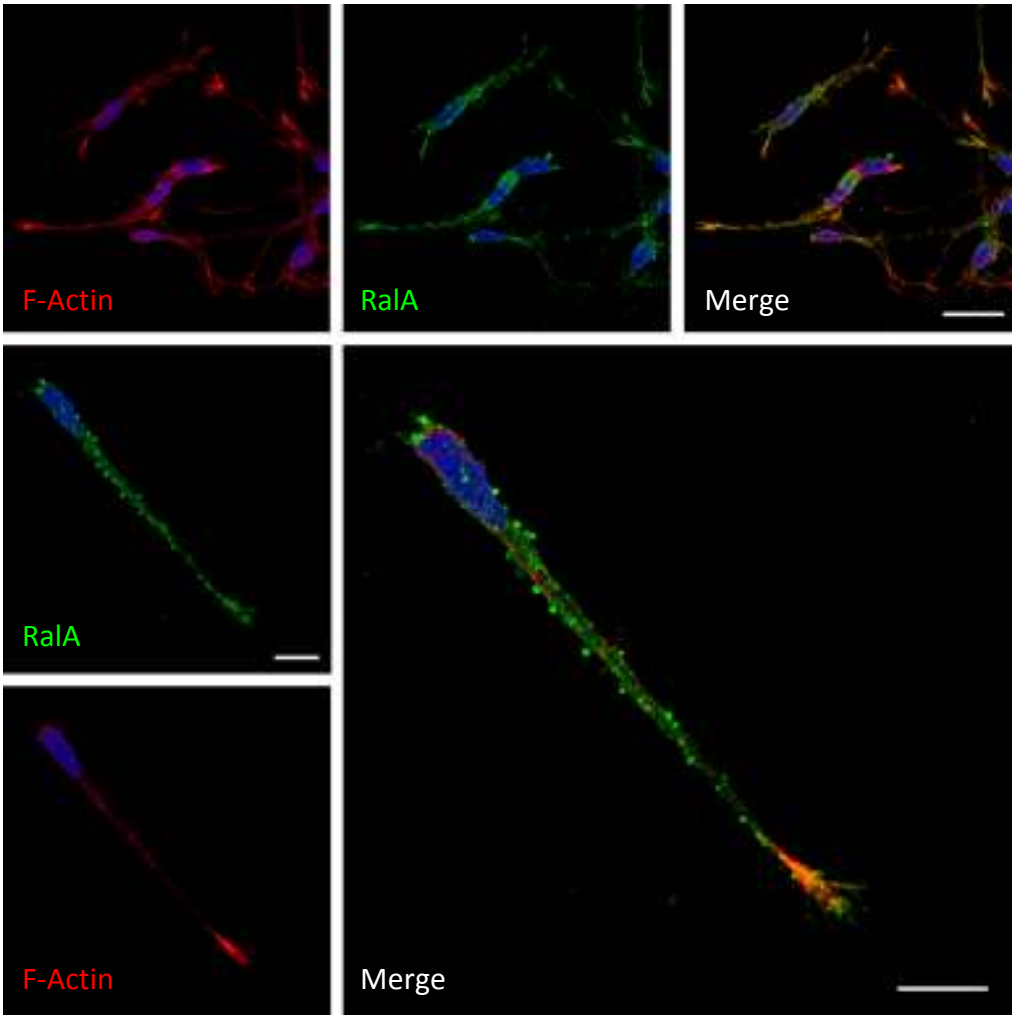

Figure 4.1: RalA is expressed in rat RMS neuroblasts. RMS explants from P5-P7 rat pups were embedded in Matrigel and allowed to migrate for 24 hours prior to fixation. Explants were stained for RalA (green) and F-Actin (red). RalA is strongly expressed in migratory neuroblasts and shows areas of accumulation along the surface of the cell membrane. Bar = 20 µm for top right panel. Bar = 10 µm for all other panels.

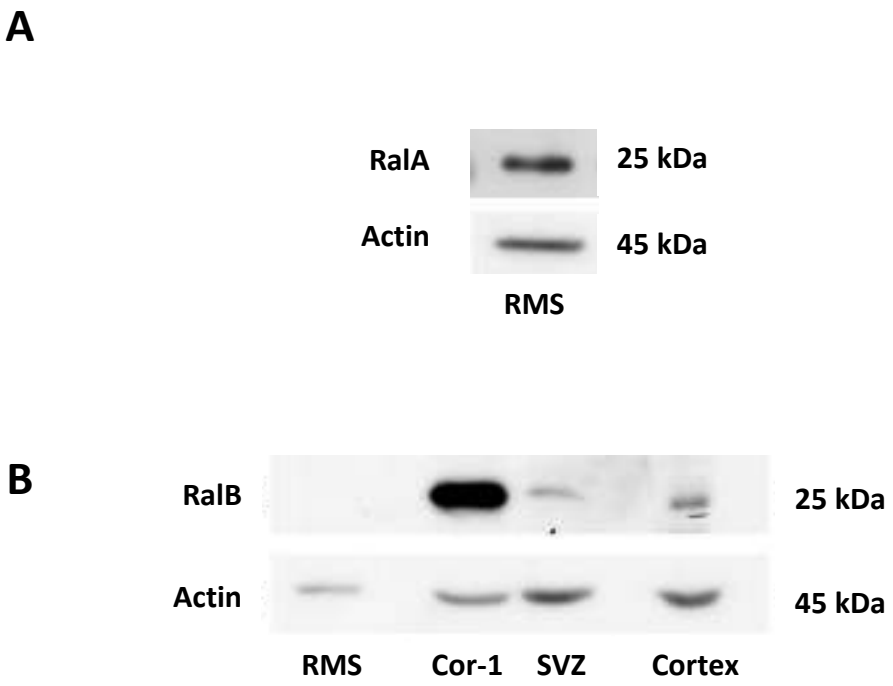

Figure 4.2: RalB can be detected in the SVZ, Cor-1 cells, and embryonic rat cortex, but not in the RMS. (A) RalA is strongly expressed in lysates of dissociated RMS neuroblasts from a P5 rat pup. **(B)** Lysates of dissociated rat RMS neuroblasts (P5), Cor-1 cells, SVZ homogenate, and rat embryonic cortex homogenate were analysed via Western blotting for RalB expression. RalB is highly expressed in Cor-1 cells and can be detected in lysates from postnatal SVZ and developing rat cortex, but not in lysates from rat RMS neuroblasts.

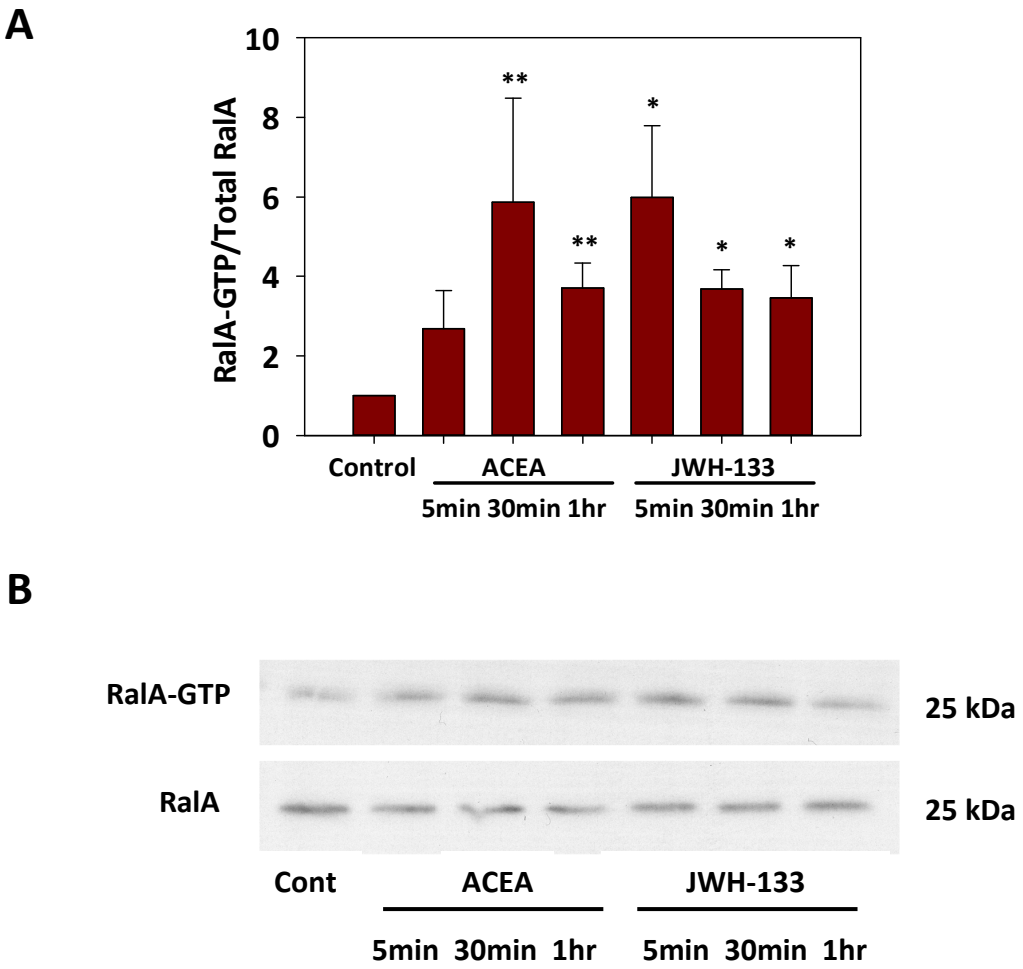

Figure 4.3: Stimulation of CB receptors activates RalA in rat primary neuroblasts. Dissociated RMS neuroblasts from P5-P7 rat pups were cultured for 48 hours on polyornithine/laminin coated plates. Neuroblasts were treated with CB1 agonist (ACEA 0.5 µM) or CB2 agonist (JWH-133 0.5 µM) for the indicated time and lysed. Active RalA was extracted from lysates using agarose beads bound to the RalA effector RalBP1. Samples were run on a Western blot and the amount of active RalA was measured compared to total RalA. **(A)** Western blot quantitative densitometric analysis shows that stimulation of CB receptors activates RalA in neuroblasts. Each bar represents the mean ± SEM; **P < 0.01; n = 6 for control and ACEA; n = 3 for JWH-133, where n = independent experiments. **(B)** Representative Western blot showing increased levels of active RalA (Ral-GTP) following treatment with CB agonists.

A

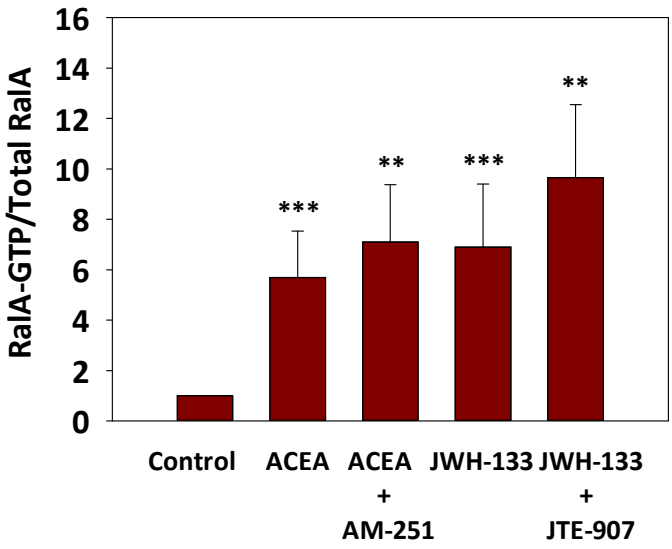

B

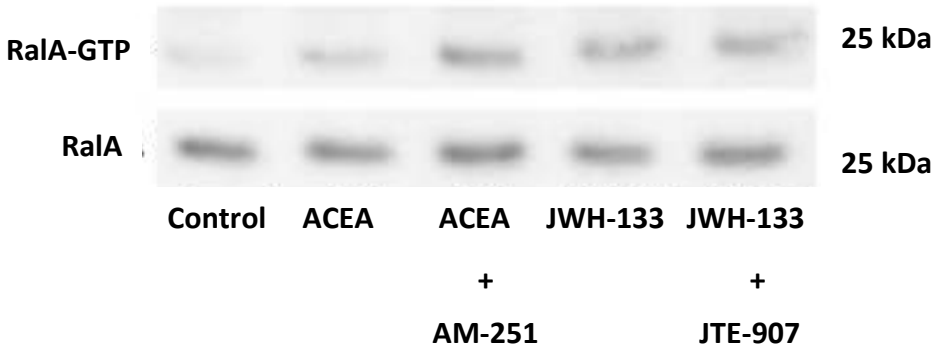

Figure 4.4: Activation of RalA by CB1 or CB2 agonist is not inhibited by CB1 antagonist AM-251 and CB2 antagonist JTE-907. Rat primary neuroblasts were pre-incubated with CB1 antagonists (AM-251 1µM), CB2 antagonist (JTE-907 1µM), or vehicle control for 1 hour prior to addition of CB1 agonist (ACEA 0.5 µM) and CB2 agonist (JWH-133 0.5 µM) for 30 minutes. Active RalA was pulled down from lysates and analysed by Western blot. **(A)** Quantitative densitometric analysis shows that RalA activation by the CB1 and CB2 agonist cannot be inhibited by AM-251 and JTE-907, respectively. Each bar represents the mean ± SEM; *P < 0.05; n = 3 independent experiments. **(B)** Representative Western blot showing levels of active RalA following treatment with CB agonists and antagonists.

One possible explanation for this unexpected result is that AM-251 is also a potent agonist for the GPR55 receptor, which is currently believed to be a novel CB receptor capable of activating Rho GTPases RhoA, Rac1, and Cdc42 (Ryberg et al. 2007). Thus, AM-251 may activate RalA through GPR55. However, it is still unclear as to why the CB2 antagonist JTE-907 enhances RalA activation in the presence of the CB2 agonist JWH-133. A different CB1 antagonist (LY-320135 1 µM), which is structurally dissimilar to AM-251, was able to suppress activation of RalA by ACEA and did not increase RalA activation when used on its own (Figure 4.5). Unexpectedly, the CB2 antagonist AM-630 enhanced RalA activation when used alone (Figure 4.5). Again, the reason for this still remains unclear, but it seems CB2 receptor signalling may be more complex than previously understood. For this reason, much of our subsequent work was focused on the CB1 receptor.

To further confirm that RalA is indeed activated following CB1 receptor stimulation, and to investigate the spatio-temporal regulation of RalA, we nucleofected rat RMS neuroblasts with a RalA FRET sensor (Raichu-RalA, kindly provided by M. Matsuda). This sensor consists of yellow fluorescent protein (YFP), RalA, the RalA binding domain for RalBP1, cyan fluorescent protein (CFP), and the C-terminal region for RalA (Figure 4.6) (Takaya et al. 2004; Yoshizaki et al. 2006). Binding of active RalA to the RalBP1 domain in the sensor induces a conformational change that brings the fluorophores into close proximity, thus resulting in FRET and enhancing YFP emission (Figure 4.6). FRET efficiency was measured using the acceptor photobleaching method, where the increase in CFP emission following bleaching of the acceptor (YFP) is used as a measure of FRET (Kenworthy 2001). Rat RMS neuroblasts show robust expression of the FRET sensor and show increase in CFP fluorescence following bleaching of the acceptor in both control and ACEA treated cells (Figure 4.7). Also, the FRET sensor appears to accumulate in highly fluorescent vesicular compartments in the dilation forming in front of the nucleus (Figure 4.7). However, there was no significant increase in FRET efficiency following treatment with ACEA for 30 minutes or 24 hours (Figure 4.8).

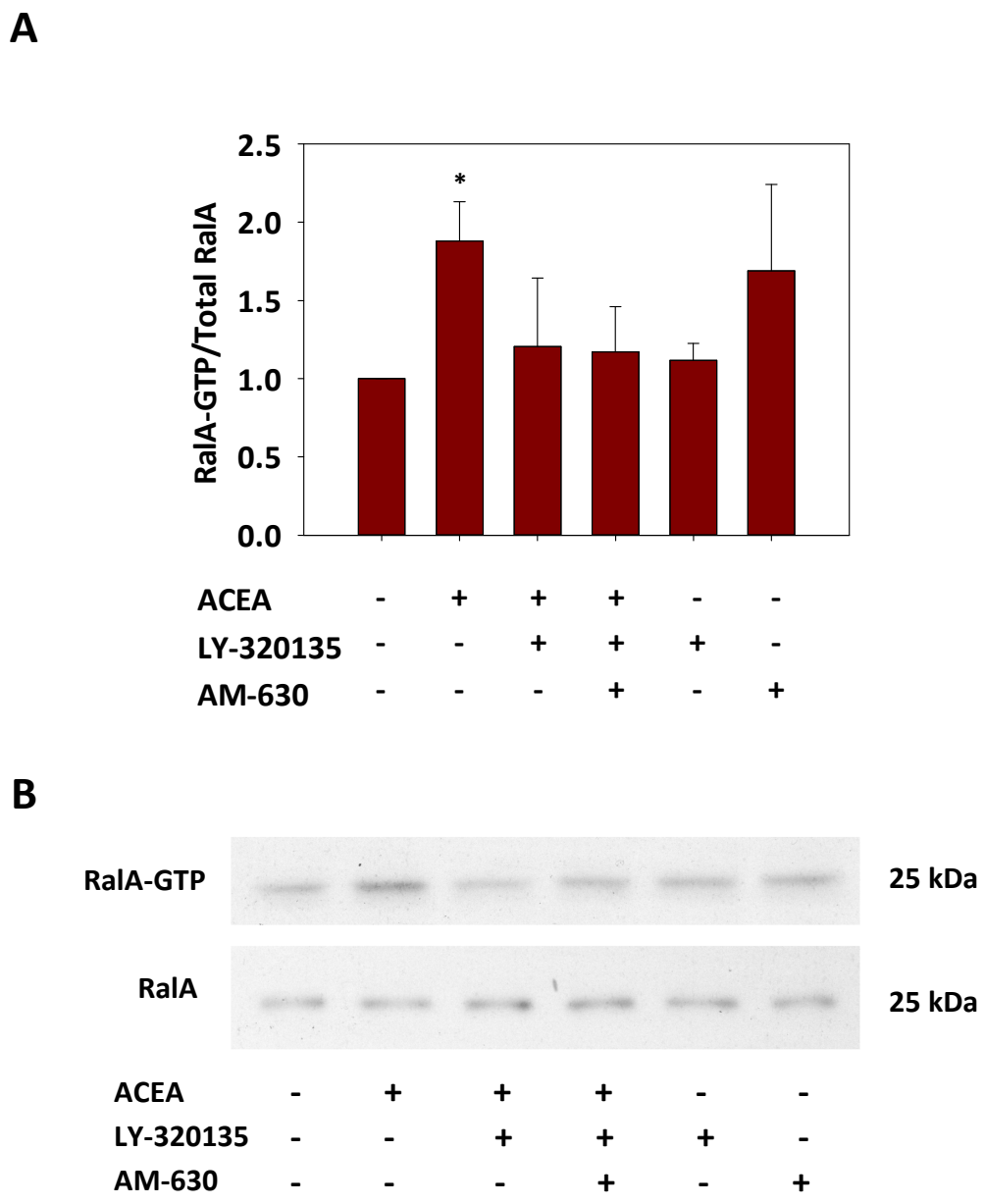

Figure 4.5: Activation of RalA by CB1 agonist is blocked by CB1 antagonist LY-320135. Rat primary neuroblasts were pre-incubated with a CB1 antagonist (LY-320135 1µM), a CB2 antagonist (AM-630 1µM), both CB1 and CB2 antagonist, or vehicle control for 1 hour prior to addition of the CB1 agonist (ACEA 0.5 µM) for 30 minutes. Active RalA was pulled down from lysates and analysed by Western blot. **(A)** Densitometric quantification of Western blots showing that RalA activation by CB1 agonist can be inhibited by the CB1 receptor antagonist LY-320135. Each bar represents the mean ± SEM; *P < 0.05; n = 3 independent experiments. **(B)** Representative Western blot showing activation of RalA by the CB1 agonist ACEA and inhibition of this activation by the CB1 antagonist LY-320135.

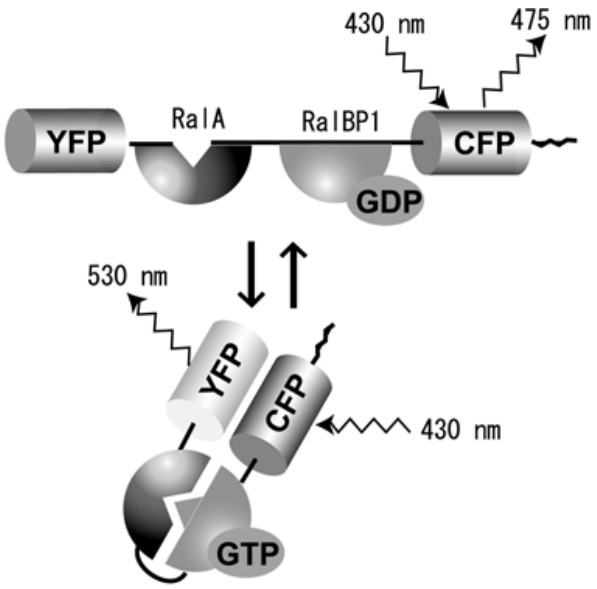

Figure 4.6: Schematic diagram of the RalA FRET sensor (Raichu-RalA). The sensor consists of yellow fluorescent protein (YFP), RalA, the RalA binding domain for RalBP1, cyano fluorescent protein (CFP), and the C-terminal region for RalA. When in the inactive state, exposing the sensor to light of wavelength 430 nm, results in emission of CFP only at 475 nm. Upon GTP loading (activation) of RalA, the effector RalBP1 binds to RalA, inducing a conformational change that brings the fluorophores into close proximity, thus allowing the YFP fluorophore to absorb CFP emission and emit fluorescence. Adapted from Yoshizaki, Aoki et al. (2006).

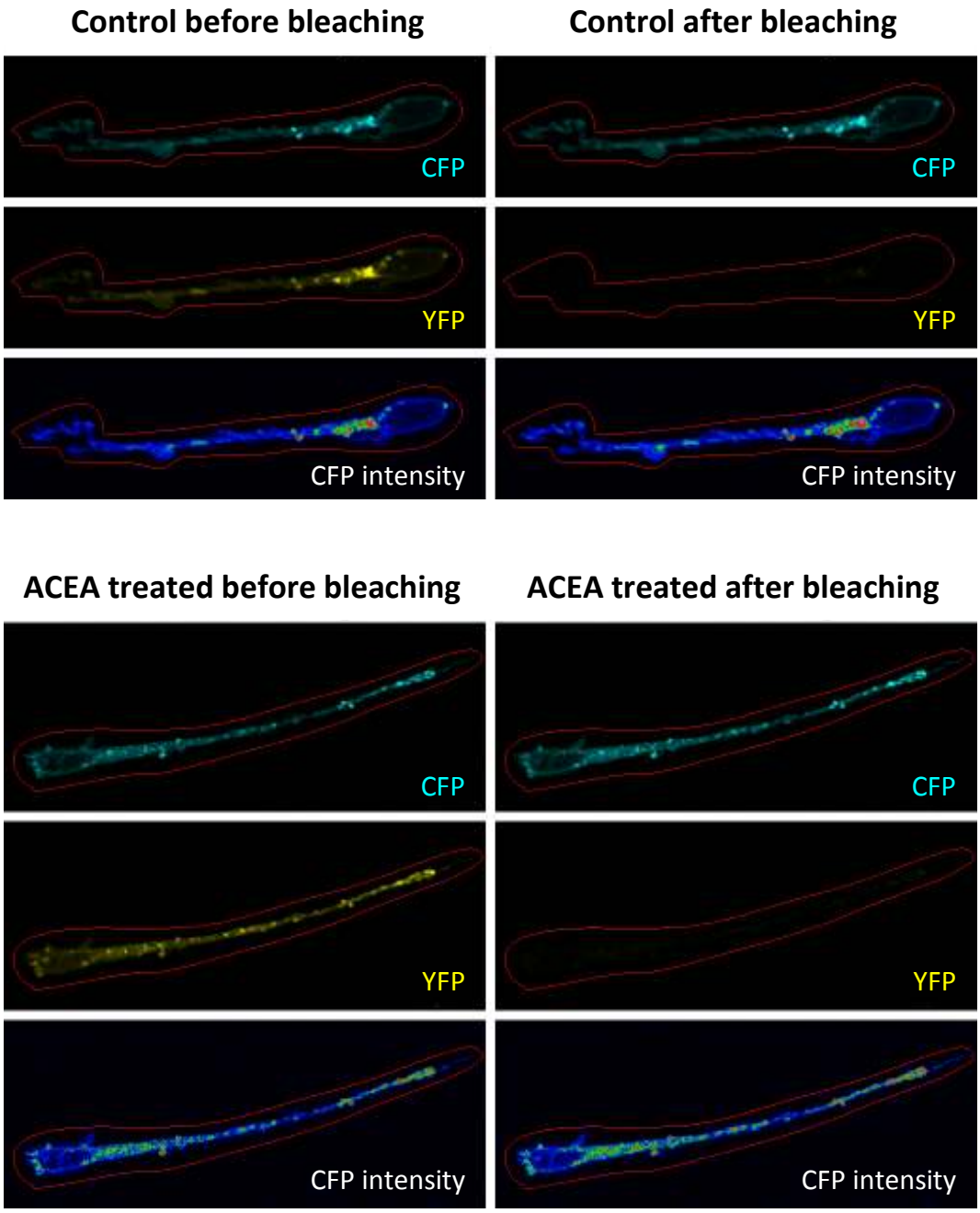

Figure 4.7 Raichu RalA is expressed in rat RMs neuroblasts. Rat RMS neuroblasts nucleofected with the RalA FRET sensor were embedded in Matrigel with or without CB1 agonist ACEA 0.5 µM. Neuroblasts were fixed 24 hours later, and FRET was measured using the acceptor photobleaching method. Panels show the levels of CFP and YFP in control and ACEA treated neuroblasts before and after bleaching of the acceptor (YFP). Bottom panels show CFP intensity as visualised by a heat map (low – high: blue – red). Red line indicates the area selected for bleaching. Imaging and bleaching were performed using the Zeiss LSM 710 confocal microscope.

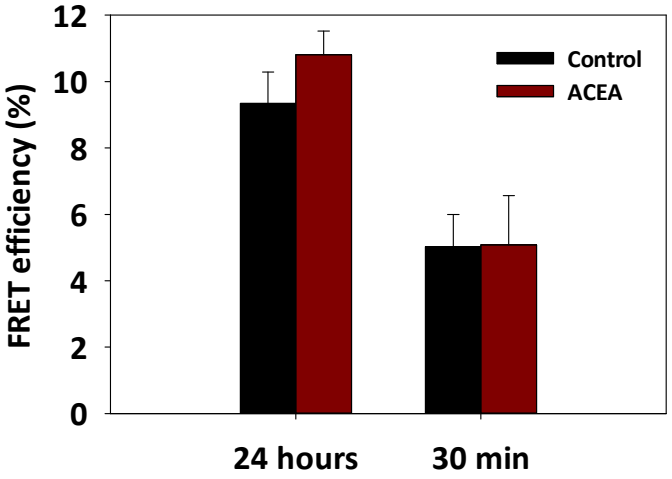

Figure 4.8 CB1 agonist does not increase FRET efficiency in rat RMs neuroblasts. Rat RMS neuroblasts nucleofected with the RalA FRET sensor were re-aggregated overnight and then embedded in Matrigel. Cultures were treated with CB1 agonist ACEA 0.5 μM for 24 hours during the entire migration period, or for 30 minutes 24 hours post embedding in Matrigel. FRET was measured in fixed cells using the acceptor photobleaching method. No significant difference was observed in FRET efficiency between control and neuroblasts treated with ACEA for 24 hours or 30 minutes. Note that FRET efficiency appears to be quite variable even between the two control groups at the two different time points. Each bar represents the mean ± SEM; n = 4 for 24 hours; n = 2 for 30 min, where n = independent experiments. Between 15 -20 cells were analysed per condition in each experiment.

Throughout these experiments we noticed a fair degree of variability in FRET efficiency even between control cells from both time points (9.3% ± 0.9 for 24 hours and 5.0% ± 1.0 for 30 min) (Figure 4.8). Further optimisation of the experimental/transfection conditions and of the criteria for FRET efficiency detection may be needed to establish whether FRET can be reliably applied for the study of GTPase activation in primary neuroblasts.

4.2.3 RalA can be knocked down with a siRNA oligo in rat RMS neuroblasts

In order to investigate RalA function in neuroblast migration, we first attempted to inhibit RalA expression using nucleofection of siRNA oligos. Rat RMS neuroblasts nucleofected with a validated RalA siRNA oligo (Lalli and Hall 2005) display a visible reduction in RalA immunoreactivity 72 hours after nucleofection when compared with control cells (Figure 4.9). The efficiency of RalA knockdown, as analysed by Western blotting, was approximately 50% and 70%, 48 hours and 72 hours post nucleofection, respectively (Figure 4.10). To confirm that inhibition of RalA expression does not affect cell viability, we stained control and RalA siRNA oligo nucleofected RMS neuroblasts for cleaved caspase 3, a marker of apoptosis (Fernandes-Alnemri et al. 1994). There was no significant difference in cleaved caspase 3-positivity between control and RalA-depleted cells, with approximately 5% of neuroblasts being positive for activated caspase in both groups (Figure 4.11). The small percentage of neuroblasts undergoing apoptosis in these cultures is most likely due to the nucleofection procedure itself, and does not appear to be due to RalA depletion. Hence, RalA does not appear to be required for neuroblast viability, and any potential effects caused by RalA knockdown on migration would be a reflection of the protein's function rather than a consequence of reduced cell viability.

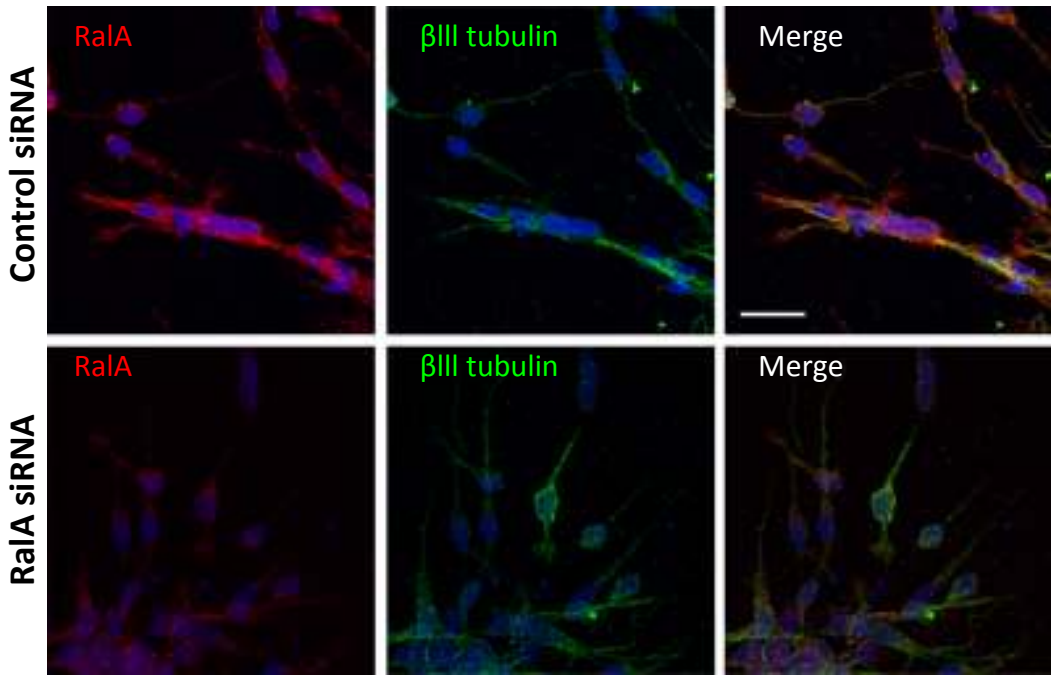

Figure 4.9: RalA expression can be knocked down with siRNA oligos in rat RMS neuroblasts (1). Dissociated rat RMS neuroblasts from P5-P7 pups were nucleofected with a control or RalA siRNA oligo and re-aggregated into clusters. Aggregates were embedded in Matrigel 48 hours post nucleofection and allowed to migrate for 24 hours. Neuroblasts were fixed and stained for RalA (red) and βIII tubulin (green). RalA expression is significantly reduced following nucleofection with RalA siRNA oligo in comparison with a control siRNA oligo. Bar = 20 µm.

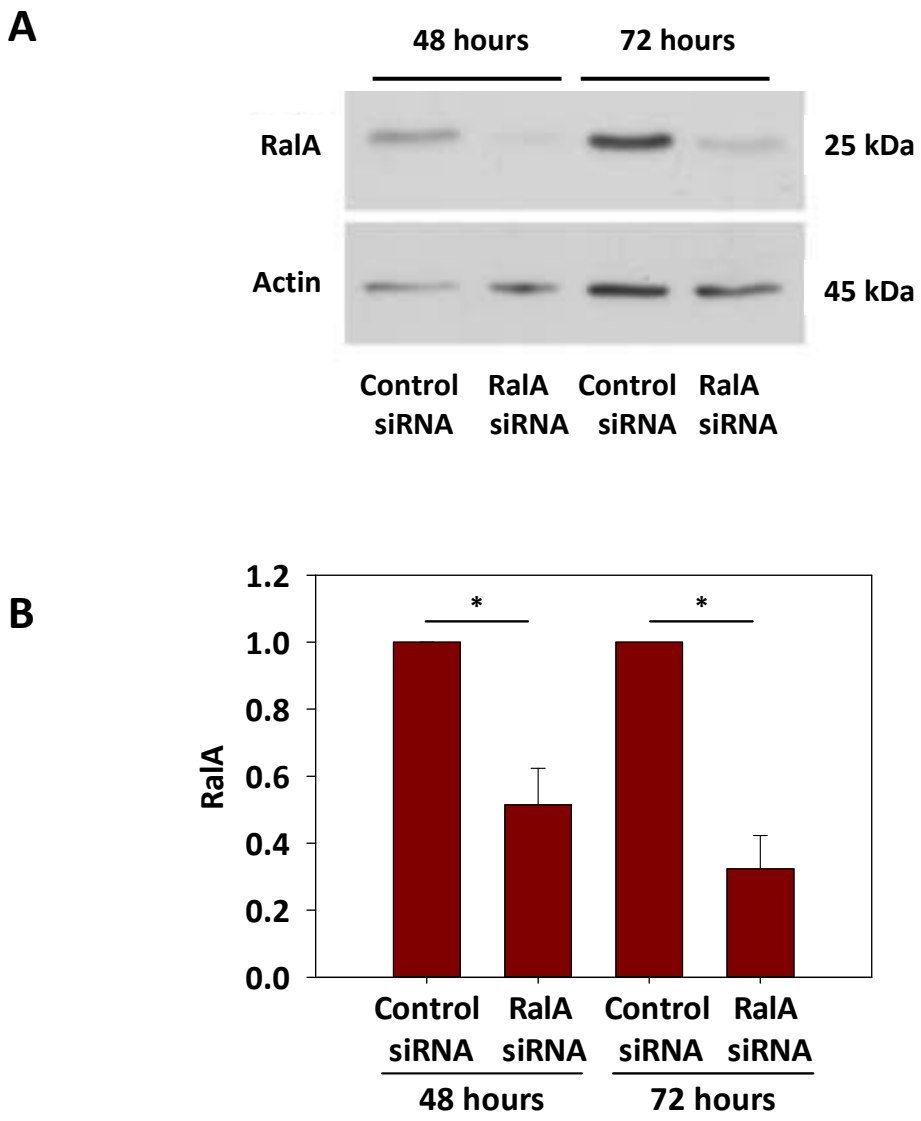

Figure 4.10: RalA expression can be knocked down with siRNA oligos in rat RMS neuroblasts (2). Dissociated rat RMS neuroblasts from P5-P7 pups were nucleofected with a control or RalA siRNA oligo and cultured for 48-72 hours. Lysates were probed for RalA expression via Western blot analysis. **(A)** Western blot showing reduced expression of RalA at both 48 and 72 hours post nucleofection with a RalA siRNA oligo. **(B)** Densitometric quantitative analysis shows significant reduction in RalA expression at both 48 and 72 hours after nucleofection of a RalA siRNA oligo. Each bar represents the mean ± SEM; *P < 0.05; n = 4 independent experiments.

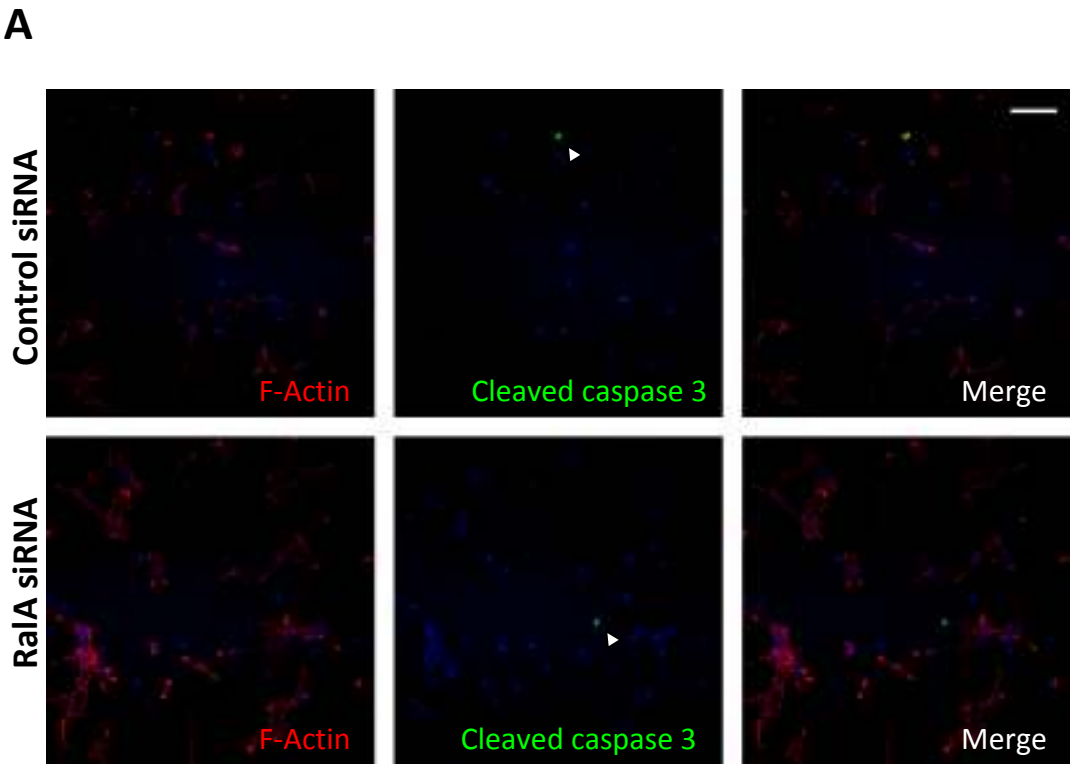

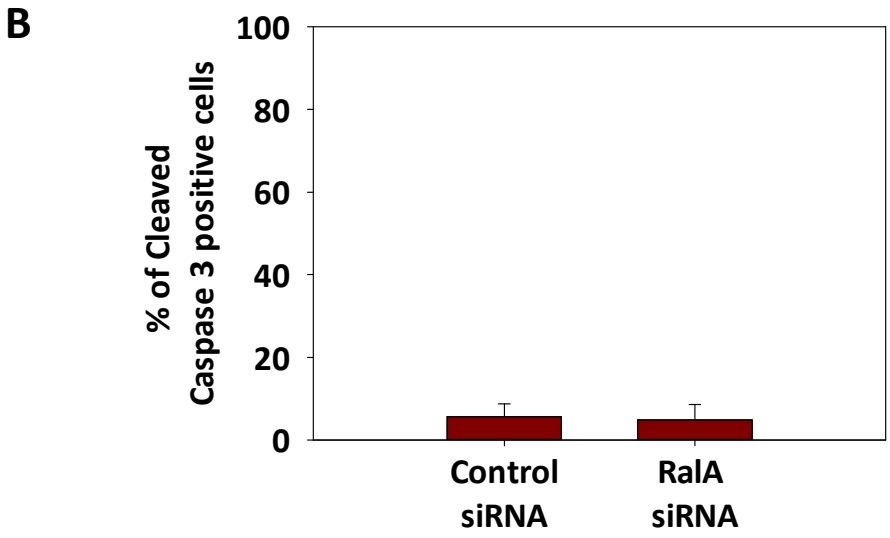

Figure 4.11: Knockdown of RalA does not affect viability of rat RMS neuroblasts. Dissociated rat RMS neuroblasts from P5-P7 pups were nucleofected with a control or RalA siRNA oligo and cultured for 48 hours on coverslips coated with polyornithine/laminin. **(A)** Coverslips were fixed and stained for F-Actin (red) and cleaved caspase 3 (green). Arrowheads point to cleaved caspase 3 positive cells. Bar = 50 µm **(B)** Quantification of cleaved caspase 3 positive cells after nucleofection with control or RalA siRNA oligo shows no difference in the % of cells undergoing apoptosis. Each bar represents the mean ± SEM; n = 3 independent experiments.

4.2.4 RalA is required for CB1 receptor-promoted migration of rat RMS neuroblasts *in vitro*

Next, we attempted to test our hypothesis that RalA is necessary for CB1-promoted migration of rat RMS neuroblasts *in vitro*. To do this, neuroblasts nucleofected with a control or RalA siRNA oligo were re-aggregated into clusters and embedded in Matrigel 48 hours post nucleofection. Aggregates were left to migrate for 24 hours ± CB1 agonist ACEA 0.5 µM, after which aggregates were fixed, and the distance migrated by neuroblasts was measured (refer to page 97 in the Methods for details of the quantification procedure). Representative images for each condition (Figure 4.12A) show that siRNA-mediated knockdown of RalA abolishes CB1 agonist-induced migration of neuroblasts out of aggregates. Quantification of the distance migrated (Figure 4.12B) also confirms that ACEA significantly increases the distance migrated by neuroblasts, and this effect is lost when RalA is depleted.

4.2.5 RalA is required for CB-promoted migration of rat RMS neuroblasts in situ

To further validate the requirement of active RalA for CB-promoted migration of neuroblasts, we prepared brain slice cultures from mice electroporated with a pCAG-IRES-EGFP plasmid expressing a myc-tagged dominant negative RalA (pCAG-DN RalA-IRES-EGFP), incubated them with CB1+CB2 agonists (1 µM), and performed time-lapse analysis of labelled neuroblasts in the RMS. Since GFP expression in cells electroporated with pCAG-DN RalA-IRES-EGFP was not sufficient enough to be detected by our spinning disk microscope, we co-electroporated pCAG-DN RalA-IRES-EGFP with a pCX-EGFP plasmid in a 3:1 ratio. To verify the expression of myc-tagged DN RalA following co-electroporation with pCX-EGFP, we performed double immunostaining of neuroblasts for cMyc and GFP. Although not all transfected cells express both GFP and DN RalA when co-electroporated (Figure 4.13), perturbing RalA function in at least some cells appears to be sufficient to significantly antagonise CB1 and CB2 agonist-mediated increases in the distance migrated (129.6 µm ± 10.9 for GFP; 190.8 µm ± 9.6 for GFP + CB agonists; 156.8 µm ± 20.4 for DN RalA + CB agonists) (Figure 4.14 top panel) and velocity (43.3 µm/hour ± 3.6 for GFP; 63.6 µm/hour ± 3.1 for GFP + CB agonists; 51.5 µm/hour ± 7.1 for DN RalA + CB agonists) (Figure 4.14 middle panel), as well as the reduction in the time spent

A

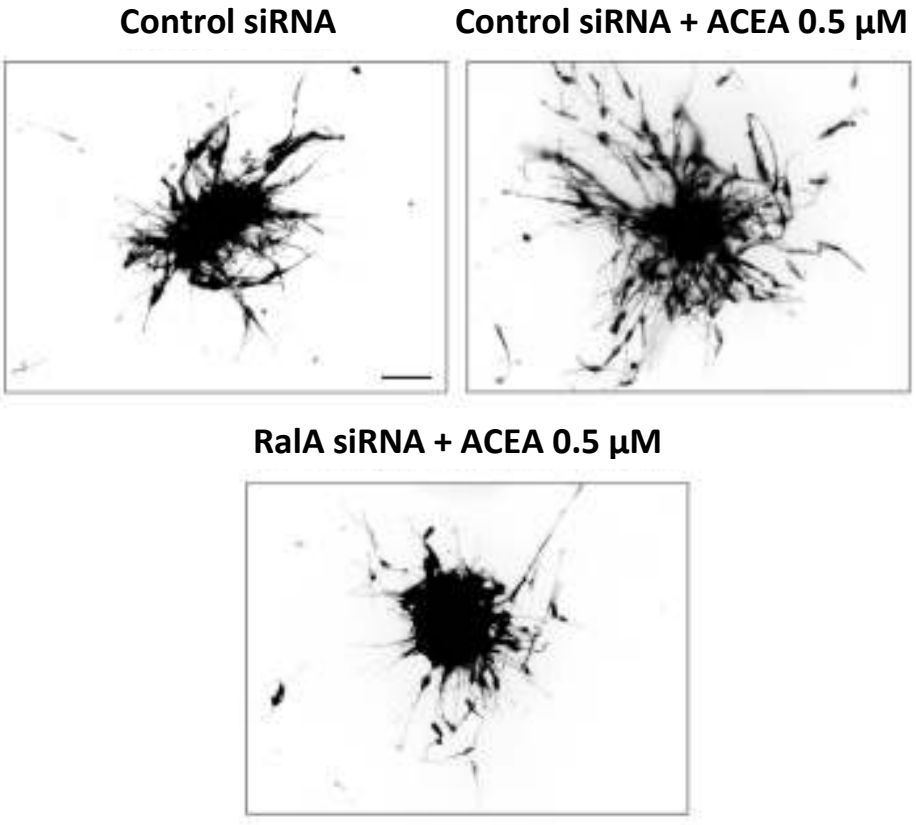
Control siRNA
Control siRNA + ACEA 0.5 µM
RalA siRNA + ACEA 0.5 µM

B

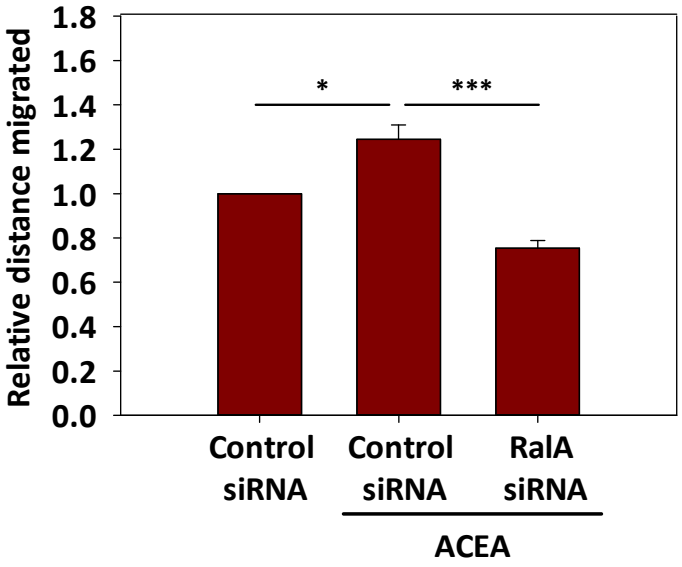
Relative distance migrated
1.8
1.6
1.4
1.2
1.0
0.8
0.6
0.4
0.2
0.0
*
***
Control siRNA
Control siRNA
RalA siRNA
ACEA

Figure 4.12: RalA is required for CB1 receptor-promoted migration of rat RMS neuroblasts *in vitro*. Dissociated rat RMS neuroblasts from P5-P7 pups were nucleofected with a control or RalA siRNA oligo and re-aggregated into clusters. Aggregates were embedded in Matrigel 48 hours post nucleofection and allowed to migrate for 24 hours with or without the CB1 agonist ACEA (0.5 µM), which was present throughout the migration period. **(A)** Images of aggregates 24 hours post embedding in Matrigel. Bar = 50 µm. **(B)** Quantification of the distance migrated shows that enhancement of neuroblast migration by the CB1 agonist ACEA is inhibited by RalA knockdown. Each bar represents the mean ± SEM; *P < 0.05; ***P < 0.001; n = 4 independent experiments.

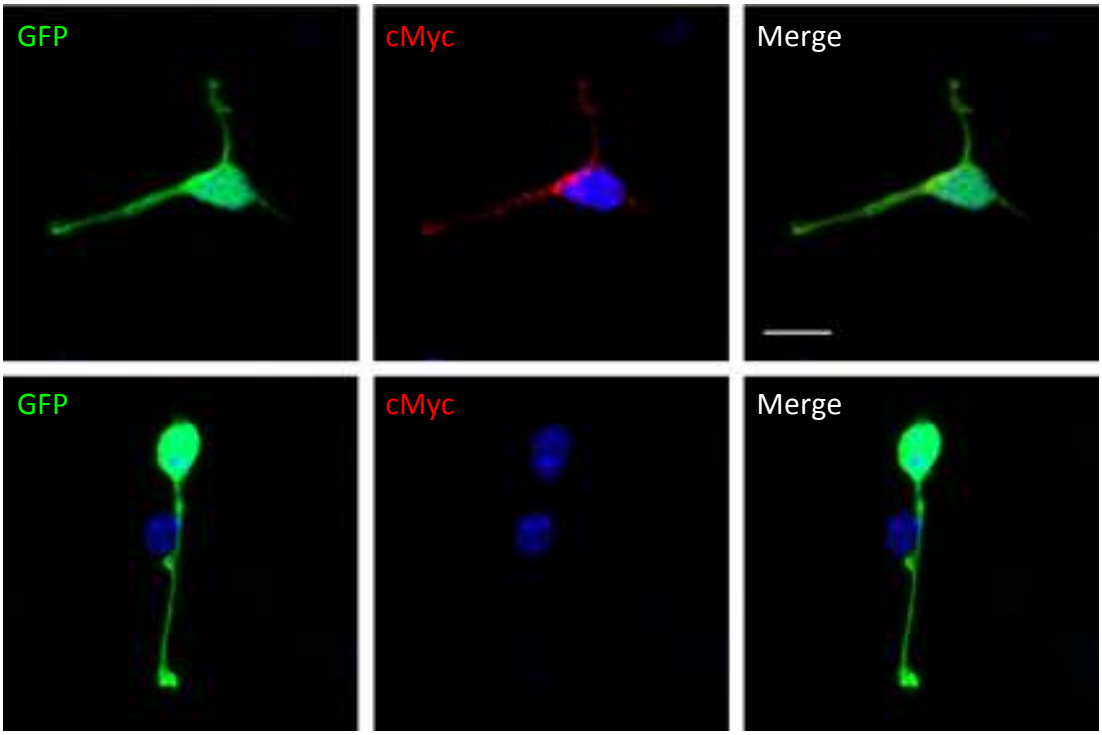

Figure 4.13: Not all RMS neuroblasts express both GFP and myc-tagged DN RalA following co-electroporation of DN RalA + pCX-EGFP in a 3:1 ratio. P2 mouse pups were electroporated with a plasmid expressing a myc-tagged dominant negative (DN) RalA and pCX-EGFP in a 3:1 ratio. Mice were sacrificed 5 days later, and RMS neuroblasts were dissociated and plated onto polyornithine/laminin-coated coverslips. Neuroblasts were fixed and stained for GFP and the myc tag 48 hours later. Only some cells expressing GFP also express the myc-tagged DN RalA. Bar = 10 µm.

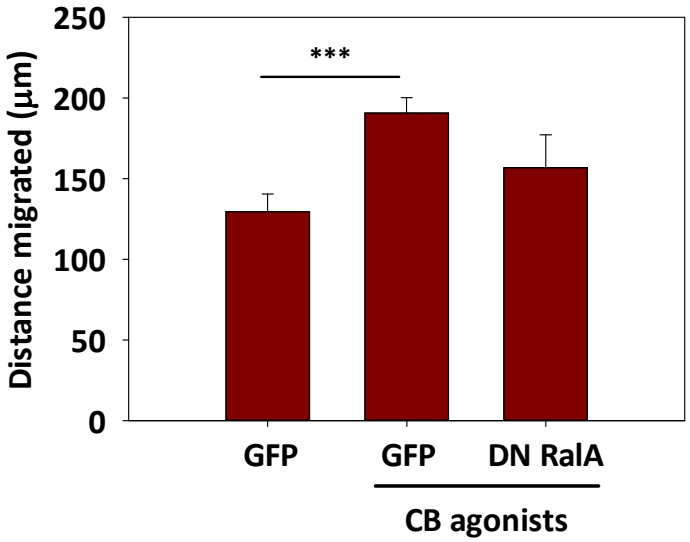
Distance migrated (µm)
250
200
150
100
50
0
***
GFP
GFP
DN RalA
CB agonists

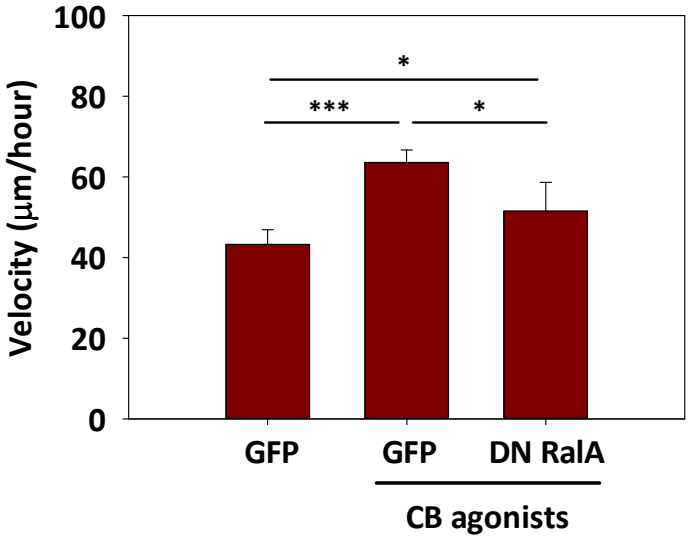
Velocity (µm/hour)
100
80
60
40
20
0
*
***
*
GFP
GFP
DN RalA
CB agonists

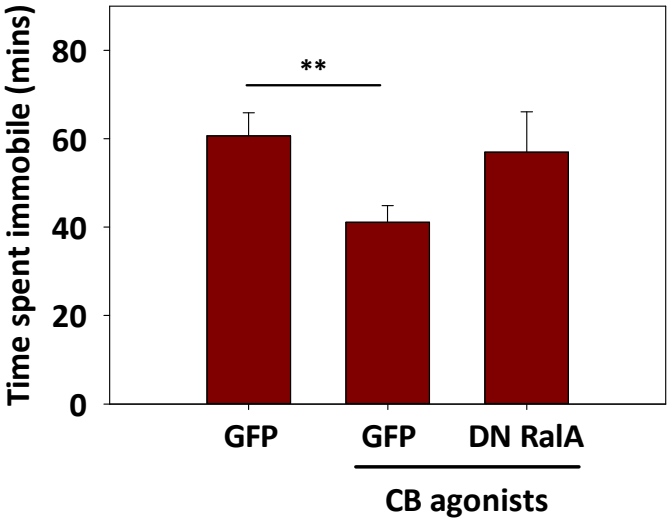
Time spent immobile (mins)
80
60
40
20
0
**
GFP
GFP
DN RalA
CB agonists

Figure 4.14: CB-promoted migration of RMS neuroblasts is inhibited by DN RalA in the brain slice assay. P2 mice were electroporated in the right ventricle with pCX-EGFP or pCAG-DN RalA-IRES-EGFP + pCX-EGFP in a 3:1 ratio. Animals were sacrificed 3-7 days later, and brain slices with GFP positive neuroblasts in the RMS were incubated with or without CB agonists (ACEA 1 μM + JWH-133 1 μM) for 1 hour prior to imaging. Slices were imaged every 3 minutes for 3 hours in the presence of CB agonists throughout the imaging period. Enhancement of distance migrated (top panel) and velocity (middle panel), and reduction in time spent immobile (bottom panel) caused by CB agonists are inhibited by DN RalA. Each bar represents the mean ± SEM; *P < 0.05; **P < 0.01; ***P < 0.001; n = 8 for control; n = 9 for CB agonists; n = 3 DN RalA + pCX-EGFP, where n = independent experiments. Approximately 15 to 30 cells were tracked for every experiment.

immobile (60.7 min ± 5.2 for GFP; 41.2 min ± 3.7 for GFP + CB agonists; 57.0 min ± 9.2 for DN RalA + CB agonists) (Figure 4.14 bottom panel) to some degree. The failure to completely inhibit the effects of the CB agonists in this assay is most probably due to the presence of neuroblasts only expressing pCX-EGFP, and therefore does not reflect the full extent to which perturbing RalA function affects CB-promoted neuroblast migration. Collectively, our data provides compelling evidence for a role for RalA in regulating CB-promoted migration of RMS neuroblasts.

4.2.6 Growth factors (HGF and GDNF) known to regulate RMS neuroblast migration also activate RalA

The RMS does not take a simple straight route from the SVZ to the OB; instead it follows a tortuous path to its final destination. How neuroblasts are guided so precisely along the stream still remains a mystery. The current school of thought assumes that various chemoattractants, and signalling molecules act at different points in the stream to continuously guide neuroblasts to the OB (Cayre et al. 2009; Leong and Turnley 2011). For example, the chemorepellent Slit is thought to be active specifically in the caudal part of the RMS where it is believed to propel neuroblasts from the SVZ into the stream (Hu 1999; Wu et al. 1999; Ward et al. 2003). Numerous chemoattractants, growth factors and signalling molecules have been demonstrated to influence RMS neuroblast migration. In order to respond to these signals, not only must RMS neuroblasts express the appropriate receptor, they must also transduce the signal to the cytoskeleton to elicit the correct response. So how do neuroblasts co-ordinate such a large variety of signals? We hypothesised that multiple signals arising from different receptors may converge onto specific “hub” molecules that can orchestrate the regulation of the cytoskeleton. RalA may represent one of these molecules operating downstream of different stimuli and signalling pathways.

In order to validate this hypothesis, we treated rat RMS neuroblasts with growth factors known to regulate RMS neuroblast migration, such as HGF and GDNF, (Paratcha et al. 2006; Wang et al. 2011), and measured RalA activation using a

pulldown assay. Figure 4.15 shows that both HGF 50 ng/ml and GDNF 100 ng/ml activate RalA after 5 mins, 30 mins, and 1 hour of incubation. This effect is statistically significant with 30 minutes of HGF 50 ng/ml. Although the extent of activation is variable, as observed by the large SEM, both HGF and GDNF increase RalA activation beyond basal levels at all time points. This degree of variability in the proportion of active RalA at any one time is not surprising given that GTPases are in constant equilibrium between the active and inactive forms. In summary, growth factors known to promote neuroblast migration, such as HGF and GDNF, may also be able to activate RalA.

Together, our results suggest a model in which different migratory signals present in the RMS may converge onto a molecular switch, such as RalA, which in turn could participate in the regulation of neuroblast migration.

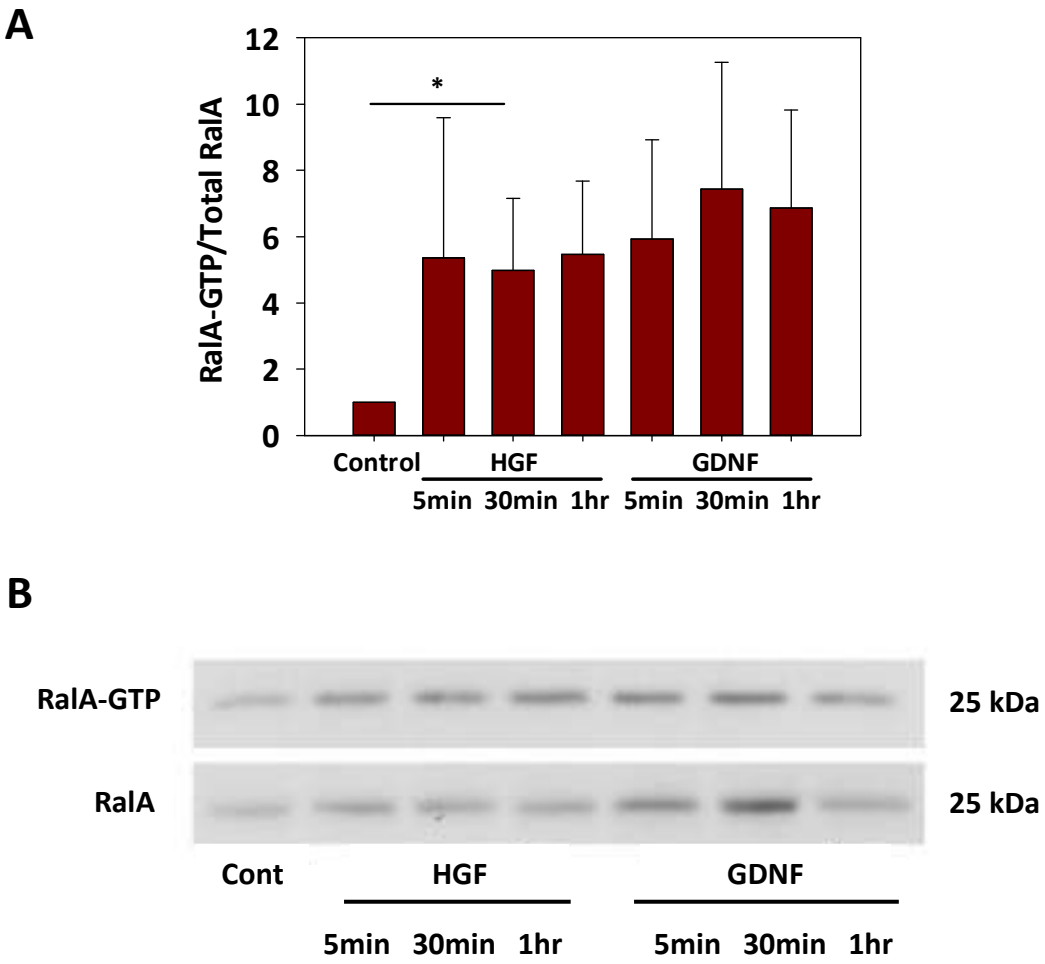

Figure 4.15: HGF and GDNF activate RalA in rat primary neuroblasts. Dissociated RMS neuroblasts cultured for 48 hours on polyornithine/laminin coated plates were treated with HGF 50 ng/ml or GDNF 100 ng/ml for the indicated time and lysed. Active RalA was examined with a pulldown assay. **(A)** Densitometric quantification of Western blots showing that both HGF and GDNF activate RalA in neuroblasts. Each bar represents the mean ± SEM; *P < 0.05; n = 5 for HGF and GDNF 30 min; n = 3 for all other treatments, where n = independent experiments. **(B)** Representative Western blot showing increased levels of active RalA (Ral-GTP) following treatment with HGF or GDNF.

4.3 Discussion

In Chapter 3, we showed that CB signalling regulates the migration of Cor-1 cells, as well as mouse and rat RMS neuroblasts. Moreover, we demonstrated for the first time that an eCB tone controls neuroblast migration *in vivo*, thus adding these lipid mediators to the already existing list of factors that influence the migration of neuroblasts in the RMS. In this chapter, we address the question of the downstream target of the CB receptors that could be involved in neuroblast migration. Here, we propose that the small GTPase RalA is an ideal candidate for this role, and examine whether CB-promoted migration of neuroblasts is reliant on RalA activity.

Since the Ral-GTPases comprise two closely related members, RalA and RalB, which are often associated with overlapping functions, we examined the expression of both isoforms in RMS neuroblasts. We find that RalA is abundant in migratory neuroblasts and has a unique pattern of expression, with diffuse punctuate staining throughout the cell body and leading process, and areas of accumulation at sites along the plasma membrane. In contrast, RalB could not be detected in RMS neuroblasts by Western blot analysis. Unfortunately due to the lack of a reliable RalB antibody suitable for immunocytochemistry, we were not able to investigate the expression and localisation of RalB in isolated neuroblasts. Intriguingly, RalB expression was particularly high in the motile and proliferative Cor-1 cell line, and was also detectable in SVZ homogenates. This could either suggest that RalB is expressed in proliferative regions such as the SVZ but not in the RMS, or that a weaker expression of RalB in neuroblasts requires loading of larger quantities of protein for detection. Either way, the preferential expression of RalA in RMS neuroblasts, suggests that this isoform may act as the principal functioning Ral protein in these cells.

We also show that both CB1 (ACEA) and CB2 (JWH-133) agonists consistently increase the activation of RalA beyond basal levels by 3 - 6 folds, even up to an hour after addition of the agonists. Unexpectedly, the CB1 antagonist AM251, and the

CB2 antagonist JTE-907 were not able to inhibit RalA activation by the CB1 and CB2 agonists, respectively. In fact, the combined effect of the CB2 agonist and antagonist (JTE-907) was greater than the agonist alone. On the other hand, a different CB1 antagonist, LY-320135, which is structurally dissimilar to AM-251, was able to block activation of RalA in response to ACEA. To our surprise, the CB2 antagonist AM-630 increased RalA activation in neuroblasts when used alone. However, AM-630 has been shown to act as a weak partial agonist at the CB1 receptor, which may account for these observations (Ross et al. 1999; Howlett et al. 2002). It is particularly puzzling that neither AM-251 nor JTE-907 could inhibit RalA activation in this assay, but were capable of inhibiting neuroblast migration stimulated by the CB1 and CB2 agonists in the Matrigel migration assay (Chapter 3). There are several factors that may have contributed to this discrepancy. Firstly, for technical reasons we were forced to perform the pulldown assay to detect active RalA on isolated neuroblasts plated on polyornithine/laminin-coated plates, a substrate on which they do not migrate. Thus the signalling cascades associated with migration in Matrigel may be altered or not active in this assay. Secondly, AM251 is also known to be an agonist for the orphan receptor GPR55, which is currently believed to be a novel CB receptor capable of activating RhoA, Rac1, and Cdc42 (Ryberg et al. 2007). Thirdly, all the CB antagonists used in this study are in fact classified as inverse agonists, and are therefore capable of inducing CB receptor signalling, albeit in an opposite manner to the agonists (Rodriguez de Fonseca et al. 2005). Another fact to consider is that RalA can mediate distinct effects simultaneously by coupling to different effectors (Feig 2003; van Dam and Robinson 2006). For example, RalA binding to different subunits of the exocyst complex has been suggested to account for discrete aspects of cell polarisation (Hazelett and Yeaman 2012). So, although several of the antagonists appear to activate RalA, or enhance the activation of RalA by the agonists, we cannot discern from this assay whether the spatial regulation or choice of target effector is the same as with the agonist alone.

In an effort to visualise the spatial activation of RalA in migrating neuroblasts, we attempted to perform FRET imaging using the Raichu-RalA sensor, a tool

successfully used in other cellular models to examine spatio-temporal regulation of RalA (Takaya et al. 2004; Yoshizaki et al. 2006). Unfortunately, we found that the expression levels of the sensor, as well as the FRET efficiency was considerably variable even amongst control neuroblasts, which may lead to artefacts and confuse the interpretation of the results. However, we noticed that in neuroblasts apparently undergoing nucleokinesis, the Raichu-RalA sensor had a tendency to accumulate in highly fluorescent vesicular compartments in the dilatation in front of the nucleus, an area known to be a site of active endocytic/exocytic traffic (Shieh et al. 2011). Understanding whether these areas can truthfully reflect real sites of active RalA in migrating neuroblasts will require further optimisation of the experimental conditions and imaging parameters.

To investigate the importance of RalA in CB agonist-promoted migration of RMS neuroblasts, we used a previously validated siRNA oligo targeted against RalA to inhibit protein expression in neuroblasts by almost 70% without any effect on cell viability. Importantly, CB-promoted migration of neuroblasts in Matrigel was completely abolished following depletion of RalA, and was in fact marginally lower than the control. This observation led us to speculate whether RalA was also important, not only for CB-promoted migration, but also for basal motility (examined in detail in Chapter 5). We further validated these observations using *ex vivo* cultures, where we show that CB-promoted migration of neuroblasts in the brain slice assay is also reliant on the activity of RalA.

In conclusion, RalA is the main isoform expressed by migrating neuroblasts. Stimulation of either the CB1 or CB2 receptor leads to activation of RalA, which appears to be important for CB-promoted migration of neuroblasts both *in vitro* and *ex vivo*. Finally, other growth factors known to regulate neuroblast migration in the RMS, such as GDNF and HGF (Paratcha et al. 2006; Garzotto et al. 2008), also activate RalA. Thus, different signalling cascades that influence neuroblast migration may impinge on RalA as a common target.

Chapter 5: RalA is required for RMS neuroblast migration *in vitro* and *in vivo*

5.1 Introduction

Due to the capacity of Ral GTPases to be activated by a number of upstream signalling cues, as well as couple to several effector molecules - such as RalBP1, the exocyst complex, the actin binding protein filamin, and the transcription factor ZONAB – Ral proteins are able to participate in a wide variety of biological functions (Cantor et al. 1995; Ohta et al. 1999; Moskalenko et al. 2002; Frankel et al. 2005). The discovery that Ral-GEFs were effectors for Ras GTPases, and that Ral proteins were able to mediate oncogenic transformation downstream of Ras, led to these previously less well-known Ras family members becoming a topic of much interest (Urano et al. 1996; White et al. 1996). Ral GTPase interaction with RalBP1 is now believed to be responsible for its function in endocytosis, and has been shown to be a mechanism by which receptor mediated endocytosis of the EGF receptor is achieved (Shen et al. 2001). Instead, interaction with the exocyst complex is recognised as the mechanism regulating exocytosis of secretory vesicles. Currently, delivery of basolateral membrane proteins in polarised epithelial cells (Moskalenko et al. 2002), secretion of dense granules by platelets (Kawato et al. 2008), insulin release by pancreatic β cells (Lopez et al. 2008), as well as glutamate secretion by neurones (Polzin et al. 2002), have all been shown to be reliant on a Ral-exocyst interaction. With regards to morphology, RalA is responsible for the formation of lamellipodia mediated by EGF in Cos cells (Takaya et al. 2004), and can also induce filopodia formation in fibroblasts by recruiting the actin binding protein filamin (Ohta et al. 1999), or by directly regulating the actin cytoskeleton through an interaction with the exocyst (Sugihara et al. 2002). Similarly, a Ral-exocyst relationship has been implicated in neurite branching and is believed to mediate changes to the actin cytoskeleton in response to integrin mediated signalling (Lalli and Hall 2005). In addition, the RalA-exocyst pathway also participates in neuronal polarity by targeting the delivery of the Par complex to initiate axon polarisation (Lalli 2009). Hence, Ral proteins have an inherent ability to regulate morphology,

polarity, adhesion, and cytoskeletal dynamics, all of which are also necessary for cell migration. Indeed, the migration of myoblasts in response to chemotactic factors, such as FGF-2, HGF, and IGF-1, is reliant on Ras activation of Ral (Suzuki et al. 2000), whilst the migration of human prostate cancer cells was found to be dependent on the interaction of RalA with the exocyst complex (Hazelett and Yeaman 2012). In addition, in a metastatic cancer cell line, Ral-exocyst was found to promote migration by delivery of α5 integrin, an adhesion molecule necessary for formation of cell-substratum interaction, to the leading edge (Spiczka and Yeaman 2008).

To this point we have determined that RalA is required for CB-promoted migration of neuroblasts, and that other factors known to regulate neuroblast migration in the RMS also activate RalA. These observations, together with the recognised functions of RalA in other systems, led us to ask whether RalA is simply required to enhance migration in response to motogens and chemoattractants, or whether it has a more fundamental role in neuroblast migration. Using several molecular biological approaches, as well as genetic deletion of RalA, we show that this GTPase is required for polarised migration and correct morphology of neuroblasts both *in vitro* and *in vivo*. We also demonstrate that RalB is not necessary for neuroblast migration and cannot fully compensate for the loss of RalA.

5.2 Results

5.2.1 RalA depletion inhibits RMS neuroblast migration *in vitro*

We have shown in Chapter 4 that RalA is required for CB-promoted migration of RMS neuroblasts, and that other pro-migratory molecules known to regulate neuroblast migration in the RMS can also activate RalA. We also know that RMS neuroblasts have an innate capacity to migrate when cultured in Matrigel, and that a basal level of active RalA is present in this system. Here, we turn our attention to examining the role of RalA in intrinsic neuroblast migration.

Firstly, to determine whether RalA is necessary for intrinsic neuroblast migration, we inhibited RalA expression using a siRNA oligo, and examined the ability of RMS neuroblasts to migrate *in vitro* using the Matrigel migration assay. Representative images and quantification of the results show that migration of neuroblasts out of aggregates is inhibited following RalA depletion by almost 40% (Figure 5.1). Close examination of neuroblast morphology reveals that loss of RalA expression leads to elongation of the leading process (Figure 5.2A), resulting in a significant increase in the average process length (Figure 5.2B). To further examine the effect of RalA knockdown on migration and to ascertain the reason for this change in morphology, we analysed time-lapse movies of control and RalA-depleted neuroblasts migrating in Matrigel. Knocking down RalA significantly impaired neuroblast migration (Figure 5.3 and Supplementary movie 5 & 6). Quantitative tracking analysis of neuroblasts confirmed that RalA-depleted neuroblasts migrated significantly less than control cells (distance migrated: 100.7 μm ± 5.9 for control, and 66.0 μm ± 2.9 for RalA deficient cells) and had a slower speed of migration (Velocity: 24.8 μm/hour ± 1.3 for control and 16.7 μm/hour ± 0.7 for RalA deficient cells) (Figure 5.4A-B and Supplementary movie 5 & 6). Also, RalA-depleted neuroblasts spent a significantly greater period of time immobile (94.6 mins ± 3.9) during the 4 hour tracking period when compared with control cells (82.1 mins ± 4.2) (Figure 5.4C). Analysis of time-lapse movies at high magnification (40X) shows that RalA-depleted neuroblasts are still able to extend a highly dynamic leading process, even though this seems to undergo retraction more frequently compared to control cells. As a consequence, the nuclei of RalA depleted neuroblasts fail to move forward (Supplementary movie 7 & 8). Based on this observation, we performed detailed tracking analysis of nuclear movement to identify defects in nucleokinesis. A sample trace showing the movement of a nucleus of a control and RalA-depleted neuroblast (Figure 5.5A) illustrates that control nuclei undergo periods of inactivity followed by large saltatory movements (jumps > 5 μm). In RalA-depleted neuroblasts, these large saltatory nuclear movements appear to be absent. Indeed, our results reveal that RalA depletion caused a 6-fold reduction in the % of “productive” saltatory nuclear movements (jumps > 5 μm) from a norm of 3% to approximately 0.5% (Figure 5.5B). In addition, classification of each nuclear movement made by every tracked cell

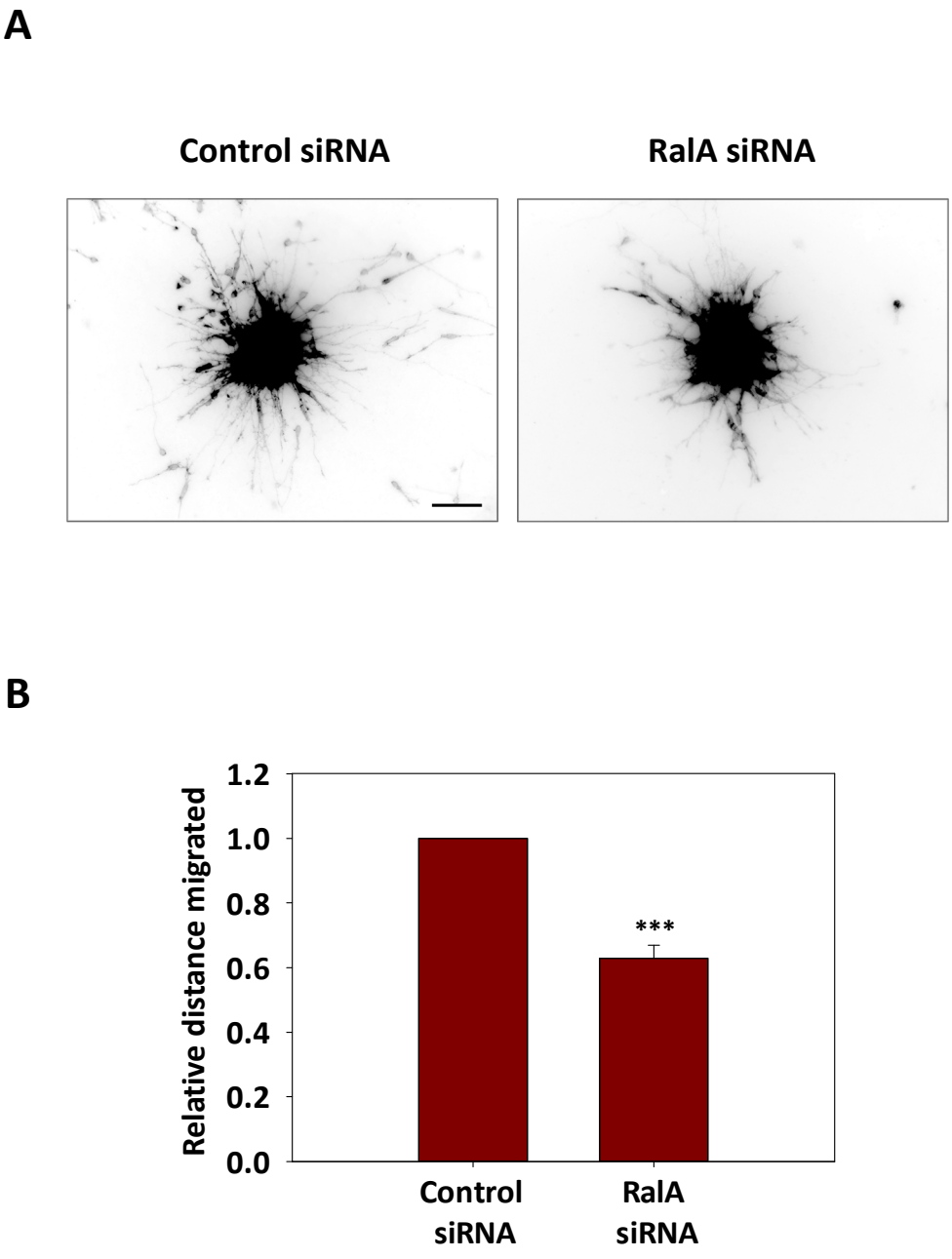

Figure 5.1: RalA is required for migration of rat RMS neuroblasts *in vitro*. Rat RMS neuroblasts nucleofected with a control or RalA siRNA oligo were re-aggregated into clusters, embedded in Matrigel 48 hours post nucleofection, and allowed to migrate for 24 hours. **(A)** Images of a control and RalA siRNA oligo nucleofected aggregate 24 hours post embedding in Matrigel. Bar = 50 µm. **(B)** Quantification of the distance migrated shows that neuroblast migration is inhibited by RalA knockdown. Each bar represents the mean ± SEM; ***P < 0.001; n = 3 independent experiments.

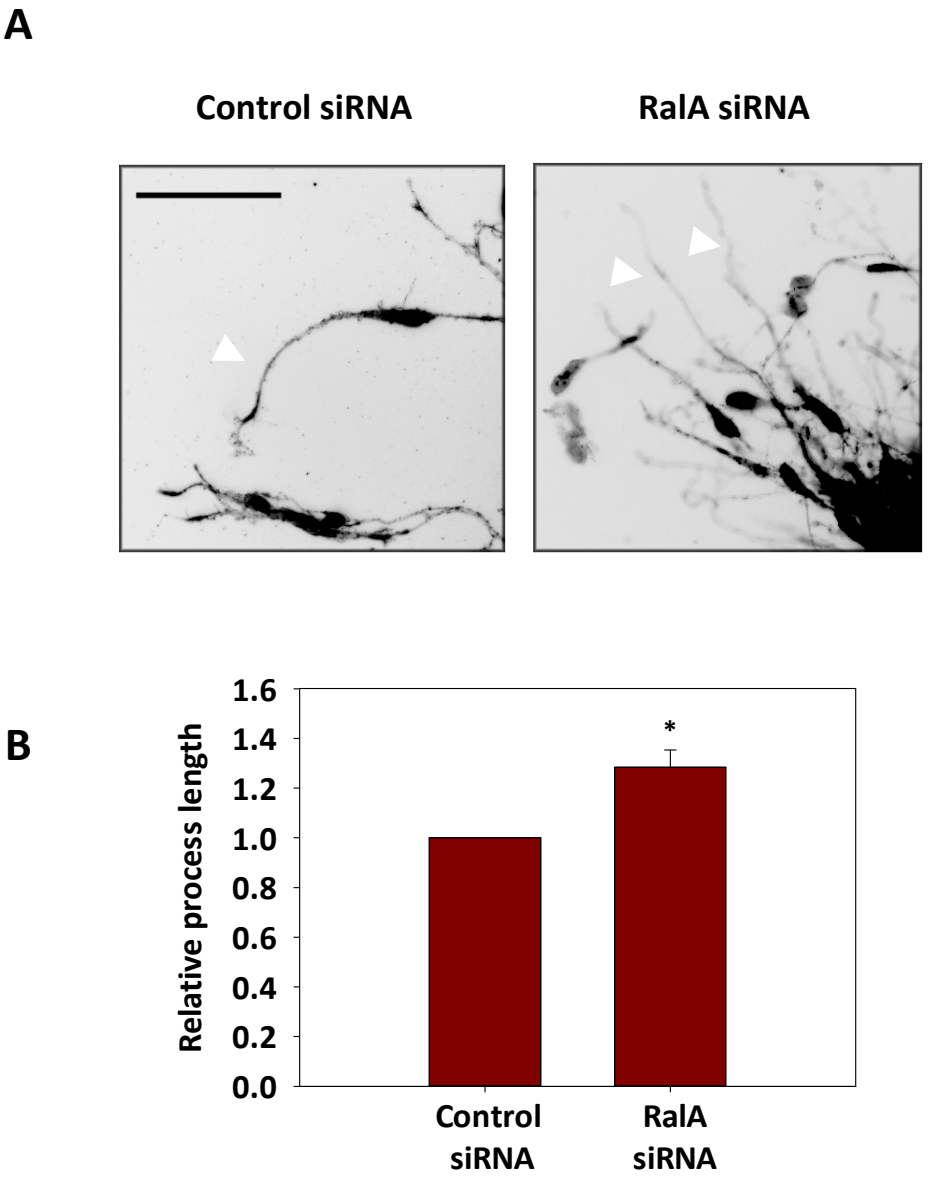

Figure 5.2: RalA knockdown alters the morphology of rat RMS neuroblasts *in vitro*. Rat RMS neuroblasts nucleofected with a control or RalA siRNA oligo were re-aggregated into clusters, embedded in Matrigel 48 hours post nucleofection, and allowed to migrate for 24 hours. **(A)** High magnification images of a control and RalA siRNA oligo nucleofected aggregate embedded in Matrigel. Arrowheads highlight leading processes of control and RalA depleted neuroblasts. Bar = 50 µm. **(B)** Quantification of process length reveals that neuroblasts depleted of RalA have significantly longer processes. Each bar represents the mean ± SEM; *P < 0.05; n = 3 independent experiments. A total of 362 cells were measured for control neuroblasts and 268 cells were measured for RalA depleted neuroblasts.

Control siRNA

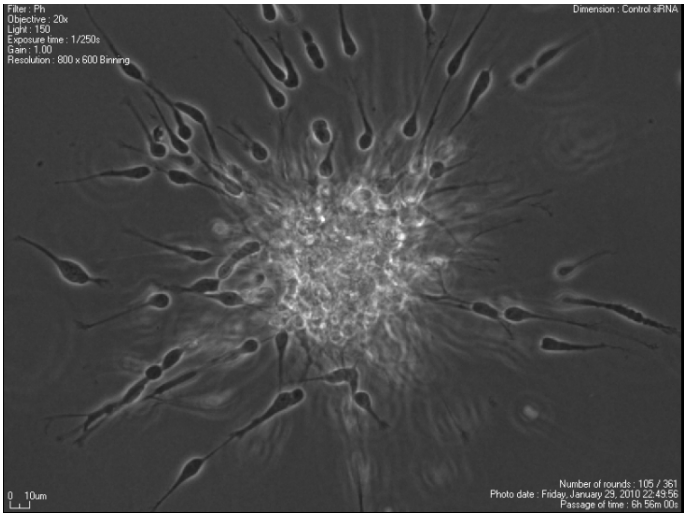

RalA siRNA

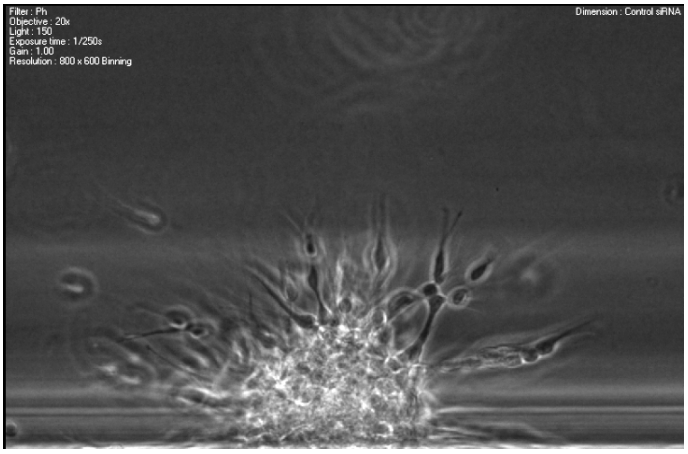

Figure 5.3: Time-lapse imaging of RalA depleted rat RMS neuroblast aggregates. Control and RalA depleted neuroblast aggregates were embedded in Matrigel in a 4 chamber 35mm Hi-Q4 culture dish (Nikon) 48 hours after nucleofection. Images were captured on a Nikon Biostation with a 20X objective every 3 minutes for 24 hours. The figure shows snapshots from movies of control and RalA depleted aggregates taken after 9 hours of migration. Please also see supplementary movie 5 and 6 - playing speed: 5 frames/second.

A

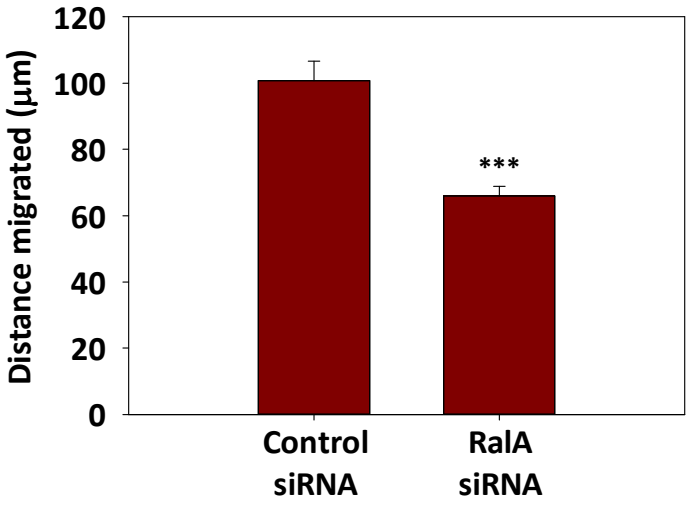
Distance migrated (µm)
120
100
80
60
40
20
0
***
Control siRNA
RalA siRNA

B

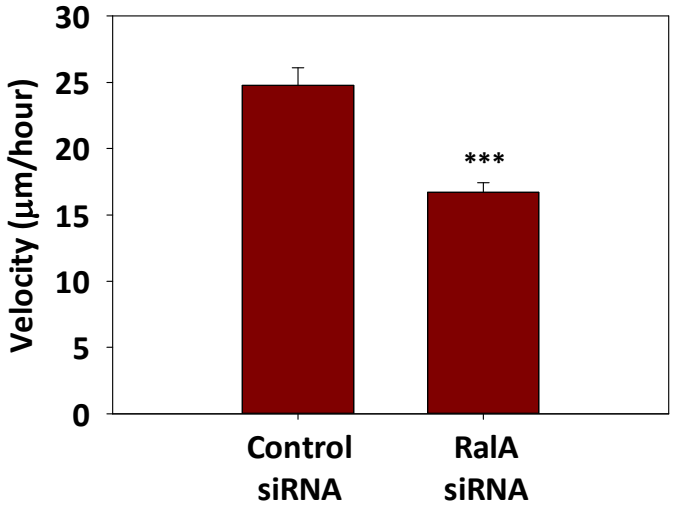
Velocity (µm/hour)
30
25
20
15
10
5
0
***
Control siRNA
RalA siRNA

C

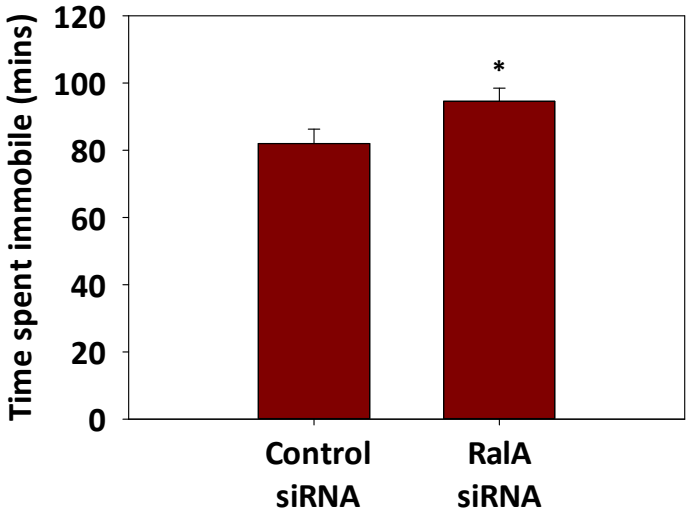
Time spent immobile (mins)
120
100
80
60
40
20
0
*
Control siRNA
RalA siRNA

Figure 5.4: RalA depletion significantly impairs RMS neuroblast migration *in vitro*. Time-lapse images of control and RalA depleted rat neuroblast aggregates, migrating in Matrigel in a 4 chamber 35mm Hi-Q4 culture dish (Nikon), were captured on the Nikon Biostation with a 20X objective every 3 minutes for 24 hours. The movement of individual cells was tracked using Volocity software (Perkin Elmer) for a period of 4 hours during the first 9 hours of filming. **(A)** Mean distance migrated by neuroblasts is significantly decreased in RalA depleted neuroblasts in comparison to the control. **(B)** Similarly, the mean velocity of RalA depleted neuroblasts is significantly lower than that of control neuroblasts. **(C)** The time spent immobile is significantly greater in RalA depleted neuroblasts. Each bar represents the mean ± SEM; *P < 0.05; ***P < 0.001; n = 80 cells from 2 independent experiments.

A

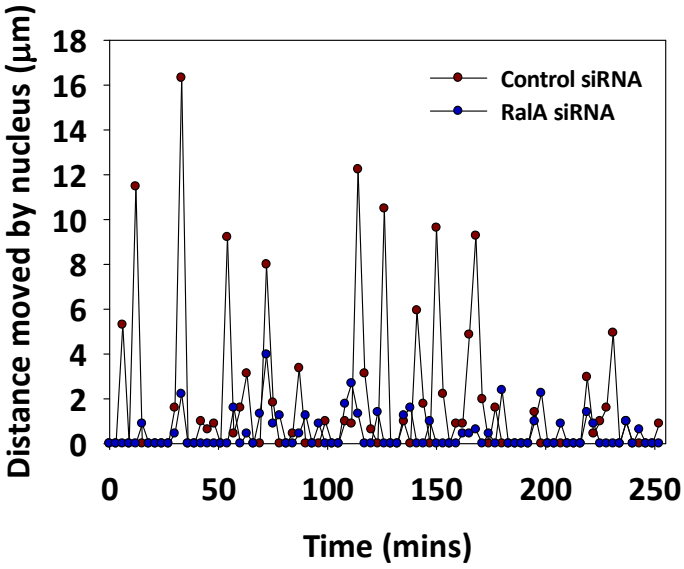
Distance moved by nucleus (µm)
18
16
14
12
10
8
6
4
2
0
Control siRNA
RalA siRNA
0
50
100
150
200
250
Time (mins)

B

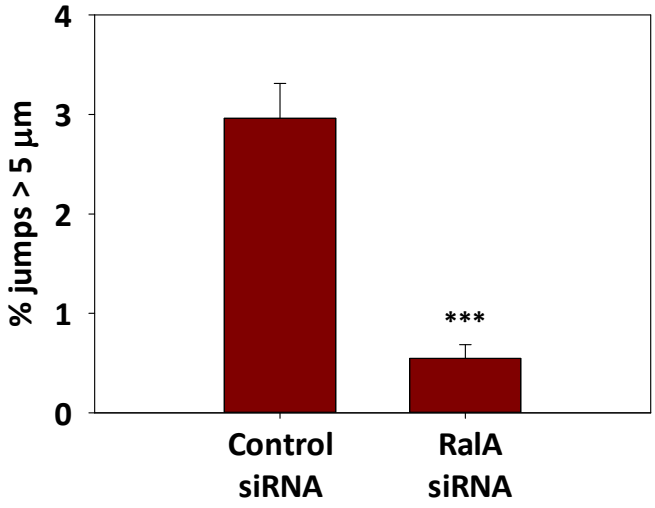
% jumps > 5 µm
4
3
2
1
0
***
Control siRNA
RalA siRNA

C

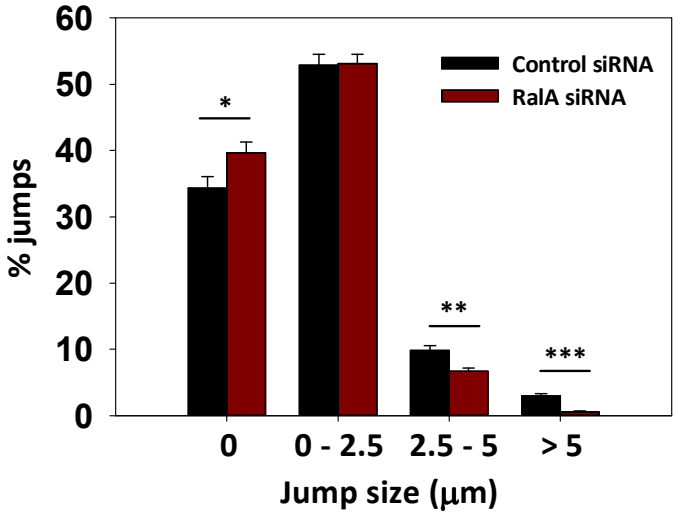
% jumps
60
50
40
30
20
10
0
Control siRNA
RalA siRNA
*
**
***
0
0 - 2.5
2.5 - 5
> 5
Jump size (µm)

Figure 5.5: RalA depletion impairs efficient nucleokinesis in rat RMS neuroblasts *in vitro*. Quantitative tracking analysis of control and RalA-depleted neuroblast aggregates migrating in Matrigel. Nuclei were tracked using Volocity software (Perkin Elmer) for a period of 4 hours during the first 9 hours of filming. **(A)** Sample trace showing the nuclear movement of a control and RalA depleted neuroblast. **(B)** RalA knockdown significantly decreases the percentage of "productive" nuclear jumps greater than 5 μm. **(C)** The jumps made by each tracked nucleus over a 4 hour period were classified according to their length. RalA depleted cells had a greater number of pauses (0 μm), and made significantly fewer jumps that were 2.5 – 5 μm or > 5μm. Each bar represents the mean ± SEM; *P < 0.05; **P < 0.01; ***P < 0.001; n = 80 cells from 2 independent experiments.

shows that RalA knockdown resulted in fewer nuclear jumps that were between 2.5 µm – 5 µm (9.9% ± 0.7 for control and 6.7% ± 0.5 for RalA knockdown), a similar % of jumps that were between 0 µm – 2.5 µm (52.8% ± 1.6 for control and 53.1% ± 1.4 for RalA knockdown), and a greater number of pauses (34.3% ± 1.8 for control and 39.7% ± 1.6) (Figure 5.5C). These results lead us to believe that RalA may be involved in regulating nucleokinesis, and is required for efficient migration of neuroblasts *in vitro*.

To prove that inhibition of neuroblast migration is specifically due to the loss of RalA, we attempted to rescue the migratory defect caused by RalA knockdown using a pCAG-IRES-EGFP plasmid (Jacobs et al. 2007; Causeret et al. 2009) containing a wild type (WT) RalA version that is resistant to siRNA-mediated knockdown (please refer to Methods, page 88). Neuroblasts were co-transfected with a control or RalA siRNA oligo together with a GFP plasmid or WT RalA. Neuroblasts transfected with RalA siRNA oligo are visibly impaired in their ability to migrate out of aggregates compared to control siRNA transfected cells (GFP-positive cells in Figure 5.6A top and middle panels). Internal control cells (GFP-negative) migrate to a similar extent in all conditions (Figure 5.6A-B). This implies that the migratory defect induced by RalA depletion is a cell autonomous effect. Moreover, co-transfection of RalA siRNA and the siRNA-resistant WT RalA restored neuroblast migration to control levels (Figure 5.6A-B). Altogether, this data validates our initial findings that RalA is involved in regulating RMS neuroblasts *in vitro*, possibly through co-ordination of events that regulate nucleokinesis.

5.2.2 Stable knockdown of RalA with a shRNA plasmid vector

We have been able to successfully demonstrate the function of RalA in neuroblast migration *in vitro* using siRNA oligos as a method of gene silencing. However, siRNA based approaches are limited by the fact that they only exert their effect for a few days before being degraded (Hasuwa et al. 2002). Achieving successful inhibition of protein expression *in vivo* may be more difficult and require a more efficient and continuous inhibition of protein expression over longer periods. Hence, to gain further evidence to support a role for RalA in neuroblast migration *in vivo,* we used

A

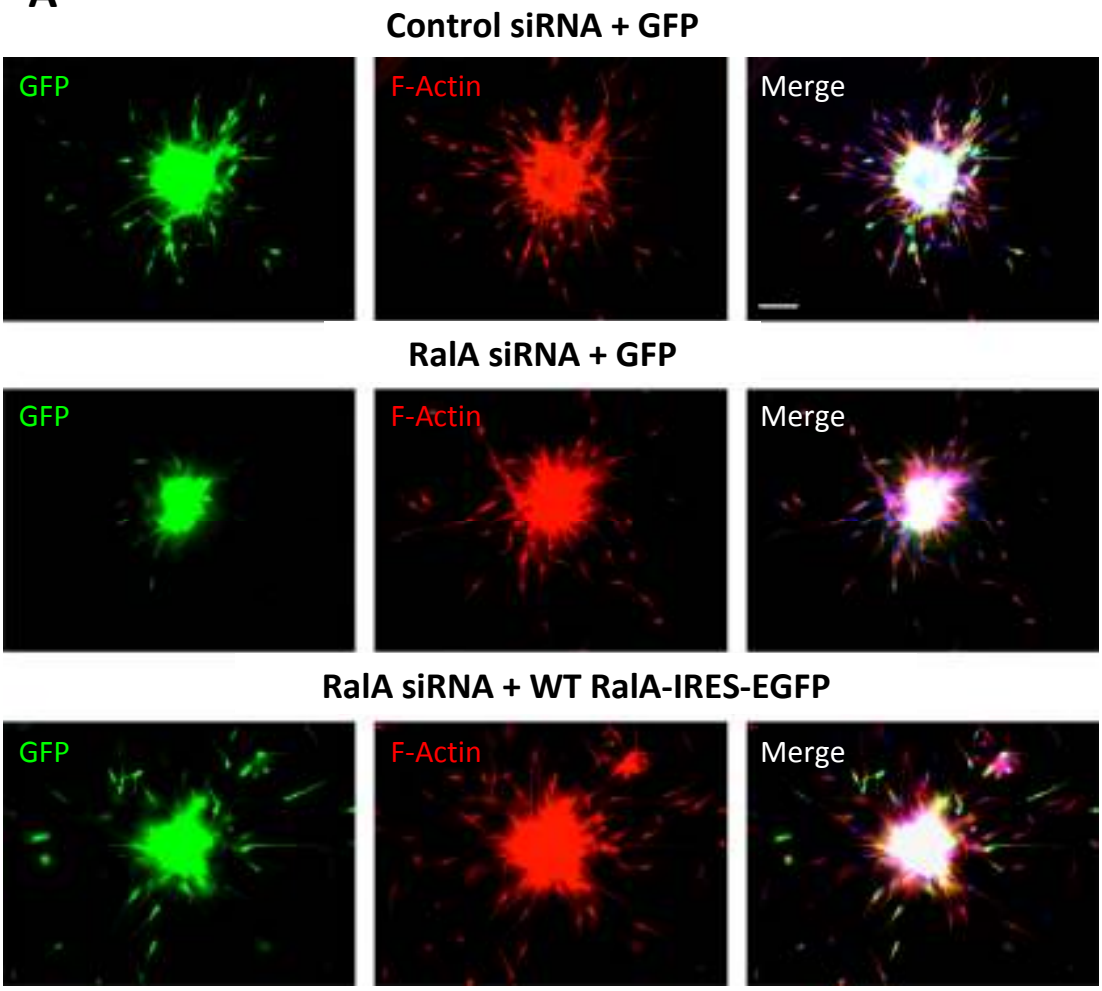
Control siRNA + GFP
GFP
F-Actin
Merge
RalA siRNA + GFP
GFP
F-Actin
Merge
RalA siRNA + WT RalA-IRES-EGFP
GFP
F-Actin
Merge

B

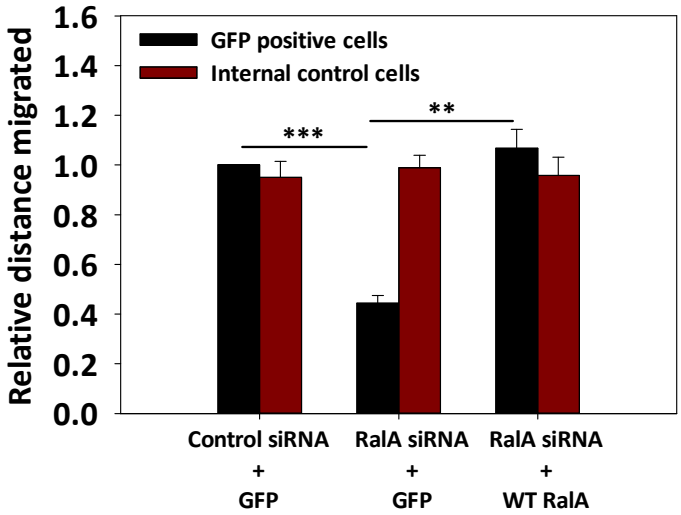
Relative distance migrated
1.6
1.4
1.2
1.0
0.8
0.6
0.4
0.2
0.0
GFP positive cells
Internal control cells
***
**
Control siRNA + GFP
RalA siRNA + GFP
RalA siRNA + WT RalA

Figure 5.6: Impaired migration caused by RalA siRNA can be rescued with a siRNA-resistant WT RalA. **(A)** Rat RMS neuroblasts were nucleofected with control siRNA + GFP, RalA siRNA + GFP, or RalA siRNA + pCAG-WT RalA-IRES-EGFP construct resistant to knockdown. Images show transfected (green) and non-transfected (red only) neuroblasts migrating out of aggregates 24 hours post embedding in Matrigel. Bar = 50 μm. **(B)** Distance migrated out of aggregates was quantified for both transfected (GFP positive) and non-transfected (internal control) neuroblasts. Inhibition of migration by RalA siRNA oligo is successfully rescued by siRNA-resistant WT RalA. Each bar represents the mean ± SEM; **P < 0.01; ***P < 0.001; n = 3 independent experiments.

a vector-based approach to achieve stable knockdown of our protein. We cloned four RalA shRNA sequences ((1), (2), (3) and (4)) targeting different regions of RalA, and one control shRNA sequence into the pCA-b-EGFPm5 silencer 3 (a kind gift from Matthieu Vermeren) (Bron et al. 2004). The efficiency of RalA depletion by each shRNA construct was evaluated using Western blot analysis. Nucleofection of rat neuroblasts with 3 μg of RalA shRNA (4) results in a 25% reduction in RalA expression at 48 hours, and a 30% reduction by 72 hours (Figure 5.7). Higher amounts of plasmid (5 μg) produced a 30% reduction in RalA expression by 72 hours, but did not have an effect at 48 hours (Figure 5.7). In contrast, 5 μg of RalA shRNA (1) had no effect on protein expression by 48 hours, and caused a 30% reduction by 72 hours (Figure 5.8). 5 μg of RalA shRNA (2) caused a 40% reduction in protein expression by 48 hours, but unexpectedly caused a 3-fold increase in RalA expression by 72 hours (Figure 5.8). Although we were able to achieve some degree of protein knockdown, RalA targeting shRNA plasmid vectors were not as efficient as siRNA oligos. Nevertheless, we assessed the effects of RalA targeting shRNA on neuroblast migration using the *in vitro* Matrigel experiment. Since this assay measures the migratory ability of neuroblasts between 48 to 72 hours post nucleofection, and RalA shRNA (4) produced reasonable knockdown (30%) of protein expression by 72 hours, this construct was selected for analysis.

Neuroblasts expressing either control or RalA shRNA vector (GFP-positive cells) migrate to a similar extent after 24 hours in Matrigel (Figure 5.9A). Quantification reveals no significant difference in the relative distance migrated by control neuroblast and RalA shRNA expressing neuroblasts (Figure 5.9B).

Next, we sought to determine whether prolonged expression (5 days) of the shRNA plasmid vectors could affect neuroblast migration *in vivo*. To test this we electroporated constructs into the right lateral ventricles of P2 mouse pups. Mice were sacrificed 5 days later and brains were fixed, sliced, and stained for GFP, or live slices were cultured for time-lapse imaging of GFP labelled neuroblasts migrating in the RMS.

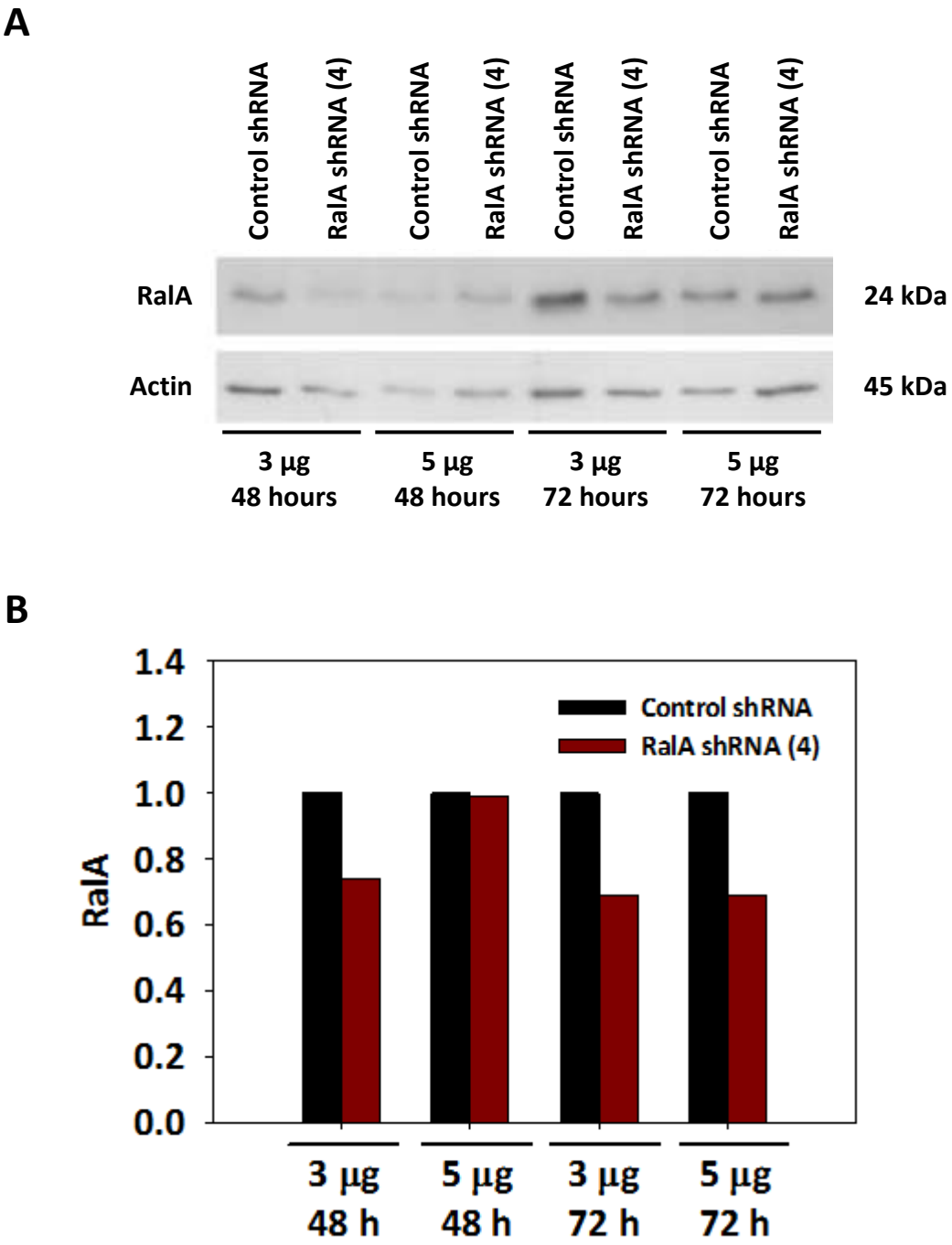

Figure 5.7: RalA expression can be partially knocked down with RalA shRNA (4) in rat RMS neuroblasts. Dissociated rat RMS neuroblasts from P5-P7 pups were nucleofected with a GFP expressing control shRNA or RalA shRNA (4) construct and cultured for 48-72 hours. Lysates were probed for RalA expression via Western blot analysis. **(A)** Western blot showing reduced expression of RalA at both 48 and 72 hours post nucleofection. **(B)** Quantification of Western blot. n = 1 experiment.

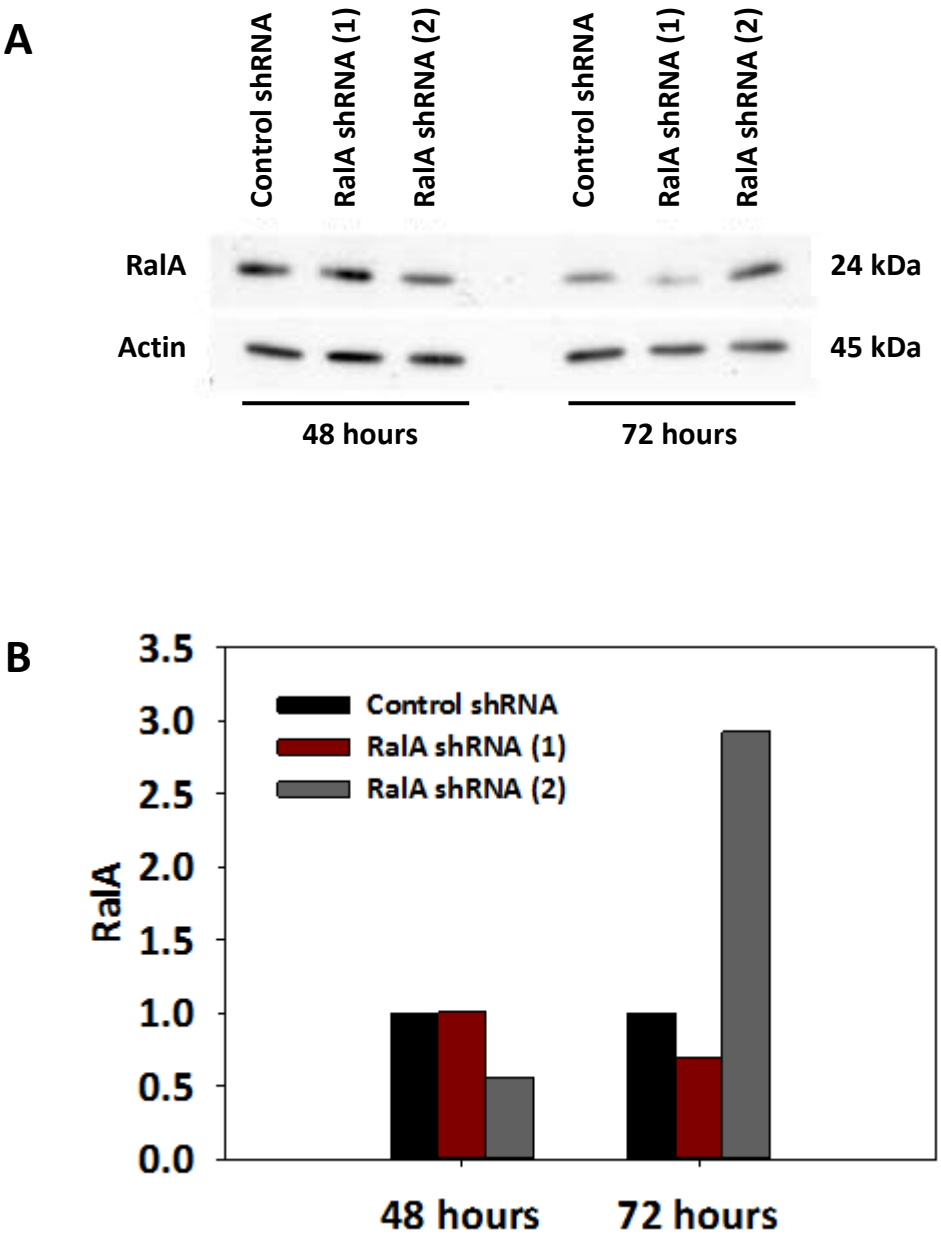

Figure 5.8: RalA expression cannot be knocked down with RalA shRNA (1) or RalA shRNA (2) in rat RMS neuroblasts. Dissociated rat RMS neuroblasts from P5-P7 pups were nucleofected with 5 µg of a GFP expressing control shRNA, RalA shRNA (1), or RalA shRNA (2) construct and cultured for 48-72 hours. Lysates were probed for RalA expression via Western blot analysis. **(A)** Western blot showing expression of RalA at both 48 and 72 hours post nucleofection. **(B)** Quantification of Western blot. n = 1 experiment.

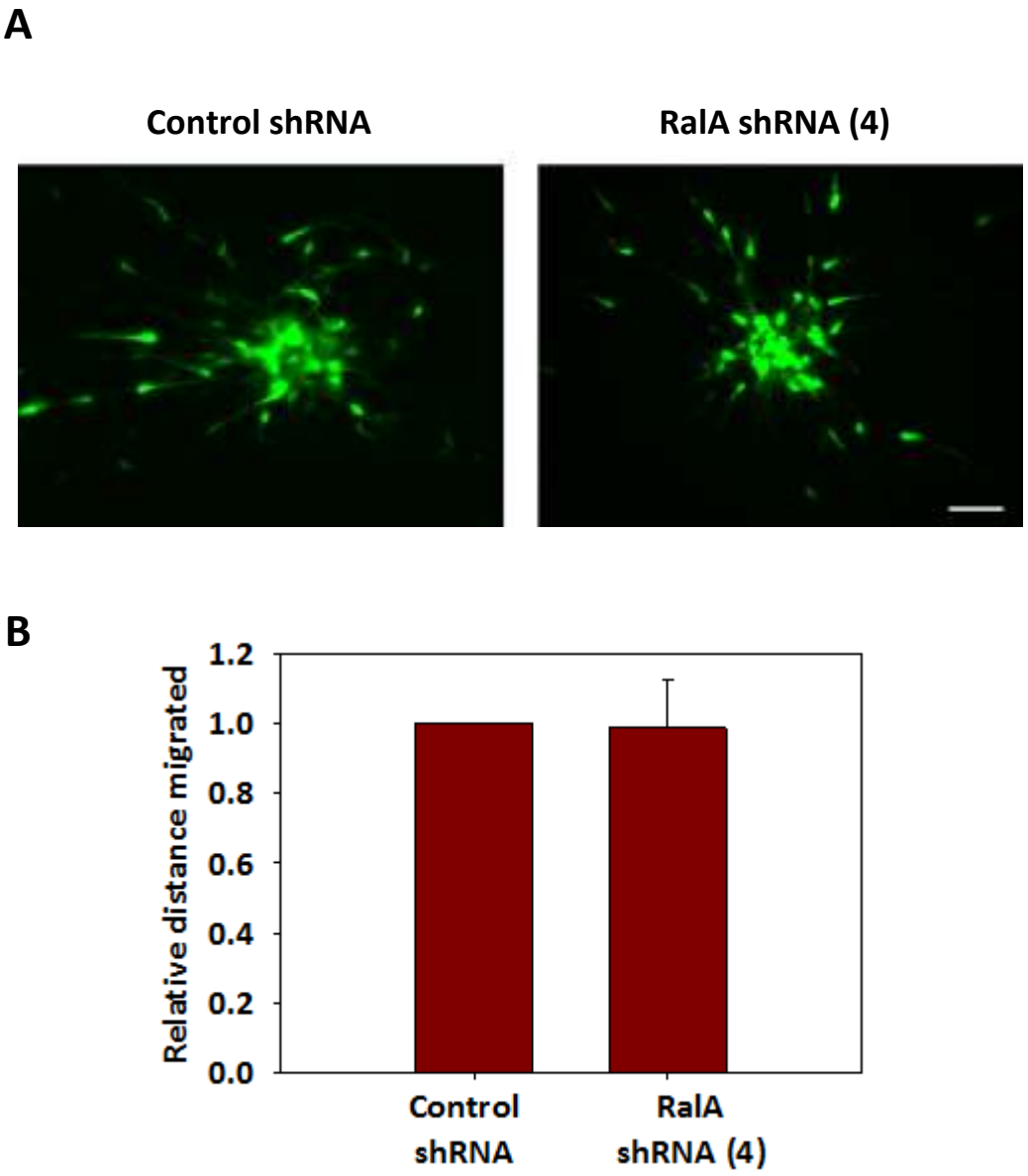

Figure 5.9: RalA shRNA (4) does not impair the migration of rat RMS neuroblasts *in vitro*. Dissociated rat RMS neuroblasts were nucleofected with either a control shRNA or RalA shRNA (4) vector also expressing GFP. Neuroblasts were re-aggregated into clusters and embedded in Matrigel 48 hours post nucleofection. The distance migrated by GFP positive neuroblasts was measured. **(A)** Aggregates expressing control shRNA and RalA shRNA (4) 24 hours after embedding in Matrigel. Bar = 50 µm. **(B)** Quantification of the distance migrated shows no significant difference between control shRNA and RalA shRNA (4) expressing neuroblasts. Each bar represents the mean ± SEM; n = 3 independent experiments.

Control and RalA shRNA ((1), (2), (3) or (4)) constructs show robust expression 5 days after electroporation as observed by GFP immune reactivity in fixed brain slices (Figure 5.10A). The great majority of neuroblasts from all conditions displayed a single leading process oriented towards the OB (Figure 5.10A). Quantitative analysis of morphology shows that none of the RalA shRNA constructs had a notable effect on process length (Figure 5.10B). In all conditions labelled neuroblasts were present throughout the entire stream (general observation - data not shown).

Analysis of time-lapse movies reveals that RalA shRNA (4) expressing neuroblasts have a slightly reduced average migrated distance (136.4 µm ± 8.7 for control shRNA and 119.1 µm ± 7.2 for RalA shRNA (4)) and velocity (45.4 µm/hour ± 2.9 for control shRNA and 39.6 µm/hour ± 2.3 for RalA shRNA) in comparison to control shRNA expressing cells (Figure 5.11 top and middle). Neuroblasts expressing RalA shRNA (4) also spent a longer time immobile (78.8 mins ± 5.5) than control cells (68.2 ± 2.6) (Figure 5.11 bottom). However, none of these effects were statistically significant. Parameters describing persistence of movement for control and RalA shRNA (Figure 5.12) were similar for both groups (Displacement: 59.6 µm± 8.2 for control shRNA and 61.7 µm ± 6.2 for RalA shRNA; Meandering Index: 0.48 ± 0.025 for control shRNA and 0.48 ± 0.027 for RalA shRNA). Categorisation of neuroblasts into migratory phenotypes also showed no difference between the two groups in the percentage of neuroblasts that were exploratory, intermediate, or migratory (Figure 5.12 bottom).

In summary, we were not able to perturb neuroblast migration, either *in vitro* or *in vivo*, using a RalA targeting shRNA plasmid vector. This is most likely due to the moderate inhibition of protein expression (30% knockdown) achieved with our constructs. Thus, further approaches to study the function of RalA *in vivo* and long-term need to take into account the robust expression of endogenous RalA in this system.

A

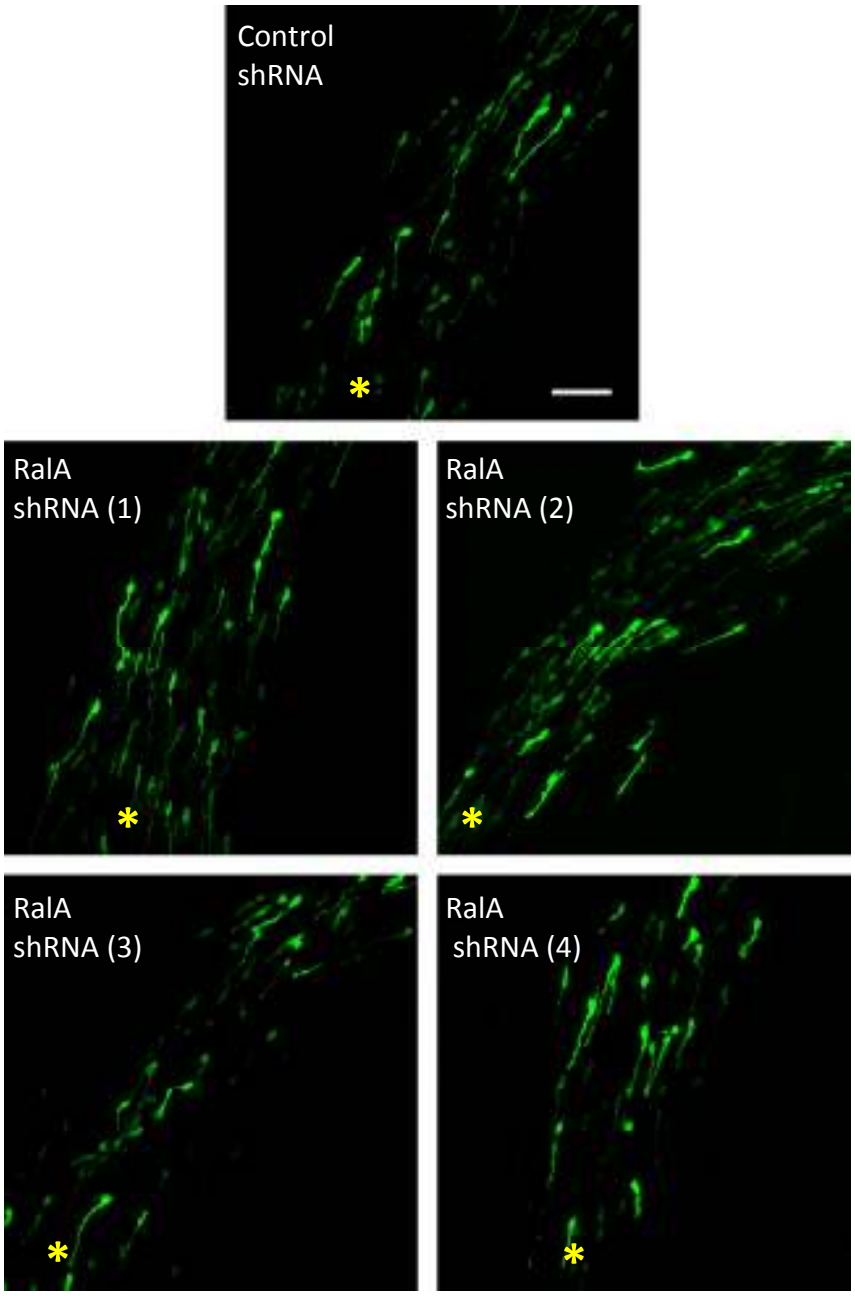
Control
shRNA
RalA
shRNA (1)
RalA
shRNA (2)
RalA
shRNA (3)
RalA
shRNA (4)

B

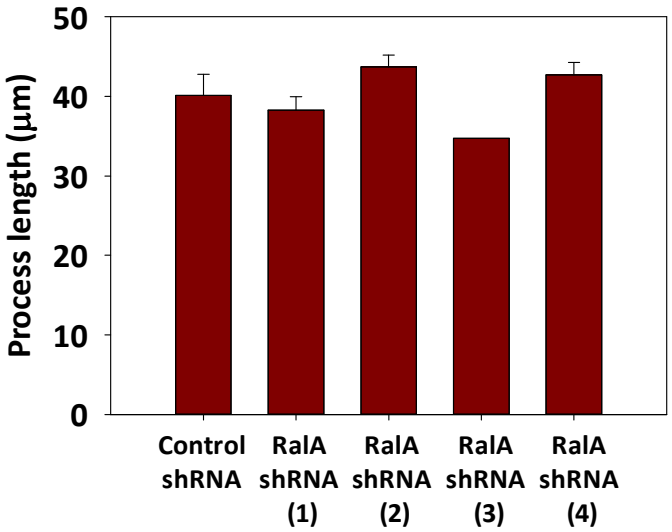

Figure 5.10: RalA shRNA does not affect process length of mouse RMS neuroblasts *in vivo*. Constructs expressing GFP and control shRNA or RalA shRNA (1-4) were electroporated into the right ventricle of P2 mouse pups. Animals were sacrificed 5 days later and brains were fixed, sliced and stained for GFP. **(A)** Representative images of neuroblasts expressing control, RalA (1), RalA (2), RalA (3) and RalA (4) shRNA constructs. Yellow asterisks indicate relative position of OB. Bar = 50 µm. **(B)** Quantification of process length shows no significant difference between control shRNA and RalA shRNA (1-4) expressing neuroblasts. Each bar represents the mean ± SEM; n = 4 for control shRNA; n = 3 for RalA shRNA (1); n = 4 for RalA shRNA (2); n = 1 for RalA shRNA (3); n = 4 for RalA shRNA (4), where n = number of brains analysed.

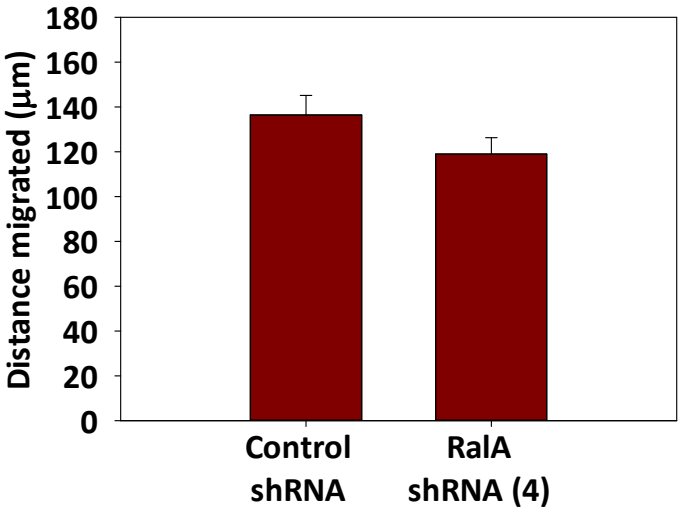
Distance migrated (µm)
180
160
140
120
100
80
60
40
20
0
Control shRNA
RalA shRNA (4)

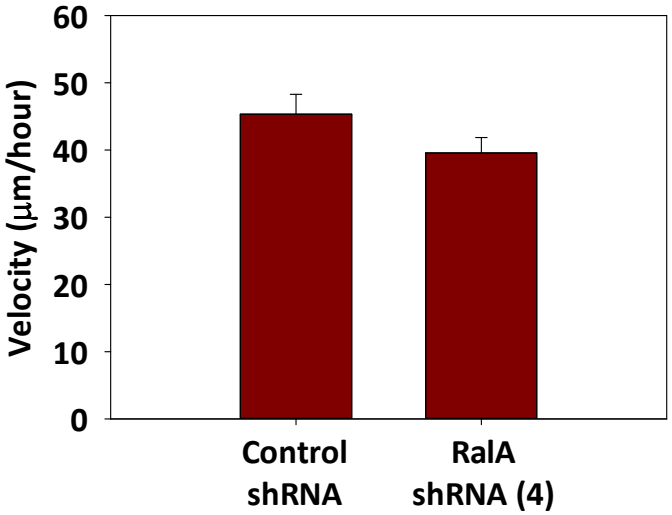
Velocity (µm/hour)
60
50
40
30
20
10
0
Control shRNA
RalA shRNA (4)

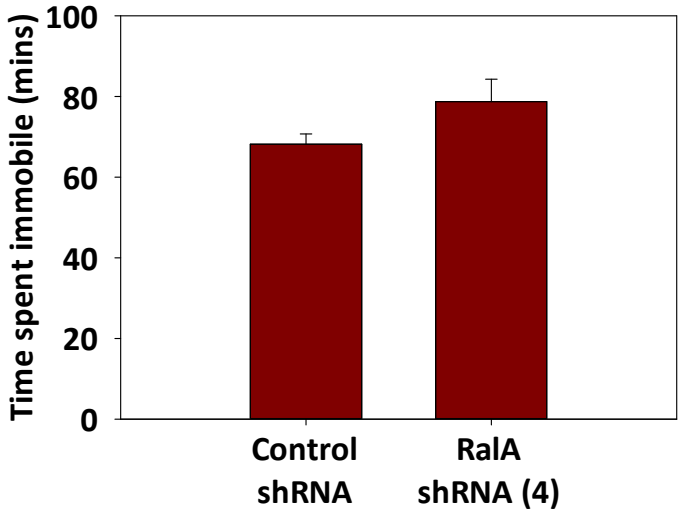
Time spent immobile (mins)
100
80
60
40
20
0
Control shRNA
RalA shRNA (4)

Figure 5.11: RalA shRNA (4) does not affect migration of neuroblasts *in vivo*. Constructs expressing GFP and control shRNA or RalA shRNA (4) were electroporated into the right ventricle of P2 mouse pups. Animals were sacrificed 3-7 days later and brain slices with GFP positive neuroblasts in the RMS were cultured for 1 hour prior to imaging. Slices were imaged at the end of the stream (region C) every 3 minutes for 3 hours. The distance (top), velocity (middle) and time spent immobile (bottom) were not significantly different between RalA shRNA (4) and control shRNA expressing neuroblasts. Each bar represents the mean ± SEM; n = 3 for control shRNA, n = 5 for RalA shRNA (4), where n = independent experiments.

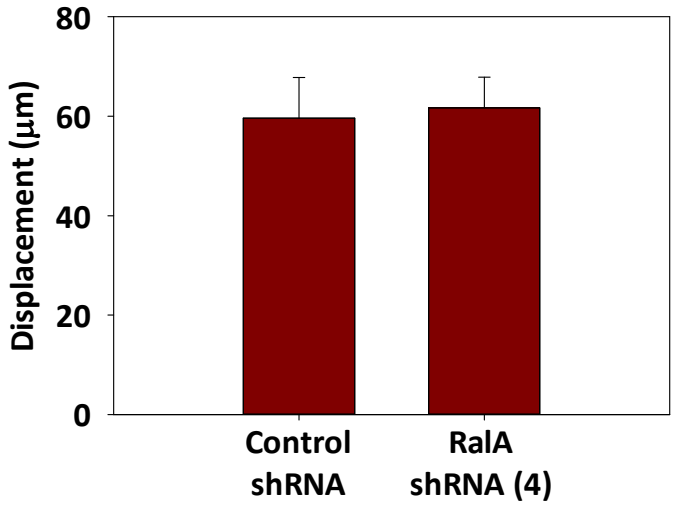
Displacement (µm)
80
60
40
20
0
Control shRNA
RalA shRNA (4)

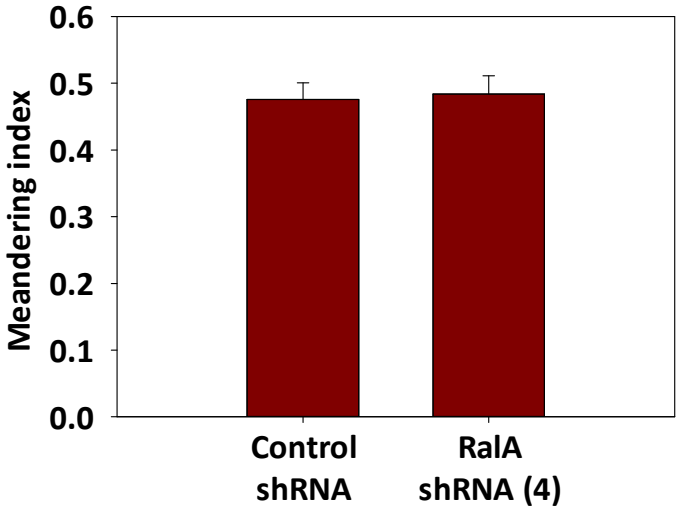
Meandering index
0.6
0.5
0.4
0.3
0.2
0.1
0.0
Control shRNA
RalA shRNA (4)

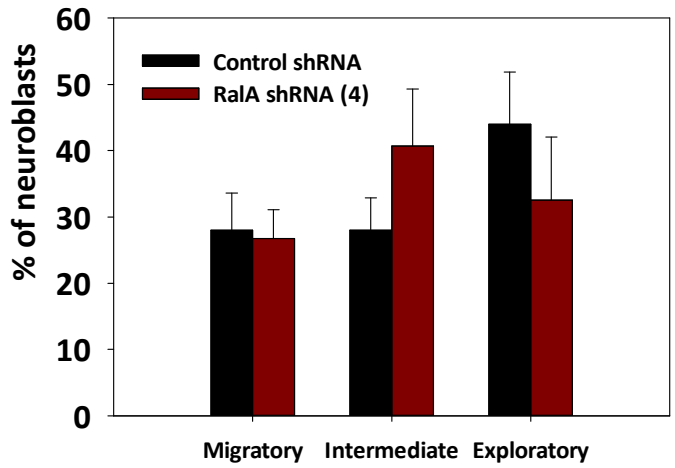
% of neuroblasts
60
50
40
30
20
10
0
Control shRNA
RalA shRNA (4)
Migratory
Intermediate
Exploratory

Figure 5.12: RalA shRNA (4) does not affect persistence *in vivo*. Constructs expressing GFP and control shRNA or RalA shRNA (4) were electroporated into the right ventricle of P2 mouse pups. Animals were sacrificed 3-7 days later and brain slices with GFP positive neuroblasts in the RMS were cultured for 1 hour prior to imaging. Slices were imaged at the end of the stream (region C) every 3 minutes for 3 hours. The persistence of neuroblast movement was analysed using the meandering index (MI; total displacement/total distance). The migratory behaviour of neuroblasts was classified as being exploratory (MI < 0.4), intermediate (MI 0.4 – 0.6) or migratory (MI > 0.6). RalA shRNA (4) did not significantly affect the displacement (top); meandering index (middle); or the % of neuroblasts with exploratory, intermediate, or migratory phenotype (bottom). Each bar represents the mean ± SEM; n = 3 for control shRNA, n = 5 for RalA shRNA (4) where n = independent experiments.

5.2.3 Ectopic expression of dominant negative RalA affects orientation and morphology of RMS neuroblasts *in vivo* but not *in vitro*

As an alternative to knockdown with shRNA vectors, we attempted to disrupt RalA signalling *in vitro* and *in vivo* by expressing myc-tagged mutant RalA proteins (wild type (WT RalA), dominant negative (DN RalA), constitutively active (CA RalA) and fast cycling (FC RalA)) previously used to perturb RalA function in neurones (Lalli and Hall 2005; Lalli 2009). Due to poor expression of the pRK5-myc plasmids in RMS neuroblasts (data not shown), we re-cloned WT and mutant RalA proteins obtained from the original pRK5 vector into a pCAG-IRES-EGFP plasmid suitable for expression in neuroblasts both *in vitro* and *in vivo* (Jacobs et al. 2007; Causeret et al. 2009).

First, we tested the effect of RalA mutants on the migration of rat RMS neuroblasts *in vitro*. To confirm that neuroblasts successfully express both the mutant RalA protein and GFP, we performed double immunostaining for the myc tag and GFP in rat neuroblasts nucleofected with pCAG-DN RalA-IRES-EGFP. Figure 5.13 shows that all cells expressing GFP also express myc-tagged DN RalA. This expression is robust 48 hours post nucleofection and there appears to be a transfection efficiency of approximately 50% (Figure 5.13). Hence, this construct allows robust, simultaneous, expression of both GFP and the myc tagged mutant protein with a reasonably high efficiency of transfection. Comparison of the distance migrated out of aggregates by rat neuroblasts embedded in Matrigel shows that there was no significant difference in the distance migrated between neuroblasts expressing just pCX-EGFP or empty pCAG-IRES-EGFP vector (EV), and untransfected internal control cells, thus demonstrating that nucleofection of the vector *per se* has no effect on basal neuroblast migration (Figure 5.14). However, there was also no significant difference in the migration of neuroblasts expressing WT RalA or DN RalA, and cells expressing just GFP or EV (Figure 5.14). Hence, expression of either WT or DN RalA proteins does not appear to affect rat RMS neuroblast migration *in vitro*.

Although the Matrigel migration assay is a useful *in vitro* tool for identifying and examining candidate molecules that influence neuronal migration, we must bear in

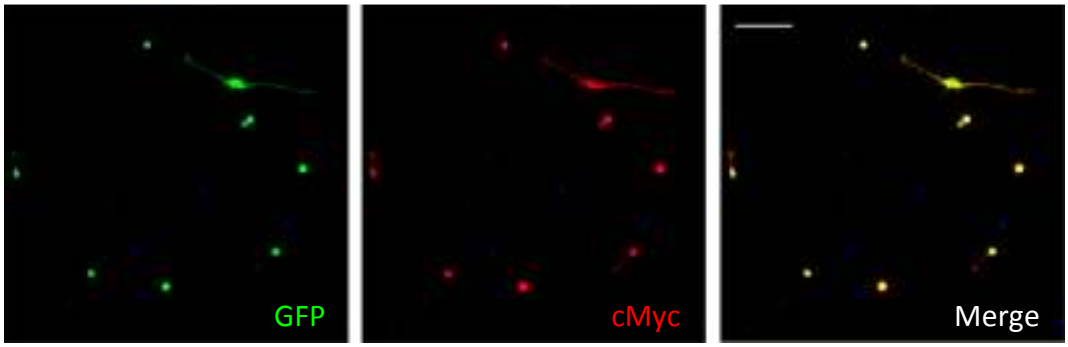

Figure 5.13: Rat RMS neuroblasts nucleofected with pCAG-DN RalA-IRES-EGFP express both GFP and myc-tagged DN RalA. Rat RMS neuroblasts were nucleofected with a pCAG-DN RalA-IRES-EGFP plasmid expressing a myc-tagged dominant negative (DN) RalA. Neuroblasts were plated onto polyornithine/laminin-coated coverslips and were fixed and stained for GFP and the myc tag 48 hours after plating. As expected, all GFP-expressing cells also express myc-tagged DN RalA. Bar = 50 µm.

A

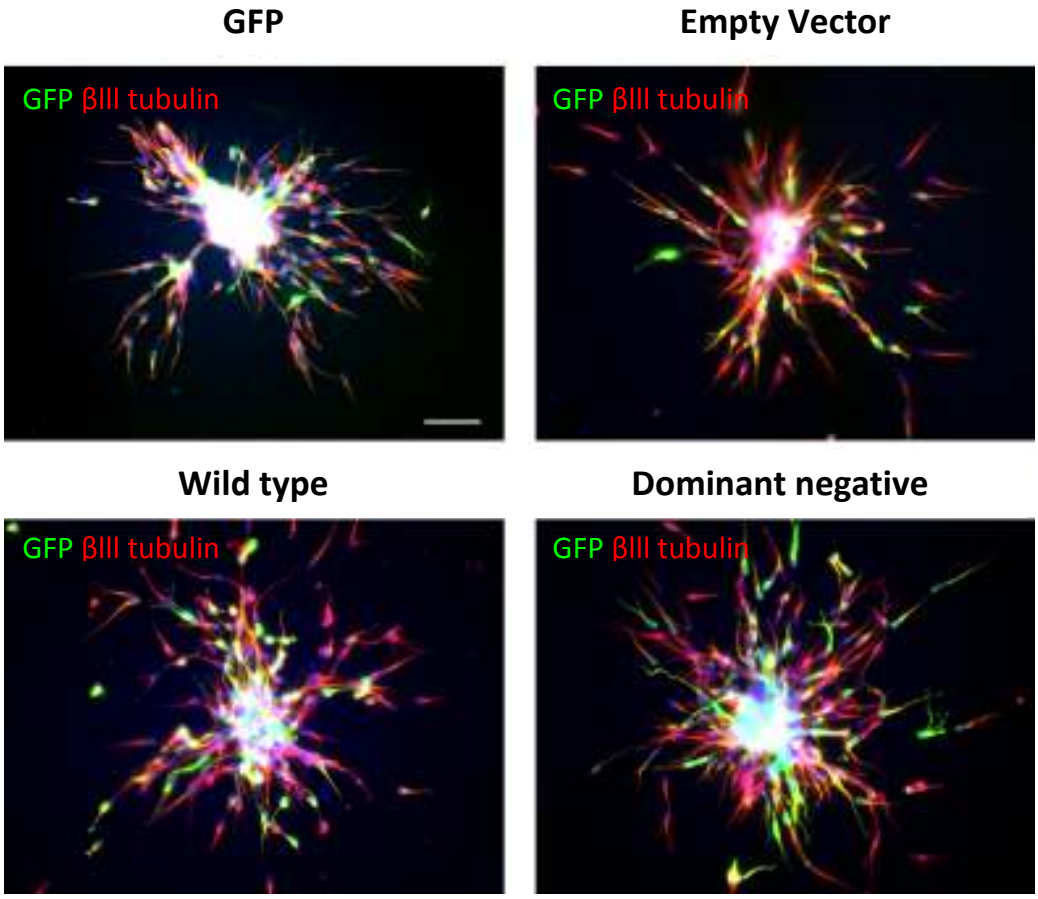
GFP
Empty Vector
GFP βIII tubulin
GFP βIII tubulin
Wild type
Dominant negative
GFP βIII tubulin
GFP βIII tubulin

B

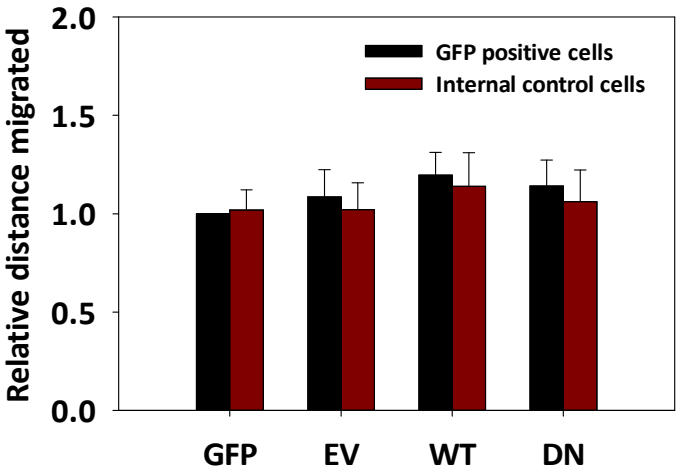
Relative distance migrated
2.0
1.5
1.0
0.5
0.0
GFP positive cells
Internal control cells
GFP
EV
WT
DN

Figure 5.14: Expression of DN RalA does not affect migration of rat RMS neuroblasts *in vitro*. Rat RMS neuroblasts were nucleofected with pCX-EGFP or one of the following pCAG-IRES-EGFP constructs: empty vector (EV), wild type (WT) RalA, or dominant negative (DN) RalA. Neuroblasts were re-aggregated into clusters and embedded into Matrigel 24 hours post nucleofection. **(A)** Representative Images of GFP, EV, WT and DN RalA nucleofected aggregates, immunostained for GFP (green) and βIII tubulin (red), 24 hours after embedding in Matrigel. Bar = 50 µm **(B)** Quantification of distance migrated shows no significant difference in migration between the nucleofected cells (GFP positive cells) and non-nucleofected cells (internal control) in all samples. Each bar represents the mean ± SEM; n = 3 independent experiments.

mind that this model does not fully re-capitulate the complex architecture and signalling cues present in the RMS. Thus, failure of RalA mutants to disrupt migration *in vitro* does not necessarily exclude a role for RalA in neuroblast migration.

To verify a role for RalA in neuroblast migration *in vivo*, we electroporated myc-tagged RalA mutants (WT, DN, CA, and FC) cloned in the pCAG-IRES-EGFP vector, the empty pCAG-IRES-EGFP vector (EV), or pCX-EGFP into the lateral ventricles of P2 mouse pups. Brains were collected 5 days post electroporation, fixed, sliced, and stained for GFP. As expected, following electroporation of DN RalA, all mouse neuroblasts expressing GFP are also immune-reactive for myc-tagged DN RalA (Figure 5.15), thereby verifying the concomitant expression of both myc-tagged RalA mutants and GFP *in vivo*. Neuroblasts expressing GFP, EV, WT RalA, CA RalA or FC RalA appear very similar in morphology, with the majority of neuroblasts extending their leading process towards the OB (Figure 5.16). However, neuroblasts expressing DN RalA have noticeably shorter leading processes, with many cells oriented away from the OB (Figure 5.16). Quantitative morphological analysis shows that the expression of DN RalA leads to a 26% reduction in average process length (25.7 µm ± 2.1) when compared with GFP expressing neuroblasts (34.7 µm ± 0.6) (Figure 5.17A). Interestingly, over-expression of RalA (WT RalA) did not cause a change in the average process length (38.1 µm ± 1.7) when compared with GFP (34.7 µm ± 0.6) or EV (36.8 µm ± 0.8) (Figure 5.17A). In contrast, a significant increase in the average process length was seen with both CA RalA (43.1 µm ± 2.1) and FC RalA (45.2 µm ± 1.9) mutants, consistent with the idea that RalA has to be in the active form to elicit a response (Figure 5.17A). Thus, simply over-expressing the WT protein is not enough to elicit a morphological response, and only the active (FC RalA and CA RalA) or inactive (DN RalA) mutants cause a change in morphology. The vast majority of GFP, EV, CA RalA, or FC RalA-expressing neuroblasts are highly polarised towards the OB. Indeed, only a small % (< 5.5%) is oriented away from the OB in these conditions (Figure 5.17B). In sharp contrast, expression of DN RalA caused a substantial increase in the % of misoriented neuroblasts (16.5% ± 2.7) (Figure 5.17B). Remarkably, despite the dramatic change in morphology and

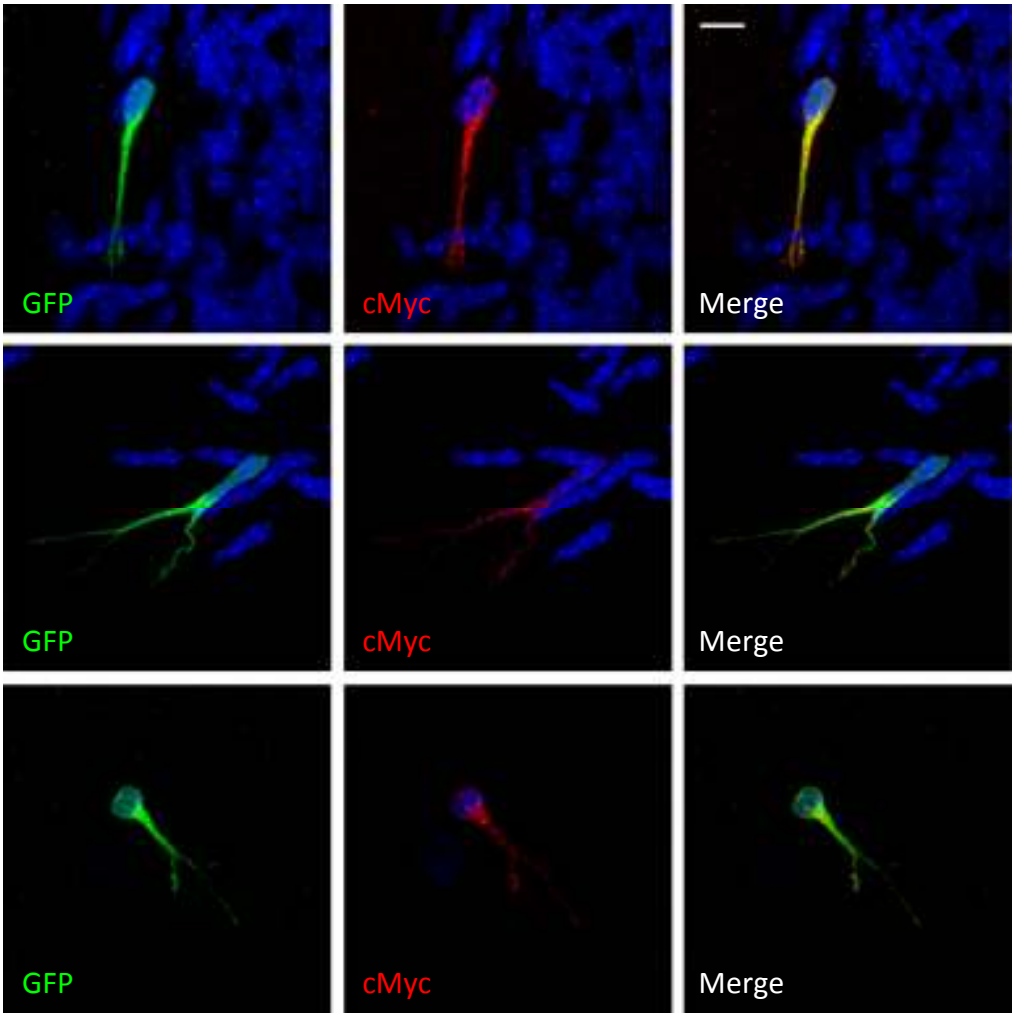

Figure 5.15: Mouse RMS neuroblasts electroporated with pCAG-DN RalA-IRES-EGFP express both GFP and myc-tagged DN RalA. P2 mouse pups were electroporated with a pCAG-DN RalA-IRES-EGFP plasmid expressing a myc-tagged dominant negative (DN) RalA. Mice were sacrificed 5 days later, and RMS explants were embedded in Matrigel, fixed and stained for GFP and the myc tag 24 hours after embedding. All cells expressing GFP also express myc-tagged DN RalA. Bar = 10 µm.

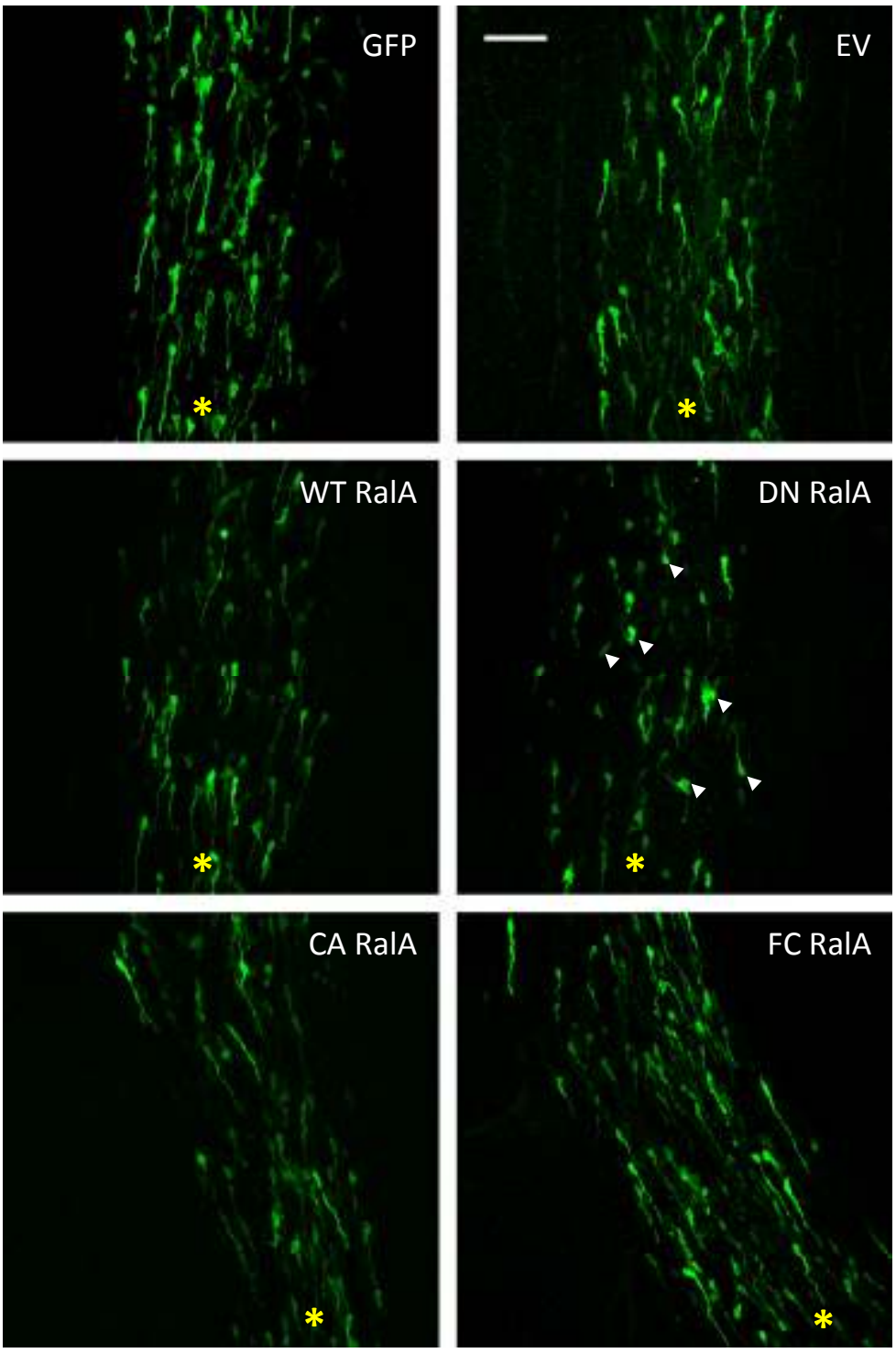
GFP
EV
WT RalA
DN RalA
CA RalA
FC RalA

Figure 5.16: RalA is important for neuroblast morphology and directionality *in vivo* (1). P2 mice were electroporated with pCX-EGFP or one of the following pCAG-IRES-EGFP constructs: empty vector (EV), wild type (WT) RalA, dominant negative (DN) RalA, constitutively active (CA) RalA, or fast cycling (FC) RalA. Mice were sacrificed 5 days later and brains were fixed, sliced, and immunostained for GFP. Representative projections from confocal z-stacks of 75 µm-thick brain slices. Yellow asterisks indicate relative position of the OB. White arrowheads indicate misoriented neuroblasts. Bar = 50 µm.

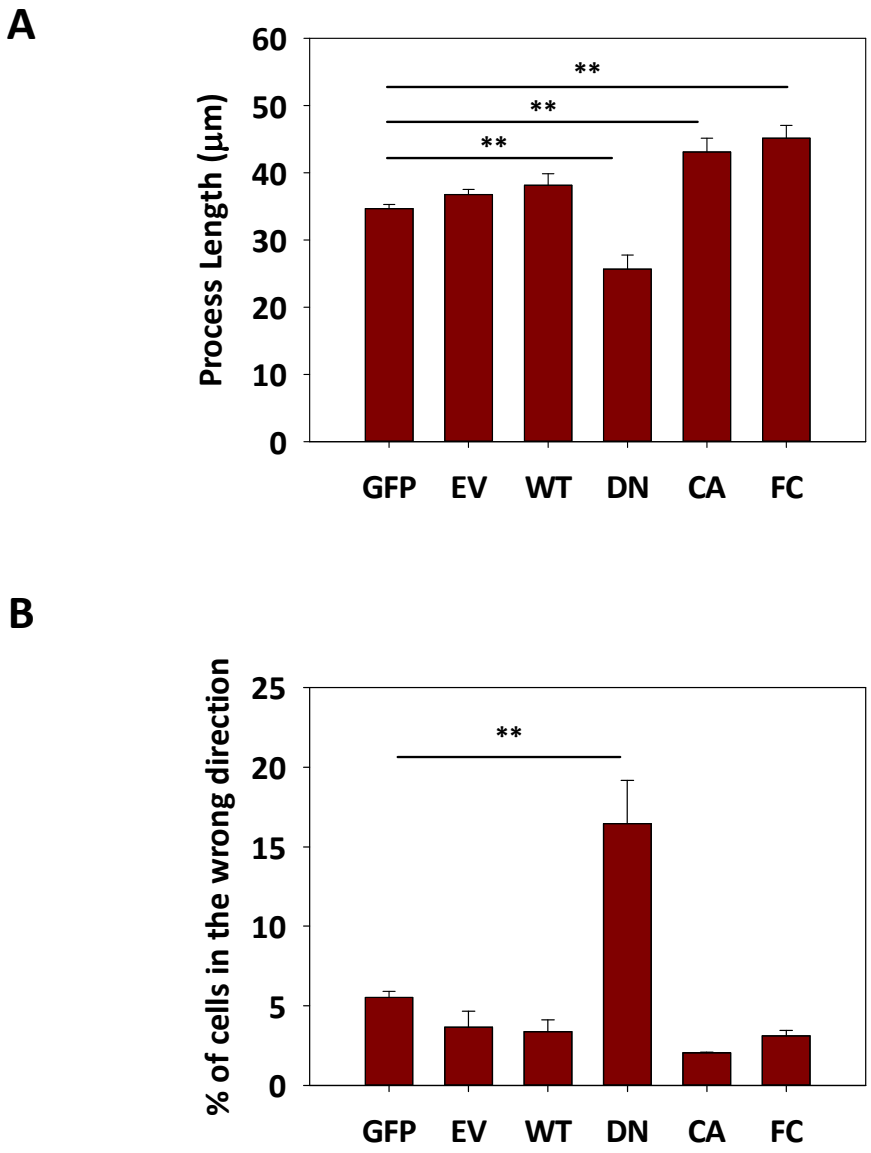

Figure 5.17: RalA is important for neuroblast morphology and directionality *in vivo* (2). P2 mice were electroporated with pCX-EGFP or one of the following pCAG-IRES-EGFP constructs: empty vector (EV), wild type (WT) RalA, dominant negative (DN) RalA, constitutively active (CA) RalA, or fast cycling (FC) RalA. Mice were sacrificed 5 days later and brains were fixed, sliced, and stained for GFP. **(A)** Expression of DN RalA leads to a significant reduction in process length, whereas expression of CA or FC RalA results in an increase in process length. **(B)** Expression of DN RalA disrupts the polarised orientation of neuroblasts towards the OB. Each bar represents the mean ± SEM; **P < 0.01; n = 6 for GFP, n = 8 for EV, n = 5 for WT, DN, and FC, n = 3 for CA, where n = number of brains analysed.

orientation caused by DN RalA, labelled neuroblasts were found throughout the RMS (general observation – data not shown). In conclusion, our data suggests that RalA is important for correct morphology and orientation of RMS neuroblasts *in vivo*.

5.2.4 Overexpression of RalA enhances RMS neuroblast migration in situ

To further investigate the effects of RalA on the migratory properties of neuroblasts, brains of mice electroporated with RalA mutants were sliced and cultured for time-lapse imaging. However, the intensity of the GFP signal in neuroblasts electroporated with the pCAG-RalA mutant-IRES-EGFP constructs was too weak to be detected by our spinning disk microscope. Therefore, we co-electroporated the RalA mutants with pCX-EGFP in a 3:1 ratio to ensure expression of the mutant RalA construct and pCX-EGFP. However, even with these conditions, immunostaining for the myc tag and GFP shows that not all neuroblasts that express GFP also express mutant RalA (Chapter 4, Figure 4.13). Despite the fact that only some neuroblasts express both constructs, overexpressing RalA with the WT mutant in at least some cells significantly enhanced the migrated distance (129.6 µm ± 10.9 for control and 178.8 µm ± 13.7 for WT RalA) and velocity (43.3 µm/hour ± 3.6 for control and 60.0 µm/hour ± 4.4 for WT RalA) in comparison to pCX-EGFP only expressing controls (Figure 5.18 top and middle). The time spent immobile was also reduced from 60.7 min ± 5.2 for the control, to 46.9 min ± 4.5 for WT RalA (Figure 5.18 bottom). Thus, overexpression of RalA significantly enhances RMS neuroblast migration in the brain slice assay.

5.2.5 Deletion of RalA and RalB affects orientation and morphology of neuroblasts *in vivo*

So far we have demonstrated a role for RalA in regulating neuroblast migration *in vitro* using siRNA based gene silencing, we have confirmed that overexpressing RalA enhances RMS neuroblast migration in situ, and we have also shown that RalA regulates morphology and directionality *in vivo* using RalA mutants. However, given that RalA is so abundant in RMS neuroblasts, it is unlikely that partial inhibition of

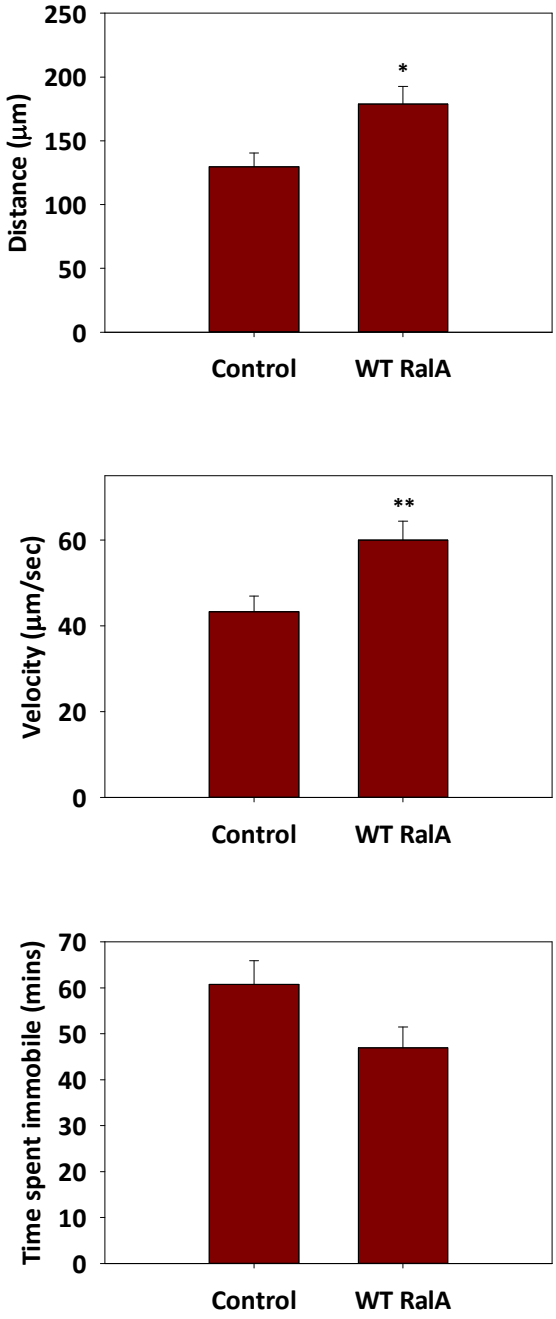

Figure 5.18: Overexpression of RalA promotes neuroblast migration in the brain slice assay. P2 mice were electroporated in the right ventricle with pCX-EGFP or pCAG-WT RalA-IRES-EGFP + pCX-EGFP in a 3:1 ratio. Animals were sacrificed 3-7 days later, and brain slices with GFP positive neuroblasts in the RMS were cultured and imaged every 3 minutes for 3 hours. Overexpression of RalA increases the distance migrated (top panel) and velocity (middle panel), and reduced the time spent immobile (bottom panel). Each bar represents the mean ± SEM; *P < 0.05; **P < 0.01; n = 8 brain slices for control; n = 5 brain slices for WT RalA.

protein expression with siRNA oligos or perturbing endogenous RalA function with the DN mutant will reveal the full extent of RalA function in neuroblast migration. The only way to obtain a complete picture of RalA function in our system is to delete the RalA gene itself. For this reason we extended our research to Ral conditional knockout models, which were kindly provided by Dr. Pascal Peschard and Prof. Chris Marshall (Institute of Cancer Research, London).

In our studies, we used RalA conditional knockout mice based on the Cre-lox system ($RalA^{lox/lox}$) (Peschard et al, *in press*), as this allows us to selectively delete RalA from a subpopulation of RMS neuroblasts. Also, since RalA null mice display embryonic lethality (Peschard et al, in press), the Cre-lox system allows us to specifically investigate RalA function in neuroblast migration without affecting development. Although we were not able to detect significant expression of RalB in RMS neuroblasts (Chapter 4), we also used a RalA conditional knockout mouse based on a RalB null mouse background ($RalA^{lox/lox}/RalB^{-/-}$) (Peschard et al, *in press*) to eliminate potential compensation of RalA loss by RalB. Deletion of RalA was achieved by electroporation of a pCAG-Cre-IRES2-EGFP plasmid (Woodhead et al. 2006) into the lateral ventricle of P2 mouse pups. The expression of Cre in cells derived from $RalA^{lox/lox}$ and $RalA^{lox/lox}/RalB^{-/-}$ mice has been previously shown by our collaborators to result in the successful loss of RalA expression (Peschard et al, *in press*). Mice were sacrificed 5 days post electroporation, and brains were fixed, sliced and stained for GFP.

Representative images of Cre-GFP expressing neuroblasts in wild type (WT), $RalA^{lox/lox}$, and $RalA^{lox/lox}/RalB^{-/-}$ mice 5 days post electroporation show that cells lacking RalA appear to have a shorter leading process, with several neuroblasts lacking a leading process altogether (Figure 5.19). In addition, a greater number of neuroblasts were oriented away from the OB when compared with wild type. The phenotype is even more striking in $RalA^{lox/lox}/RalB^{-/-}$ mice, with neuroblasts having very short leading processes or no process at all, and a substantially large number of neuroblasts oriented away from the OB (Figure 5.19). Quantitative morphological analysis reveals that the leading process is significantly shorter

WT

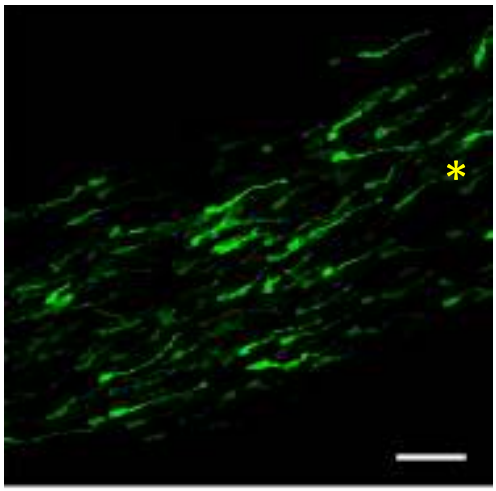

$RalA^{lox/lox}$

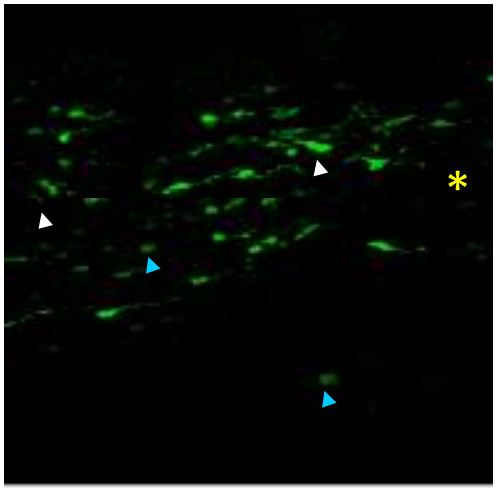

$RalA^{lox/lox}/RalB^{-/-}$

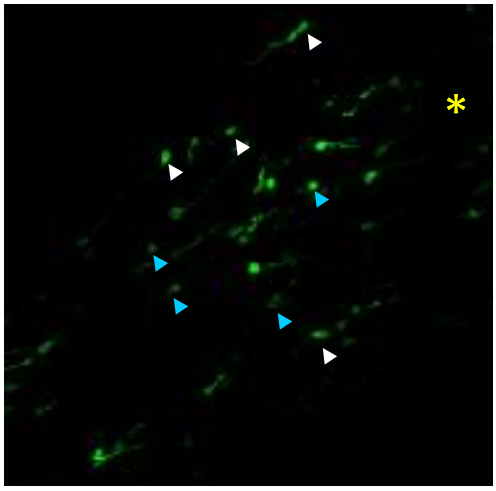

Figure 5.19: Deletion of RalA/RalB disrupts neuroblast polarised morphology and directionality (1). A pCAG-Cre-IRES2-EGFP plasmid was electroporated into the right lateral ventricle of WT, $RalA^{lox/lox}$, or $RalA^{lox/lox}/RalB^{-/-}$ P2 mouse pups. Mice were sacrificed 5 days later and the right hemisphere was fixed, sliced and stained for GFP. Representative images of RMS neuroblasts expressing the Cre-GFP construct in WT, $RalA^{lox/lox}$, or $RalA^{lox/lox}/RalB^{-/-}$ mice. Yellow asterisks indicate the relative position of the OB, white arrowheads point to misoriented neuroblasts, and blue arrowheads point to neuroblasts lacking a leading process. Both $RalA^{lox/lox}$ and $RalA^{lox/lox}/RalB^{-/-}$ animals have a greater number of neuroblasts oriented away from the bulb, as well as a significantly higher proportion of neuroblasts without a leading process. Bar = 50 µm.

in RalA$^{lox/lox}$ mice (39.5 µm ± 1.6), when compared with WT animals (49.8 µm ± 1.1), and is almost halved in RalA$^{lox/lox}$/RalB$^{-/-}$ mice (25.5 µm ± 0.7) (Figure 5.20, top panel). Only 1.1% ± 0.5 of neuroblasts are either oriented in the wrong direction or have no process in WT animals, whereas in RalA$^{lox/lox}$ and RalA$^{lox/lox}$/RalB$^{-/-}$ mice this figure is increased to 7.2% ± 1.3 and 7.8% ± 1.2, respectively (Figure 5.20, middle panel). Looking exclusively at the number of neuroblasts without a process, just 0.1% ± 0.1 of cells do not have a process in WT neuroblasts, whereas 3.5% ± 1.0 of RalA$^{lox/lox}$ neuroblasts and 28.5% ± 3.3 of RalA$^{lox/lox}$/RalB$^{-/-}$ neuroblasts lack a leading process (Figure 5.20, bottom panel).

To determine whether RalA/RalB deletion affects neuroblast migration, we divided the RMS into distinct anatomical regions (Figure 5.21A) as previously described by others (Belvindrah et al. 2011), and counted the number of labelled cells in regions B, C and D of the RMS. Looking at the total number of labelled neuroblasts in the stream, we find that there is no major difference between RalA$^{lox/lox}$ (299 ± 71) and WT mice (282 ± 20) (Figure 5.21B). However, the number of labelled neuroblasts entering the stream in RalA$^{lox/lox}$/RalB$^{-/-}$ mice (119 ± 18) is less than half that of WT (Figure 5.21B). Looking at the average number of labelled neuroblasts in regions B, C, and D (Figure 5.21C), we saw no significant difference between WT and RalA$^{lox/lox}$ mice (Region B: 49 ± 12 for WT and 40 ± 24 for RalA$^{lox/lox}$; Region C: 76 ± 8 for WT and 105 ± 35 for RalA$^{lox/lox}$; Region D: 158 ± 8 for WT and 154 ± 34 for RalA$^{lox/lox}$). However, there are far fewer labelled neuroblasts present in all regions for RalA$^{lox/lox}$/RalB$^{-/-}$ mice (Region B: 24 ± 5; Region C: 38 ± 6; Region D: 57 ± 11) when compared with WT, with the greatest difference being in the OB (region D). Though there is some variation between experiments in the quantity of plasmid injected into the lateral ventricle and electroporation efficiency, the difference seen between WT and RalA$^{lox/lox}$/RalB$^{-/-}$ samples is far too great to be attributed to these differences. In addition, looking at Cre-GFP electroporated RalA$^{lox/lox}$/RalB$^{-/-}$ brain slices (Figure 5.24), we can see that despite the lack of GFP positive neuroblasts in the RMS, there is considerable labelling of cells at the injection site, which appears greater than that seen in WT (Figure 5.22) and RalA$^{lox/lox}$ (Figure 5.23) brain slices.

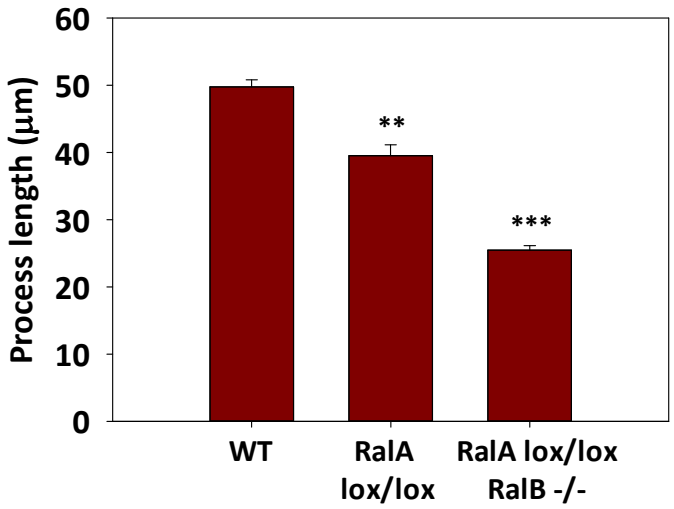
Process length (µm)
60
50
40
30
20
10
0
**
***
WT
RalA lox/lox
RalA lox/lox RalB -/-

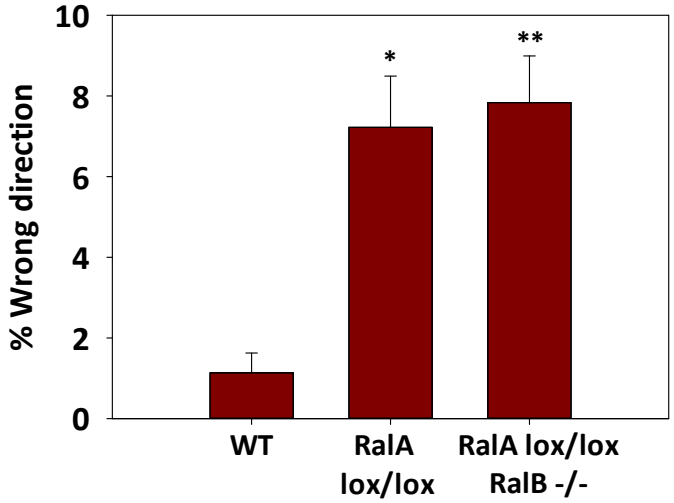
% Wrong direction
10
8
6
4
2
0
*
**
WT
RalA lox/lox
RalA lox/lox RalB -/-

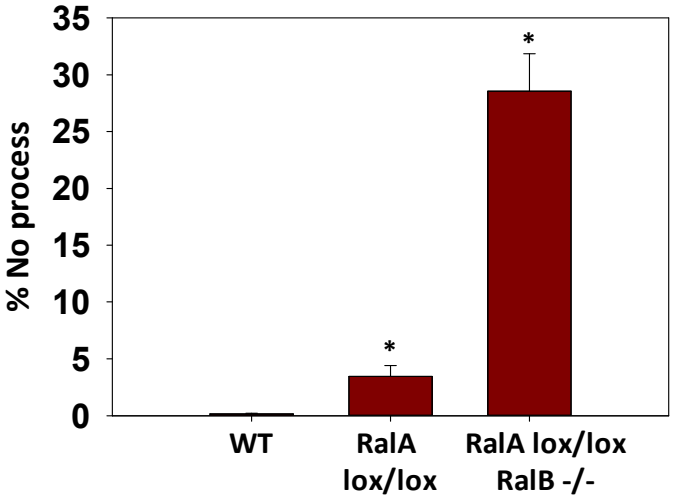
% No process
35
30
25
20
15
10
5
0
*
*
WT
RalA lox/lox
RalA lox/lox RalB -/-

Figure 5.20: Deletion of RalA/RalB disrupts neuroblast polarised morphology and directionality (2). A pCAG-Cre-IRES2-EGFP plasmid was electroporated into the right lateral ventricle of WT, $RalA^{lox/lox}$, or $RalA^{lox/lox}/RalB^{-/-}$ P2 mouse pups. Mice were sacrificed 5 days later and the right hemisphere was fixed, sliced and stained for GFP. Deletion of RalA, or RalA and RalB, causes a significant reduction in process length (top panel), and an increase in the % neuroblasts oriented away from the OB (middle panel) or without a leading process (bottom panel). Each bar represents the mean ± SEM; *P < 0.05; **P < 0.01; ***P < 0.001; n = 4 brains for WT, n = 5 brains for $RalA^{lox/lox}$, n = 11 brains for $RalA^{lox/lox}/RalB^{-/-}$.

A

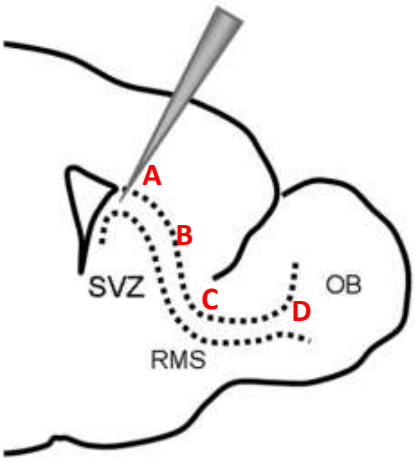
A
B
C
D
SVZ
OB
RMS

B

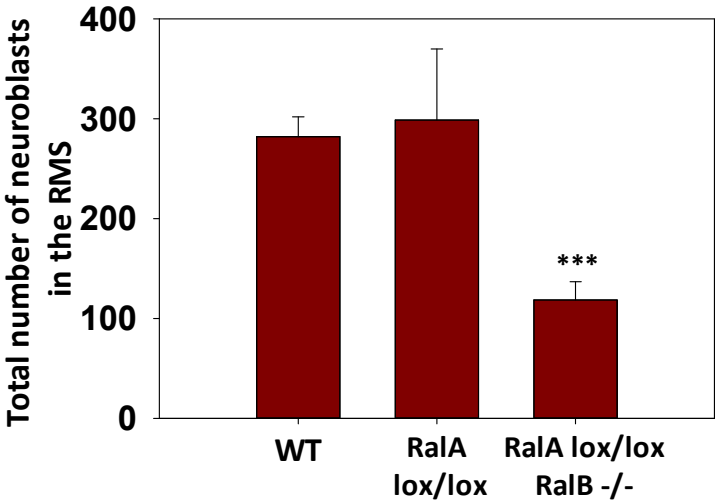
Total number of neuroblasts in the RMS
400
300
200
100
0
***
WT
RalA lox/lox
RalA lox/lox RalB -/-

C

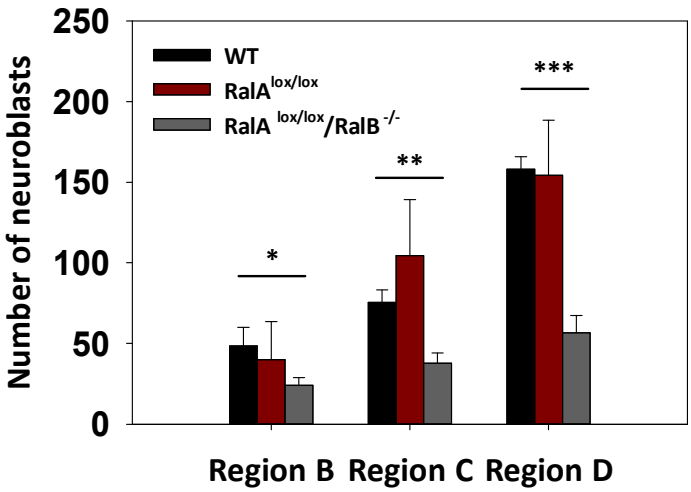
Number of neuroblasts
250
200
150
100
50
0
WT
RalA lox/lox
RalA lox/lox/RalB -/-
*
**
***
Region B
Region C
Region D

Figure 5.21: Effect of RalA/RalB deletion on neuroblast migration. A pCAG-Cre-IRES2-EGFP plasmid was electroporated into the right lateral ventricle of WT, $RalA^{lox/lox}$, or $RalA^{lox/lox}/RalB^{-/-}$ P2 mouse pups. Mice were sacrificed 5 days later and the right hemisphere was fixed, sliced and stained for GFP. **(A)** A schematic diagram showing the site of injection in the lateral ventricle. The RMS (dotted lines) was divided into anatomically distinct regions for the purpose of quantification. Region **A** is the injection site, region **B** is the descending arm of the RMS, region **C** is the RMS "elbow" preceding the OB, and region **D** is within the OB. **(B)** The total number of labelled cells within the stream is significantly less in $RalA^{lox/lox}/RalB^{-/-}$ mice in comparison to WT mice. **(C)** There are far fewer neuroblasts in all regions of the stream of $RalA^{lox/lox}/RalB^{-/-}$ mice in comparison to the control. Each bar represents the mean ± SEM; *P < 0.05; **P < 0.01; ***P < 0.001; n = 4 brains for WT, n = 4 brains for $RalA^{lox/lox}$, n = 10 brains for $RalA^{lox/lox}/RalB^{-/-}$.

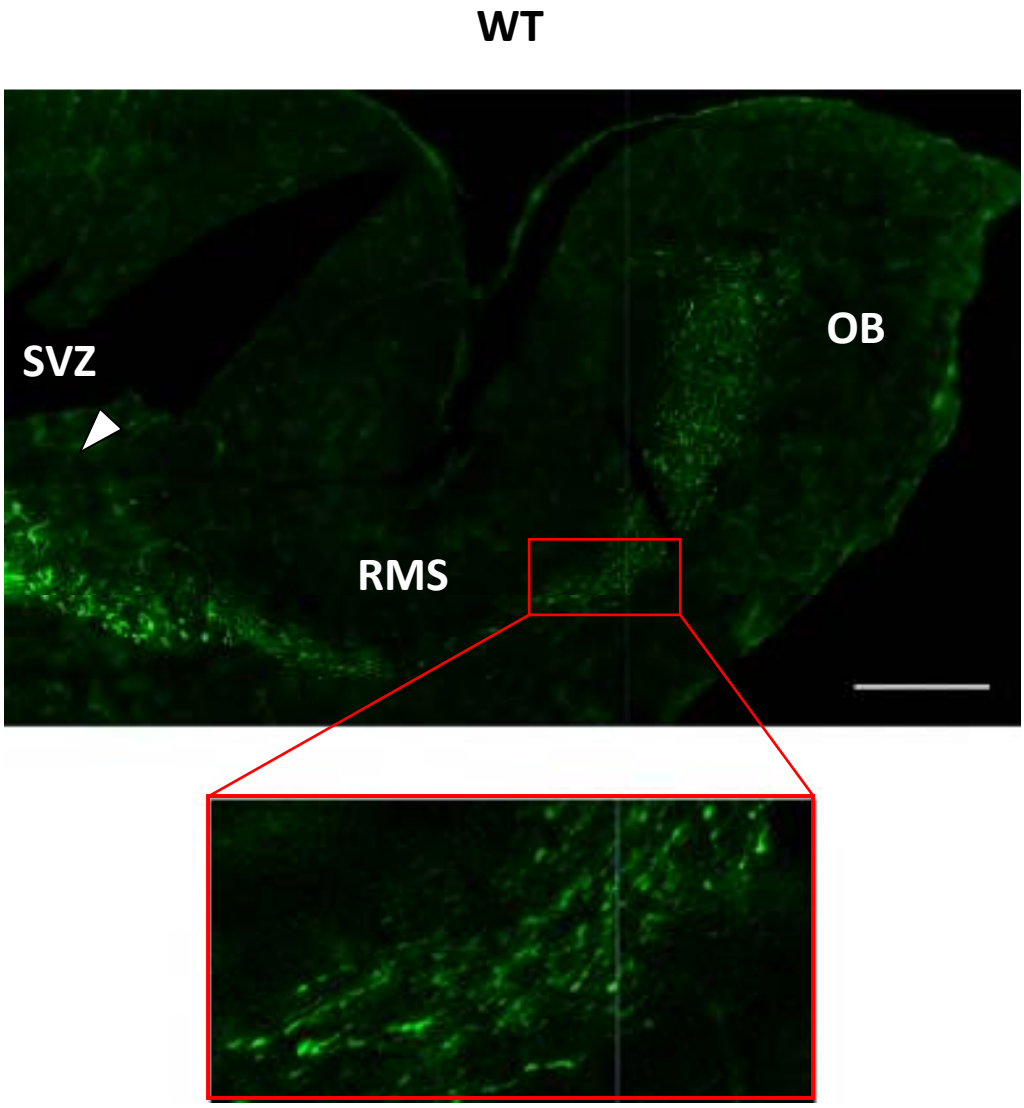

Figure 5.22: Cre-GFP expression in RMS neuroblasts in WT mice. A PCAG-Cre-IRES2-EGFP plasmid was electroporated into the right lateral ventricle of WT P2 mouse pups. Mice were sacrificed 5 days later and the right hemisphere was fixed, sliced and stained for GFP. Representative image of a WT mouse brain slice showing Cre-GFP labelled neuroblasts in the RMS. There is robust labelling of cells at the injection site and GFP-expressing cells can be seen throughout the RMS. White arrowhead indicates the site of injection. Bar = 500 µm.

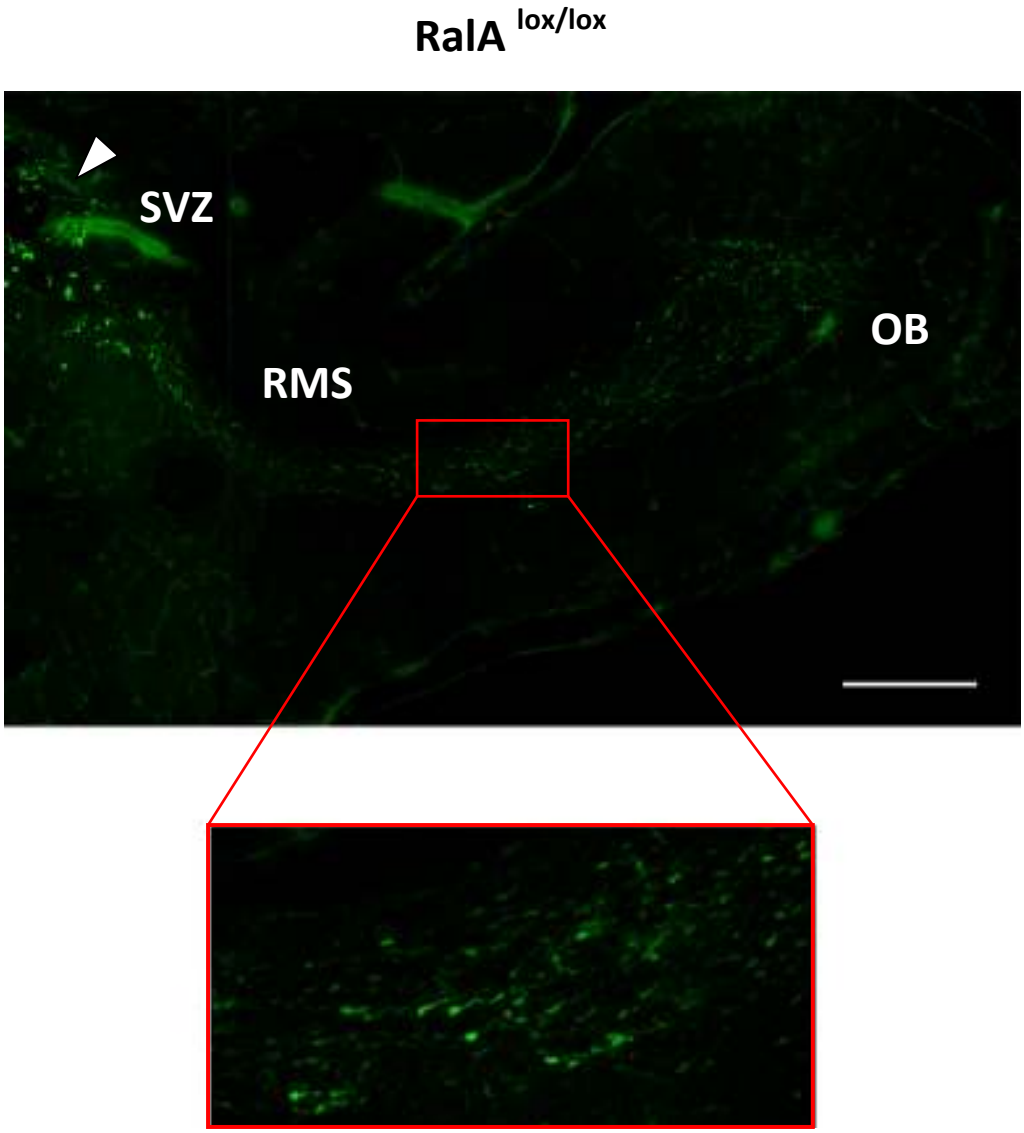

Figure 5.23: Cre-GFP expression in RMS neuroblasts in RalA$^{lox/lox}$ mice. A PCAG-Cre-IRES2-EGFP plasmid was electroporated into the right lateral ventricle of RalA$^{lox/lox}$ P2 mouse pups. Mice were sacrificed 5 days later and the right hemisphere was fixed, sliced and stained for GFP. Representative image of a RalA$^{lox/lox}$ mouse brain slice showing Cre-GFP labelled neuroblasts in the RMS. The number of GFP labelled neuroblasts entering the stream appears to be comparable to wild type mice. White arrowhead indicates the site of injection. Bar = 500 µm.

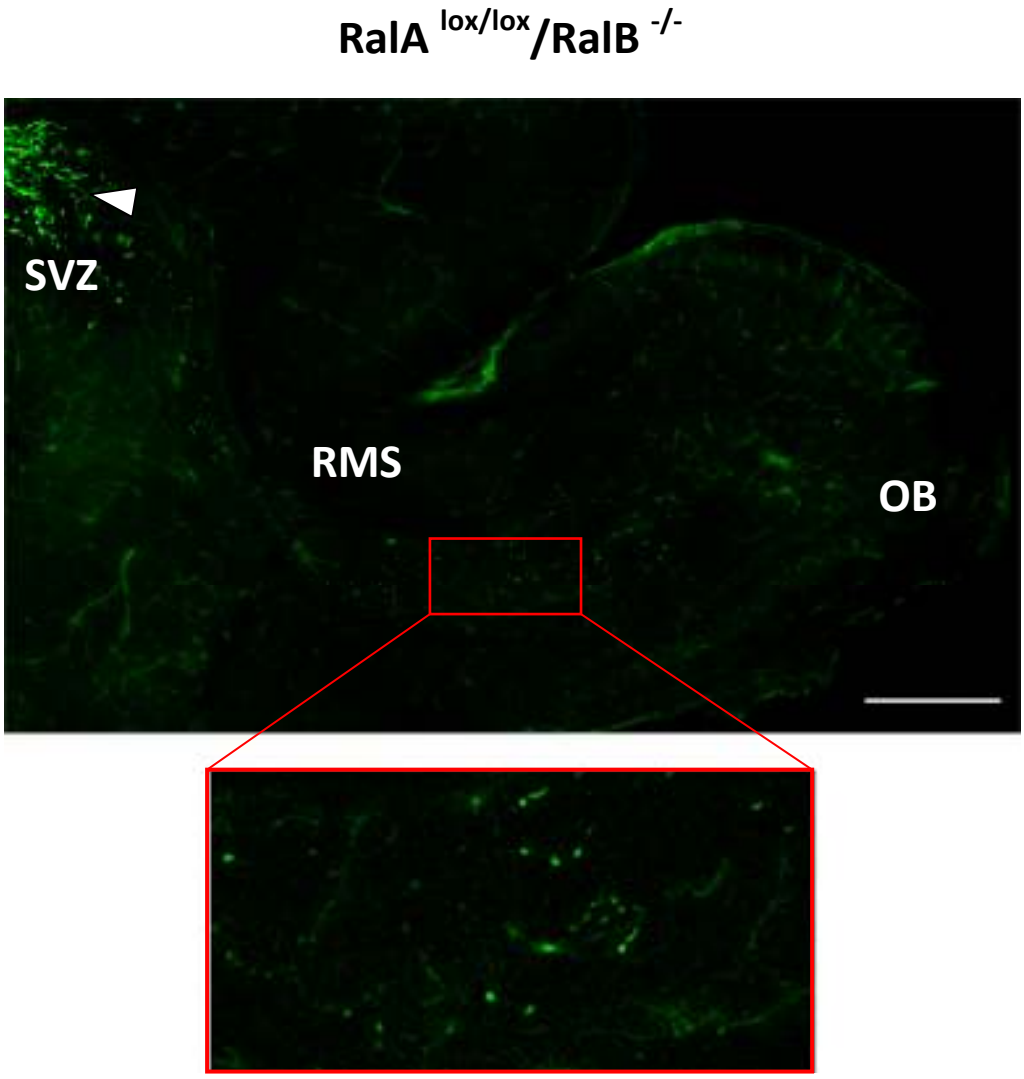

Figure 5.24: Cre-GFP expression in RMS neuroblasts in RalA$^{lox/lox}$/RalB$^{-/-}$ mice. A PCAG-Cre-IRES2-EGFP plasmid was electroporated into the right lateral ventricle of RalA$^{lox/lox}$/RalB$^{-/-}$ P2 mouse pups. Mice were sacrificed 5 days later and the right hemisphere was fixed, sliced and stained for GFP. Representative image of a RalA$^{lox/lox}$/RalB$^{-/-}$ mouse brain slice showing Cre-GFP labelled neuroblasts in the RMS. Although there is robust expression of GFP at the injection site, there are considerably fewer GFP positive neuroblasts in the stream in comparison to wild type animals and RalA$^{lox/lox}$ animals. White arrowhead indicates the site of injection. Bar = 500 µm.

To examine the function of RalB loss on RMS neuroblast migration, we electroporated pCX-EGFP into the lateral ventricles of $RalA^{lox/lox}/RalB^{-/-}$ mice. Preliminary observations show that deletion of RalB does not noticeably affect morphology, orientation, or the extent of migration along the RMS (Figure 5.25) (Dr Katarzyna Falenta – work in progress). Interestingly, analysis of DAPI nuclear staining shows that the gross RMS morphology and cell density appears to be comparable between $RalA^{lox/lox}$, $RalA^{lox/lox}/RalB^{-/-}$, and WT mice (Figure 5.26). Taken together, these observations suggest that deletion of RalB alone does not affect the generation or migration of RMS neuroblasts.

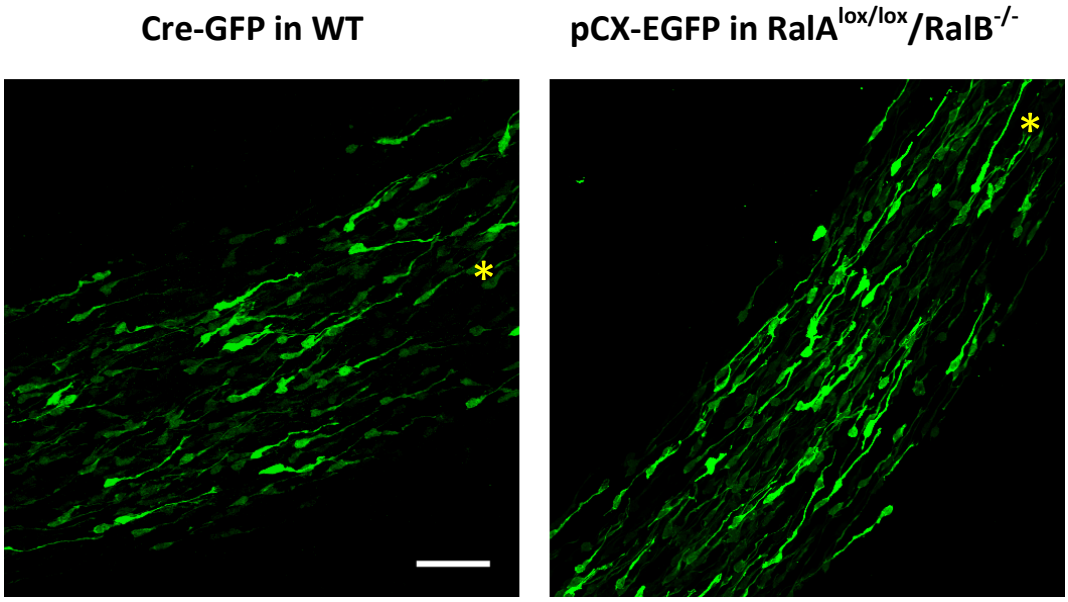

Figure 5.25: Neuroblast morphology and migration appears normal in RalB deficient mice. Comparison of a pCAG-Cre-IRES2-EGFP plasmid electroporated into the right lateral ventricle of a WT mouse, and pCX-EGFP electroporated into the lateral ventricle of a RalA$^{lox/lox}$/RalB$^{-/-}$ mouse. Mice were sacrificed 5 days later and the right hemisphere was fixed, sliced and stained for GFP. Representative images of RMS neuroblasts expressing the Cre-GFP construct in WT mice (left) and neuroblasts expressing pCX-EGFP in RalA$^{lox/lox}$/RalB$^{-/-}$ mice (right). Yellow asterisks indicate the relative position of the OB. The morphology of neuroblasts lacking RalB is comparable to that of WT neuroblasts, with the majority of neuroblasts being oriented towards the OB. Bar = 50 µm. Images kindly provided by Dr Katarzyna Falenta.

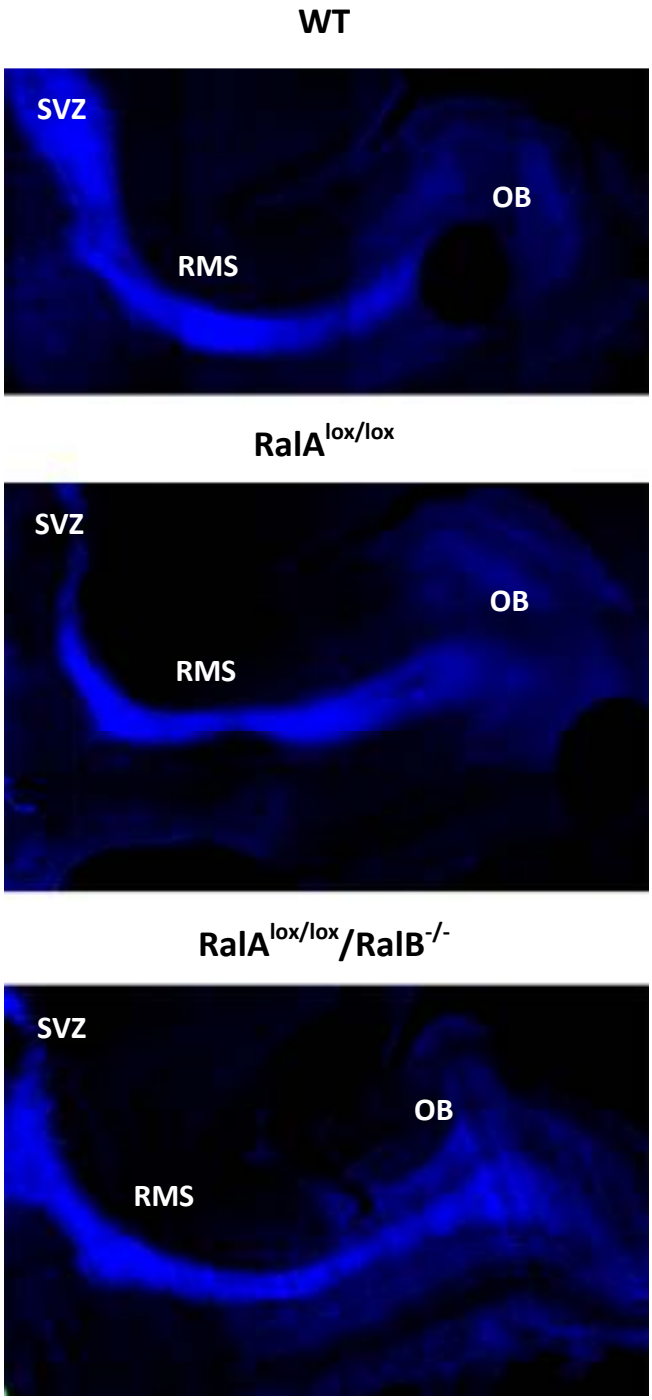

Figure 5.26: RMS morphology of WT, RalA$^{lox/lox}$, and RalA$^{lox/lox}$/RalB$^{-/-}$ mice. Brain slices of P7 WT, RalA$^{lox/lox}$, and RalA$^{lox/lox}$/RalB$^{-/-}$ mice were fixed and incubated with the nuclear stain DAPI to visualise the morphology of the RMS. Representative images show that the RMS forms of RalA$^{lox/lox}$ and RalA$^{lox/lox}$/RalB$^{-/-}$ mice is morphologically similar to WT samples.

5.3 Discussion

The Ral GTPases are important regulators of migration in a number of cell types, including myoblasts, B cells, multiple myeloma, and prostate cancer cells (Suzuki et al. 2000; Oxford et al. 2005; de Gorter et al. 2008; Spiczka and Yeaman 2008). Our earlier findings demonstrate that the RalA isoform is highly expressed by migrating neuroblasts. Not only is this GTPase activated by both motogenic and chemotactic factors, it is also required for CB-promoted migration. In this part of the study, using the techniques we established in Chapters 3 and 4, we focus our attention on investigating whether RalA has a more fundamental role in neuroblast migration in the RMS.

Here we show using a siRNA based approach, that RalA depleted neuroblasts are significantly impaired in their ability to migrate *in vitro*. These neuroblasts have a lower velocity, show a dramatic reduction in the migrated distance, and spend a greater amount of time immobile. Furthermore, despite having a dynamic leading process, RalA depleted neuroblasts have a significantly lower frequency (6-fold reduction) of productive nuclear movements, and appear to "struggle" during nucleokinesis. This apparent uncoupling of leading process extension and nucleokinesis, also appears to lead to a substantial increase in the average process length of RalA deficient cells. Time-lapse experiments show that these protrusions undergo cycles of extension and collapse, as if failing to adhere properly to the matrix. This is particularly interesting since RalA has been shown to regulate the migration of non-neuronal cells by co-ordinating the delivery of integrin subunits required for cell-substratum adhesion (Spiczka and Yeaman 2008). Moreover, both β1 and β8 integrins have been shown to play a vital role in the chain migration of neuroblasts in the RMS (Belvindrah et al. 2007; Mobley and McCarty 2011).

We also demonstrate that this impairment in migration specifically arises from the loss of RalA, since inhibition of migration is fully rescued by co-transfection of a siRNA-resistant WT RalA version. Moreover, we show that the function of RalA is

cell autonomous, since untransfected neuroblasts in RalA siRNA-nucleofected cultures are comparable to control cells in their ability to migrate.

To translate our *in vitro* findings to an *in vivo* model, we cloned control and RalA-targeting shRNA sequences (RalA shRNA 1-4) into an expression vector. These plasmids were used to inhibit RalA expression in the Matrigel migration assay, and were also electroporated *in vivo* for analysis of neuroblast morphology in fixed brains slices as well as time-lapse analysis of cultured slices. Unfortunately, we did not observe any significant difference between control and RalA shRNA expressing neuroblasts in any of the assays examined. The most likely explanation for this failure of RalA shRNA constructs to inhibit neuroblast migration is that they only produced relatively moderate knockdown (25-40%) of RalA. In comparison, the RalA siRNA oligo, which produced dramatic changes in morphology and migration, could inhibit RalA expression by up to 70%. Since RalA is abundant in these cells, it may be necessary to inhibit protein expression by a considerable amount before any migratory defects begin to manifest. Therefore, we decided to try an alternative approach based on the expression of mutant RalA proteins previously shown to perturb RalA function in different types of neurones (Lalli and Hall 2005; Lalli 2009). Analysis of fixed brain slices from mouse pups that had been electroporated with the RalA mutants revealed that neuroblasts expressing DN RalA were misoriented and showed a significant reduction in leading process length. On the other hand, cells expressing CA or FC RalA showed a slight, but significant increase in the leading process length without any change to orientation. Thus, the expression of RalA appears to be important for correct neuroblast morphology as wells as orientation. Surprisingly, despite the striking results seen with the DN RalA mutant *in vivo*, the same construct did not perturb migration *in vitro*. In addition, whilst disturbing RalA function with DN RalA caused a shortening of the leading process *in vivo*, depletion of RalA with siRNA caused a significant increase in leading process length *in vitro*. One possibility for these differences could be that all Matrigel migration assays were performed with rat RMS cultures, which were necessary for the greater amount of starting material required for nucleofection procedures, as opposed to the mouse model used for *in vivo* electroporation studies. There has been some

suggestion of subtle differences between the migration of mouse and rat RMS neuroblasts in slice cultures. For instance, Nam et al. (2007) describe that mouse RMS neuroblasts only move by translocation (leading process extension and nuclear translocation occur as distinct consecutive steps) and not by locomotion (leading process extension and nuclear translocation occur simultaneously). Instead, Kakita and Goldman (1999) showed that rat neuroblasts migrate by both translocation and locomotion. Another possibility is that these observed discrepancies may have arisen from the differences between neuroblast migration in Matrigel versus migration in the native RMS. Indeed, neuronal precursors can switch their mode of migration as well as morphology when faced with different environments. For example, during development, migrating cortical neurones adopt a multipolar morphology after entering the SVZ, and then switch to a bipolar form before commencing towards the cortical plate (Noctor et al. 2004). Furthermore, the migration of RMS neuroblasts is also subject to subtle changes that occur both spatially and temporally. For instance, neuroblasts transition from vasculature-independent to vasculature-dependent migration in the early stages of postnatal development (Bovetti et al. 2007; Saghatelyan 2009; Snapyan et al. 2009; Bozoyan et al. 2012), and from chain to single cell migration in response to detachment signals present in the OB (Hack et al. 2002; Saghatelyan et al. 2004; Ng et al. 2005). Hence, the morphological differences seen following impairment of RalA function in these two assays may arise from distinct modes of migration adopted by neuroblasts in these specific environments. Nevertheless, perturbing RalA activity *in vitro* with siRNA and *in vivo* with DN RalA significantly impairs RMS neuroblast morphology and migration, thus supporting a role for RalA in this process.

To examine the full significance of RalA function in the RMS, we deleted RalA using electroporation of Cre-GFP into the lateral ventricle of $RalA^{lox/lox}$ and $RalA^{lox/lox}/RalB^{-/-}$ mice (Peschard et al, in press). Neuroblasts in the RMS are strictly polarised towards the OB, with only 1% of cells in wild type mice being misoriented. Here, we show that deletion of RalA results in a significant increase in the percentage of misoriented neuroblasts in the RMS (7%). Moreover, loss of RalA leads to significant shortening of the leading process, with some neuroblasts completely lacking a

leading process altogether. Deletion of both RalA and RalB leads to an even more striking phenotype, with an even greater reduction in the leading process length and % of cells without a process. The number of misoriented neuroblasts however is similar to that of $RalA^{lox/lox}$ mice, with approximately 8% of cells facing away from the OB in both cases. In addition, the loss of RalB alone does not appear to affect neuroblast morphology or orientation, suggesting that RalA is primarily responsible for regulating these functions. Despite this drastic change in morphology and orientation, Cre-GFP expressing neuroblasts, including those lacking a leading process, can be seen throughout the RMS in $RalA^{lox/lox}$ and $RalA^{lox/lox}/RalB^{-/-}$ mice. One possible explanation could be that due to the compact nature of the stream, the subpopulation of labelled neuroblasts get "carried along" by the continuous current of migrating cells. Future work will therefore need to include time-lapse imaging of these neuroblasts in the stream to characterise their capacity to migrate.

Intriguingly, deletion of both Ral isoforms results in a striking reduction of labelled neuroblasts found in the RMS when compared with wild type and $RalA^{lox/lox}$ animals, despite a similar extent of cell labelling at the injection site. This could suggest one of several possibilities (discussed in detail in Chapter 7.4). Firstly, the loss of RalA and RalB may severely impair the migration of RMS neuroblasts causing them to be "trapped" in the SVZ. If this is the case, both RalA and RalB would be needed for proper migration of neuroblasts. Another possibility is that the loss of both Ral proteins could lead to a defect in the proliferation of SVZ NS cells, which normally give rise to migratory neuroblasts (Doetsch et al. 1997; Garcia-Verdugo et al. 1998; Doetsch et al. 1999), and is the main cell type labelled by electroporation (Boutin et al. 2008). Our initial finding that RalB was abundant in highly proliferative cells such as the Cor-1 NS cell line led us to speculate whether RalB could be involved in neural precursor proliferation in the SVZ. However, the morphology of the RMS in $RalA^{lox/lox}/RalB^{-/-}$ mice is comparable to that of wild type littermates, thus suggesting that RalB *per se* is not absolutely necessary for proliferation of SVZ neural stem cells, though we cannot rule out the possibility that RalA may compensate for the loss of RalB. Finally, the loss of both Ral isoforms could adversely affects cell viability or cell fate. Work in progress in the lab is aimed at analysing these

possibilities by establishing the identity of cells lacking RalA and RalB following Cre electroporation, as well as assessing potential effects on proliferation and viability arising from the deletion of RalA and/or RalB.

Chapter 6: Potential effectors and activators of RalA

6.1 Introduction

The migration of neural precursors is regarded as a cyclic process involving extension of a leading process in response to integration of extracellular guidance cues, followed by translocation of the nucleus in the direction of migration (Lambert de Rouvroit and Goffinet 2001; Marin et al. 2006). Each of these distinct steps is co-ordinated by a number of proteins that regulate specific aspects of cell migration (reviewed in detail in Introduction Chapter 1.5). In our search to elucidate the molecular control of cell migration in the RMS, we have identified RalA as a regulator of neuroblast migration. To further our understanding of the RalA signalling mechanism in this system, we focus our attention in this chapter on uncovering the potential activators and effectors of RalA.

Ral-GTPases can be activated by one of several mechanisms. Other members of the Ras superfamily, including Ras and Rap GTPases, have been shown to regulate Ral function by activating Ral specific GEFs (Bos et al. 2007). Although Rap GTPases appear to have a higher affinity for Ral-GEFS than Ras, in mammalian cells Ral-GEFS are recognised as the primary effectors for Ras proteins (Ferro and Trabalzini 2010). However, under certain circumstances, Rap GTPases have been shown to be responsible for GEF-mediated activation of Ral (Wolthuis et al. 1996). For example, CB1 receptor mediated neurite outgrowth as well as orientation of multipolar neurones in the developing cortex have been shown to be reliant on the activation of Ral by Rap1 (He et al. 2005; Jossin and Cooper 2011). Ral GTPases can also be activated by rises in intracellular Ca^{2+}, although it is not yet clear as to whether this occurs through the actions of a Ca^{2+} sensitive GEF or through binding of Ral by calmodulin, which occurs in a Ca^{2+} dependent manner (Hofer et al. 1998; Wolthuis et al. 1998; Clough et al. 2002). In addition, the mitotic kinase Aurora A has been shown to directly activate Ral proteins by phosphorylation of Ser-194 at the C-terminus, a mechanism that is specific to RalA (Kashatus et al. 2011).

Once activated, Ral GTPases can participate in a variety of signalling cascades through the regulation of their effectors, which include RalBP1, the exocyst complex, filamin, and ZONAB (Cantor et al. 1995; Ohta et al. 1999; Moskalenko et al. 2002; Frankel et al. 2005). Hence, to narrow our search, we specifically examined the relationship between RalA and molecules known to be involved in neuronal migration such as CDK5 (Hirota et al. 2007; Rakic et al. 2009), Pak1 (Nikolic 2008; Causeret et al. 2009; Kreis and Barnier 2009), p27-kip1 (Nguyen et al. 2006), MLC-2 (Bellion et al. 2005), and N-Cadherin (Jossin and Cooper 2011), as well as a Ral effector the exocyst complex (Moskalenko et al. 2002).

6.2 Results

6.2.1 Activators of RalA: Rap GTPases

Rap GTPases are able to bind and activate Ral-GEFs, and have been shown to be the primary activators of Ral proteins in *Drosophila* (Mirey et al. 2003). Furthermore, CB receptor-mediated neurite outgrowth and reelin-induced migration of cortical neurones in the developing brain are both dependent on a Rap-Ral relationship (He et al. 2005; Jossin and Cooper 2011). Since we found that CB agonists-promoted migration of RMS neuroblasts was reliant on RalA (Chapter 4), we speculated that Rap1 may be responsible for coupling CB receptor signalling to RalA activation, as seen in neurite outgrowth (He et al. 2005). To confirm this hypothesis, we examined rat RMS neuroblast lysates by Western blotting for Rap1A/B expression. Figure 6.1 shows that Rap1A/B is hardly detectable in neuroblast lysates. In contrast, SVZ and rat embryonic cortex homogenates, as well as Cor-1 cell lysates all show strong expression of Rap1. To determine whether Rap1 could act downstream of the CB1 receptor, we tested whether the CB1 agonist ACEA could activate Rap1 using a pulldown assay, where dissociated rat RMS neuroblasts treated with ACEA 0.5 µM for 5 minutes, 30 minutes and 1 hour, were subsequently lysed and incubated with agarose beads bound to the Rap binding domain of Ral-GDS (a Ral-specific GEF), which only binds the active form of Rap (Rap-GTP) (van Triest et al. 2001). Using a Rap1B specific antibody, we were not able to detect protein expression in either the input or the pulldown samples (Figure 6.2). As a

positive control, the same antibody detected a single band at 21 kDa in rat embryonic cortex corresponding to the expected band for Rap1B (Figure 6.2). A Rap1A antibody was also tested in the same assay but failed to detect any bands in the input or pulldown samples (data not shown). Hence, Rap1 appears to be weakly expressed in rat neuroblasts, and unfortunately it was not possible to measure activation of this GTPase due to limitations in the sensitivity of the pulldown assay and the low available starting material (primary neuroblasts).

6.2.2 Signalling downstream of RalA: Regulation of nucleokinesis

In the first part of nucleokinesis in migrating neuronal cells, the centrosome and Golgi move into a swelling in front of the nucleus in the direction of migration, a process that has been demonstrated to be important for SVZ neural precursor migration (Higginbotham et al. 2006). We showed previously that RalA depletion causes a nucleokinesis defect *in vitro* (Chapter 5, Figure 5.5), whilst deletion of RalA led to misorientation of neuroblasts *in vivo* (Chapter 5, Figure 5.21). Thus, to assess whether lack of RalA impairs centrosome polarisation, we examined the orientation of the centrosome in relation to the leading process in control and RalA-depleted RMS neuroblasts migrating in Matrigel, by immunostaining for the centrosomal marker γ tubulin (Wiese and Zheng 2006). The centrosome can be visualised as a bright spot and is usually located between the nucleus and the leading process (Figure 6.3A). For the purpose of quantification, the cell body was divided into four quadrants, with quadrant 1 representing the area between the nucleus and leading process (Figure 6.3B). The number of cells with centrosomes in each quadrant was counted for both control and RalA-depleted neuroblasts. Figure 6.3C shows that the centrosome is nearly always positioned between the nucleus and leading process (quadrant 1) with 89.7 % ± 0.5 of control neuroblasts and 97.0 % ± 0.3 of RalA-depleted neuroblasts having their centrosome in quadrant 1. Thus, positioning of the centrosome does not appear to be impaired following RalA depletion in these experimental conditions. However, since we are examining a snapshot in time using fixed samples, we noticed that only a few cells were actively undergoing nucleokinesis, as identified by the appearance of a characteristic swelling in front of the nucleus (Figure 6.3A, white arrowheads).

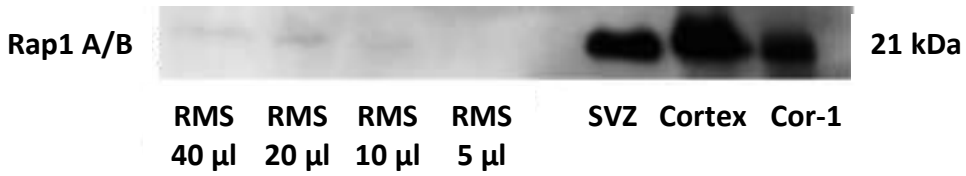

Figure 6.1: Rap1 A/B expression in rat RMS neuroblasts, SVZ, rat embryonic cortex and Cor-1 cells. Dissociated rat RMS neuroblasts were plated in 6 well plates coated with polyornithine/laminin at a density of 1,000,000 cells/well. Neuroblasts were lysed after 48 hours in culture. Different volumes of RMS lysates (5-40 µl), SVZ homogenate, rat embryonic cortex homogenate and Cor-1 cell lysate were analysed by Western blotting for expression of Rap1 A/B.

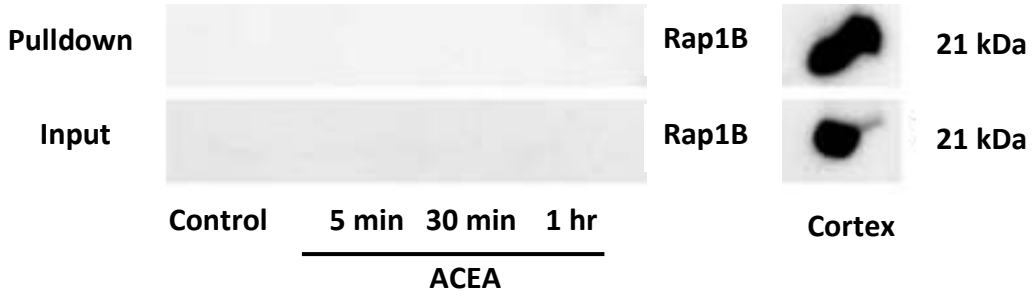

Figure 6.2: Expression of Rap1B in rat embryonic cortex and rat RMS neuroblasts after treatment with CB1 agonist. Dissociated rat RMS neuroblasts plated on polyornithine/laminin-coated wells were cultured for 48 hours before treatment with the CB1 agonist ACEA (0.5 µM for 5 min, 30 min and 1 hr). Lysates were incubated with agarose beads bound to the Ral GDS-Rap binding domain to extract active Rap1. Input and pulldown samples were run on a SDS-polyacrylamide gel alongside an embryonic rat cortex homogenate as a positive control. Western blots were probed for Rap1B expression. Rap1B is not detectable in input or pulldown samples derived from rat RMS neuroblasts, whereas it is abundant in rat embryonic cortex with a single band being detected at 21 kDa.

A

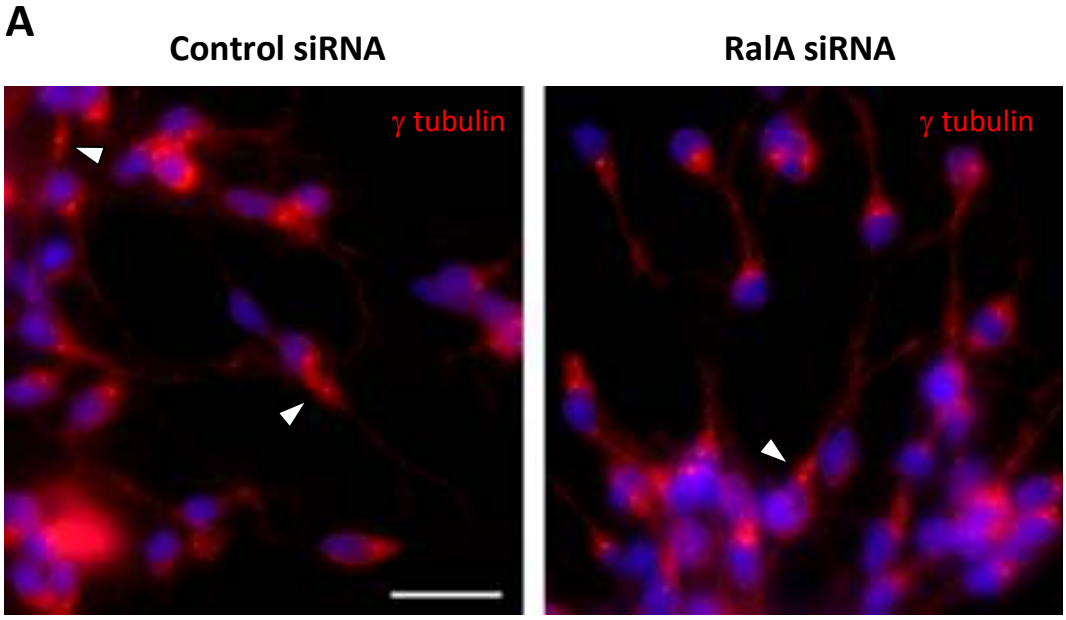
Control siRNA
RalA siRNA
γ tubulin
γ tubulin

B

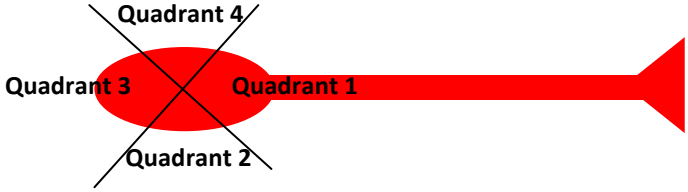
Quadrant 4
Quadrant 3
Quadrant 1
Quadrant 2

C

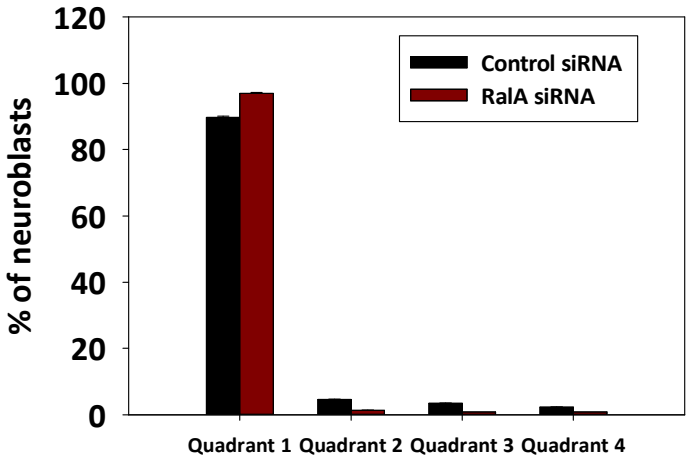
120
100
80
60
40
20
0
% of neuroblasts
Control siRNA
RalA siRNA
Quadrant 1
Quadrant 2
Quadrant 3
Quadrant 4

Figure 6.3: Depletion of RalA does not alter the position of the centrosome. Rat RMS neuroblasts were nucleofected with either a control or RalA siRNA, re-aggregated and embedded in Matrigel 48 hours post nucleofection. Cells were fixed 24 hours later and immunostained for the centrosomal marker γ-tubulin. **(A)** Representative images of control (left) and RalA-depleted cells (right). The centrosome can be seen as a bright spot between the nucleus and leading process. White arrowheads point to neuroblasts that are midway through nucleokinesis as evidenced by the cytoplasmic swelling in front of the nucleus. Bar = 20 μm. **(B)** Schematic representation showing how each neuroblast was divided into quadrants to quantify the position of the centrosome in relation to the leading process. **(C)** A graph showing the % of neuroblasts that had their centrosome located in quadrant 1, 2, 3 or 4. The centrosome is nearly always located between the nucleus and leading process (quadrant 1) in both control and RalA depleted cells. Each bar represents the mean ± SEM; n = 261 cells for control and 460 cells for RalA siRNA.

The second part of nucleokinesis, the forward movement of the nucleus, relies on pulling forces associated with the dynein motor complex as well as actomyosin contraction at the rear of the cell (Bellion et al. 2005; Schaar and McConnell 2005; Tsai and Gleeson 2005). Hence, we examined the phosphorylation state of myosin ll light chain (MLC2), the actin-based motor protein responsible for contraction of the cell rear (Schaar and McConnell 2005). Unexpectedly, antibodies for MLC2 and p-MLC2 detected a single band at 65 kDa rather than the expected 18 kDa (Figure 6.4A). To rule out possible aggregation of the protein after lysis, samples were sonicated before Western analysis. However, this produced a triplet of bands around 60 - 70 kDa for MLC2, and no detectable bands for p-MLC2 (Figure 6.4B). Similarly, our analysis of the phosphorylation states of proteins associated with the dynein motor complex, such as DCX and Nudel, which may be involved in generating the pulling forces necessary for nuclear translocation (Niethammer et al. 2000; Sasaki et al. 2000; Shu et al. 2004; Tanaka et al. 2004) proved inconclusive (data not shown).

6.2.3 Signalling downstream of RalA: Pak1

The p21-activated kinase (Pak) family members are serine/threonine kinases known to regulate both actin and microtubule dynamics, and have established roles in neuronal polarity, axon guidance, and cortical neuron migration during development (Fan et al. 2003; Shekarabi et al. 2005; Jacobs et al. 2007; Smith et al. 2008; Causeret et al. 2009). The Pak family consist of 6 members divided into group l (Pak 1, 2, and 3) and group ll (Pak 4, 5, and 6) Paks based on their sequence, structure, and biochemical properties (Kreis and Barnier 2009). Though they are the major effectors for the Rho GTPases Rac and Cdc42, they can also be activated by a number of molecules through phosphorylation at various sites. For example, the T212 site which is specifically found on Pak1, is the target residue for CDK5 (Chong et al. 2001; Thiel et al. 2002). Importantly, perturbing Pak1 function in cortical neurones leads to misorientation of migrating cells and a disorganised leading process (Causeret et al. 2009), reminiscent of the phenotype seen with RalA deletion in RMS neuroblasts (Chapter 5).

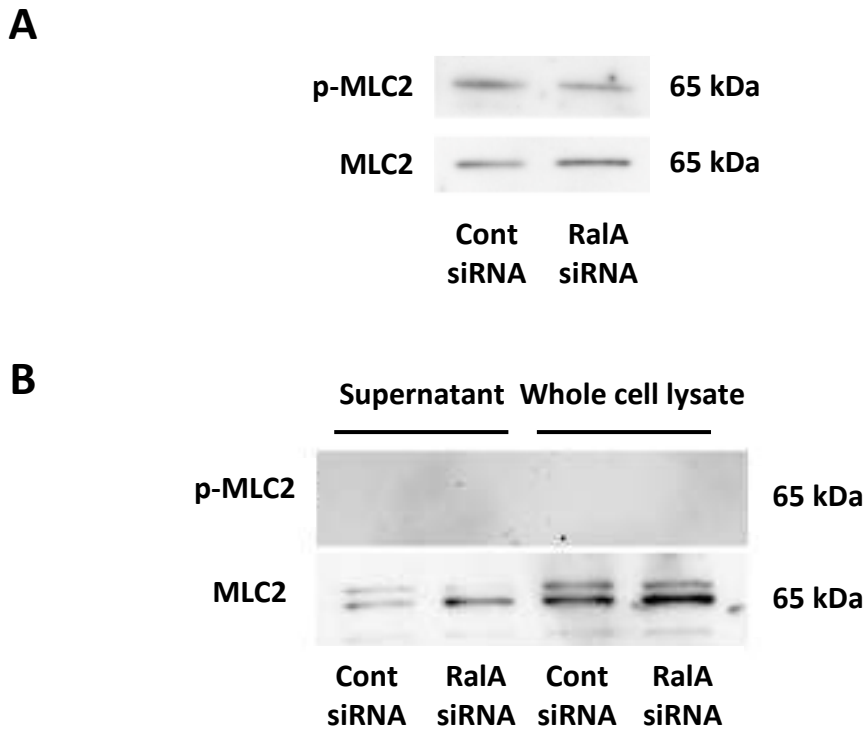

Figure 6.4: MLC2 and p-MLC2 expression after RalA knockdown in rat RMS neuroblasts. Dissociated rat RMS neuroblasts were nucleofected with a control or RalA siRNA oligo, plated onto polyornithine/laminin-coated wells and cultured for 48 hours. **(A)** Lysates were analysed by Western blotting for expression of MLC2 and p-MLC2. A single band is detected for both antibodies, but at a much higher molecular weight than the expected 18 kDa. **(B)** Control and RalA-depleted neuroblasts were lysed and centrifuged to obtain just the supernatant, or whole cell lysates were used. Samples were sonicated before Western analysis. A triplet of bands can be detected for MLC2, although the band is not of the expected molecular weight. No bands were detected with the p-MLC2 antibody.

In addition, the actin-binding protein filamin, an effector for RalA, has also been shown to activate Pak (Vadlamudi et al. 2002). Hence, we speculated whether RalA mediated its effects through regulation of Pak activity. We sought to address this issue primarily by analysing Pak1 phosphorylation as a marker of activation using Western blot analysis (Nikolic 2008; Kreis and Barnier 2009).

To test the hypothesis that Pak1 acts downstream of CB signalling and RalA, we investigated Pak1 expression and phosphorylation in rat RMS neuroblasts following treatment with CB1 agonist, in control and RalA-depleted cells using Western blot analysis. Using an antibody recognising an epitope on the C-terminus of PAK1 (αPak c-19; Santa Cruz) we detected two bands in rat neuroblast lysates (Figure 6.5A). The lower band at 65 kDa corresponds to the molecular weight of Pak1, whilst the identity of the upper band at 70 kDa is not clear. Interestingly, treatment of neuroblasts with ACEA, or RalA knockdown, or RalA knockdown followed by ACEA treatment results in upregulation of this unknown protein (Figure 6.5A-B). Although Pak1 has multiple phosphorylation sites which specifically regulate activation and inactivation of its catalytic domain, it is unlikely that the upper band is a result of Pak phosphorylation given the 5 kDa difference between the two bands. Nevertheless, to further examine whether the upper band was due to phosphorylation of the protein we also tested the effects of an inhibitor of CDK5, a kinase known to phosphorylate Pak (Rashid et al. 2001; Banerjee et al. 2002). Unexpectedly, the CDK5 inhibitor Roscovitine (Leitch et al. 2009) significantly upregulated the expression of the unknown protein when used alone or in combination with ACEA (Figure 6.6A-B).

In an attempt to determine the identity of the unknown band, we examined expression of other Pak family members following knockdown of RalA, treatment with ACEA, or knockdown of RalA followed by ACEA treatment. A Pak2 antibody detected a doublet of bands (at around 61 kDa) in neuroblasts (Figure 6.7A). A Pak3-specific antibody detected a band at 65 kDa (Figure 6.7B), and a Pak4-specific antibody detected a single band at 72 kDa (Figure 6.7C).

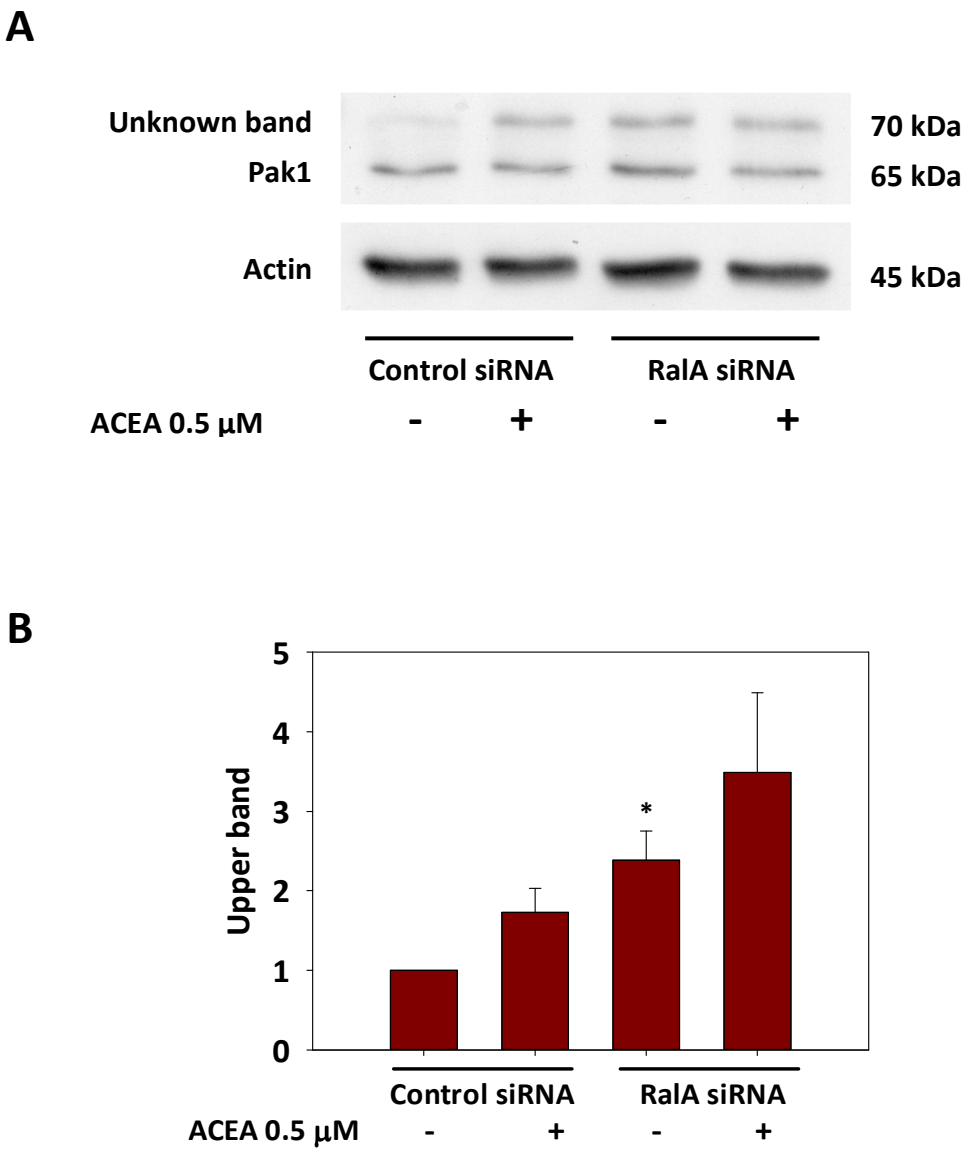

Figure 6.5: CB treatment or knockdown of RalA causes increased expression of an unknown band when probed for Pak1 (αPak c-19; Santa Cruz). Dissociated rat RMS neuroblasts nucleofected with control or RalA siRNA oligo were plated onto polyornithine/laminin coated wells and cultured for 48 hours before being treated with either vehicle or ACEA 0.5 µM for 30 minutes. Lysates were analysed by Western blot for expression of Pak1 using an antibody that recognises the c-terminus of Pak1 (αPak c-19; Santa Cruz). **(A)** Representative Western blot showing control and RalA siRNA nucleofected neuroblasts probed for Pak1 shows an increase in the expression of an unknown band (70 kDa) following knockdown with RalA siRNA, treatment with ACEA, or both. **(B)** Densitometric analysis of the Western blot. Each bar represents the mean ± SEM; *P < 0.05; n = 4 independent experiments.

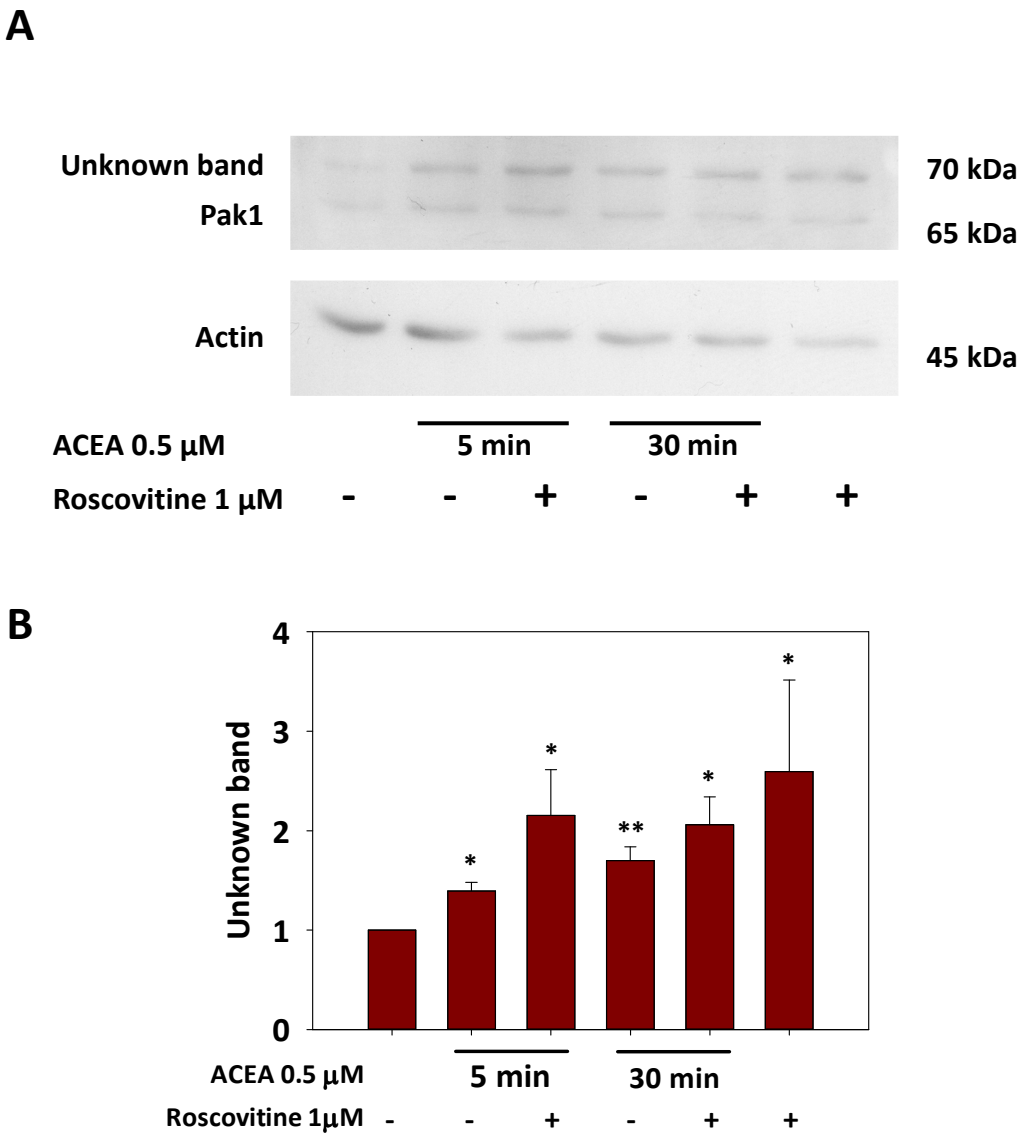

Figure 6.6: Treatment with CB1 agonist, CDK5 inhibitor, or both causes an increase in the expression of an unknown band when probed for Pak1 (αPak c-19; Santa Cruz). Dissociated rat RMS neuroblasts were plated onto polyornithine/laminin coated wells and cultured for 48 hours before being treated with the indicated drugs. CDK5 inhibitor Roscovitine 1 µM was pre-incubated for 1 hour before addition of CB1 agonist ACEA 0.5 µM. Lysates were analysed by Western blot for expression of using an antibody that recognises the C-terminus of Pak1 (αPak c-19; Santa Cruz). **(A)** Western blot probed for Pak1 showing an increase in the expression of an unknown band (70 kDa) following knockdown treatment with ACEA, Roscovitine, or both drugs. **(B)** Densitometric analysis of the Western blot shows that there is a significant increase in the expression of the 70 kDa unknown protein after CDK5 inhibition, CB1 receptor activation, or both. Each bar represents the mean ± SEM *P < 0.05; **P < 0.01; n = 4 independent experiments.

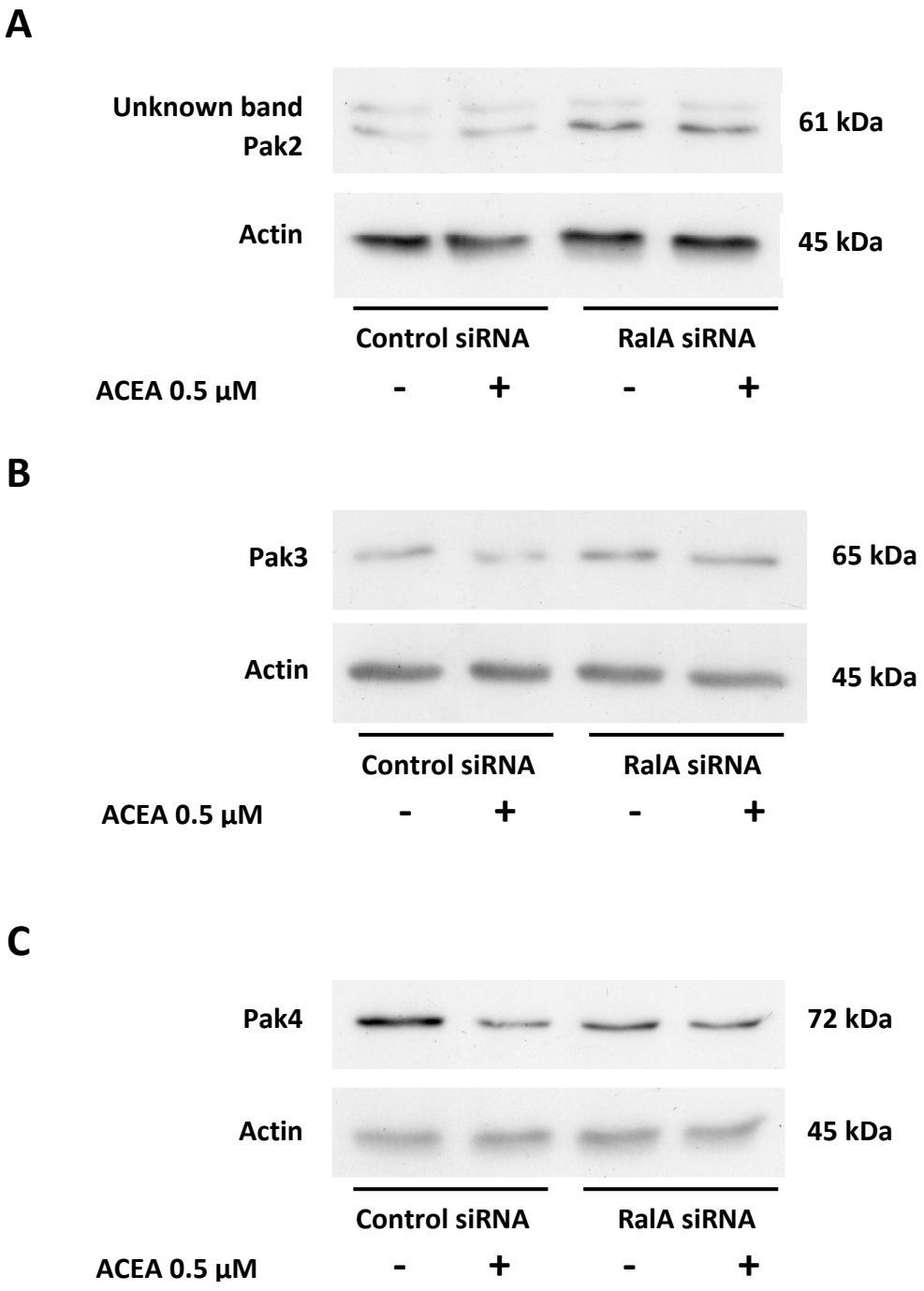

Figure 6.7: Expression of Pak family members after RalA knockdown and treatment with CB1 agonist ACEA. Dissociated rat RMS neuroblasts were nucleofected with a control or RalA siRNA oligo, plated onto polyornithine/laminin-coated wells and cultured for 48 hours. Neuroblasts were treated with vehicle or ACEA 0.5 µM for 30 minutes prior to being lysed and analysed by Western blotting for expression of the p21 activated family of kinases: Pak 2 **(A)**, Pak 3 **(B)**, and Pak 4 **(C)**.

A pan antibody that recognises Pak 1, 2, and 3 detected a single band at 90 kDa and a doublet of bands at around 70 kDa (Figure 6.8). None of these bands showed upregulation following RalA depletion or ACEA treatment. Finally an alternative Pak1 antibody that recognises an epitope on the N-terminus was tested (Cell signalling). This antibody produced a doublet of closer bands (Figure 6.9), running at approximately 68 kDa. Given the close proximity of the two bands, the upper band detected by this Pak1 antibody could very well be phospho-Pak1. However, a change in band intensity was not observed following RalA depletion. On visual inspection alone, there does not seem to be a reduction in the band intensity of phosphorylated Pak1 following treatment with CDK5 inhibitor Roscovitine (1 μM) (Figure 6.9), suggesting that other kinases may have a role in regulating the phosphorylation state of Pak1 in RMS neuroblasts. The stark differences seen between the two Pak1 antibodies together with the screening analysis we performed on other Paks, indicate that the upper band we originally detected using the first Pak1 antibody is unlikely to be a Pak family member.

6.2.4 Signalling downstream of RalA: CDK5

CDK5 is best recognised for its regulation of the CNS cytoarchitecture. Loss of CDK5 function results in disruption of neuronal migration, leading to abnormal layering of several brain structures, including the cerebral cortex, cerebellum, hippocampus and olfactory bulb (Ohshima et al. 1996; Chae et al. 1997; Gilmore et al. 1998; Kwon and Tsai 1998). Due to its ability to phosphorylate a number of microtubule associated proteins, it is currently believed that disrupting CDK5 activity adversely affects neuronal migration as a result of impaired nucleokinesis (Marin et al. 2010). Since time-lapse analysis of RalA depleted neuroblasts in Matrigel showed evidence of a nucleokinesis defect (Chapter 5), and CDK5 has been implicated in RMS neuroblast migration (Hirota et al. 2007), we speculated whether CB signalling, RalA, and CDK5 may co-operate to regulate RMS neuroblast migration. To test this hypothesis, we treated rat RMS explants embedded in Matrigel with the CDK5 inhibitor Roscovitine (1 μM) and measured the distance migrated after 9 hours.

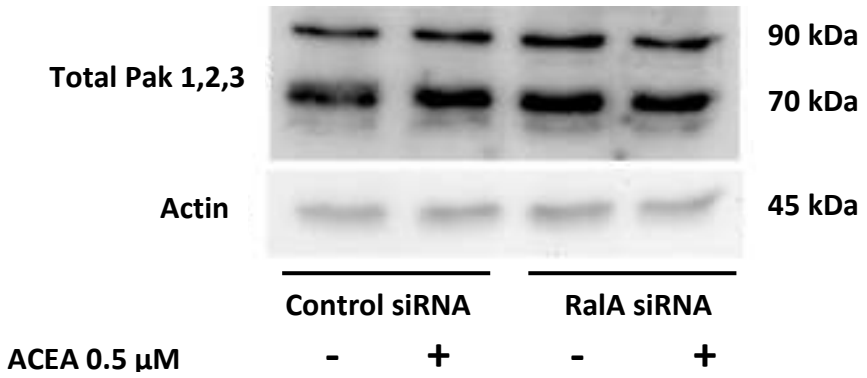

Figure 6.8: Pak 1, 2, 3 expression after RalA knockdown and treatment with CB1 agonist ACEA. Dissociated rat RMS neuroblasts were nucleofected with a control or RalA siRNA oligo, plated onto polyornithine/laminin-coated wells and cultured for 48 hours. Neuroblasts were treated with vehicle or ACEA 0.5 µM for 30 minutes prior to being lysed and analysed by Western blotting for expression of total Pak 1,2,3.

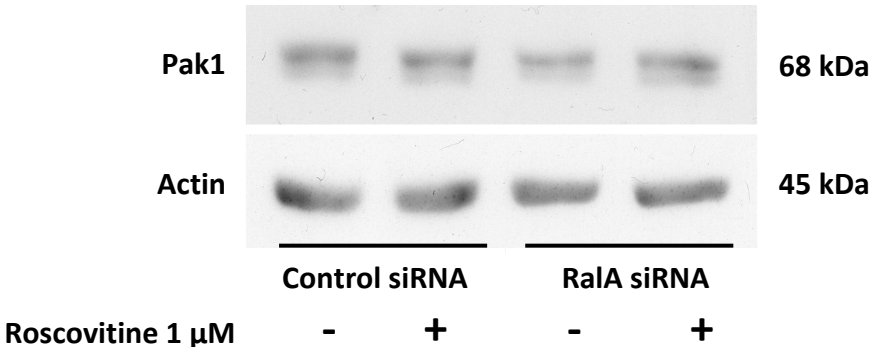

Figure 6.9: Pak1 expression after RalA knockdown and treatment with CDK5 inhibitor Roscovitine. Dissociated rat RMS neuroblasts were nucleofected with a control or RalA siRNA oligo, plated onto polyornithine/laminin-coated wells and cultured for 48 hours. Neuroblasts were treated with vehicle or Roscovitine 1 µM for 1 hour prior to being lysed and analysed by Western blotting for expression of Pak1 using a cell signalling antibody that recognises the amino terminus of Pak1.

A shorter migration period of 9 hours was chosen, as opposed to the usual 24 hour period, since inhibition of migration is more notable at this time point (general observation from time lapse imaging). Unexpectedly, Roscovitine did not inhibit neuroblast migration out of explants. Intriguingly, the combined effect of ACEA and Roscovitine on the distance migrated by neuroblasts was significantly greater than the control (Figure 6.10A-B). We were not able to examine CDK5 activity by Western analysis of the phosphorylated protein in relation to RalA expression, due to technical difficulties using the phospho-antibody (Data not shown).

Although we were not able to come to a definitive conclusion as to the role of CDK5 in RMS neuroblast migration using the CDK5 inhibitor Roscovitine, we attempted to examine other targets associated with nucleokinesis, some of which are also substrates of CDK5. One such example is p27kip1, which relies on phosphorylation by CDK5 to regulate cortical neuron migration in development (Kawauchi et al. 2006; Nguyen et al. 2006). However, our results showed no significant change in the phosphorylation of p27kip1 following treatment with ACEA, RalA depletion, or both (Figure 6.11).

6.2.5 Signalling downstream of RalA: N-Cadherin

Another potential downstream target of Ral GTPases we examined was N-Cadherin. In development, the migration of multipolar cortical neurones in response to reelin depends on the delivery of N-Cadherin to the plasma membrane by Rap1, a process that was also suggested to involve the activation of Ral (Jossin and Cooper 2011). Since Ral GTPases have long been known to regulate polarised delivery of membrane proteins (Shipitsin and Feig 2004), and adhesion molecules have been shown to be crucial for chain migration of RMS neuroblasts (Emsley and Hagg 2003; Belvindrah et al. 2007; Mobley and McCarty 2011), we examined whether RalA may regulate neuroblast migration by regulating N-Cadherin trafficking. Immunohistochemical analysis of P8 mouse brains showed that N-Cadherin (cytoplasmic) is enriched along the entire RMS (Figure 6.12A-B).

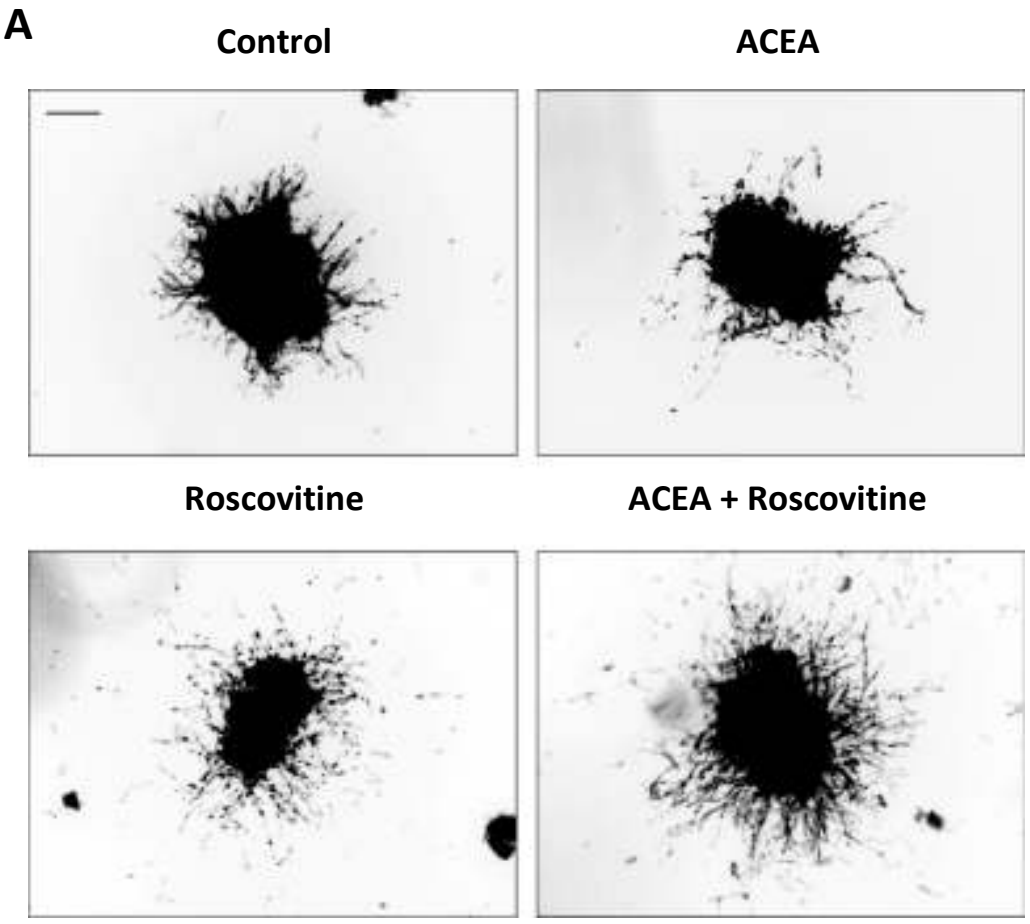
A
Control
ACEA
Roscovitine
ACEA + Roscovitine
B
Relative distance migrated
1.8
1.6
1.4
1.2
1.0
0.8
0.6
0.4
0.2
0.0
*
ACEA 0.5 μM - + - +
Roscovitine 1 μM - - + +

Figure 6.10: Inhibition of CDK5 enhances migration out of explants and enhances the pro-migratory effects of CB1 agonist ACEA. Rat RMS explants were embedded in Matrigel and allowed to migrate for 9 hours in the presence of vehicle control, ACEA 0.5 µM, Roscovitine 1 µM, or both drugs. **(A)** Representative images of explants after 9 hours of migration. **(B)** Quantification of the distance migrated out of explants. ACEA and Roscovitine promote migration of neuroblasts out of explants, and appear to have a synergistic effect when applied together. Each bar represents the mean ± SEM; *P < 0.05; n = 4 independent experiments.

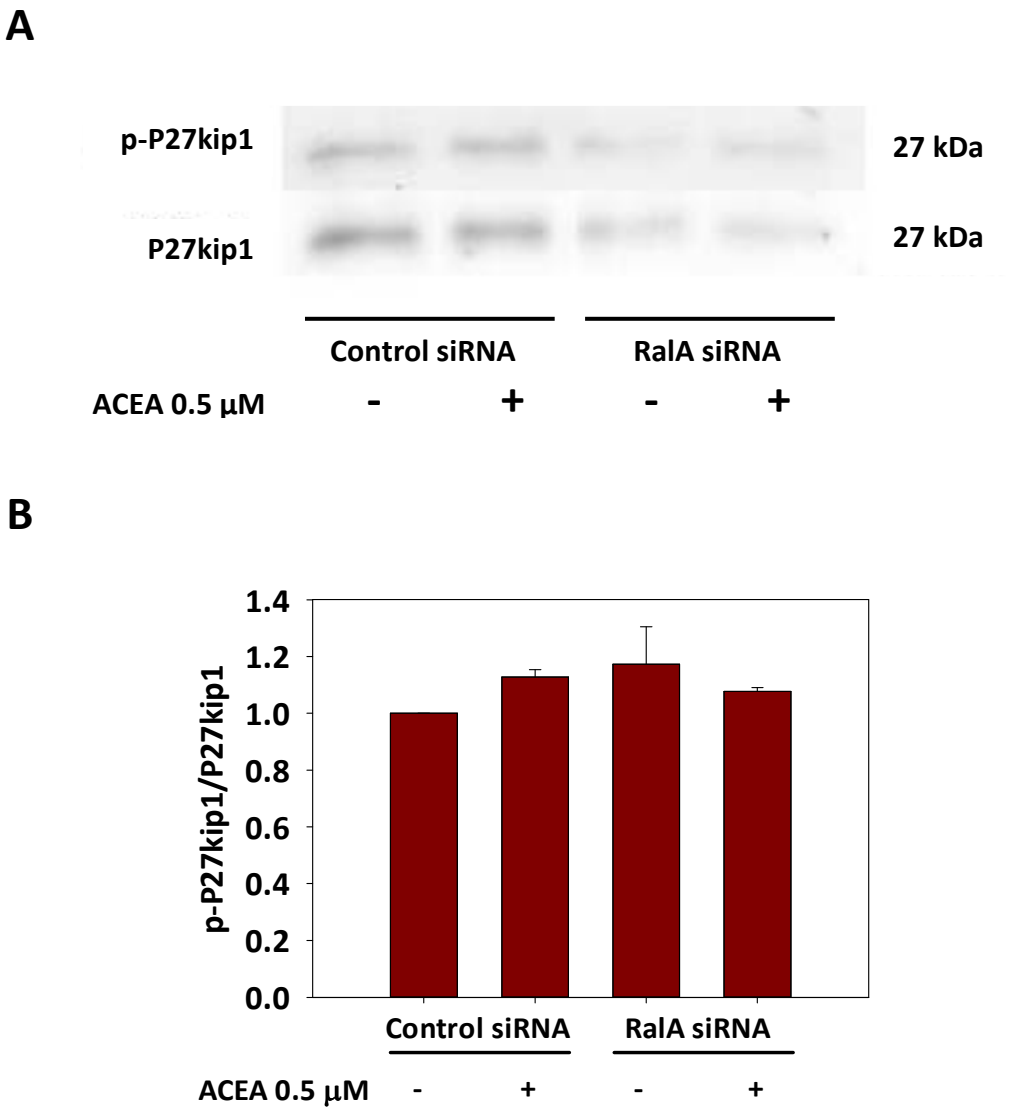

Figure 6.11: P-27kip1 and p-P27kip1 expression after RalA knockdown and treatment with CB1 agonist ACEA. Dissociated rat RMS neuroblasts were nucleofected with a control or RalA siRNA oligo, plated onto polyornithine/laminin coated wells and cultured for 48 hours**. (A)** Neuroblasts were treated with vehicle or ACEA 0.5 µM for 30 minutes prior to being lysed and analysed by Western blotting for expression of the p-P27kip1 and P27kip1. **(B)** Quantification of p-P27kip (normalised to P27kip1) relative to control. Each bar represents the mean ± SEM; n = 2 independent experiments.

A

N-Cadherin cytoplasmic

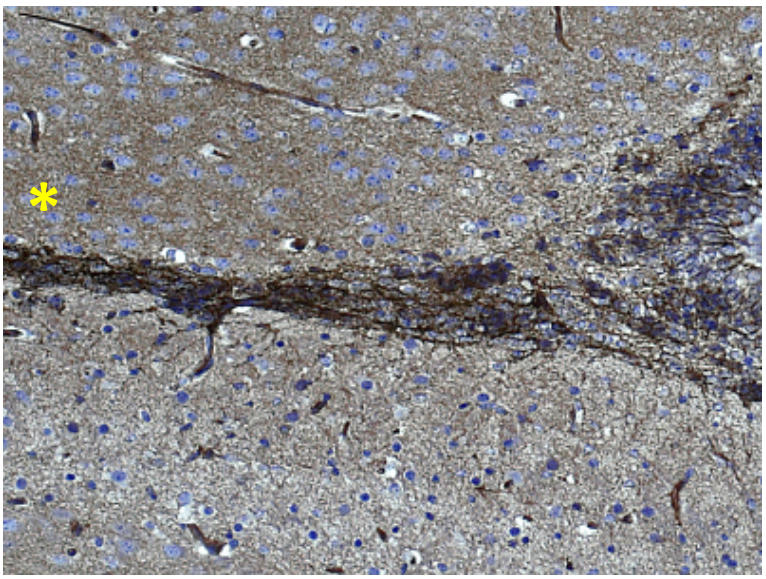

B

N-Cadherin a.a 811-824

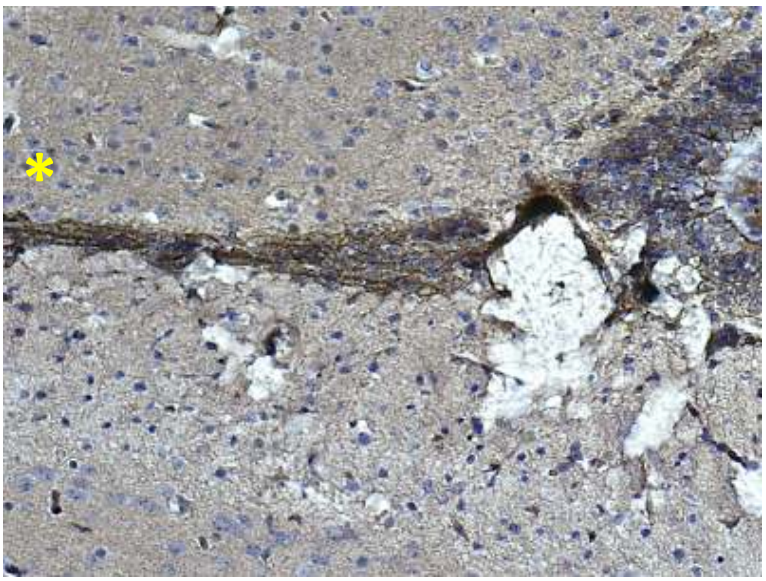

Figure 6.12: N-Cadherin is strongly expressed in the mouse RMS. Sagittal sections of P8 mouse brain containing the RMS were examined for N-Cadherin expression using immunohistochemical analysis. Images correspond to the beginning section of the RMS just adjacent to the SVZ. The RMS shows robust expression of N-Cadherin as detected with an antibody recognising the cytoplasmic domain **(A)**, and an antibody recognising amino acid sequence 811-824 **(B)**. Yellow asterisks indicate direction of the OB and hence direction of migration.

We were not able to examine the expression of N-Cadherin in migrating neuroblasts *in vitro* due to technical difficulties associated with the use of some antibodies with Matrigel embedded cultures (data not shown). Thus, to analyse potential changes in N-Cadherin distribution and/or expression following RalA depletion, we stained control and RalA depleted rat neuroblasts plated on polyornithine/laminin-coated coverslips for cytoplasmic and external N-Cadherin (Figure 6.13A and 6.14 respectively). Cytoplasmic N-Cadherin showed punctuate staining along the cell body and protrusion. Although initial visual inspection from preliminary experiments seemed to indicate a change in the intensity of cytoplasmic N-Cadherin following RalA knockdown, quantification of N-Cadherin mean intensity relative to F-Actin showed no change in expression levels of the adhesion molecule (Figure 6.13B). Also, no change in the distribution of N-Cadherin was apparent after RalA depletion (Data not shown). An external N-Cadherin antibody showed punctuate staining that was localised to the cell body. Upon visual inspection, we observed no apparent change in external N-Cadherin distribution following RalA depletion (Figure 6.14).

6.2.6 Signalling downstream of RalA: The exocyst complex

The exocyst complex, one of the major Ral effectors, is responsible for mediating the functions of RalA in migration, secretion, polarity, and cytoskeletal dynamics (Moskalenko et al. 2002; Sugihara et al. 2002; Lalli and Hall 2005; Oxford et al. 2005; Spiczka and Yeaman 2008; Lalli 2009). Our lab has previously shown that RalA activation promotes an association between the exocyst and the PAR complex. This interaction is required for the proper targeting of the PAR complex to the tips of nascent axons, and is an essential event in neuronal polarisation (Lalli 2009). Solecki et al. (2004) also showed that the positioning of the centrosome during cerebellar granule cell migration is dependent on the PAR complex. Current work by other members of the Lalli Lab (Dr Katarzyna Falenta) indicates that an exocyst-PAR association may also be involved in regulating the polarised migration of RMS neuroblasts. This association appears to be mediated by a specific region of the Exo84 exocyst subunit, which is able to directly bind the PAR complex component Par6.

A

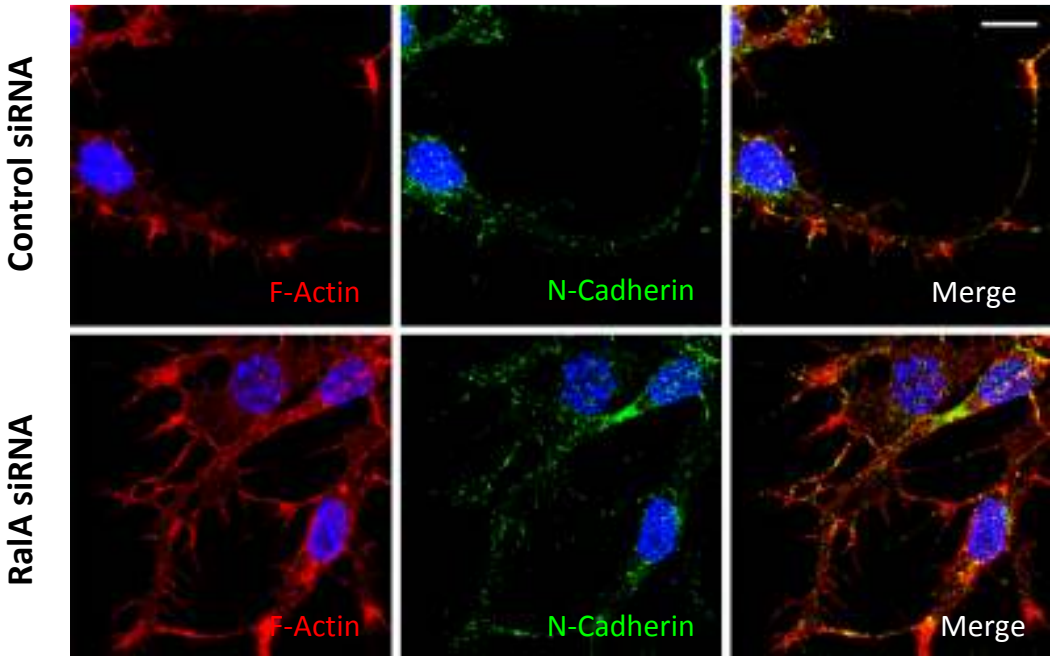
Control siRNA
RalA siRNA
F-Actin
N-Cadherin
Merge
F-Actin
N-Cadherin
Merge

B

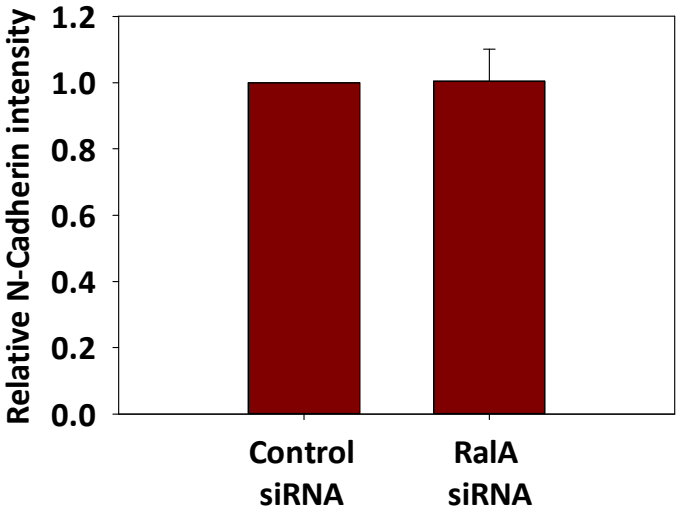
Relative N-Cadherin intensity
1.2
1.0
0.8
0.6
0.4
0.2
0.0
Control siRNA
RalA siRNA

Figure 6.13: N-Cadherin expression in rat RMS neuroblast after RalA depletion. Dissociated rat RMS neuroblasts were nucleofected with a control or RalA siRNA oligo, plated onto polyornithine/laminin-coated wells and cultured for 48 hours. Cells were then fixed, permeabilised, and stained with an N-Cadherin antibody recognising the cytoplasmic region of the protein. Bar = 10 µm. **(A)** Representative images of control and RalA depleted neuroblasts stained for N-Cadherin. **(B)** Quantification of N-Cadherin intensity (normalised to actin) relative to the control. No significant difference was observed in the intensity of N-Cadherin staining between control and RalA-depleted cells. Each bar represents the mean ± SEM; n = 3 independent experiments. Approximately 12-20 images were analysed per condition per experiment.

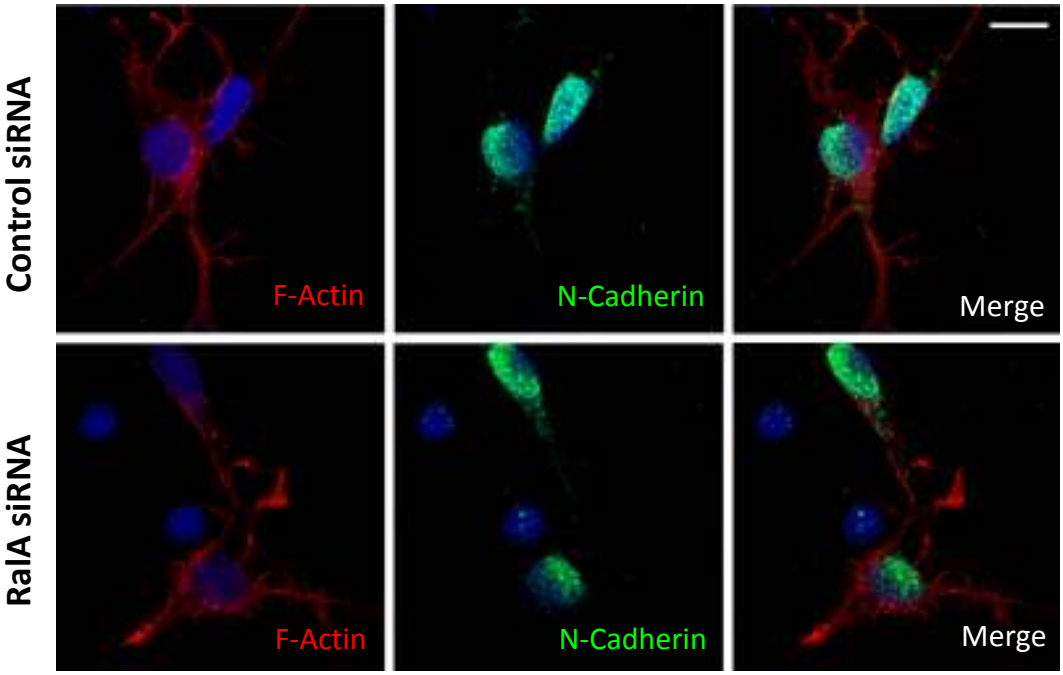

Figure 6.14: External N-Cadherin expression in rat RMS neuroblast after RalA depletion. Dissociated rat RMS neuroblasts were nucleofected with a control or RalA siRNA oligo, plated onto polyornithine/laminin-coated wells and cultured for 48 hours. Cells were then fixed and stained for external N-Cadherin (Sigma). External N-Cadherin expression appears punctate and is mainly localised to the cell body. Bar = 10 µm.

Importantly, active RalA promotes this interaction *in vitro* (Amlan Das and Wei Guo, unpublished). Our preliminary results imply that this interaction may also be functional in neuroblast migration *in vivo*. A pCAG-IRES-EGFP construct expressing the Par6-binding fragment of Exo84 (Exo84 Int Frag) was electroporated into the lateral ventricles of P2 mouse pups. Brains were collected 5 days post electroporation, fixed, sliced, and stained for GFP. Perturbing the Exo84-Par6 association caused a significant increase in the % of misoriented neuroblasts (5.5% ± 0.4 for GFP control and 12.7% ± 3.0 for Exo84 Int Frag) (Figure 6.15B). These results imply that an exocyst-Par6 association may be involved in the polarised migration of RMS neuroblasts.

A

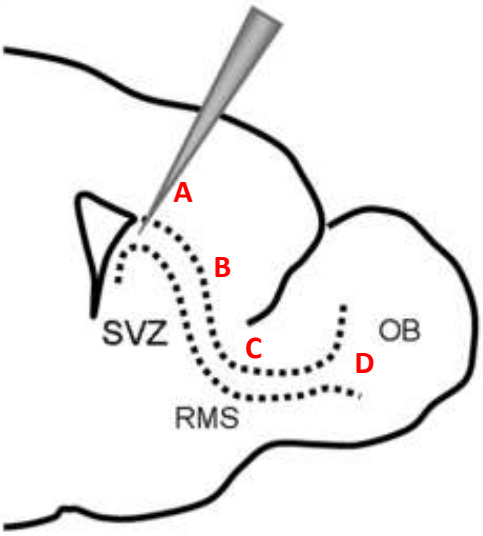
A
B
SVZ
C
OB
D
RMS

B

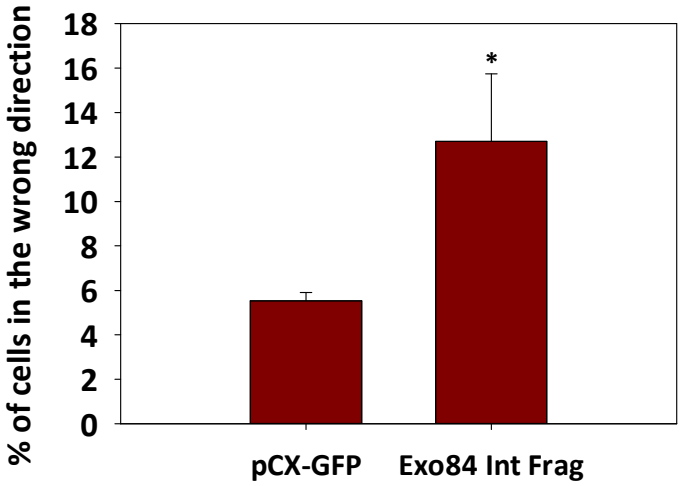
% of cells in the wrong direction
18
16
14
12
10
8
6
4
2
0
*
pCX-GFP
Exo84 Int Frag

Figure 6.15: Perturbing Exo84 function affects orientation and migration of RMS neuroblasts. A pCX-EGFP or pCAG-Exo84 Int Frag-IRES-EGFP was electroporated into the right lateral ventricle of P2 mouse pups. Mice were sacrificed 5 days later and the right hemisphere was fixed, sliced and stained for GFP. **(A)** A schematic diagram showing the site of injection in the lateral ventricle. The RMS (dotted lines) was divided into anatomically distinct regions for the purpose of quantification. Region **A** is the injection site, region **B** is the descending arm of the RMS, region **C** is the RMS "elbow" preceding the OB, and region **D** is within the OB. Perturbing the Exo84-Par6 interaction significantly increases the % of misoriented cells **(B)**. Each bar represents the mean ± SEM; *P < 0.05; n = 4 independent experiments. (Data kindly provided by Dr Katarzyna Falenta).

6.3 Discussion

During the course of this study we have uncovered a role for RalA in RMS neuroblast migration. In this final chapter, we attempted to identify upstream activators as well as downstream targets of RalA.

Rap GTPases have been shown to act upstream of Ral in neuronal migration during development and CB-promoted neurite outgrowth (He et al. 2005; Jossin and Cooper 2011). Here we show that Rap1 is weakly expressed by RMS neuroblasts. However, due to the low sensitivity of the pulldown assay used to measure Rap activation, and the limited amount of starting material that is available to us, we were not able to examine Rap activity in relation to CB receptor activation.

Since our time-lapse analysis of RalA depleted cells in Matrigel showed an impairment of nucleokinesis, we looked for defects in the two stages of this process: movement of the centrosome in the direction of migration, and translocation of the nucleus from pulling forces generated by the dynein motor complex and actomyosin contraction at the rear of the cell (Tsai and Gleeson 2005). Analysis of centrosome position revealed no difference in orientation between RalA depleted and control cells. However, since our analysis was conducted in fixed neuroblast cultures, and only looks at a snapshot in time, very few neuroblasts in our analysis were undergoing nuclear translocation. Hence time-lapse imaging of neuroblasts expressing a fluorescently-tagged centrosomal marker, a common method used to track centrosomal movement (Solecki et al. 2004), may be necessary to fully analyse whether RalA regulates centrosome polarisation and movement. Although we attempted to examine the activation state of molecules associated with the dynein motor complex (Nudel), and those localised to the perinuclear microtubule cage (DCX), as well as those involved in actomyosin contraction (MLC-2) (Tsai and Gleeson 2005), we were not able to arrive at a conclusion as to whether there is impairment of these molecular regulators of nuclear translocation following RalA knockdown due to technical difficulties associated with the phospho-antibodies for these targets.

Next, we examined a range of molecules (CDK5, Pak, p27kip1, N-Cadherin) shown to regulate RMS neuroblast migration or the migration of other neuronal cell types (Gilmore et al. 1998; Ohshima et al. 1999; Xie et al. 2003; Nikolic 2004; Kawauchi et al. 2006; Nguyen et al. 2006; Hirota et al. 2007; Causeret et al. 2009; Jossin and Cooper 2011; Valiente et al. 2011). Even though we showed that Pak 1-4 were expressed by RMS neuroblasts, we could not obtain convincing evidence supporting their activation downstream of CB/RalA signalling.

Despite the recent report that CDK5 is required for RMS neuroblasts migration (Hirota et al. 2007), inhibiting CDK5 activity with Roscovitine did not perturb neuroblast migration out of explants in our studies. One possible explanation for this difference may be that inhibition of CDK5 activity in our experiment was achieved with Roscovitine, which may have off-target effects, as opposed to the more robust genetic approach used by Hirota et al. (2007). Although Roscovitine was shown to inhibit RMS neuroblast migration in Matrigel by Paratcha et al. (2006), this study used a particularly high concentration of 20 µM compared with 1 µM used by us. Since the IC_{50} of Roscovitine is only 200 nM, the concentration we used should have been sufficient to inhibit CDK5 activity without the occurrence of drastic off-target effects. Unexpectedly, treatment with ACEA combined with inhibition of CDK5 activity with Roscovitine enhanced migration of neuroblasts. Based on our results, the role of CDK5 is not particularly clear. Measurement of kinase activity or the use of a siRNA-mediated strategy may be a more effective method for examining a potential relationship between CDK5 and CB/RalA signalling.

Ral GTPases can regulate the delivery of N-Cadherin to the plasma membrane during neuronal migration in the developing cortex (Jossin and Cooper 2011). Though we were able to show robust expression of N-Cadherin in the RMS of neonatal mice, we did not observe any change in the distribution of N-Cadherin following knockdown of RalA. However, due to technical difficulties arising from the use of N-Cadherin antibodies with Matrigel-embedded cultures, N-Cadherin expression was examined in neuroblasts cultured on polyornithine/laminin coated-

coverslips, a plating condition that allows immunostaining but on the other hand does not favour migration. Thus, the signalling and trafficking mechanisms associated with migrating neuroblasts may not be present in this system, and may therefore not truthfully reflect the state of neuroblasts migrating in Matrigel or within the RMS. Consistent with this idea, a recent report demonstrates that the role of adhesion molecules in cell migration is different in a 2D and 3D environment (Fraley et al. 2010). Alternatively, to determine whether a relationship between RalA and N-Cadherin exists in RMS neuroblasts, one could examine the localisation of N-Cadherin in Cre-GFP electroporated $RalA^{lox/lox}$ and $RalA^{lox/lox}/RalB^{-/-}$ brain slices.

Finally, we investigated whether perturbing the function of a well-known Ral effector, the exocyst complex, would re-capitulate the phenotype observed following genetic deletion of RalA. Given the newly discovered ability of Exo84 to interact with Par6 in a Ral-dependent fashion (Wei Guo and Amlan Das, unpublished observations), and the fact that disrupting such an interaction impairs neuronal polarisation (Lalli, unpublished), we asked whether disrupting this association could also impair polarised neuroblast migration *in vivo*. Interestingly, the expression of the Par6-binding region of the Exo84 exocyst subunit closely mimics the polarisation defect observed after genetic deletion of RalA (compare Figure 6.15B with Figure 5.20 middle panel). Almost 12.7% ± 3.0 of neuroblasts were misoriented following disruption of the Exo84-Par6 association, whilst 5.5% ± 0.4 of neuroblasts were misoriented in control samples. These results suggest that an association between Exo84 of the exocyst complex and Par6 of the polarity complex may have a role in regulating the polarised migration of neuroblasts. Future work is aimed at investigating whether RalA may regulate neuroblast polarisation by favouring an Exo84-Par6 association. This could be validated *in vivo* by electroporation of RalA mutants uncoupled from specific exocyst subunits, such as Sec5 and Exo84 (Fukai et al. 2003).

In summary, we have attempted to elucidate the Ral signalling cascade in RMS neuroblast migration. Our preliminary data suggests that a well known effector of Ral GTPases, the exocyst complex, may also have a role in this system. Further work will be required to validate a potential role for Ral-exocyst in adult neurogenesis.

Chapter 7: General discussion

The acceptance of ongoing neurogenesis has revolutionised our understanding of the mammalian brain from an immutable structure to one which is permissive to change and adaptation. The two recognised neurogenic regions of the adult brain, the SVZ of the lateral ventricles and the DG of the hippocampus, contain a unique niche that facilitates the continued existence and proliferation of NS cells. In the SVZ, slowly proliferating adult NS cells give rise to chains of migratory neuroblasts that undergo long-distance tangential migration to the OB via the highly restricted route of the RMS. Remarkably, these cells are able to migrate to sites of injury in the rodent and human brains, where they appear to contribute to CNS repair (Arvidsson et al. 2002; Zhang et al. 2004; Ohab et al. 2006; Ekonomou et al. 2011; Ekonomou et al. 2012). These findings have brought to light exciting new possibilities of employing stem cells existing within the CNS as a tool for regenerative therapies. However, the concept of neuronal replacement from adult NS cells is still viewed by many as a formidable task, mostly due to the limited neurogenic capacity of the adult human brain (Sanai et al. 2011). Yet our understanding of the CNS is still in its infancy, and to dismiss the regenerative potential of adult NS cells may be as detrimental to the progress of neuroscience as refuting the works of Altman and Kaplan was to neurogenesis some decades ago (Kaplan 2001). Thus, to further the possibility of employing NS cells residing in the adult brain for therapeutic purposes, it is imperative to study the mechanisms that govern the different stages of neurogenesis: proliferation, migration and differentiation.

The primary goal of this thesis was to investigate the guidance of RMS neuroblast migration and the molecular mechanisms regulating this process in the postnatal brain. In doing so, we have uncovered a novel role for the eCB system in RMS neuroblast migration. In addition, we show that CB signalling may promote migration through the activation of the small GTPase RalA. Moreover, other guidance molecules previously shown to regulate RMS neuroblast migration, such as HGF and GDNF, also activate RalA. We demonstrate for the first time that RalA is

required for correct neuroblast orientation and morphology. Based on the analysis of genetic mouse models, we demonstrate that deleting both RalA and RalB leads to a dramatic reduction of neuroblasts in the RMS as well as impairment of polarised morphology.

7.1 Modelling RMS neuroblast migration

The study of RMS neuroblast migration is a relatively new field, which has emerged over the last few decades since the discovery of long distance migration in the adult CNS (Lois and Alvarez-Buylla 1994; Lois et al. 1996). In our attempt to investigate the molecular mechanisms that regulate this process, we established a range of migration assays based on widely used published protocols. Our initial studies were performed on the Cor-1 cell line, a highly proliferative and motile NS stem cell model which expresses markers of neurogenic radial glia (Conti et al. 2005; Pollard et al. 2006) as wells as markers of migratory neuroblasts. Although this model has proven useful as a tool for high throughput screening and was used to identify the eCB system as a regulator of neuroblast migration, there are several notable differences between Cor-1 cell and RMS neuroblast migration which may lead to discrepancies between these two systems. For example, Cor-1 cells migrate on 2D surfaces, and show evidence of inter-kinetic nuclear movement and contact mediated inhibition of locomotion. In contrast, primary RMS neuroblasts are only motile in a 3D matrix such as Matrigel, and migrate in chains, forming close associations with neighbouring cells. Nevertheless, the Cor-1 cell line provides a useful screening tool that may be used as a first step in identifying regulators of neural precursor migration.

The *in vitro* Matrigel migration assay is currently the most widely used tool for studying the significance of potential guidance cues regulating the migration of RMS neuroblasts. This technique provides a 3D environment which recapitulates the chain migration of neuroblasts *in vivo*, and is a simple effective method that can be used to examine the effects of motogens, attractants, repellents and inhibitors of neuroblast migration (Ward et al. 2003; Ward and Rao 2005). We adapted this

technique to assess the migratory capacity of neuroblasts following transfection/nucleofection with siRNA or mutant proteins. This method has been pivotal in furthering our understanding of neuroblast migration, but also comes with certain limitations and subtle differences from the *in vivo* situation, which we discovered during the course of our investigation. For example, disruption of RalA function leads to migration defects *in vitro* and *in vivo* but with different changes to morphology (increase in leading process length *in vitro* Vs reduction in leading process length *in vivo*). Also, in contrast to the situation *in vivo*, neuroblasts in Matrigel do not proliferate. Hence, although the Matrigel migration assay has proven to be a useful model system, and has led to the identification of several key molecules, including Slit, BDNF and eCBs, which have all been shown to influence neuronal migration *in vivo*, it is necessary to validate *in vitro* findings in an *in vivo/ex vivo* model where possible.

More recently, the development of electroporation procedures to efficiently transfect SVZ neuroblasts has greatly facilitated the study of neuroblast migration in the native architecture of the RMS (Boutin et al. 2008). Analysis of fixed brain slices following electroporation is a useful method for studying the role of target proteins on neuroblast migration, and is the method that most closely reflects the *in vivo* situation. However, the limitations of this procedure lies in the fact that it only provides a snapshot of a given time-point and does not fully reflect the dynamic nature of neuroblast migration. Due to the RMS being located deep within the CNS, conventional fluorescence time-lapse microscopy is not compatible for imaging this region in the intact brain. Whilst magnetic resonance imaging (MRI) of iron-oxide labelled neuroblasts, and positron emission tomography (PET) have been used to monitor neuroblast migration *in vivo*, these techniques are limited by low resolution and slower acquisition times (Vreys et al. 2009; Nieman et al. 2010; Granot et al. 2011; Vande Velde et al. 2012). Hence, time-lapse imaging of fluorescently labelled migratory neuroblasts is currently only possible in cultured brains slices (approximately 300 μm thick). This assay has the advantage of containing all cellular and matrix components of the stream, and has a resolution and speed of acquisition that is good enough to visualise even the highly dynamic

changes of the growth cone on the tips of the leading processes. However, during our studies we observed one main difference between neuroblasts in fixed brains slices and those in live slice cultures. In fixed brain slices, nearly all neuroblasts are oriented towards the OB. However, in the brain slice assay, many cells often turn and migrate in the opposite direction. Whilst several papers have described this as "normal behaviour" of neuroblasts and have used this as evidence to suggest that the same occurs *in vivo* (Kakita and Goldman 1999; Nam et al. 2007), our data from fixed brain slices suggests that this is most likely an artefact of the slice preparation and may arise from the loss or dilution of diffusible guidance cues in this assay. Another method in which a fibre optic probe was used to image labelled neuroblasts in the intact brain has been suggested as a less invasive alternative, and also described migration of neuroblasts in the opposite direction (Davenne et al. 2005). Despite the fact that this is probably the least disruptive technique, we cannot rule out tissue damage from the insertion of the probe, which may influence neuroblast migration.

In summary, a variety of *in vitro* and *in vivo* migration assays are currently available for the study of neuroblast migration. Whilst *in vitro* studies are useful for the identification of compounds that have potential to regulate this process, it is necessary to validate these results in a more physiological context to identify the true regulators of migration in the RMS. While *in vivo* electroporation has become a very valuable tool to achieve this objective, the development of new imaging technologies will undoubtedly be instrumental in understanding the dynamics of neurogenesis in the intact brain.

7.2 The role of endocannabinoid signalling in postnatal neurogenesis

The eCB system has long been recognised for its ability to inhibit neurotransmitter release via retrograde signalling in the adult brain (Pertwee 2006). The numerous psychoactive properties of cannabis (altered perception, euphoria, hallucination, enhanced appetite, reduced spontaneous motor activity, immobility, analgesia and impairment of short-term memory) have now been attributed to regulation of

GABA and glutamate release by the CB1 receptor (Wilson and Nicoll 2001; Alger 2002; Piomelli 2003) (Figure 7.1B). In the developing brain, the CB1 receptor partakes in axon guidance by coupling signalling via the FGF receptor to axonal growth (Williams et al. 2003) (Figure 7.1A). Recently, the Doherty lab has also demonstrated a role for the eCB system in regulating the proliferation of adult SVZ neural stem cells (Gao et al. 2010) (Figure 7.1C). Importantly, genetic deletion of DAG-L resulted in a significant reduction in SVZ neurogenesis, thus highlighting 2-AG as the primary eCB regulating the proliferation of adult NS cells (Gao et al. 2010). In addition, the decline in neurogenesis associated with ageing could be rescued by pharmacological activation of the CB2 receptor (Goncalves et al. 2008). These findings have significant implications since much of the scepticism surrounding the therapeutic potential of adult NS cells arises from the limited neurogenic capacity of the adult human brain (Spalding et al. 2005; Sanai et al. 2011; Bergmann et al. 2012). Hence, the discovery that neurogenesis can be reactivated in the aged brain via restoration of an eCB tone raises the possibility of reactivating neurogenesis in the otherwise dormant adult human SVZ.

In this study, we sought to assess a role for CB signalling in regulating another aspect of SVZ neurogenesis: the migration of neural progenitors along the RMS. Our results demonstrate that an endogenous cannabinoid tone regulates this process through both the CB1 and CB2 receptors. Pharmacological inhibition of eCB signalling leads to a loss of polarised neuroblast morphology and impairs efficient nucleokinesis (Oudin et al. 2011). Interestingly, we found several similarities between eCB signalling in RMS neuroblast migration and axon guidance during development. Firstly, both DAG-L, the enzyme responsible for the synthesis of 2-AG, and the CB receptors are both expressed by migratory neuroblasts (Figure 7.1D), suggesting the existence of an autocrine/paracrine signalling loop as seen with axon guidance (Bisogno et al. 2003). Secondly, preliminary data suggests that signalling via the FGF receptor may be responsible for driving eCB tone in the RMS (PhD thesis of Madeleine Oudin). In the context of contact-mediated axon guidance, cell adhesion molecules - N-Cadherin, L1 and NCAM – stimulate the production of 2-AG via activation of the FGF receptor (Williams et al. 2003). In the SVZ, adhesion

molecules such as integrins have a crucial role in regulating the proliferation of adult NS cells (Kazanis et al. 2010), whilst both integrins and PSA-NCAM are required for the efficient migration of neuroblasts in the RMS (Rutishauser et al. 1985; Hu et al. 1996; Belvindrah et al. 2007; Mobley and McCarty 2011). We have also shown that N-Cadherin is expressed by neuroblasts throughout the RMS. Given that the expression of β1 integrins is up-regulated by adult NS cells when they are stimulated to proliferate (Kazanis et al. 2010), and the fact that neurogenesis can be induced by eCB signalling in the aged brain (Goncalves et al. 2008), whether adhesion molecule signalling drives eCB tone to regulate proliferation and migration in adult neurogenesis is an interesting point to address.

Adult neurogenesis in the SVZ consists of three distinct stages: proliferation of adult NS cells in the SVZ, migration of neuroblasts along the RMS, and differentiation in the OB. Research conducted in our lab has uncovered a role for the eCB system in regulating both proliferation and migration in the postnatal brain. In the developing CNS, eCB signalling also orchestrates the formation of synapses (Berghuis et al. 2007). Whether a similar mechanism exists in the integration of adult-born neurones in the OB is not known. Thus, whether eCB signalling can participate in all three stages of adult neurogenesis would be an important aspect to investigate.

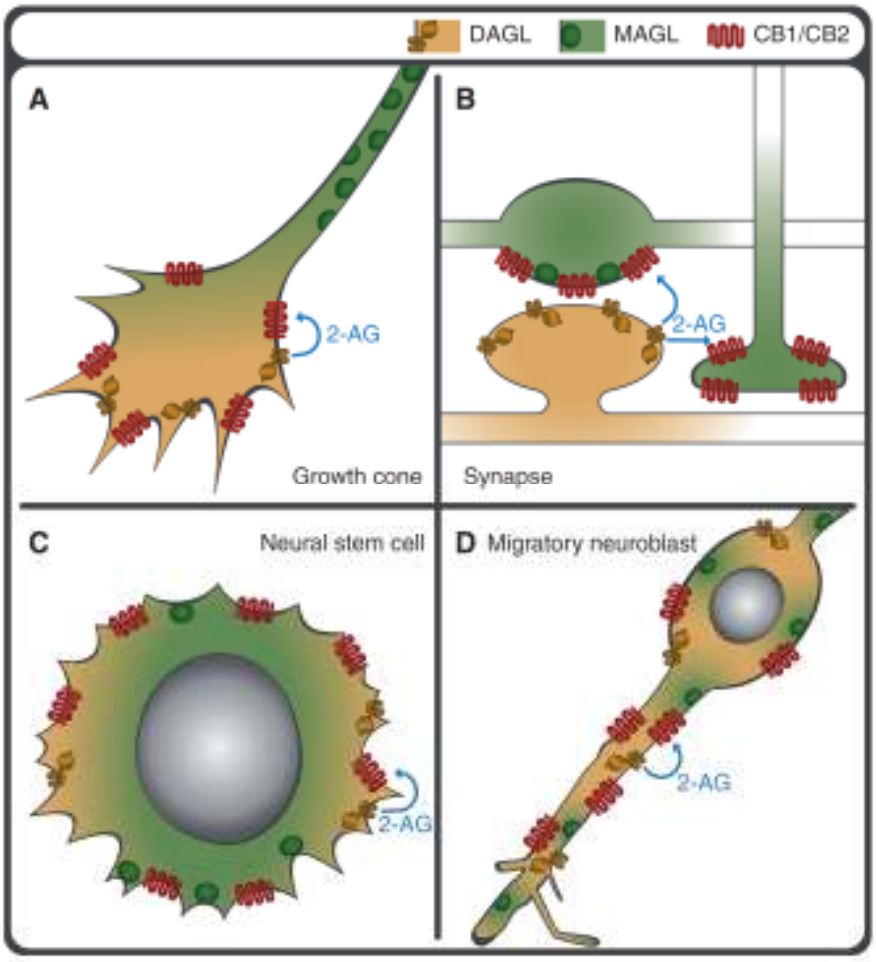

Figure 7.1: The multiple roles of the eCB system in the CNS. A schematic representation of the roles of the eCB 2-AG in the CNS. The distribution of the synthetic enzyme (DAG-L), CB receptors (CB1/CB2), and degradative enzyme (MAG-L) in axonal growth **(A)**, retrograde signalling **(B)**, NS cell proliferation **(C)** and neuroblast migration **(D)** are shown for each signalling system. Adapted from Oudin et al. (2011).

7.3 A cannabinoid-RalA signalling pathway regulates RMS neuroblast migration

The migration of neuroblasts in the RMS is not reliant on a single factor, but appears to be finely orchestrated by a number of growth factors, chemorepellents, chemoattractants, migration inhibitors, motogens, and adhesion molecules acting at different points along this route (Cayre et al. 2009). Despite the wealth of information regarding the extracellular signals that influence this process, exactly how multiple signals arising from the RMS are synchronised and translated to the molecular machinery of the cell remains largely unknown.

We propose that RalA may represent a potential point of convergence for migratory cues in RMS neuroblast migration, since in primary postnatal neuroblasts this GTPase is activated not only by CB agonists, but also by other known guidance factors such as HGF and GDNF (Paratcha et al. 2006; Garzotto et al. 2008). Moreover, RalA appears to be necessary for CB-promoted migration of RMS neuroblasts both *in vitro* and *ex vivo* (Chapter 4, Figure 4.12 and 4.14 respectively). Inhibiting RalA function or antagonising the CB receptor results in shortening of the leading process *in vivo*, and causes a nucleokinesis defect where there is a significant reduction in the number of productive saltatory nuclear movements. Interestingly however, CB antagonists also cause an increase in secondary branching, whereas deletion of RalA leads to only shortening, and sometimes loss of the leading process, but not secondary branching. These findings could imply that some, but not all of the effects of the CB receptors are mediated via RalA. Our *in vitro* data from explant cultures in Matrigel also suggest that the eCBs may regulate more than one aspect of neuroblast migration. For example, CB agonists not only enhance the distance migrated by neuroblasts, but they also increased the number of cells migrating out of the explants. These two properties can occur independently. For example, BDNF enhances the number of migrating cells but not the distance migrated (Chiaramello et al. 2007). Hence the CB system appears to regulate distinct aspects of neuroblast migration, and at least some of these effects may be mediated by RalA. In the developing CNS, CB1 receptor signalling regulates

polarisation of the growth cone cytoskeleton through the activation of another small GTPase, RhoA (Berghuis et al. 2007). Whether this ability is conserved in migratory neuroblasts remains to be investigated.

7.4 The redundant and exclusive functions of RalA and RalB in adult neurogenesis

The two isoforms belonging to the Ral GTPase family, RalA and RalB, are highly similar, sharing approximately 85% sequence identity and only differing in the C-terminal region. Yet despite this similarity, the function of these two proteins can be complimentary or antagonistic, redundant or exclusive to a particular isoform (Zhao and Rivkees 2000; Chien and White 2003; Shipitsin and Feig 2004; Lalli and Hall 2005; Oxford et al. 2005; Cascone et al. 2008; Ljubicic et al. 2009). In the context of RMS neuroblast migration, we have shown that RalA is the predominant isoform expressed by these cells and is activated downstream of CB-receptor signalling as well as by other molecules shown to regulate neuroblast migration. The expression of RalA is not only important for CB-promoted migration of neuroblasts, but is also required for efficient nucleokinesis, as well as correct morphology and orientation in the RMS. It is worth noting that similar to controls, neuroblasts lacking RalA can be found at the entrance to the OB 5 days post electroporation. However, this does not necessarily rule out the existence of a migratory defect. Given the compact nature of the stream, and the close association between migratory neuroblasts, it is possible that RalA-deficient neuroblasts get carried along by the "current" in the RMS. In support of this hypothesis, Hu et al. (1996) demonstrated that PSA-NCAM deficient neuroblasts were able to migrate normally when transplanted in a wild type RMS, but not vice versa, and suggested that abnormal neuroblasts may be towed along the RMS by other neuroblasts. Time-lapse imaging of Cre-GFP labelled neuroblasts in $RalA^{lox/lox}$ mice may help clarify this issue.

Although we were not able to detect RalB expression in RMS neuroblasts by Western analysis, we cannot exclude the presence of this Ral isoform in these cells,

even though this is likely to be less abundant than RalA. Preliminary observations of pCX-EGFP labelled neuroblasts in $RalA^{lox/lox}/RalB^{-/-}$ mice indicate that neuroblast morphology and migration do not appear to be significantly affected by the absence of RalB, thereby suggesting that RalB may be dispensable for proper neuroblast migration and polarisation. Consistent with this idea, the disrupted orientation defect caused by RalA deletion could not be compensated by the presence of RalB in Cre-expressing $RalA^{lox/lox}$ neuroblasts, and is not worsened by the absence of RalB in Cre-expressing $RalA^{lox/lox}/RalB^{-/-}$ cells (Figure 5.20, middle panel). Hence the regulatory role of Ral GTPases in the polarised migration of RMS neuroblasts appears to be one that is exclusive to RalA.

Interestingly, whilst the loss of RalA affected morphology and orientation of neuroblasts, it did not affect the total number of Cre-GFP-labelled cells entering the stream. In contrast, deletion of both RalA and RalB led to a drastic reduction in the number of Cre-GFP labelled neuroblasts in the RMS. There could be several possible reasons for this. Firstly, the loss of both GTPases could result in a severe migration defect resulting in neuroblasts failing to leave the SVZ. Another interesting possibility is that RalA and RalB may have a role in regulating NS cell or transient amplifying cell proliferation in the SVZ. The electroporation procedure we used to introduce plasmids into migratory neuroblasts labels mostly radial glia-like adult NS cells, which then proliferate to produce transient amplifying progenitors that ultimately give rise to migratory neuroblasts (Boutin et al. 2008). Thus, the drastic reduction in Cre-GFP labelled neuroblasts entering the RMS may also result from a proliferation defect resulting from the loss of RalA and RalB. This hypothesis is also partly based on the fact that both Ral GTPases have been previously shown to regulate proliferation in several types of cancers (Urano et al. 1996; Lu et al. 2000; Hamad et al. 2002; Yu and Feig 2002). Moreover, our collaborators found that the expression of either RalA or RalB was sufficient to drive K-Ras mediated carcinomas, whilst deletion of both RalA and RalB in $RalA^{lox/lox}/RalB^{-/-}$ mice led to mitotic catastrophe arising from a failure of chromosomal segregation during cell division (Peschard et al, *in press*). Interestingly, both RalA and RalB have been shown to participate in cytokinesis in non-neuronal cells by regulating the formation of the

cleavage furrow and mediating abscission, respectively (Cascone et al. 2008). Furthermore, this function of Ral GTPases was reliant on an association with the exocyst complex (Cascone et al. 2008). Recently, Carmena et al. (2011) reported that organisation of the mitotic spindle in asymmetric division of NS cells in *Drosophila* involved an association between Rap-Ral signalling and members of the Par complex, namely aPKC and Par6. Whether RalA and RalB have a similar role in the control of cell division of adult NS cells is currently an unexplored field of research, but given our recent observations this may be a function worth investigating.

Alternatively, deleting both Ral proteins may lead to reduced survival, thus leading to fewer labelled cells present in the stream. A role for RalB in promoting cell survival has been described in tumourigeneis (Chien and White 2003). RalB was found not to be necessary for the survival of normal cells, but was required to promote the survival of tumourogenic cells by offsetting the increased tendency for apoptosis arising from enhanced cell proliferation brought about by RalA (Chien and White 2003; Bodemann and White 2008). Interestingly, deletion of both RalA and RalB was shown to have no effect on tumour cell survival since the balance between proliferation and survival is restored. So, if RalA and RalB have a similar role in the SVZ, we would expect deletion of RalB alone to have a drastic effect on survival whilst deletion of both isoforms to have no effect, which is contrary to our observations, where only deletion of both isoforms causes a severe reduction in the number of labelled neuroblasts. Hence, to uncover which of these three scenarios is true, we are currently investigating changes to proliferation and survival following the loss of RalA and RalB, as well as using time-lapse analysis to assess the migratory capacity of these neuroblasts. In summary, RalA appears to have an exclusive role in regulating RMS neuroblast polarised morphology, whilst RalA and RalB may potentially have redundant roles in the regulation of neural precursor proliferation/survival.

In conclusion, we have shown that an eCB tone regulates the migration of RMS neuroblasts in the postnatal brain. CB receptor-promoted migration is reliant on the activation of the small GTPase RalA, which appears to be required for efficient nucleokinesis *in vitro* and for polarised neuroblast morphology *in vivo*. Furthermore, other growth factors known to regulate neuroblast migration also activate RalA, implying that this GTPase may be a point of convergence for migratory signals in the RMS. Future work will be centred on examining downstream targets of RalA, as well as clarifying the phenotype caused by the loss of RalA and RalB in the postnatal SVZ neurogenic niche.

Publications arising from this thesis

Oudin MJ, Gajendra S, Williams G, Hobbs C, Lalli G and Doherty P (2011). Endocannabinoids regulate the migration of subventricular zone-derived neuroblasts in the postnatal brain. J Neurosci **31**(11): 4000-4011.

Gajendra S, Das A, Falenta K, Peschard P, Marshall CJ, Doherty P, Guo W and Lalli G. An Exo84-Par6 interaction promoted by RalA regulates neuronal polarization and neuroblast migration. *In preparation*

Gajendra S, Oudin M, Zhou Y, Doherty P and Lalli G. RalA acts downstream of cannabinoid signalling to regulate neuroblast migration. *In preparation*

Sonego M, Gajendra S, Hobbs C, Doherty P and Lalli G. The role of fascin in neuroblast migration. *In preparation*

Gajendra S, Sonego M and Lalli G. New insights into signalling events controlling neuronal migration. Int Rev Cell Mol Biol, *In preparation*

References

Abercrombie M and Heaysman JE (1953). Observations on the social behaviour of cells in tissue culture. I. Speed of movement of chick heart fibroblasts in relation to their mutual contacts. Exp Cell Res **5**(1): 111-131.

Abercrombie M and Heaysman JE (1954). Observations on the social behaviour of cells in tissue culture. II. Monolayering of fibroblasts. Exp Cell Res **6**(2): 293-306.

Abrous DN, Koehl M and Le Moal M (2005). Adult neurogenesis: from precursors to network and physiology. Physiol Rev **85**(2): 523-569.

Adams JP and Sweatt JD (2002). Molecular psychology: roles for the ERK MAP kinase cascade in memory. Annu Rev Pharmacol Toxicol **42**: 135-163.

Aggarwal SK, Carter GT, Sullivan MD, ZumBrunnen C, Morrill R and Mayer JD (2009). Medicinal use of cannabis in the United States: historical perspectives, current trends, and future directions. J Opioid Manag **5**(3): 153-168.

Aguado T, Palazuelos J, Monory K, Stella N, Cravatt B, Lutz B, Marsicano G, Kokaia Z, Guzman M and Galve-Roperh I (2006). The endocannabinoid system promotes astroglial differentiation by acting on neural progenitor cells. J Neurosci **26**(5): 1551-1561.

Alexanian AR and Kurpad SN (2005). Quiescent neural cells regain multipotent stem cell characteristics influenced by adult neural stem cells in co-culture. Exp Neurol **191**(1): 193-197.

Alger BE (2002). Retrograde signaling in the regulation of synaptic transmission: focus on endocannabinoids. Prog Neurobiol **68**(4): 247-286.

Alonso M, Lepousez G, Wagner S, Bardy C, Gabellec MM, Torquet N and Lledo PM (2012). Activation of adult-born neurons facilitates learning and memory. Nat Neurosci.

Altman DG and Bland JM (2005). Standard deviations and standard errors. BMJ **331**(7521): 903.

Altman J (1962). Are new neurons formed in the brains of adult mammals? Science **135**: 1127-1128.

Altman J (1963). Autoradiographic investigation of cell proliferation in the brains of rats and cats. Anat Rec **145**: 573-591.

Altman J (1969). Autoradiographic and histological studies of postnatal neurogenesis. IV. Cell proliferation and migration in the anterior forebrain, with special reference to persisting neurogenesis in the olfactory bulb. J Comp Neurol **137**(4): 433-457.

Altman J and Das GD (1965). Autoradiographic and histological evidence of postnatal hippocampal neurogenesis in rats. J Comp Neurol **124**(3): 319-335.

Alvarez-Buylla A (1997). Mechanism of migration of olfactory bulb interneurons. Semin Cell Dev Biol **8**(2): 207-213.

Alvarez-Buylla A, Buskirk DR and Nottebohm F (1987). Monoclonal antibody reveals radial glia in adult avian brain. J Comp Neurol **264**(2): 159-170.

Alvarez-Buylla A and Nottebohm F (1988). Migration of young neurons in adult avian brain. Nature **335**(6188): 353-354.

Anderson SA, Eisenstat DD, Shi L and Rubenstein JL (1997). Interneuron migration from basal forebrain to neocortex: dependence on Dlx genes. Science **278**(5337): 474-476.

Andrade N, Komnenovic V, Blake SM, Jossin Y, Howell B, Goffinet A, Schneider WJ and Nimpf J (2007). ApoER2/VLDL receptor and Dab1 in the rostral migratory stream function in postnatal neuronal migration independently of Reelin. Proc Natl Acad Sci U S A **104**(20): 8508-8513.

Anton ES, Ghashghaei HT, Weber JL, McCann C, Fischer TM, Cheung ID, Gassmann M, Messing A, Klein R, Schwab MH, Lloyd KC and Lai C (2004). Receptor tyrosine kinase ErbB4 modulates neuroblast migration and placement in the adult forebrain. Nat Neurosci **7**(12): 1319-1328.

Arevalo-Martin A, Garcia-Ovejero D, Rubio-Araiz A, Gomez O, Molina-Holgado F and Molina-Holgado E (2007). Cannabinoids modulate Olig2 and polysialylated neural cell adhesion molecule expression in the subventricular zone of post-natal rats through cannabinoid receptor 1 and cannabinoid receptor 2. Eur J Neurosci **26**(6): 1548-1559.

Arvidsson A, Collin T, Kirik D, Kokaia Z and Lindvall O (2002). Neuronal replacement from endogenous precursors in the adult brain after stroke. Nat Med **8**(9): 963-970.

Austin CP and Cepko CL (1990). Cellular migration patterns in the developing mouse cerebral cortex. Development **110**(3): 713-732.

Bagley JA and Belluscio L (2010). Dynamic imaging reveals that brain-derived neurotrophic factor can independently regulate motility and direction of neuroblasts within the rostral migratory stream. Neuroscience **169**(3): 1449-1461.

Banerjee M, Worth D, Prowse DM and Nikolic M (2002). Pak1 phosphorylation on t212 affects microtubules in cells undergoing mitosis. Curr Biol **12**(14): 1233-1239.

Batista-Brito R, Close J, Machold R and Fishell G (2008). The distinct temporal origins of olfactory bulb interneuron subtypes. J Neurosci **28**(15): 3966-3975.

Batista CM, Kippin TE, Willaime-Morawek S, Shimabukuro MK, Akamatsu W and van der Kooy D (2006). A progressive and cell non-autonomous increase in striatal neural stem cells in the Huntington's disease R6/2 mouse. J Neurosci **26**(41): 10452-10460.

Beffert U, Morfini G, Bock HH, Reyna H, Brady ST and Herz J (2002). Reelin-mediated signaling locally regulates protein kinase B/Akt and glycogen synthase kinase 3beta. J Biol Chem **277**(51): 49958-49964.

Begbie J, Doherty P and Graham A (2004). Cannabinoid receptor, CB1, expression follows neuronal differentiation in the early chick embryo. J Anat **205**(3): 213-218.

Bellion A, Baudoin JP, Alvarez C, Bornens M and Metin C (2005). Nucleokinesis in tangentially migrating neurons comprises two alternating phases: forward migration of the Golgi/centrosome associated with centrosome splitting and myosin contraction at the rear. J Neurosci **25**(24): 5691-5699.

Belvindrah R, Hankel S, Walker J, Patton BL and Muller U (2007). Beta1 integrins control the formation of cell chains in the adult rostral migratory stream. J Neurosci **27**(10): 2704-2717.

Belvindrah R, Nissant A and Lledo PM (2011). Abnormal neuronal migration changes the fate of developing neurons in the postnatal olfactory bulb. J Neurosci **31**(20): 7551-7562.

Benraiss A, Chmielnicki E, Lerner K, Roh D and Goldman SA (2001). Adenoviral brain-derived neurotrophic factor induces both neostriatal and olfactory neuronal recruitment from endogenous progenitor cells in the adult forebrain. J Neurosci **21**(17): 6718-6731.

Berghuis P, Dobszay MB, Wang X, Spano S, Ledda F, Sousa KM, Schulte G, Ernfors P, Mackie K, Paratcha G, Hurd YL and Harkany T (2005). Endocannabinoids regulate interneuron migration and morphogenesis by transactivating the TrkB receptor. Proc Natl Acad Sci U S A **102**(52): 19115-19120.

Berghuis P, Rajnicek AM, Morozov YM, Ross RA, Mulder J, Urban GM, Monory K, Marsicano G, Matteoli M, Canty A, Irving AJ, Katona I, Yanagawa Y, Rakic P, Lutz B, Mackie K and Harkany T (2007). Hardwiring the brain: endocannabinoids shape neuronal connectivity. Science **316**(5828): 1212-1216.

Bergmann O, Liebl J, Bernard S, Alkass K, Yeung MS, Steier P, Kutschera W, Johnson L, Landen M, Druid H, Spalding KL and Frisen J (2012). The age of olfactory bulb neurons in humans. Neuron **74**(4): 634-639.

Bhardwaj RD, Curtis MA, Spalding KL, Buchholz BA, Fink D, Bjork-Eriksson T, Nordborg C, Gage FH, Druid H, Eriksson PS and Frisen J (2006). Neocortical neurogenesis in humans is restricted to development. Proc Natl Acad Sci U S A **103**(33): 12564-12568.

Bhattacharya M, Anborgh PH, Babwah AV, Dale LB, Dobransky T, Benovic JL, Feldman RD, Verdi JM, Rylett RJ and Ferguson SS (2002). Beta-arrestins regulate a Ral-GDS Ral effector pathway that mediates cytoskeletal reorganization. Nat Cell Biol **4**(8): 547-555.

Bignami A and Dahl D (1974). Astrocyte-specific protein and neuroglial differentiation. An immunofluorescence study with antibodies to the glial fibrillary acidic protein. J Comp Neurol **153**(1): 27-38.

Bisogno T, Howell F, Williams G, Minassi A, Cascio MG, Ligresti A, Matias I, Schiano-Moriello A, Paul P, Williams EJ, Gangadharan U, Hobbs C, Di Marzo V and Doherty P (2003). Cloning of the first sn1-DAG lipases points to the spatial and temporal regulation of endocannabinoid signaling in the brain. J Cell Biol **163**(3): 463-468.

Blankman JL, Simon GM and Cravatt BF (2007). A comprehensive profile of brain enzymes that hydrolyze the endocannabinoid 2-arachidonoylglycerol. Chem Biol **14**(12): 1347-1356.

Bodemann BO and White MA (2008). Ral GTPases and cancer: linchpin support of the tumorigenic platform. Nat Rev Cancer **8**(2): 133-140.

Bolteus AJ and Bordey A (2004). GABA release and uptake regulate neuronal precursor migration in the postnatal subventricular zone. J Neurosci **24**(35): 7623-7631.

Bos JL, Rehmann H and Wittinghofer A (2007). GEFs and GAPs: critical elements in the control of small G proteins. Cell **129**(5): 865-877.

Boutin C, Diestel S, Desoeuvre A, Tiveron MC and Cremer H (2008). Efficient in vivo electroporation of the postnatal rodent forebrain. PLoS ONE **3**(4): e1883.

Bovetti S, Bovolin P, Perroteau I and Puche AC (2007). Subventricular zone-derived neuroblast migration to the olfactory bulb is modulated by matrix remodelling. Eur J Neurosci **25**(7): 2021-2033.

Bovetti S, Hsieh YC, Bovolin P, Perroteau I, Kazunori T and Puche AC (2007). Blood vessels form a scaffold for neuroblast migration in the adult olfactory bulb. J Neurosci **27**(22): 5976-5980.

Bozoyan L, Khlghatyan J and Saghatelyan A (2012). Astrocytes control the development of the migration-promoting vasculature scaffold in the postnatal brain via VEGF signaling. J Neurosci **32**(5): 1687-1704.

Breton-Provencher V, Lemasson M, Peralta MR, 3rd and Saghatelyan A (2009). Interneurons produced in adulthood are required for the normal functioning of the olfactory bulb network and for the execution of selected olfactory behaviors. J Neurosci **29**(48): 15245-15257.

Bron R, Eickholt BJ, Vermeren M, Fragale N and Cohen J (2004). Functional knockdown of neuropilin-1 in the developing chick nervous system by siRNA hairpins phenocopies genetic ablation in the mouse. Dev Dyn **230**(2): 299-308.

Bronner-Fraser M, Wolf JJ and Murray BA (1992). Effects of antibodies against N-cadherin and N-CAM on the cranial neural crest and neural tube. Dev Biol **153**(2): 291-301.

Brose K, Bland KS, Wang KH, Arnott D, Henzel W, Goodman CS, Tessier-Lavigne M and Kidd T (1999). Slit proteins bind Robo receptors and have an evolutionarily conserved role in repulsive axon guidance. Cell **96**(6): 795-806.

Buck L and Axel R (1991). A novel multigene family may encode odorant receptors: a molecular basis for odor recognition. Cell **65**(1): 175-187.

Buckley NE, Hansson S, Harta G and Mezey E (1998). Expression of the CB1 and CB2 receptor messenger RNAs during embryonic development in the rat. Neuroscience **82**(4): 1131-1149.

Cabral GA, Raborn ES, Griffin L, Dennis J and Marciano-Cabral F (2008). CB2 receptors in the brain: role in central immune function. Br J Pharmacol **153**(2): 240-251.

Cadas H, di Tomaso E and Piomelli D (1997). Occurrence and biosynthesis of endogenous cannabinoid precursor, N-arachidonoyl phosphatidylethanolamine, in rat brain. J Neurosci **17**(4): 1226-1242.

Cadas H, Gaillet S, Beltramo M, Venance L and Piomelli D (1996). Biosynthesis of an endogenous cannabinoid precursor in neurons and its control by calcium and cAMP. J Neurosci **16**(12): 3934-3942.

Camonis JH and White MA (2005). Ral GTPases: corrupting the exocyst in cancer cells. Trends Cell Biol **15**(6): 327-332.

Cantor SB, Urano T and Feig LA (1995). Identification and characterization of Ral-binding protein 1, a potential downstream target of Ral GTPases. Mol Cell Biol **15**(8): 4578-4584.

Carleton A, Petreanu LT, Lansford R, Alvarez-Buylla A and Lledo PM (2003). Becoming a new neuron in the adult olfactory bulb. Nat Neurosci **6**(5): 507-518.

Carmena A, Makarova A and Speicher S (2011). The Rap1-Rgl-Ral signaling network regulates neuroblast cortical polarity and spindle orientation. J Cell Biol **195**(4): 553-562.

Casarosa S, Fode C and Guillemot F (1999). Mash1 regulates neurogenesis in the ventral telencephalon. Development **126**(3): 525-534.

Cascone I, Selimoglu R, Ozdemir C, Del Nery E, Yeaman C, White M and Camonis J (2008). Distinct roles of RalA and RalB in the progression of cytokinesis are supported by distinct RalGEFs. EMBO J **27**(18): 2375-2387.

Causeret F, Terao M, Jacobs T, Nishimura YV, Yanagawa Y, Obata K, Hoshino M and Nikolic M (2009). The p21-activated kinase is required for neuronal migration in the cerebral cortex. Cereb Cortex **19**(4): 861-875.

Cayre M, Canoll P and Goldman JE (2009). Cell migration in the normal and pathological postnatal mammalian brain. Prog Neurobiol **88**(1): 41-63.

Chae T, Kwon YT, Bronson R, Dikkes P, Li E and Tsai LH (1997). Mice lacking p35, a neuronal specific activator of Cdk5, display cortical lamination defects, seizures, and adult lethality. Neuron **18**(1): 29-42.

Chazal G, Durbec P, Jankovski A, Rougon G and Cremer H (2000). Consequences of neural cell adhesion molecule deficiency on cell migration in the rostral migratory stream of the mouse. J Neurosci **20**(4): 1446-1457.

Chen CX, Soto I, Guo YL and Liu Y (2011). Control of secondary granule release in neutrophils by Ral GTPase. J Biol Chem **286**(13): 11724-11733.

Chiaramello S, Dalmasso G, Bezin L, Marcel D, Jourdan F, Peretto P, Fasolo A and De Marchis S (2007). BDNF/ TrkB interaction regulates migration of SVZ precursor cells via PI3-K and MAP-K signalling pathways. Eur J Neurosci **26**(7): 1780-1790.

Chien Y and White MA (2003). RAL GTPases are linchpin modulators of human tumour-cell proliferation and survival. EMBO Rep **4**(8): 800-806.

Chong C, Tan L, Lim L and Manser E (2001). The mechanism of PAK activation. Autophosphorylation events in both regulatory and kinase domains control activity. J Biol Chem **276**(20): 17347-17353.

Clough RR, Sidhu RS and Bhullar RP (2002). Calmodulin binds RalA and RalB and is required for the thrombin-induced activation of Ral in human platelets. J Biol Chem **277**(32): 28972-28980.

Cochard P and Paulin D (1984). Initial expression of neurofilaments and vimentin in the central and peripheral nervous system of the mouse embryo in vivo. J Neurosci **4**(8): 2080-2094.

Comte I, Kim Y, Young CC, van der Harg JM, Hockberger P, Bolam PJ, Poirier F and Szele FG (2011). Galectin-3 maintains cell motility from the subventricular zone to the olfactory bulb. J Cell Sci **124**(Pt 14): 2438-2447.

Conover JC, Doetsch F, Garcia-Verdugo JM, Gale NW, Yancopoulos GD and Alvarez-Buylla A (2000). Disruption of Eph/ephrin signaling affects migration and proliferation in the adult subventricular zone. Nat Neurosci **3**(11): 1091-1097.

Conti L, Pollard SM, Gorba T, Reitano E, Toselli M, Biella G, Sun Y, Sanzone S, Ying QL, Cattaneo E and Smith A (2005). Niche-independent symmetrical self-renewal of a mammalian tissue stem cell. PLoS Biol **3**(9): e283.

Costa MR, Wen G, Lepier A, Schroeder T and Gotz M (2008). Par-complex proteins promote proliferative progenitor divisions in the developing mouse cerebral cortex. Development **135**(1): 11-22.

Cravatt BF, Giang DK, Mayfield SP, Boger DL, Lerner RA and Gilula NB (1996). Molecular characterization of an enzyme that degrades neuromodulatory fatty-acid amides. Nature **384**(6604): 83-87.

Cremer H, Lange R, Christoph A, Plomann M, Vopper G, Roes J, Brown R, Baldwin S, Kraemer P, Scheff S and et al. (1994). Inactivation of the N-CAM gene in mice results in size reduction of the olfactory bulb and deficits in spatial learning. Nature **367**(6462): 455-459.

Curtis MA, Kam M, Nannmark U, Anderson MF, Axell MZ, Wikkelso C, Holtas S, van Roon-Mom WM, Bjork-Eriksson T, Nordborg C, Frisen J, Dragunow M, Faull RL and Eriksson PS (2007). Human neuroblasts migrate to the olfactory bulb via a lateral ventricular extension. Science **315**(5816): 1243-1249.

Davenne M, Custody C, Charneau P and Lledo PM (2005). In vivo imaging of migrating neurons in the mammalian forebrain. Chem Senses **30 Suppl 1**: i115-116.

de Gorter DJ, Reijmers RM, Beuling EA, Naber HP, Kuil A, Kersten MJ, Pals ST and Spaargaren M (2008). The small GTPase Ral mediates SDF-1-induced migration of B cells and multiple myeloma cells. Blood **111**(7): 3364-3372.

Derkinderen P, Toutant M, Burgaya F, Le Bert M, Siciliano JC, de Franciscis V, Gelman M and Girault JA (1996). Regulation of a neuronal form of focal adhesion kinase by anandamide. Science **273**(5282): 1719-1722.

Derkinderen P, Valjent E, Toutant M, Corvol JC, Enslen H, Ledent C, Trzaskos J, Caboche J and Girault JA (2003). Regulation of extracellular signal-regulated kinase by cannabinoids in hippocampus. J Neurosci **23**(6): 2371-2382.

Dhavan R and Tsai LH (2001). A decade of CDK5. Nat Rev Mol Cell Biol **2**(10): 749-759.

Di Marzo V, Fontana A, Cadas H, Schinelli S, Cimino G, Schwartz JC and Piomelli D (1994). Formation and inactivation of endogenous cannabinoid anandamide in central neurons. Nature **372**(6507): 686-691.

Dinh TP, Carpenter D, Leslie FM, Freund TF, Katona I, Sensi SL, Kathuria S and Piomelli D (2002). Brain monoglyceride lipase participating in endocannabinoid inactivation. Proc Natl Acad Sci U S A **99**(16): 10819-10824.

Doetsch F (2003). A niche for adult neural stem cells. Curr Opin Genet Dev **13**(5): 543-550.

Doetsch F and Alvarez-Buylla A (1996). Network of tangential pathways for neuronal migration in adult mammalian brain. Proc Natl Acad Sci U S A **93**(25): 14895-14900.

Doetsch F, Caille I, Lim DA, Garcia-Verdugo JM and Alvarez-Buylla A (1999). Subventricular zone astrocytes are neural stem cells in the adult mammalian brain. Cell **97**(6): 703-716.

Doetsch F, Garcia-Verdugo JM and Alvarez-Buylla A (1997). Cellular composition and three-dimensional organization of the subventricular germinal zone in the adult mammalian brain. J Neurosci **17**(13): 5046-5061.

Doetsch F, Petreanu L, Caille I, Garcia-Verdugo JM and Alvarez-Buylla A (2002). EGF converts transit-amplifying neurogenic precursors in the adult brain into multipotent stem cells. Neuron **36**(6): 1021-1034.

Doherty P, Ashton SV, Moore SE and Walsh FS (1991). Morphoregulatory activities of NCAM and N-cadherin can be accounted for by G protein-dependent activation of L- and N-type neuronal Ca2+ channels. Cell **67**(1): 21-33.

Doherty P, Cohen J and Walsh FS (1990). Neurite outgrowth in response to transfected N-CAM changes during development and is modulated by polysialic acid. Neuron **5**(2): 209-219.

Doherty P, Fruns M, Seaton P, Dickson G, Barton CH, Sears TA and Walsh FS (1990). A threshold effect of the major isoforms of NCAM on neurite outgrowth. Nature **343**(6257): 464-466.

Easter SS, Jr., Ross LS and Frankfurter A (1993). Initial tract formation in the mouse brain. J Neurosci **13**(1): 285-299.

Ehninger D and Kempermann G (2008). Neurogenesis in the adult hippocampus. Cell Tissue Res **331**(1): 243-250.

Ekonomou A, Ballard CG, Pathmanaban ON, Perry RH, Perry EK, Kalaria RN and Minger SL (2011). Increased neural progenitors in vascular dementia. Neurobiol Aging **32**(12): 2152-2161.

Ekonomou A, Johnson M, Perry RH, Perry EK, Kalaria RN, Minger SL and Ballard CG (2012). Increased neural progenitors in individuals with cerebral small vessel disease. Neuropathol Appl Neurobiol **38**(4): 344-353.

Emsley JG and Hagg T (2003). alpha6beta1 integrin directs migration of neuronal precursors in adult mouse forebrain. Exp Neurol **183**(2): 273-285.

Eriksson PS, Perfilieva E, Bjork-Eriksson T, Alborn AM, Nordborg C, Peterson DA and Gage FH (1998). Neurogenesis in the adult human hippocampus. Nat Med **4**(11): 1313-1317.

Etienne-Manneville S and Hall A (2003). Cell polarity: Par6, aPKC and cytoskeletal crosstalk. Curr Opin Cell Biol **15**(1): 67-72.

Fan X, Labrador JP, Hing H and Bashaw GJ (2003). Slit stimulation recruits Dock and Pak to the roundabout receptor and increases Rac activity to regulate axon repulsion at the CNS midline. Neuron **40**(1): 113-127.

Farooqui AA, Rammohan KW and Horrocks LA (1989). Isolation, characterization, and regulation of diacylglycerol lipases from the bovine brain. Ann N Y Acad Sci **559**: 25-36.

Feig LA (2003). Ral-GTPases: approaching their 15 minutes of fame. Trends Cell Biol **13**(8): 419-425.

Feig LA, Urano T and Cantor S (1996). Evidence for a Ras/Ral signaling cascade. Trends Biochem Sci **21**(11): 438-441.

Felder CC, Joyce KE, Briley EM, Glass M, Mackie KP, Fahey KJ, Cullinan GJ, Hunden DC, Johnson DW, Chaney MO, Koppel GA and Brownstein M (1998). LY320135, a novel cannabinoid CB1 receptor antagonist, unmasks coupling of the CB1 receptor to stimulation of cAMP accumulation. J Pharmacol Exp Ther **284**(1): 291-297.

Fenwick RB, Prasannan S, Campbell LJ, Nietlispach D, Evetts KA, Camonis J, Mott HR and Owen D (2009). Solution structure and dynamics of the small GTPase RalB in its active conformation: significance for effector protein binding. Biochemistry **48**(10): 2192-2206.

Fernandes-Alnemri T, Litwack G and Alnemri ES (1994). CPP32, a novel human apoptotic protein with homology to Caenorhabditis elegans cell death protein Ced-3 and mammalian interleukin-1 beta-converting enzyme. J Biol Chem **269**(49): 30761-30764.

Ferro E and Trabalzini L (2010). RalGDS family members couple Ras to Ral signalling and that's not all. Cell Signal **22**(12): 1804-1810.

Fraley SI, Feng Y, Krishnamurthy R, Kim DH, Celedon A, Longmore GD and Wirtz D (2010). A distinctive role for focal adhesion proteins in three-dimensional cell motility. Nat Cell Biol **12**(6): 598-604.

Frankel P, Aronheim A, Kavanagh E, Balda MS, Matter K, Bunney TD and Marshall CJ (2005). RalA interacts with ZONAB in a cell density-dependent manner and regulates its transcriptional activity. EMBO J **24**(1): 54-62.

Fukai S, Matern HT, Jagath JR, Scheller RH and Brunger AT (2003). Structural basis of the interaction between RalA and Sec5, a subunit of the sec6/8 complex. EMBO J **22**(13): 3267-3278.

Funamoto S, Meili R, Lee S, Parry L and Firtel RA (2002). Spatial and temporal regulation of 3-phosphoinositides by PI 3-kinase and PTEN mediates chemotaxis. Cell **109**(5): 611-623.

Gage FH (2000). Mammalian neural stem cells. Science **287**(5457): 1433-1438.

Gage FH (2002). Neurogenesis in the adult brain. J Neurosci **22**(3): 612-613.

Gage FH, Coates PW, Palmer TD, Kuhn HG, Fisher LJ, Suhonen JO, Peterson DA, Suhr ST and Ray J (1995). Survival and differentiation of adult neuronal progenitor cells transplanted to the adult brain. Proc Natl Acad Sci U S A **92**(25): 11879-11883.

Gao Y, Vasilyev DV, Goncalves MB, Howell FV, Hobbs C, Reisenberg M, Shen R, Zhang MY, Strassle BW, Lu P, Mark L, Piesla MJ, Deng K, Kouranova EV, Ring RH, Whiteside GT, Bates B, Walsh FS, Williams G, Pangalos MN, Samad TA and Doherty P (2010). Loss of retrograde endocannabinoid signaling and reduced adult neurogenesis in diacylglycerol lipase knock-out mice. J Neurosci **30**(6): 2017-2024.

Garcia-Gonzalez D, Clemente D, Coelho M, Esteban PF, Soussi-Yanicostas N and de Castro F (2010). Dynamic roles of FGF-2 and Anosmin-1 in the migration of neuronal precursors from the subventricular zone during pre- and postnatal development. Exp Neurol **222**(2): 285-295.

Garcia-Verdugo JM, Doetsch F, Wichterle H, Lim DA and Alvarez-Buylla A (1998). Architecture and cell types of the adult subventricular zone: in search of the stem cells. J Neurobiol **36**(2): 234-248.

Garcia AD, Doan NB, Imura T, Bush TG and Sofroniew MV (2004). GFAP-expressing progenitors are the principal source of constitutive neurogenesis in adult mouse forebrain. Nat Neurosci **7**(11): 1233-1241.

Garzotto D, Giacobini P, Crepaldi T, Fasolo A and De Marchis S (2008). Hepatocyte growth factor regulates migration of olfactory interneuron precursors in the rostral migratory stream through Met-Grb2 coupling. J Neurosci **28**(23): 5901-5909.

Gates MA, Thomas LB, Howard EM, Laywell ED, Sajin B, Faissner A, Gotz B, Silver J and Steindler DA (1995). Cell and molecular analysis of the developing and adult mouse subventricular zone of the cerebral hemispheres. J Comp Neurol **361**(2): 249-266.

Gatley SJ, Gifford AN, Volkow ND, Lan R and Makriyannis A (1996). 123I-labeled AM251: a radioiodinated ligand which binds in vivo to mouse brain cannabinoid CB1 receptors. Eur J Pharmacol **307**(3): 331-338.

Gatley SJ, Lan R, Pyatt B, Gifford AN, Volkow ND and Makriyannis A (1997). Binding of the non-classical cannabinoid CP 55,940, and the diarylpyrazole AM251 to rodent brain cannabinoid receptors. Life Sci **61**(14): PL 191-197.

Gilmore EC, Ohshima T, Goffinet AM, Kulkarni AB and Herrup K (1998). Cyclin-dependent kinase 5-deficient mice demonstrate novel developmental arrest in cerebral cortex. J Neurosci **18**(16): 6370-6377.

Giuffrida A, Beltramo M and Piomelli D (2001). Mechanisms of endocannabinoid inactivation: biochemistry and pharmacology. J Pharmacol Exp Ther **298**(1): 7-14.

Glass M and Felder CC (1997). Concurrent stimulation of cannabinoid CB1 and dopamine D2 receptors augments cAMP accumulation in striatal neurons: evidence for a Gs linkage to the CB1 receptor. J Neurosci **17**(14): 5327-5333.

Gleeson JG, Lin PT, Flanagan LA and Walsh CA (1999). Doublecortin is a microtubule-associated protein and is expressed widely by migrating neurons. Neuron **23**(2): 257-271.

Goi T, Rusanescu G, Urano T and Feig LA (1999). Ral-specific guanine nucleotide exchange factor activity opposes other Ras effectors in PC12 cells by inhibiting neurite outgrowth. Mol Cell Biol **19**(3): 1731-1741.

Goldman SA and Nottebohm F (1983). Neuronal production, migration, and differentiation in a vocal control nucleus of the adult female canary brain. Proc Natl Acad Sci U S A **80**(8): 2390-2394.

Goldstein B and Macara IG (2007). The PAR proteins: fundamental players in animal cell polarization. Dev Cell **13**(5): 609-622.

Goncalves MB, Suetterlin P, Yip P, Molina-Holgado F, Walker DJ, Oudin MJ, Zentar MP, Pollard S, Yanez-Munoz RJ, Williams G, Walsh FS, Pangalos MN and Doherty P (2008). A diacylglycerol lipase-CB2 cannabinoid pathway regulates adult subventricular zone neurogenesis in an age-dependent manner. Mol Cell Neurosci **38**(4): 526-536.

Gonzalez-Perez O, Romero-Rodriguez R, Soriano-Navarro M, Garcia-Verdugo JM and Alvarez-Buylla A (2009). EGF Induces the Progeny of Subventricular Zone Type B Cells to Migrate and Differentiate into Oligodendrocytes. Stem Cells.

Gopal PP, Simonet JC, Shapiro W and Golden JA (2010). Leading process branch instability in Lis1+/- nonradially migrating interneurons. Cereb Cortex **20**(6): 1497-1505.

Gould E (2007). How widespread is adult neurogenesis in mammals? Nat Rev Neurosci **8**(6): 481-488.

Granot D, Scheinost D, Markakis EA, Papademetris X and Shapiro EM (2011). Serial monitoring of endogenous neuroblast migration by cellular MRI. Neuroimage **57**(3): 817-824.

Grindstaff KK, Yeaman C, Anandasabapathy N, Hsu SC, Rodriguez-Boulan E, Scheller RH and Nelson WJ (1998). Sec6/8 complex is recruited to cell-cell contacts and specifies transport vesicle delivery to the basal-lateral membrane in epithelial cells. Cell **93**(5): 731-740.

Grosheva I, Shtutman M, Elbaum M and Bershadsky AD (2001). p120 catenin affects cell motility via modulation of activity of Rho-family GTPases: a link between cell-cell contact formation and regulation of cell locomotion. J Cell Sci **114**(Pt 4): 695-707.

Gupta A, Tsai LH and Wynshaw-Boris A (2002). Life is a journey: a genetic look at neocortical development. Nat Rev Genet **3**(5): 342-355.

Hack I, Bancila M, Loulier K, Carroll P and Cremer H (2002). Reelin is a detachment signal in tangential chain-migration during postnatal neurogenesis. Nat Neurosci **5**(10): 939-945.

Hakanen J, Duprat S and Salminen M (2011). Netrin1 is required for neural and glial precursor migrations into the olfactory bulb. Dev Biol **355**(1): 101-114.

Hamad NM, Elconin JH, Karnoub AE, Bai W, Rich JN, Abraham RT, Der CJ and Counter CM (2002). Distinct requirements for Ras oncogenesis in human versus mouse cells. Genes Dev **16**(16): 2045-2057.

Han K, Kim MH, Seeburg D, Seo J, Verpelli C, Han S, Chung HS, Ko J, Lee HW, Kim K, Heo WD, Meyer T, Kim H, Sala C, Choi SY, Sheng M and Kim E (2009). Regulated RalBP1 binding to RalA and PSD-95 controls AMPA receptor endocytosis and LTD. PLoS Biol **7**(9): e1000187.

Hanks SK, Calalb MB, Harper MC and Patel SK (1992). Focal adhesion protein-tyrosine kinase phosphorylated in response to cell attachment to fibronectin. Proc Natl Acad Sci U S A **89**(18): 8487-8491.

Harkany T, Guzman M, Galve-Roperh I, Berghuis P, Devi LA and Mackie K (2007). The emerging functions of endocannabinoid signaling during CNS development. Trends Pharmacol Sci **28**(2): 83-92.

Hasuwa H, Kaseda K, Einarsdottir T and Okabe M (2002). Small interfering RNA and gene silencing in transgenic mice and rats. FEBS Lett **532**(1-2): 227-230.

Hatten ME (1999). Central nervous system neuronal migration. Annu Rev Neurosci **22**: 511-539.

Haubensak W, Attardo A, Denk W and Huttner WB (2004). Neurons arise in the basal neuroepithelium of the early mammalian telencephalon: a major site of neurogenesis. Proc Natl Acad Sci U S A **101**(9): 3196-3201.

Hazelett CC and Yeaman C (2012). Sec5 and Exo84 Mediate Distinct Aspects of RalA-Dependent Cell Polarization. PLoS ONE **7**(6): e39602.

He JC, Gomes I, Nguyen T, Jayaram G, Ram PT, Devi LA and Iyengar R (2005). The G alpha(o/i)-coupled cannabinoid receptor-mediated neurite outgrowth involves Rap regulation of Src and Stat3. J Biol Chem **280**(39): 33426-33434.

Hehnly H and Doxsey S (2012). Polarity sets the stage for cytokinesis. Mol Biol Cell **23**(1): 7-11.

Henrique D and Schweisguth F (2003). Cell polarity: the ups and downs of the Par6/aPKC complex. Curr Opin Genet Dev **13**(4): 341-350.

Higginbotham H, Tanaka T, Brinkman BC and Gleeson JG (2006). GSK3beta and PKCzeta function in centrosome localization and process stabilization during Slit-mediated neuronal repolarization. Mol Cell Neurosci **32**(1-2): 118-132.

Hillard CJ, Manna S, Greenberg MJ, DiCamelli R, Ross RA, Stevenson LA, Murphy V, Pertwee RG and Campbell WB (1999). Synthesis and characterization of potent and selective agonists of the neuronal cannabinoid receptor (CB1). J Pharmacol Exp Ther **289**(3): 1427-1433.

Hirota Y, Ohshima T, Kaneko N, Ikeda M, Iwasato T, Kulkarni AB, Mikoshiba K, Okano H and Sawamoto K (2007). Cyclin-dependent kinase 5 is required for control of neuroblast migration in the postnatal subventricular zone. J Neurosci **27**(47): 12829-12838.

Hofer F, Berdeaux R and Martin GS (1998). Ras-independent activation of Ral by a Ca(2+)-dependent pathway. Curr Biol **8**(14): 839-842.

Horton S, Meredith A, Richardson JA and Johnson JE (1999). Correct coordination of neuronal differentiation events in ventral forebrain requires the bHLH factor MASH1. Mol Cell Neurosci **14**(4-5): 355-369.

Howlett AC, Barth F, Bonner TI, Cabral G, Casellas P, Devane WA, Felder CC, Herkenham M, Mackie K, Martin BR, Mechoulam R and Pertwee RG (2002). International Union of Pharmacology. XXVII. Classification of cannabinoid receptors. Pharmacol Rev **54**(2): 161-202.

Hu H (1999). Chemorepulsion of neuronal migration by Slit2 in the developing mammalian forebrain. Neuron **23**(4): 703-711.

Hu H and Rutishauser U (1996). A septum-derived chemorepulsive factor for migrating olfactory interneuron precursors. Neuron **16**(5): 933-940.

Hu H, Tomasiewicz H, Magnuson T and Rutishauser U (1996). The role of polysialic acid in migration of olfactory bulb interneuron precursors in the subventricular zone. Neuron **16**(4): 735-743.

Huffman JW, Liddle J, Yu S, Aung MM, Abood ME, Wiley JL and Martin BR (1999). 3-(1',1'-Dimethylbutyl)-1-deoxy-delta8-THC and related compounds: synthesis of selective ligands for the CB2 receptor. Bioorg Med Chem **7**(12): 2905-2914.

Hurtado-Chong A, Yusta-Boyo MJ, Vergano-Vera E, Bulfone A, de Pablo F and Vicario-Abejon C (2009). IGF-I promotes neuronal migration and positioning in the olfactory bulb and the exit of neuroblasts from the subventricular zone. Eur J Neurosci.

Huttenlocher A, Lakonishok M, Kinder M, Wu S, Truong T, Knudsen KA and Horwitz AF (1998). Integrin and cadherin synergy regulates contact inhibition of migration and motile activity. J Cell Biol **141**(2): 515-526.

Hynes RO (2002). Integrins: bidirectional, allosteric signaling machines. Cell **110**(6): 673-687.

Imura T, Kornblum HI and Sofroniew MV (2003). The predominant neural stem cell isolated from postnatal and adult forebrain but not early embryonic forebrain expresses GFAP. J Neurosci **23**(7): 2824-2832.

Iwamura H, Suzuki H, Ueda Y, Kaya T and Inaba T (2001). In vitro and in vivo pharmacological characterization of JTE-907, a novel selective ligand for cannabinoid CB2 receptor. J Pharmacol Exp Ther **296**(2): 420-425.

Jacobs T, Causeret F, Nishimura YV, Terao M, Norman A, Hoshino M and Nikolic M (2007). Localized activation of p21-activated kinase controls neuronal polarity and morphology. J Neurosci **27**(32): 8604-8615.

Jacques TS, Relvas JB, Nishimura S, Pytela R, Edwards GM, Streuli CH and ffrench-Constant C (1998). Neural precursor cell chain migration and division are regulated through different beta1 integrins. Development **125**(16): 3167-3177.

Jaffe AB and Hall A (2005). Rho GTPases: biochemistry and biology. Annu Rev Cell Dev Biol **21**: 247-269.

Jankovski A and Sotelo C (1996). Subventricular zone-olfactory bulb migratory pathway in the adult mouse: cellular composition and specificity as determined by heterochronic and heterotopic transplantation. J Comp Neurol **371**(3): 376-396.

Jiang W, Zhang Y, Xiao L, Van Cleemput J, Ji SP, Bai G and Zhang X (2005). Cannabinoids promote embryonic and adult hippocampus neurogenesis and produce anxiolytic- and antidepressant-like effects. J Clin Invest **115**(11): 3104-3116.

Jiao J and Chen DF (2008). Induction of neurogenesis in nonconventional neurogenic regions of the adult central nervous system by niche astrocyte-produced signals. Stem Cells **26**(5): 1221-1230.

Jin K, Wang X, Xie L, Mao XO, Zhu W, Wang Y, Shen J, Mao Y, Banwait S and Greenberg DA (2006). Evidence for stroke-induced neurogenesis in the human brain. Proc Natl Acad Sci U S A **103**(35): 13198-13202.

Jin K, Xie L, Kim SH, Parmentier-Batteur S, Sun Y, Mao XO, Childs J and Greenberg DA (2004). Defective adult neurogenesis in CB1 cannabinoid receptor knockout mice. Mol Pharmacol **66**(2): 204-208.

Jin R, Junutula JR, Matern HT, Ervin KE, Scheller RH and Brunger AT (2005). Exo84 and Sec5 are competitive regulatory Sec6/8 effectors to the RalA GTPase. EMBO J **24**(12): 2064-2074.

Johansson CB, Momma S, Clarke DL, Risling M, Lendahl U and Frisen J (1999). Identification of a neural stem cell in the adult mammalian central nervous system. Cell **96**(1): 25-34.

Jossin Y and Cooper JA (2011). Reelin, Rap1 and N-cadherin orient the migration of multipolar neurons in the developing neocortex. Nat Neurosci **14**(6): 697-703.

Jullien-Flores V, Mahe Y, Mirey G, Leprince C, Meunier-Bisceuil B, Sorkin A and Camonis JH (2000). RLIP76, an effector of the GTPase Ral, interacts with the AP2 complex: involvement of the Ral pathway in receptor endocytosis. J Cell Sci **113 (Pt 16)**: 2837-2844.

Kakita A and Goldman JE (1999). Patterns and dynamics of SVZ cell migration in the postnatal forebrain: monitoring living progenitors in slice preparations. Neuron **23**(3): 461-472.

Kanatani S, Tabata H and Nakajima K (2005). Neuronal migration in cortical development. J Child Neurol **20**(4): 274-279.

Kanoh H, Yamada K and Sakane F (2002). Diacylglycerol kinases: emerging downstream regulators in cell signaling systems. J Biochem **131**(5): 629-633.

Kaplan MS (2001). Environment complexity stimulates visual cortex neurogenesis: death of a dogma and a research career. Trends Neurosci **24**(10): 617-620.

Kaplan MS and Hinds JW (1977). Neurogenesis in the adult rat: electron microscopic analysis of light radioautographs. Science **197**(4308): 1092-1094.

Kashatus DF, Lim KH, Brady DC, Pershing NL, Cox AD and Counter CM (2011). RALA and RALBP1 regulate mitochondrial fission at mitosis. Nat Cell Biol **13**(9): 1108-1115.

Kawato M, Shirakawa R, Kondo H, Higashi T, Ikeda T, Okawa K, Fukai S, Nureki O, Kita T and Horiuchi H (2008). Regulation of platelet dense granule secretion by the Ral GTPase-exocyst pathway. J Biol Chem **283**(1): 166-174.

Kawauchi T, Chihama K, Nabeshima Y and Hoshino M (2006). Cdk5 phosphorylates and stabilizes p27kip1 contributing to actin organization and cortical neuronal migration. Nat Cell Biol **8**(1): 17-26.

Kazanis I, Lathia JD, Vadakkan TJ, Raborn E, Wan R, Mughal MR, Eckley DM, Sasaki T, Patton B, Mattson MP, Hirschi KK, Dickinson ME and ffrench-Constant C (2010). Quiescence and activation of stem and precursor cell populations in the subependymal zone of the mammalian brain are associated with distinct cellular and extracellular matrix signals. J Neurosci **30**(29): 9771-9781.

Kempermann G (2006). Adult neurogenesis: Stem cells and neuronal development in the adult brain. New York, Oxford University Press.

Kenworthy AK (2001). Imaging protein-protein interactions using fluorescence resonance energy transfer microscopy. Methods **24**(3): 289-296.

Kerever A, Schnack J, Vellinga D, Ichikawa N, Moon C, Arikawa-Hirasawa E, Efird JT and Mercier F (2007). Novel extracellular matrix structures in the neural stem cell niche capture the neurogenic factor fibroblast growth factor 2 from the extracellular milieu. Stem Cells **25**(9): 2146-2157.

Kidd T, Bland KS and Goodman CS (1999). Slit is the midline repellent for the robo receptor in Drosophila. Cell **96**(6): 785-794.

Kim J, Isokawa M, Ledent C and Alger BE (2002). Activation of muscarinic acetylcholine receptors enhances the release of endogenous cannabinoids in the hippocampus. J Neurosci **22**(23): 10182-10191.

Kim Y, Comte I, Szabo G, Hockberger P and Szele FG (2009). Adult mouse subventricular zone stem and progenitor cells are sessile and epidermal growth factor receptor negatively regulates neuroblast migration. PLoS ONE **4**(12): e8122.

Kirschenbaum B, Doetsch F, Lois C and Alvarez-Buylla A (1999). Adult subventricular zone neuronal precursors continue to proliferate and migrate in the absence of the olfactory bulb. J Neurosci **19**(6): 2171-2180.

Koizumi H, Higginbotham H, Poon T, Tanaka T, Brinkman BC and Gleeson JG (2006). Doublecortin maintains bipolar shape and nuclear translocation during migration in the adult forebrain. Nat Neurosci **9**(6): 779-786.

Konno D, Yoshimura S, Hori K, Maruoka H and Sobue K (2005). Involvement of the phosphatidylinositol 3-kinase/rac1 and cdc42 pathways in radial migration of cortical neurons. J Biol Chem **280**(6): 5082-5088.

Kosodo Y (2012). Interkinetic nuclear migration: beyond a hallmark of neurogenesis. Cell Mol Life Sci.

Kreis P and Barnier JV (2009). PAK signalling in neuronal physiology. Cell Signal **21**(3): 384-393.

Kreitzer AC and Regehr WG (2001). Retrograde inhibition of presynaptic calcium influx by endogenous cannabinoids at excitatory synapses onto Purkinje cells. Neuron **29**(3): 717-727.

Kriegstein A and Alvarez-Buylla A (2009). The Glial Nature of Embryonic and Adult Neural Stem Cells. Annu Rev Neurosci **32**: 149-184.

Kriegstein AR and Noctor SC (2004). Patterns of neuronal migration in the embryonic cortex. Trends Neurosci **27**(7): 392-399.

Kruegel J and Miosge N (2010). Basement membrane components are key players in specialized extracellular matrices. Cell Mol Life Sci **67**(17): 2879-2895.

Kwon YT and Tsai LH (1998). A novel disruption of cortical development in p35(-/-) mice distinct from reeler. J Comp Neurol **395**(4): 510-522.

Lalli G (2009). RalA and the exocyst complex influence neuronal polarity through PAR-3 and aPKC. J Cell Sci **122**(Pt 10): 1499-1506.

Lalli G and Hall A (2005). Ral GTPases regulate neurite branching through GAP-43 and the exocyst complex. J Cell Biol **171**(5): 857-869.

Lambert de Rouvroit C and Goffinet AM (2001). Neuronal migration. Mech Dev **105**(1-2): 47-56.

Law AK, Pencea V, Buck CR and Luskin MB (1999). Neurogenesis and neuronal migration in the neonatal rat forebrain anterior subventricular zone do not require GFAP-positive astrocytes. Dev Biol **216**(2): 622-634.

Lazarini F, Mouthon MA, Gheusi G, de Chaumont F, Olivo-Marin JC, Lamarque S, Abrous DN, Boussin FD and Lledo PM (2009). Cellular and behavioral effects of cranial irradiation of the subventricular zone in adult mice. PLoS ONE **4**(9): e7017.

Leitch AE, Haslett C and Rossi AG (2009). Cyclin-dependent kinase inhibitor drugs as potential novel anti-inflammatory and pro-resolution agents. Br J Pharmacol **158**(4): 1004-1016.

Leong SY and Turnley AM (2011). Regulation of adult neural precursor cell migration. Neurochem Int **59**(3): 382-393.

Leventhal C, Rafii S, Rafii D, Shahar A and Goldman SA (1999). Endothelial trophic support of neuronal production and recruitment from the adult mammalian subependyma. Mol Cell Neurosci **13**(6): 450-464.

Liang CC, Park AY and Guan JL (2007). In vitro scratch assay: a convenient and inexpensive method for analysis of cell migration in vitro. Nat Protoc **2**(2): 329-333.

Lim DA and Alvarez-Buylla A (1999). Interaction between astrocytes and adult subventricular zone precursors stimulates neurogenesis. Proc Natl Acad Sci U S A **96**(13): 7526-7531.

Lim DA, Tramontin AD, Trevejo JM, Herrera DG, Garcia-Verdugo JM and Alvarez-Buylla A (2000). Noggin antagonizes BMP signaling to create a niche for adult neurogenesis. Neuron **28**(3): 713-726.

Liu G and Rao Y (2003). Neuronal migration from the forebrain to the olfactory bulb requires a new attractant persistent in the olfactory bulb. J Neurosci **23**(16): 6651-6659.

Ljubicic S, Bezzi P, Vitale N and Regazzi R (2009). The GTPase RalA regulates different steps of the secretory process in pancreatic beta-cells. PLoS ONE **4**(11): e7770.

Lledo PM, Merkle FT and Alvarez-Buylla A (2008). Origin and function of olfactory bulb interneuron diversity. Trends Neurosci **31**(8): 392-400.

Lois C and Alvarez-Buylla A (1994). Long-distance neuronal migration in the adult mammalian brain. Science **264**(5162): 1145-1148.

Lois C, Garcia-Verdugo JM and Alvarez-Buylla A (1996). Chain migration of neuronal precursors. Science **271**(5251): 978-981.

Lopez JA, Kwan EP, Xie L, He Y, James DE and Gaisano HY (2008). The RalA GTPase is a central regulator of insulin exocytosis from pancreatic islet beta cells. J Biol Chem **283**(26): 17939-17945.

Lu Z, Hornia A, Joseph T, Sukezane T, Frankel P, Zhong M, Bychenok S, Xu L, Feig LA and Foster DA (2000). Phospholipase D and RalA cooperate with the epidermal growth factor receptor to transform 3Y1 rat fibroblasts. Mol Cell Biol **20**(2): 462-467.

Luo L (2000). Rho GTPases in neuronal morphogenesis. Nat Rev Neurosci **1**(3): 173-180.

Luskin MB (1993). Restricted proliferation and migration of postnatally generated neurons derived from the forebrain subventricular zone. Neuron **11**(1): 173-189.

Luskin MB (1998). Neuroblasts of the postnatal mammalian forebrain: their phenotype and fate. J Neurobiol **36**(2): 221-233.

Marin O and Rubenstein JL (2001). A long, remarkable journey: tangential migration in the telencephalon. Nat Rev Neurosci **2**(11): 780-790.

Marin O, Valdeolmillos M and Moya F (2006). Neurons in motion: same principles for different shapes? Trends Neurosci **29**(12): 655-661.

Marin O, Valiente M, Ge X and Tsai LH (2010). Guiding neuronal cell migrations. Cold Spring Harb Perspect Biol **2**(2): a001834.

Marins M, Xavier AL, Viana NB, Fortes FS, Froes MM and Menezes JR (2009). Gap junctions are involved in cell migration in the early postnatal subventricular zone. Dev Neurobiol **69**(11): 715-730.

Martin TD and Der CJ (2012). Differential involvement of RalA and RalB in colorectal cancer. Small Gtpases **3**(2): 126-130.

Martinez-Molina N, Kim Y, Hockberger P and Szele FG (2011). Rostral migratory stream neuroblasts turn and change directions in stereotypic patterns. Cell Adh Migr **5**(1): 83-95.

Martino G and Pluchino S (2006). The therapeutic potential of neural stem cells. Nat Rev Neurosci **7**(5): 395-406.

Mason HA, Ito S and Corfas G (2001). Extracellular signals that regulate the tangential migration of olfactory bulb neuronal precursors: inducers, inhibitors, and repellents. J Neurosci **21**(19): 7654-7663.

Massouh M and Saghatelyan A (2010). De-routing neuronal precursors in the adult brain to sites of injury: role of the vasculature. Neuropharmacology **58**(6): 877-883.

Matsuda LA, Lolait SJ, Brownstein MJ, Young AC and Bonner TI (1990). Structure of a cannabinoid receptor and functional expression of the cloned cDNA. Nature **346**(6284): 561-564.

May RM (1991). Cajal's Degeneration and Regeneration of the Nervous System translated by Raoul M May. New York, Oxford University Press.

Mechoulam R and Gaoni Y (1965). A Total Synthesis of Dl-Delta-1-Tetrahydrocannabinol, the Active Constituent of Hashish. J Am Chem Soc **87**: 3273-3275.

Mechoulam R and Parker LA (2012). The Endocannabinoid System and the Brain. Annu Rev Psychol.

Mercier F and Arikawa-Hirasawa E (2012). Heparan sulfate niche for cell proliferation in the adult brain. Neurosci Lett **510**(2): 67-72.

Mercier F, Kitasako JT and Hatton GI (2002). Anatomy of the brain neurogenic zones revisited: fractones and the fibroblast/macrophage network. J Comp Neurol **451**(2): 170-188.

Merkle FT, Mirzadeh Z and Alvarez-Buylla A (2007). Mosaic organization of neural stem cells in the adult brain. Science **317**(5836): 381-384.

Metin C, Denizot JP and Ropert N (2000). Intermediate zone cells express calcium-permeable AMPA receptors and establish close contact with growing axons. J Neurosci **20**(2): 696-708.

Miller AM and Stella N (2008). CB2 receptor-mediated migration of immune cells: it can go either way. Br J Pharmacol **153**(2): 299-308.

Ming GL and Song H (2011). Adult neurogenesis in the mammalian brain: significant answers and significant questions. Neuron **70**(4): 687-702.

Mirey G, Balakireva M, L'Hoste S, Rosse C, Voegeling S and Camonis J (2003). A Ral guanine exchange factor-Ral pathway is conserved in Drosophila melanogaster and sheds new light on the connectivity of the Ral, Ras, and Rap pathways. Mol Cell Biol **23**(3): 1112-1124.

Mirzadeh Z, Merkle FT, Soriano-Navarro M, Garcia-Verdugo JM and Alvarez-Buylla A (2008). Neural stem cells confer unique pinwheel architecture to the ventricular surface in neurogenic regions of the adult brain. Cell Stem Cell **3**(3): 265-278.

Mission JP, Takahashi T and Caviness VS, Jr. (1991). Ontogeny of radial and other astroglial cells in murine cerebral cortex. Glia **4**(2): 138-148.

Miyakoshi LM, Todeschini AR, Mendez-Otero R and Hedin-Pereira C (2012). Role of the 9-O-acetyl GD3 in subventricular zone neuroblast migration. Mol Cell Neurosci **49**(2): 240-249.

Mobley AK and McCarty JH (2011). beta8 integrin is essential for neuroblast migration in the rostral migratory stream. Glia **59**(11): 1579-1587.

Mobley AK, Tchaicha JH, Shin J, Hossain MG and McCarty JH (2009). Beta8 integrin regulates neurogenesis and neurovascular homeostasis in the adult brain. J Cell Sci **122**(Pt 11): 1842-1851.

Molina-Holgado F, Rubio-Araiz A, Garcia-Ovejero D, Williams RJ, Moore JD, Arevalo-Martin A, Gomez-Torres O and Molina-Holgado E (2007). CB2 cannabinoid receptors promote mouse neural stem cell proliferation. Eur J Neurosci **25**(3): 629-634.

Monje ML, Mizumatsu S, Fike JR and Palmer TD (2002). Irradiation induces neural precursor-cell dysfunction. Nat Med **8**(9): 955-962.

Moreno MM, Linster C, Escanilla O, Sacquet J, Didier A and Mandairon N (2009). Olfactory perceptual learning requires adult neurogenesis. Proc Natl Acad Sci U S A **106**(42): 17980-17985.

Morest DK (1970). A study of neurogenesis in the forebrain of opossum pouch young. Z Anat Entwicklungsgesch **130**(4): 265-305.

Morris NR (2003). Nuclear positioning: the means is at the ends. Curr Opin Cell Biol **15**(1): 54-59.

Morshead CM, Garcia AD, Sofroniew MV and van Der Kooy D (2003). The ablation of glial fibrillary acidic protein-positive cells from the adult central nervous system results in the loss of forebrain neural stem cells but not retinal stem cells. Eur J Neurosci **18**(1): 76-84.

Moskalenko S, Henry DO, Rosse C, Mirey G, Camonis JH and White MA (2002). The exocyst is a Ral effector complex. Nat Cell Biol **4**(1): 66-72.

Moskalenko S, Tong C, Rosse C, Mirey G, Formstecher E, Daviet L, Camonis J and White MA (2003). Ral GTPases regulate exocyst assembly through dual subunit interactions. J Biol Chem **278**(51): 51743-51748.

Munro S, Thomas KL and Abu-Shaar M (1993). Molecular characterization of a peripheral receptor for cannabinoids. Nature **365**(6441): 61-65.

Murase S, Cho C, White JM and Horwitz AF (2008). ADAM2 promotes migration of neuroblasts in the rostral migratory stream to the olfactory bulb. Eur J Neurosci **27**(7): 1585-1595.

Murase S and Horwitz AF (2002). Deleted in colorectal carcinoma and differentially expressed integrins mediate the directional migration of neural precursors in the rostral migratory stream. J Neurosci **22**(9): 3568-3579.

Nadarajah B, Alifragis P, Wong RO and Parnavelas JG (2002). Ventricle-directed migration in the developing cerebral cortex. Nat Neurosci **5**(3): 218-224.

Nadarajah B, Alifragis P, Wong RO and Parnavelas JG (2003). Neuronal migration in the developing cerebral cortex: observations based on real-time imaging. Cereb Cortex **13**(6): 607-611.

Nadarajah B, Brunstrom JE, Grutzendler J, Wong RO and Pearlman AL (2001). Two modes of radial migration in early development of the cerebral cortex. Nat Neurosci **4**(2): 143-150.

Nadarajah B and Parnavelas JG (2002). Modes of neuronal migration in the developing cerebral cortex. Nat Rev Neurosci **3**(6): 423-432.

Nakatomi H, Kuriu T, Okabe S, Yamamoto S, Hatano O, Kawahara N, Tamura A, Kirino T and Nakafuku M (2002). Regeneration of hippocampal pyramidal neurons after ischemic brain injury by recruitment of endogenous neural progenitors. Cell **110**(4): 429-441.

Nam SC, Kim Y, Dryanovski D, Walker A, Goings G, Woolfrey K, Kang SS, Chu C, Chenn A, Erdelyi F, Szabo G, Hockberger P and Szele FG (2007). Dynamic features of postnatal subventricular zone cell motility: a two-photon time-lapse study. J Comp Neurol **505**(2): 190-208.

Ng KL, Li JD, Cheng MY, Leslie FM, Lee AG and Zhou QY (2005). Dependence of olfactory bulb neurogenesis on prokineticin 2 signaling. Science **308**(5730): 1923-1927.

Nguyen-Ba-Charvet KT, Picard-Riera N, Tessier-Lavigne M, Baron-Van Evercooren A, Sotelo C and Chedotal A (2004). Multiple roles for slits in the control of cell migration in the rostral migratory stream. J Neurosci **24**(6): 1497-1506.

Nguyen-Ba-Charvet KT, Plump AS, Tessier-Lavigne M and Chedotal A (2002). Slit1 and slit2 proteins control the development of the lateral olfactory tract. J Neurosci **22**(13): 5473-5480.

Nguyen Ba-Charvet KT, Brose K, Marillat V, Kidd T, Goodman CS, Tessier-Lavigne M, Sotelo C and Chedotal A (1999). Slit2-Mediated chemorepulsion and collapse of developing forebrain axons. Neuron **22**(3): 463-473.

Nguyen L, Besson A, Heng JI, Schuurmans C, Teboul L, Parras C, Philpott A, Roberts JM and Guillemot F (2006). p27kip1 independently promotes neuronal differentiation and migration in the cerebral cortex. Genes Dev **20**(11): 1511-1524.

Nie K, Molnar Z and Szele FG (2010). Proliferation but not migration is associated with blood vessels during development of the rostral migratory stream. Dev Neurosci **32**(3): 163-172.

Nieman BJ, Shyu JY, Rodriguez JJ, Garcia AD, Joyner AL and Turnbull DH (2010). In vivo MRI of neural cell migration dynamics in the mouse brain. Neuroimage **50**(2): 456-464.

Niethammer M, Smith DS, Ayala R, Peng J, Ko J, Lee MS, Morabito M and Tsai LH (2000). NUDEL is a novel Cdk5 substrate that associates with LIS1 and cytoplasmic dynein. Neuron **28**(3): 697-711.

Nikolic M (2004). The molecular mystery of neuronal migration: FAK and Cdk5. Trends Cell Biol **14**(1): 1-5.

Nikolic M (2008). The Pak1 kinase: an important regulator of neuronal morphology and function in the developing forebrain. Mol Neurobiol **37**(2-3): 187-202.

Noctor SC, Martinez-Cerdeno V, Ivic L and Kriegstein AR (2004). Cortical neurons arise in symmetric and asymmetric division zones and migrate through specific phases. Nat Neurosci **7**(2): 136-144.

O'Rourke NA, Sullivan DP, Kaznowski CE, Jacobs AA and McConnell SK (1995). Tangential migration of neurons in the developing cerebral cortex. Development **121**(7): 2165-2176.

Ocbina PJ, Dizon ML, Shin L and Szele FG (2006). Doublecortin is necessary for the migration of adult subventricular zone cells from neurospheres. Mol Cell Neurosci **33**(2): 126-135.

Ohab JJ, Fleming S, Blesch A and Carmichael ST (2006). A neurovascular niche for neurogenesis after stroke. J Neurosci **26**(50): 13007-13016.

Ohshima T, Gilmore EC, Longenecker G, Jacobowitz DM, Brady RO, Herrup K and Kulkarni AB (1999). Migration defects of cdk5(-/-) neurons in the developing cerebellum is cell autonomous. J Neurosci **19**(14): 6017-6026.

Ohshima T, Ward JM, Huh CG, Longenecker G, Veeranna, Pant HC, Brady RO, Martin LJ and Kulkarni AB (1996). Targeted disruption of the cyclin-dependent kinase 5 gene results in abnormal corticogenesis, neuronal pathology and perinatal death. Proc Natl Acad Sci U S A **93**(20): 11173-11178.

Ohta Y, Suzuki N, Nakamura S, Hartwig JH and Stossel TP (1999). The small GTPase RalA targets filamin to induce filopodia. Proc Natl Acad Sci U S A **96**(5): 2122-2128.

Ono K, Tomasiewicz H, Magnuson T and Rutishauser U (1994). N-CAM mutation inhibits tangential neuronal migration and is phenocopied by enzymatic removal of polysialic acid. Neuron **13**(3): 595-609.

Orona E, Scott JW and Rainer EC (1983). Different granule cell populations innervate superficial and deep regions of the external plexiform layer in rat olfactory bulb. J Comp Neurol **217**(2): 227-237.

Ortega-Perez I, Murray K and Lledo PM (2007). The how and why of adult neurogenesis. J Mol Histol **38**(6): 555-562.

Oudin MJ, Gajendra S, Williams G, Hobbs C, Lalli G and Doherty P (2011). Endocannabinoids regulate the migration of subventricular zone-derived neuroblasts in the postnatal brain. J Neurosci **31**(11): 4000-4011.

Oudin MJ, Hobbs C and Doherty P (2011). DAGL-dependent endocannabinoid signalling: roles in axonal pathfinding, synaptic plasticity and adult neurogenesis. Eur J Neurosci **34**(10): 1634-1646.

Oxford G, Owens CR, Titus BJ, Foreman TL, Herlevsen MC, Smith SC and Theodorescu D (2005). RalA and RalB: antagonistic relatives in cancer cell migration. Cancer Res **65**(16): 7111-7120.

Palazuelos J, Aguado T, Egia A, Mechoulam R, Guzman M and Galve-Roperh I (2006). Non-psychoactive CB2 cannabinoid agonists stimulate neural progenitor proliferation. FASEB Journal **20**(13): 2405-2407.

Palmer TD, Willhoite AR and Gage FH (2000). Vascular niche for adult hippocampal neurogenesis. J Comp Neurol **425**(4): 479-494.

Panganiban G and Rubenstein JL (2002). Developmental functions of the Distal-less/Dlx homeobox genes. Development **129**(19): 4371-4386.

Paratcha G, Ibanez CF and Ledda F (2006). GDNF is a chemoattractant factor for neuronal precursor cells in the rostral migratory stream. Mol Cell Neurosci **31**(3): 505-514.

Park HT, Wu J and Rao Y (2002). Molecular control of neuronal migration. Bioessays **24**(9): 821-827.

Park SH and Weinberg RA (1995). A putative effector of Ral has homology to Rho/Rac GTPase activating proteins. Oncogene **11**(11): 2349-2355.

Parras CM, Galli R, Britz O, Soares S, Galichet C, Battiste J, Johnson JE, Nakafuku M, Vescovi A and Guillemot F (2004). Mash1 specifies neurons and oligodendrocytes in the postnatal brain. EMBO J **23**(22): 4495-4505.

Parrish-Aungst S, Shipley MT, Erdelyi F, Szabo G and Puche AC (2007). Quantitative analysis of neuronal diversity in the mouse olfactory bulb. J Comp Neurol **501**(6): 825-836.

Pencea V, Bingaman KD, Freedman LJ and Luskin MB (2001). Neurogenesis in the subventricular zone and rostral migratory stream of the neonatal and adult primate forebrain. Exp Neurol **172**(1): 1-16.

Peretto P, Giachino C, Aimar P, Fasolo A and Bonfanti L (2005). Chain formation and glial tube assembly in the shift from neonatal to adult subventricular zone of the rodent forebrain. J Comp Neurol **487**(4): 407-427.

Pertwee RG (2006). The pharmacology of cannabinoid receptors and their ligands: an overview. Int J Obes (Lond) **30 Suppl 1**: S13-18.

Petreanu L and Alvarez-Buylla A (2002). Maturation and death of adult-born olfactory bulb granule neurons: role of olfaction. J Neurosci **22**(14): 6106-6113.

Petridis AK and El Maarouf A (2011). Brain-derived neurotrophic factor levels influence the balance of migration and differentiation of subventricular zone cells, but not guidance to the olfactory bulb. J Clin Neurosci **18**(2): 265-270.

Piomelli D (2003). The molecular logic of endocannabinoid signalling. Nat Rev Neurosci **4**(11): 873-884.

Platel JC, Dave KA and Bordey A (2008). Control of neuroblast production and migration by converging GABA and glutamate signals in the postnatal forebrain. J Physiol **586**(16): 3739-3743.

Platel JC, Heintz T, Young S, Gordon V and Bordey A (2008). Tonic activation of GLUK5 kainate receptors decreases neuroblast migration in whole-mounts of the subventricular zone. J Physiol **586**(16): 3783-3793.

Pollard SM, Conti L, Sun Y, Goffredo D and Smith A (2006). Adherent neural stem (NS) cells from fetal and adult forebrain. Cereb Cortex **16 Suppl 1**: i112-120.

Polleux F, Whitford KL, Dijkhuizen PA, Vitalis T and Ghosh A (2002). Control of cortical interneuron migration by neurotrophins and PI3-kinase signaling. Development **129**(13): 3147-3160.

Polzin A, Shipitsin M, Goi T, Feig LA and Turner TJ (2002). Ral-GTPase influences the regulation of the readily releasable pool of synaptic vesicles. Mol Cell Biol **22**(6): 1714-1722.

Porteus MH, Bulfone A, Liu JK, Puelles L, Lo LC and Rubenstein JL (1994). DLX-2, MASH-1, and MAP-2 expression and bromodeoxyuridine incorporation define molecularly distinct cell populations in the embryonic mouse forebrain. J Neurosci **14**(11 Pt 1): 6370-6383.

Quilliam LA, Rebhun JF and Castro AF (2002). A growing family of guanine nucleotide exchange factors is responsible for activation of Ras-family GTPases. Prog Nucleic Acid Res Mol Biol **71**: 391-444.

Rakic P (1985). Limits of neurogenesis in primates. Science **227**(4690): 1054-1056.

Rakic S, Yanagawa Y, Obata K, Faux C, Parnavelas JG and Nikolic M (2009). Cortical interneurons require p35/Cdk5 for their migration and laminar organization. Cereb Cortex **19**(8): 1857-1869.

Rashid T, Banerjee M and Nikolic M (2001). Phosphorylation of Pak1 by the p35/Cdk5 kinase affects neuronal morphology. J Biol Chem **276**(52): 49043-49052.

Reid CB, Liang I and Walsh C (1995). Systematic widespread clonal organization in cerebral cortex. Neuron **15**(2): 299-310.

Reynolds BA and Weiss S (1992). Generation of neurons and astrocytes from isolated cells of the adult mammalian central nervous system. Science **255**(5052): 1707-1710.

Ridley AJ, Schwartz MA, Burridge K, Firtel RA, Ginsberg MH, Borisy G, Parsons JT and Horwitz AR (2003). Cell migration: integrating signals from front to back. Science **302**(5651): 1704-1709.

Robin AM, Zhang ZG, Wang L, Zhang RL, Katakowski M, Zhang L, Wang Y, Zhang C and Chopp M (2006). Stromal cell-derived factor 1alpha mediates neural progenitor cell motility after focal cerebral ischemia. J Cereb Blood Flow Metab **26**(1): 125-134.

Rochefort C, Gheusi G, Vincent JD and Lledo PM (2002). Enriched odor exposure increases the number of newborn neurons in the adult olfactory bulb and improves odor memory. J Neurosci **22**(7): 2679-2689.

Rodriguez de Fonseca F, Del Arco I, Bermudez-Silva FJ, Bilbao A, Cippitelli A and Navarro M (2005). The endocannabinoid system: physiology and pharmacology. Alcohol Alcohol **40**(1): 2-14.

Rondaij MG, Sellink E, Gijzen KA, ten Klooster JP, Hordijk PL, van Mourik JA and Voorberg J (2004). Small GTP-binding protein Ral is involved in cAMP-mediated release of von Willebrand factor from endothelial cells. Arterioscler Thromb Vasc Biol **24**(7): 1315-1320.

Ross RA, Brockie HC, Stevenson LA, Murphy VL, Templeton F, Makriyannis A and Pertwee RG (1999). Agonist-inverse agonist characterization at CB1 and CB2 cannabinoid receptors of L759633, L759656, and AM630. Br J Pharmacol **126**(3): 665-672.

Rosse C, Hatzoglou A, Parrini MC, White MA, Chavrier P and Camonis J (2006). RalB mobilizes the exocyst to drive cell migration. Mol Cell Biol **26**(2): 727-734.

Rousselot P, Lois C and Alvarez-Buylla A (1995). Embryonic (PSA) N-CAM reveals chains of migrating neuroblasts between the lateral ventricle and the olfactory bulb of adult mice. J Comp Neurol **351**(1): 51-61.

Rusanescu G, Gotoh T, Tian X and Feig LA (2001). Regulation of Ras signaling specificity by protein kinase C. Mol Cell Biol **21**(8): 2650-2658.

Rutishauser U, Watanabe M, Silver J, Troy FA and Vimr ER (1985). Specific alteration of NCAM-mediated cell adhesion by an endoneuraminidase. J Cell Biol **101**(5 Pt 1): 1842-1849.

Ryberg E, Larsson N, Sjogren S, Hjorth S, Hermansson NO, Leonova J, Elebring T, Nilsson K, Drmota T and Greasley PJ (2007). The orphan receptor GPR55 is a novel cannabinoid receptor. Br J Pharmacol **152**(7): 1092-1101.

Saffell JL, Williams EJ, Mason IJ, Walsh FS and Doherty P (1997). Expression of a dominant negative FGF receptor inhibits axonal growth and FGF receptor phosphorylation stimulated by CAMs. Neuron **18**(2): 231-242.

Saghatelyan A (2009). Role of blood vessels in the neuronal migration. Semin Cell Dev Biol **20**(6): 744-750.

Saghatelyan A, de Chevigny A, Schachner M and Lledo PM (2004). Tenascin-R mediates activity-dependent recruitment of neuroblasts in the adult mouse forebrain. Nat Neurosci **7**(4): 347-356.

Sakamoto M, Imayoshi I, Ohtsuka T, Yamaguchi M, Mori K and Kageyama R (2011). Continuous neurogenesis in the adult forebrain is required for innate olfactory responses. Proc Natl Acad Sci U S A **108**(20): 8479-8484.

Sanai N, Nguyen T, Ihrie RA, Mirzadeh Z, Tsai H-H, Wong M, Gupta N, Berger MS, Huang E, Garcia-Verdugo J-M, Rowitch DH and Alvarez-Buylla A (2011). Corridors of migrating neurons in the human brain and their decline during infancy. Nature **478**(7369): 382-386.

Sanai N, Nguyen T, Ihrie RA, Mirzadeh Z, Tsai HH, Wong M, Gupta N, Berger MS, Huang E, Garcia-Verdugo JM, Rowitch DH and Alvarez-Buylla A (2011). Corridors of migrating neurons in the human brain and their decline during infancy. Nature.

Sanchez-Heras E, Howell FV, Williams G and Doherty P (2006). The fibroblast growth factor receptor acid box is essential for interactions with N-cadherin and all of the major isoforms of neural cell adhesion molecule. J Biol Chem **281**(46): 35208-35216.

Sancho-Tello M, Valles S, Montoliu C, Renau-Piqueras J and Guerri C (1995). Developmental pattern of GFAP and vimentin gene expression in rat brain and in radial glial cultures. Glia **15**(2): 157-166.

Sasaki S, Shionoya A, Ishida M, Gambello MJ, Yingling J, Wynshaw-Boris A and Hirotsune S (2000). A LIS1/NUDEL/cytoplasmic dynein heavy chain complex in the developing and adult nervous system. Neuron **28**(3): 681-696.

Sawamoto K, Hirota Y, Alfaro-Cervello C, Soriano-Navarro M, He X, Hayakawa-Yano Y, Yamada M, Hikishima K, Tabata H, Iwanami A, Nakajima K, Toyama Y, Itoh T, Alvarez-Buylla A, Garcia-Verdugo JM and Okano H (2011). Cellular composition and organization of the subventricular zone and rostral migratory stream in the adult and neonatal common marmoset brain. J Comp Neurol **519**(4): 690-713.

Sawamoto K, Wichterle H, Gonzalez-Perez O, Cholfin JA, Yamada M, Spassky N, Murcia NS, Garcia-Verdugo JM, Marin O, Rubenstein JL, Tessier-Lavigne M, Okano H and Alvarez-Buylla A (2006). New neurons follow the flow of cerebrospinal fluid in the adult brain. Science **311**(5761): 629-632.

Schaar BT and McConnell SK (2005). Cytoskeletal coordination during neuronal migration. Proc Natl Acad Sci U S A **102**(38): 13652-13657.

Schaller MD, Borgman CA, Cobb BS, Vines RR, Reynolds AB and Parsons JT (1992). pp125FAK a structurally distinctive protein-tyrosine kinase associated with focal adhesions. Proc Natl Acad Sci U S A **89**(11): 5192-5196.

Schliwa M, Euteneuer U, Graf R and Ueda M (1999). Centrosomes, microtubules and cell migration. Biochem Soc Symp **65**: 223-231.

Schmechel DE and Rakic P (1979). A Golgi study of radial glial cells in developing monkey telencephalon: morphogenesis and transformation into astrocytes. Anat Embryol (Berl) **156**(2): 115-152.

Segarra J, Balenci L, Drenth T, Maina F and Lamballe F (2006). Combined signaling through ERK, PI3K/AKT, and RAC1/p38 is required for met-triggered cortical neuron migration. J Biol Chem **281**(8): 4771-4778.

Seki T and Arai Y (1993). Distribution and possible roles of the highly polysialylated neural cell adhesion molecule (NCAM-H) in the developing and adult central nervous system. Neurosci Res **17**(4): 265-290.

Seri B, Garcia-Verdugo JM, Collado-Morente L, McEwen BS and Alvarez-Buylla A (2004). Cell types, lineage, and architecture of the germinal zone in the adult dentate gyrus. J Comp Neurol **478**(4): 359-378.

Seri B, Garcia-Verdugo JM, McEwen BS and Alvarez-Buylla A (2001). Astrocytes give rise to new neurons in the adult mammalian hippocampus. J Neurosci **21**(18): 7153-7160.

Shekarabi M, Moore SW, Tritsch NX, Morris SJ, Bouchard JF and Kennedy TE (2005). Deleted in colorectal cancer binding netrin-1 mediates cell substrate adhesion and recruits Cdc42, Rac1, Pak1, and N-WASP into an intracellular signaling complex that promotes growth cone expansion. J Neurosci **25**(12): 3132-3141.

Shen Y, Xu L and Foster DA (2001). Role for phospholipase D in receptor-mediated endocytosis. Mol Cell Biol **21**(2): 595-602.

Shepherd GM (1972). Synaptic organization of the mammalian olfactory bulb. Physiol Rev **52**(4): 864-917.

Shieh JC, Schaar BT, Srinivasan K, Brodsky FM and McConnell SK (2011). Endocytosis regulates cell soma translocation and the distribution of adhesion proteins in migrating neurons. PLoS ONE **6**(3): e17802.

Shipitsin M and Feig LA (2004). RalA but not RalB enhances polarized delivery of membrane proteins to the basolateral surface of epithelial cells. Mol Cell Biol **24**(13): 5746-5756.

Shirakawa R, Fukai S, Kawato M, Higashi T, Kondo H, Ikeda T, Nakayama E, Okawa K, Nureki O, Kimura T, Kita T and Horiuchi H (2009). Tuberous sclerosis tumor suppressor complex-like complexes act as GTPase-activating proteins for Ral GTPases. J Biol Chem **284**(32): 21580-21588.

Shu T, Ayala R, Nguyen MD, Xie Z, Gleeson JG and Tsai LH (2004). Ndel1 operates in a common pathway with LIS1 and cytoplasmic dynein to regulate cortical neuronal positioning. Neuron **44**(2): 263-277.

Smith SD, Jaffer ZM, Chernoff J and Ridley AJ (2008). PAK1-mediated activation of ERK1/2 regulates lamellipodial dynamics. J Cell Sci **121**(Pt 22): 3729-3736.

Snapyan M, Lemasson M, Brill MS, Blais M, Massouh M, Ninkovic J, Gravel C, Berthod F, Gotz M, Barker PA, Parent A and Saghatelyan A (2009). Vasculature guides migrating neuronal precursors in the adult mammalian forebrain via brain-derived neurotrophic factor signaling. J Neurosci **29**(13): 4172-4188.

Sohur US, Emsley JG, Mitchell BD and Macklis JD (2006). Adult neurogenesis and cellular brain repair with neural progenitors, precursors and stem cells. Philos Trans R Soc Lond B Biol Sci **361**(1473): 1477-1497.

Solecki DJ, Model L, Gaetz J, Kapoor TM and Hatten ME (2004). Par6alpha signaling controls glial-guided neuronal migration. Nat Neurosci **7**(11): 1195-1203.

Song H, Stevens CF and Gage FH (2002). Astroglia induce neurogenesis from adult neural stem cells. Nature **417**(6884): 39-44.

Song M, Kojima N, Hanamura K, Sekino Y, Inoue HK, Mikuni M and Shirao T (2008). Expression of drebrin E in migrating neuroblasts in adult rat brain: coincidence between drebrin E disappearance from cell body and cessation of migration. Neuroscience **152**(3): 670-682.

Song ZH and Bonner TI (1996). A lysine residue of the cannabinoid receptor is critical for receptor recognition by several agonists but not WIN55212-2. Mol Pharmacol **49**(5): 891-896.

Song ZH and Zhong M (2000). CB1 cannabinoid receptor-mediated cell migration. J Pharmacol Exp Ther **294**(1): 204-209.

Spalding KL, Bhardwaj RD, Buchholz BA, Druid H and Frisen J (2005). Retrospective birth dating of cells in humans. Cell **122**(1): 133-143.

Spiczka KS and Yeaman C (2008). Ral-regulated interaction between Sec5 and paxillin targets Exocyst to focal complexes during cell migration. J Cell Sci **121**(Pt 17): 2880-2891.

Stella N and Piomelli D (2001). Receptor-dependent formation of endogenous cannabinoids in cortical neurons. Eur J Pharmacol **425**(3): 189-196.

Stella N, Schweitzer P and Piomelli D (1997). A second endogenous cannabinoid that modulates long-term potentiation. Nature **388**(6644): 773-778.

Stuhmer T, Puelles L, Ekker M and Rubenstein JL (2002). Expression from a Dlx gene enhancer marks adult mouse cortical GABAergic neurons. Cereb Cortex **12**(1): 75-85.

Stumm R and Hollt V (2007). CXC chemokine receptor 4 regulates neuronal migration and axonal pathfinding in the developing nervous system: implications for neuronal regeneration in the adult brain. J Mol Endocrinol **38**(3): 377-382.

Stumm RK, Zhou C, Ara T, Lazarini F, Dubois-Dalcq M, Nagasawa T, Hollt V and Schulz S (2003). CXCR4 regulates interneuron migration in the developing neocortex. J Neurosci **23**(12): 5123-5130.

Sugihara K, Asano S, Tanaka K, Iwamatsu A, Okawa K and Ohta Y (2002). The exocyst complex binds the small GTPase RalA to mediate filopodia formation. Nat Cell Biol **4**(1): 73-78.

Suhonen JO, Peterson DA, Ray J and Gage FH (1996). Differentiation of adult hippocampus-derived progenitors into olfactory neurons in vivo. Nature **383**(6601): 624-627.

Sultan S, Mandairon N, Kermen F, Garcia S, Sacquet J and Didier A (2010). Learning-dependent neurogenesis in the olfactory bulb determines long-term olfactory memory. FASEB Journal **24**(7): 2355-2363.

Suzuki J, Yamazaki Y, Li G, Kaziro Y and Koide H (2000). Involvement of Ras and Ral in chemotactic migration of skeletal myoblasts. Mol Cell Biol **20**(13): 4658-4665.

Takahashi T, Misson JP and Caviness VS, Jr. (1990). Glial process elongation and branching in the developing murine neocortex: a qualitative and quantitative immunohistochemical analysis. J Comp Neurol **302**(1): 15-28.

Takai Y, Sasaki T and Matozaki T (2001). Small GTP-binding proteins. Physiol Rev **81**(1): 153-208.

Takaya A, Ohba Y, Kurokawa K and Matsuda M (2004). RalA activation at nascent lamellipodia of epidermal growth factor-stimulated Cos7 cells and migrating Madin-Darby canine kidney cells. Mol Biol Cell **15**(6): 2549-2557.

Tanaka T, Serneo FF, Higgins C, Gambello MJ, Wynshaw-Boris A and Gleeson JG (2004). Lis1 and doublecortin function with dynein to mediate coupling of the nucleus to the centrosome in neuronal migration. J Cell Biol **165**(5): 709-721.

Tanaka T, Serneo FF, Tseng HC, Kulkarni AB, Tsai LH and Gleeson JG (2004). Cdk5 phosphorylation of doublecortin ser297 regulates its effect on neuronal migration. Neuron **41**(2): 215-227.

Tattersfield AS, Croon RJ, Liu YW, Kells AP, Faull RL and Connor B (2004). Neurogenesis in the striatum of the quinolinic acid lesion model of Huntington's disease. Neuroscience **127**(2): 319-332.

TerBush DR, Maurice T, Roth D and Novick P (1996). The Exocyst is a multiprotein complex required for exocytosis in Saccharomyces cerevisiae. EMBO J **15**(23): 6483-6494.

Thiel DA, Reeder MK, Pfaff A, Coleman TR, Sells MA and Chernoff J (2002). Cell cycle-regulated phosphorylation of p21-activated kinase 1. Curr Biol **12**(14): 1227-1232.

Thomas LB, Gates MA and Steindler DA (1996). Young neurons from the adult subependymal zone proliferate and migrate along an astrocyte, extracellular matrix-rich pathway. Glia **17**(1): 1-14.

Thored P, Arvidsson A, Cacci E, Ahlenius H, Kallur T, Darsalia V, Ekdahl CT, Kokaia Z and Lindvall O (2006). Persistent production of neurons from adult brain stem cells during recovery after stroke. Stem Cells **24**(3): 739-747.

Tian X, Rusanescu G, Hou W, Schaffhausen B and Feig LA (2002). PDK1 mediates growth factor-induced Ral-GEF activation by a kinase-independent mechanism. EMBO J **21**(6): 1327-1338.

Tomasiewicz H, Ono K, Yee D, Thompson C, Goridis C, Rutishauser U and Magnuson T (1993). Genetic deletion of a neural cell adhesion molecule variant (N-CAM-180) produces distinct defects in the central nervous system. Neuron **11**(6): 1163-1174.

Tomasz M and Palom Y (1997). The mitomycin bioreductive antitumor agents: cross-linking and alkylation of DNA as the molecular basis of their activity. Pharmacol Ther **76**(1-3): 73-87.

Tramontin AD, Garcia-Verdugo JM, Lim DA and Alvarez-Buylla A (2003). Postnatal development of radial glia and the ventricular zone (VZ): a continuum of the neural stem cell compartment. Cereb Cortex **13**(6): 580-587.

Tsai LH and Gleeson JG (2005). Nucleokinesis in neuronal migration. Neuron **46**(3): 383-388.

Tsou K, Brown S, Sanudo-Pena MC, Mackie K and Walker JM (1998). Immunohistochemical distribution of cannabinoid CB1 receptors in the rat central nervous system. Neuroscience **83**(2): 393-411.

Uchigashima M, Narushima M, Fukaya M, Katona I, Kano M and Watanabe M (2007). Subcellular arrangement of molecules for 2-arachidonoyl-glycerol-mediated retrograde signaling and its physiological contribution to synaptic modulation in the striatum. J Neurosci **27**(14): 3663-3676.

Urano T, Emkey R and Feig LA (1996). Ral-GTPases mediate a distinct downstream signaling pathway from Ras that facilitates cellular transformation. EMBO J **15**(4): 810-816.

Vadlamudi RK, Li F, Adam L, Nguyen D, Ohta Y, Stossel TP and Kumar R (2002). Filamin is essential in actin cytoskeletal assembly mediated by p21-activated kinase 1. Nat Cell Biol **4**(9): 681-690.

Valiente M, Ciceri G, Rico B and Marin O (2011). Focal adhesion kinase modulates radial glia-dependent neuronal migration through connexin-26. J Neurosci **31**(32): 11678-11691.

Valley MT, Mullen TR, Schultz LC, Sagdullaev BT and Firestein S (2009). Ablation of mouse adult neurogenesis alters olfactory bulb structure and olfactory fear conditioning. Front Neurosci **3**: 51.

van Dam EM and Robinson PJ (2006). Ral: mediator of membrane trafficking. Int J Biochem Cell Biol **38**(11): 1841-1847.

van Triest M, de Rooij J and Bos JL (2001). Measurement of GTP-bound Ras-like GTPases by activation-specific probes. Methods Enzymol **333**: 343-348.

Vande Velde G, Couillard-Despres S, Aigner L, Himmelreich U and van der Linden A (2012). In situ labeling and imaging of endogenous neural stem cell proliferation and migration. Wiley Interdiscip Rev Nanomed Nanobiotechnol.

Varma N, Carlson GC, Ledent C and Alger BE (2001). Metabotropic glutamate receptors drive the endocannabinoid system in hippocampus. J Neurosci **21**(24): RC188.

Voigt T (1989). Development of glial cells in the cerebral wall of ferrets: direct tracing of their transformation from radial glia into astrocytes. J Comp Neurol **289**(1): 74-88.

Vreys R, Velde GV, Krylychkina O, Vellema M, Verhoye M, Timmermans JP, Baekelandt V and Van der Linden A (2009). MRI visualization of endogenous neural progenitor cell migration along the RMS in the adult mouse brain: Validation of various MPIO labeling strategies. Neuroimage.

Walsh C and Cepko CL (1992). Widespread dispersion of neuronal clones across functional regions of the cerebral cortex. Science **255**(5043): 434-440.

Wang L, Li G and Sugita S (2004). RalA-exocyst interaction mediates GTP-dependent exocytosis. J Biol Chem **279**(19): 19875-19881.

Wang TW, Zhang H, Gyetko MR and Parent JM (2011). Hepatocyte growth factor acts as a mitogen and chemoattractant for postnatal subventricular zone-olfactory bulb neurogenesis. Mol Cell Neurosci **48**(1): 38-50.

Ward M, McCann C, DeWulf M, Wu JY and Rao Y (2003). Distinguishing between directional guidance and motility regulation in neuronal migration. J Neurosci **23**(12): 5170-5177.

Ward ME and Rao Y (2005). Investigations of neuronal migration in the central nervous system. Methods Mol Biol **294**: 137-156.

Wedlich D (2005). Cell migration in development and disease. Weinheim, Wiley-VCH.

Weiner OD (2002). Regulation of cell polarity during eukaryotic chemotaxis: the chemotactic compass. Curr Opin Cell Biol **14**(2): 196-202.

White MA, Vale T, Camonis JH, Schaefer E and Wigler MH (1996). A role for the Ral guanine nucleotide dissociation stimulator in mediating Ras-induced transformation. J Biol Chem **271**(28): 16439-16442.

Whitman MC, Fan W, Rela L, Rodriguez-Gil DJ and Greer CA (2009). Blood vessels form a migratory scaffold in the rostral migratory stream. J Comp Neurol **516**(2): 94-104.

Wichterle H, Garcia-Verdugo JM and Alvarez-Buylla A (1997). Direct evidence for homotypic, glia-independent neuronal migration. Neuron **18**(5): 779-791.

Wiese C and Zheng Y (2006). Microtubule nucleation: gamma-tubulin and beyond. J Cell Sci **119**(Pt 20): 4143-4153.

Williams EJ, Walsh FS and Doherty P (1994). The production of arachidonic acid can account for calcium channel activation in the second messenger pathway underlying neurite outgrowth stimulated by NCAM, N-cadherin, and L1. J Neurochem **62**(3): 1231-1234.

Williams EJ, Walsh FS and Doherty P (2003). The FGF receptor uses the endocannabinoid signaling system to couple to an axonal growth response. J Cell Biol **160**(4): 481-486.

Williams EJ, Williams G, Howell FV, Skaper SD, Walsh FS and Doherty P (2001). Identification of an N-cadherin motif that can interact with the fibroblast growth factor receptor and is required for axonal growth. J Biol Chem **276**(47): 43879-43886.

Wilson RI and Nicoll RA (2001). Endogenous cannabinoids mediate retrograde signalling at hippocampal synapses. Nature **410**(6828): 588-592.

Winner B, Cooper-Kuhn CM, Aigner R, Winkler J and Kuhn HG (2002). Long-term survival and cell death of newly generated neurons in the adult rat olfactory bulb. Eur J Neurosci **16**(9): 1681-1689.

Winner B, Couillard-Despres S, Geyer M, Aigner R, Bogdahn U, Aigner L, Kuhn HG and Winkler J (2008). Dopaminergic lesion enhances growth factor-induced striatal neuroblast migration. J Neuropathol Exp Neurol **67**(2): 105-116.

Wittko IM, Schanzer A, Kuzmichev A, Schneider FT, Shibuya M, Raab S and Plate KH (2009). VEGFR-1 regulates adult olfactory bulb neurogenesis and migration of neural progenitors in the rostral migratory stream in vivo. J Neurosci **29**(27): 8704-8714.

Wolthuis RM, Bauer B, van 't Veer LJ, de Vries-Smits AM, Cool RH, Spaargaren M, Wittinghofer A, Burgering BM and Bos JL (1996). RalGDS-like factor (Rlf) is a novel Ras and Rap 1A-associating protein. Oncogene **13**(2): 353-362.

Wolthuis RM, Franke B, van Triest M, Bauer B, Cool RH, Camonis JH, Akkerman JW and Bos JL (1998). Activation of the small GTPase Ral in platelets. Mol Cell Biol **18**(5): 2486-2491.

Wong K, Ren XR, Huang YZ, Xie Y, Liu G, Saito H, Tang H, Wen L, Brady-Kalnay SM, Mei L, Wu JY, Xiong WC and Rao Y (2001). Signal transduction in neuronal migration: roles of GTPase activating proteins and the small GTPase Cdc42 in the Slit-Robo pathway. Cell **107**(2): 209-221.

Woodhead GJ, Mutch CA, Olson EC and Chenn A (2006). Cell-autonomous beta-catenin signaling regulates cortical precursor proliferation. J Neurosci **26**(48): 12620-12630.

Wu W, Wong K, Chen J, Jiang Z, Dupuis S, Wu JY and Rao Y (1999). Directional guidance of neuronal migration in the olfactory system by the protein Slit. Nature **400**(6742): 331-336.

Xie XQ, Melvin LS and Makriyannis A (1996). The conformational properties of the highly selective cannabinoid receptor ligand CP-55,940. J Biol Chem **271**(18): 10640-10647.

Xie Z, Sanada K, Samuels BA, Shih H and Tsai LH (2003). Serine 732 phosphorylation of FAK by Cdk5 is important for microtubule organization, nuclear movement, and neuronal migration. Cell **114**(4): 469-482.

Yang HK, Sundholm-Peters NL, Goings GE, Walker AS, Hyland K and Szele FG (2004). Distribution of doublecortin expressing cells near the lateral ventricles in the adult mouse brain. J Neurosci Res **76**(3): 282-295.

Yang XT, Bi YY and Feng DF (2011). From the vascular microenvironment to neurogenesis. Brain Res Bull **84**(1): 1-7.

Yoshizaki H, Aoki K, Nakamura T and Matsuda M (2006). Regulation of RalA GTPase by phosphatidylinositol 3-kinase as visualized by FRET probes. Biochem Soc Trans **34**(Pt 5): 851-854.

Young KM, Fogarty M, Kessaris N and Richardson WD (2007). Subventricular zone stem cells are heterogeneous with respect to their embryonic origins and neurogenic fates in the adult olfactory bulb. J Neurosci **27**(31): 8286-8296.

Yu Y and Feig LA (2002). Involvement of R-Ras and Ral GTPases in estrogen-independent proliferation of breast cancer cells. Oncogene **21**(49): 7557-7568.

Zhang H, Vutskits L, Pepper MS and Kiss JZ (2003). VEGF is a chemoattractant for FGF-2-stimulated neural progenitors. J Cell Biol **163**(6): 1375-1384.

Zhang R, Zhang Z, Zhang C, Zhang L, Robin A, Wang Y, Lu M and Chopp M (2004). Stroke transiently increases subventricular zone cell division from asymmetric to symmetric and increases neuronal differentiation in the adult rat. J Neurosci **24**(25): 5810-5815.

Zhao Z and Rivkees SA (2000). Tissue-specific expression of GTPas RalA and RalB during embryogenesis and regulation by epithelial-mesenchymal interaction. Mech Dev **97**(1-2): 201-204.